Nitroxide Mediated Radical Heterogeneous Polymerizations in Supercritical Carbon Dioxide

Pádraig O'Connor

Thesis presented for the qualification of Ph.D. degree

to the

National University of Ireland Galway

Department of Chemistry,

National University of Ireland, Galway

2012

Supervisor: Dr. Fawaz Aldabbagh

Head of School: Prof. Paul V. Murphy

Table of Contents

I would firstly like to thank my supervisor Dr. Fawaz Aldabbagh for giving me the opportunity of doing this PhD and for all his advice and guidance throughout the course of my research.

I would also like to acknowledge and thank A/Prof Per B. Zetterlund (CAMD, UNSW, Australia) for his guidance and help particularly with polymerization kinetics and modelling.

This doctoral thesis would not have been possible without the generous support of the Science Foundation of Ireland (08/RFP/MTR1201).

Thanks to Yusuke Sugihara who helped me throughout my PhD and for his significant contributions to chapter 3 and Rongbing Yang for her contribution to chapter 5.

Thanks also to my fellow chemistry postgraduates in NUI Galway, especially past and present members of the Aldabbagh group, for valued advice, discussions and keeping me sane.

Finally I must thank my family and friends for their continuous support and encouragement.

"If we knew what it was we were doing, it would not be called research, would it?"

- Albert Einstein

Abstract

Chapter 1 provides a general introduction to addition radical polymerizations and controlled/living radical polymerizations with an emphasis on nitroxide-mediated polymerization (NMP). The merits of supercritical carbon dioxide ($scCO_2$) as a polymerization medium are described, focusing on heterogeneous NMP systems.

Chapter 2 describes the work published in, *Macromolecules* **2009,** 43, 914-919. The point of particle nucleation or the critical degree of polymerization (J_{crit}) at which polymer chains become insoluble in the continuous medium ($scCO_2$) has been ascertained under a variety of experimental conditions for the precipitation NMP of styrene (St) and *tert*-butyl acrylate (*t*-BA), mediated by SG1. A simple graphical model has been developed and successfully employed, whereby J_{crit} can be predicted as a function of both target molecular weight and initial monomer loading. J_{crit} is shown to increase linearly with increasing pressure.

Chapter 3 details the work published in, *J. Polym. Sci. Part A: Polym. Chem.* **2011,** 49, 1856-1864. Chain transfer to solvent has been investigated in the conventional radical polymerization (RP) and NMP of *N*-isopropylacrylamide (NIPAM) in *N*,*N*-dimethylformamide (DMF) at 120 °C. The same chain transfer to solvent constant ($C_{tr,S}$) can account for the deviation of experimental molecular weight data from theoretical, in both conventional RP and NMP.

Chapter 4 gives an account of the work published in, *J. Polym. Sci. Part A Polym. Chem.* **2011,** 49, 1719-1723. The first controlled/living inverse suspension polymerization in $scCO_2$ is described. The NMP of NIPAM proceeded in the absence of stabilizer to high conversion with low polydispersity, affording a dry powder. The purification step entails washing with fresh $scCO_2$, and the technique thus completely avoids of the use of environmentally damaging volatile organic compounds.

Chapter 5 presents the work published in, *Eur. Poly. J.* **2012,** *doi.org/10.1016/j.eurpolymj.2012.04.011*. A new preparation of thermoresponsive poly(NIPAM) containing block copolymers, involving two successive heterogeneous controlled/living NMPs in $scCO_2$ is described. Precipitation NMPs in $scCO_2$ give functionalised macroinitiators (MIs), and a first report of the controlled/living NMP of *N*,*N*-dimethylacrylamide in $scCO_2$ is described. The MI initiates an inverse suspension NMP of NIPAM in $scCO_2$. Aqueous cloud point temperature analysis for AB block copolymers show a significant dependence on poly(NIPAM) chain length.

Abbreviations

AA	acrylic acid
AIBN	2, 2'-azobisisobutyronitrile
AN	acrylonitrile
AMRP	Aminoxyl-mediated radical polymerization
α	fractional monomer conversion
ATRP	atom transfer radical polymerization
b	block
b.p.	boiling point
CLRP	controlled/living radical polymerization
conv.	conversion
C_T	chain transfer constant
CTA	chain transfer agent
$C_{tr,M}$	chain transfer to monomer constant
DCM	dichloromethane
DMA	*N*,*N*-dimethylacrylamide
DMF	*N*,*N*-dimethyl formamide
DMS	dimethylsiloxane
DMSO	dimethyl sulfoxide
DP	degree of polymerization
DP_n	number average degree of polymerization
DPAIO	2,2-diphenyl-3-phenylimino-2,3-dihydroindol-1-iloxyl
Et	ethyl
f	initiator efficiency
f_{app}	apparent initiator efficiency
FDA	heptadecafluorodecyl acrylate
γ	gamma
g	gram
GPC	gel permeation chromatography
h	hour
Hz	hertz
[I]	initiator concentration

I_p	polydispersity index
inistab	polymeric initiator and stabilizer combined
J_{crit}	number average degree of polymerization at which precipitation occurs
K	equilibrium constant
k_{act}	rate constant for activation
k_c	rate constant for combination
k_d	rate constant for dissociation of an alkoxyamine
k_{deact}	rate constant for deactivation
k_{dec}	rate constant for decomposition of initiator
k_i	rate constant for initiation
$k_{i.th}$	rate constant for thermal self-initiation
k_p	rate constant for propagation
k_{ri}	rate constant for re-initiation
k_t	rate constant for termination
k_{tc}	rate constant for termination by combination
k_{td}	rate constant for termination by disproportionation
k_{tr}	rate constant for chain transfer
L	litre
LCST	lower critical solution temperature
[M]	monomer concentration
M	molar
MAA	methyl acrylamide
MA	methyl acrylate
MADIX	Macromolecular design via the interchange of xanthates
MCR	Mid-chain radicals
Me	methyl
mg	milligram
MI	Macroinitiator
mL	millilitre
μm	micrometer
mm	millimeter
MMA	methyl methacrylate
mmol	millimole
M_n	number average molecular weight

M_n(GPC)	number average molecular weight calculated by GPC
M_n(NMR)	number average molecular weight calculated by NMR
$M_{n,th}$	theoretical number average molecular weight
mol	mole
MPa	megapascal
MW	molecular weight
M_w	weight average molecular weight
MWD	molecular weight distribution
M_w/M_n	polydispersity
*n*BA	*n*-butyl acrylate
NIPAM	*N*-isopropylacrylamide
nm	nanometer
NMP	nitroxide mediated polymerization
NMR	nuclear magnetic resonance
4-oxo-TEMPO	4-oxo-2,2,6,6-tetramethylpiperidinyl-1-oxy
$P^{\bullet}$	propagating radical
Ph	phenyl
pK_a	$-\log_{10}$ of K_a (acid dissociation constant)
P(*M*)	number distribution
ppm	parts per million
PRE	persistent radical effect
P-T	polymeric alkoxyamine
$R^{\bullet}$	radical
R_{add}	rate of addition
RAFT	reversible addition fragmentation chain transfer
RDRP	reversible deactivation radical polymerization
R_i	rate of initiation
RI	refractive index
$R_{i,th}$	rate of thermal initiation
RP	radical polymerization
R_p	rate of polymerization
rpm	revolutions per minute
R_{pr}	rate of radical production
R_t	rate of termination

R_{tr}	rate of transfer
R-X	alkyl halide
s	second
SCF	supercritical fluid
$scCO_2$	supercritical carbon dioxide
SEM	scanning electron microscopy
SG1	*N*-*tert*-butyl-*N*-(1-diethylphosphono-2,2-dimethylpropyl) nitroxide
St	styrene
t	time
$T^{\bullet}$	nitroxide trap
$t_{1/2}$	half-life
t-BA	*tert*-butyl acrylate
TBAM	*tert*-butylacrylamide
TBP	*tert*-butyl peroxide
*t*Bu	*tert*-butyl
TEM	transmission electron microscopy
Temp.	temperature
TEMPO	2,2,6,6-tetramethylpiperidinyl-1-oxy
TFA	trifluoroacetic acid
T_g	glass transition temperature
THF	tetrahydrofuran
TIPNO	2,2,5-trimethyl-4-phenyl-3-azahexane-3-aminoxyl
UV	ultra violet
υ	kinetic chain length
VAc	vinyl acetate
VOC	volatile organic compound
wt. %	weight percent
w/*v*	weight per volume
$[X_i]$	concentration of a low molecular weight species to which chain transfer occurs

CHAPTER 1

GENERAL INTRODUCTION

1.1 Overview of Addition Chain Polymerization

It is estimated that 50% of all industrially manufactured polymers are produced by radical polymerization (RP).[1] This is because of numerous chemical and technical advantages RP has over other chain addition techniques such as anionic and cationic or coordination polymerization, which allow for many industrial applications. Chain addition polymerizations are almost always anti-Markovnikov because the generated active centre is stabilized by the substituent at the head part of the monomer. For chain growth polymerizations high molecular weight polymer is achieved at low conversions due to instantaneous rates of monomer addition or propagation. In contrast for a step growth polymerization (e.g. condensation) high conversion (>99%) of monomer is required before high MW polymer is obtained. RP is suitable for nearly all vinyl monomers such as ethylene, styrenes, (meth)acrylates, acrylamides, acrylonitriles, 1,3-dienes, vinyl chloride, vinyl alcohols and acrylic acids, and unlike anionic, and cationic polymerizations is not limited by the electronic nature of the vinyl monomer. The recognised disadvantages of anionic and cationic polymerizations are the low temperatures, scrupulous drying and purification of both monomers and solvents required, [2] the non-compatibility of monomer classes with the propagating chain [3] and the requirement for protecting groups (e.g. in the anionic polymerization of *N*-isopropylacrylamide, NIPAM,).[4] Conversion of NIPAM monomer to *N*-methoxymethyl-NIPAM to mask the acidic hydrogen, allows for anionic polymerization initiated by diphenylmethyllithium (Ph_2CHLi) in the presence of diethylzinc (Et_2Zn) in THF at -78 °C. Acidic hydrolysis of the methoxymethyl protecting groups after polymerization afforded poly(NIPAM) (Scheme 1.01).

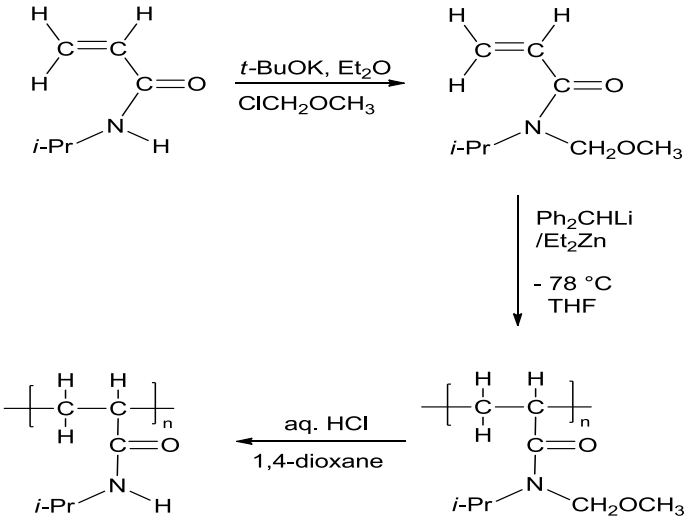

Scheme 1.01: Anionic polymerization of NIPAM

Coordination polymerization is used to produce commercial high density polyethylene (HDPE).[5] The advantage of the coordination polymerization, is the production of a linear isotactic polymer. The stereoselective polymer allows closer packing of the polymer chains, giving greater strengths and chemical resistance, over low density polyethylene (LDPE) produced by radical polymerization.[3] However coordination polymerization is of limited industrial use with only simple polyolefins, mainly poly(ethylene) and poly(propylene) derivatives of gaseous un-activated monomers prepared using this technology.

RP is compatible with several different reaction processes, such as solution, bulk and heterogeneous polymerizations, unlike other addition polymerizations that have to be carried out under specific conditions due to the reactivity of the active centre or sensitivity of the catalyst.[3] The monomer classes used in this thesis are styrene, acrylates and acrylamides, and the introduction focuses on the conventional radical polymerization and controlled/living radical polymerization (CLRP) of these monomers (in particular nitroxide-mediated polymerizations, NMPs).

1.2 Conventional Radical Polymerization

A conventional radical polymerization consists of initiation, propagation, termination and chain transfer events. Initiation takes place in two stages, firstly peroxide (e.g. *tert*-butyl peroxide, TBP) or azo-initiator (e.g. 2,2'-azoisobutyronitrile, AIBN) undergoes thermolytic decomposition to produce two initiating radicals (Scheme 1.02).

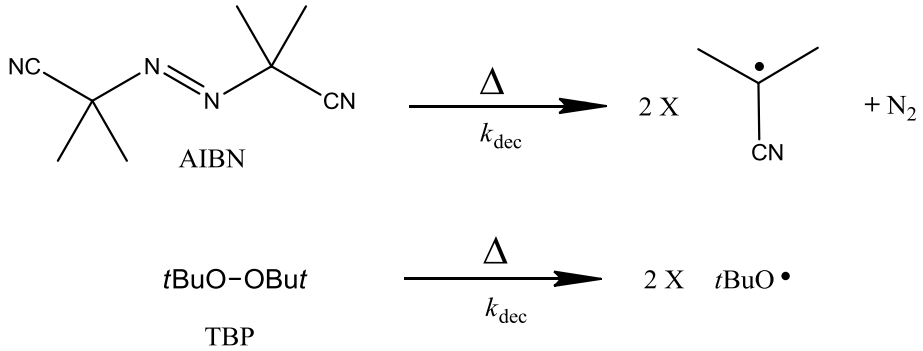

Scheme 1.02: Thermal decomposition of AIBN and TBP.

The rate constant of initiator decomposition is k_{dec} and the rate of radical production (R_{pr}) is expressed in terms of Equation 1.01.

$$R_{pr} = 2fk_{dec}[\mathrm{I}] \qquad (1.01)$$

Where [I] is the concentration of initiator, 2 denotes the decomposition of the initiating molecule into 2 identical radicals and f represents initiator efficiency. The f value is nearly always considered to be less than unity due to wastage of initiator derived radicals in side-reactions. A small portion of the 2-cyanoisopropyl radicals, ($(CH_3)_2(CN)C^{\bullet}$), produced from AIBN decomposition can disproportionate within the solvent cage to form methacrylonitrile, ($CH_2{=}CCH_3(CN)$).[6, 7] Values of f for peroxides tend to be closer to unity because of the higher reactivity of oxygen centred radicals and negligible solvent cage effects. In the case of TBP, recombination of the generated radicals reforms the initiator therefore having no effect on f.[6] TBP is a useful initiator for RP at higher temperatures, as indicated by the 10 hour initiator half-live which is achieved for AIBN at 65°C and TBP at 125°C.[8]

The second step of initiation involves the addition of an initiator derived radical onto a vinyl monomer (Scheme 1.03).

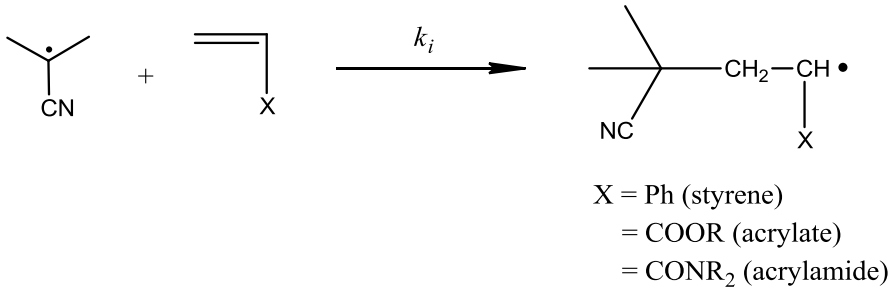

Scheme 1.03: Addition of an initiator radical onto monomer

The rate of initiator radical addition R_{add} is expressed as shown in Equation 1.02.

$$R_{add} = k_i[\mathrm{R}^{\bullet}][\mathrm{M}] \qquad (1.02)$$

Where k_i is the rate constant for the addition step, [$R^{\bullet}$] is the concentration of primary initiator radicals and [M] is the concentration of monomer present. Typically $k_{dec} << k_i$ making the rate of initiator decomposition the rate determining step and the rate of initiation can be taken as Equation 1.01.

Initiation for some monomers can also occur by a purely thermal reaction. Thermal ("spontaneous") initiation studies of acrylates and acrylamides have been reported, but it is unlikely that they have a true self-initiation mechanism.[9-12] The observed initiation without added initiators is thought to be caused by impurities present (speculated to be peroxides [13]) that cannot be removed by rigorous freeze thaw degas techniques.[14] Styrene on the other hand is know to undergo thermal initiation by probable formation of the Mayo dimer by a Diels-Alder [4+2] cycloaddition with subsequent chain transfer to monomer to form initiating radicals, as shown in Scheme 1.04.[15-17]

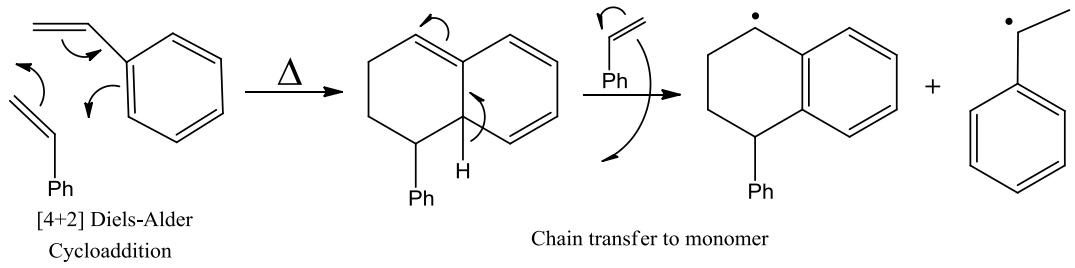

Scheme 1.04: Thermal self-initiation of styrene

Propagation involves propagating radicals ($P^{\bullet}$) successively adding to further monomer increasing the polymer chain length; this can take place hundreds to thousands of times (Scheme 1.05) until a random bimolecular chain termination occurs.

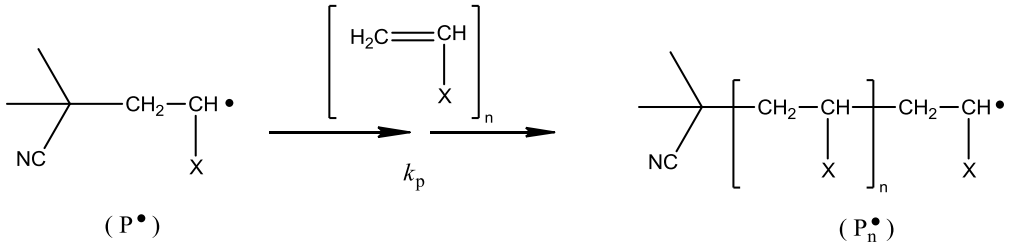

Scheme 1.05: Propagation

The rate constant for propagation, k_p, is large (typically $k_p \approx 10^2$–10^4 L mol^{-1} s^{-1})[18] for most monomers and is assumed to be independent of chain length when the degree of polymerization (*DP*) is greater than 20.[9, 19, 20] Propagation rate coefficients for radical polymerization can be accurately determined by pulsed-laser-initiated polymerization (PLP) coupled with size exclusion chromatography (SEC).[21]

The size of k_p is governed by the nature of the monomer molecule and the reactivity of the propagating radical. Styrene has a relatively low k_p, in comparison to other monomer classes (Table 1.01) due to the fact that styrene monomer is a relatively reactive monomer but its corresponding radical is efficiently resonance stabilized by the adjacent phenyl group. The rate of propagation, R_p, can be expressed as shown in Equation 1.03, where [P$^\bullet$] is the propagating radical concentration.

$$R_p = \frac{-d[\mathrm{M}]}{dt} = k_p[\mathrm{P}^\bullet][\mathrm{M}] \qquad (1.03)$$

Table 1.01: Propagation rate constants (k_p) of selected monomers

Monomer	**k_p (L mol^{-1} s^{-1})**	**Temp (°C)**
Styrene	341[22]	60
tert-Butyl acrylate	22500[23]	38.8
N-Isopropylacrylamide	20000[24]	20
N,*N*-dimethylacrylamide	15000[25]	25

Termination is the removal of propagating radicals by combination or disproportionation to form unreactive (dead) polymer chains (Scheme 1.06).

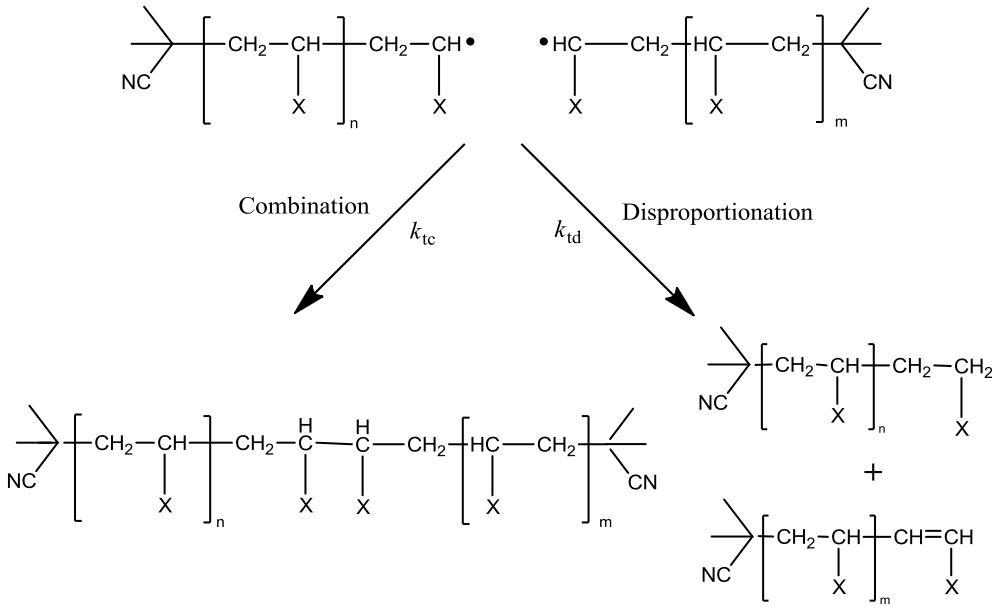

Scheme 1.06: Combination and disproportionation of two polymer chains

Bimolecular combination is the most common form of termination for most vinyl monomers (e.g. styrene,[26] acrylonitrile[27] and methyl acrylate[28]) and occurs when any two radical species come together to form one larger molecule, thus leading to high molecular weight polymer. Disproportionation is observed more readily when the propagating radical is sterically hindered (i.e. α-methyl vinyl monomers, e.g. methyl methacrylate) [26] and occurs when one radical abstracts a β-hydrogen from another radical species. Disproportionation results in one saturated and one unsaturated product, without changing the molecular weight of the polymer chain (also see chain transfer discussion below). The overall rate constant for termination (k_t) is given by $k_t = k_{tc} + k_{td}$. Equation 1.04 shows the overall rate of termination expression (R_t), 2 denotes the removal of two propagating radicals in each termination event.

$$R_t = \frac{-d[\mathrm{P}^\bullet]}{dt} = 2k_t[\mathrm{P}^\bullet]^2 \qquad (1.04)$$

In a stationary state polymerization (or where steady state kinetics apply), the radical concentration remains essentially constant. After a short time (seconds) a steady state equilibrium is reached, where the rate of initiation is approximately equal to the rate of termination and the population of propagating radicals, [P$^\bullet$] remains constant, *i.e.* R_i and R_t are equal as shown in Equation 1.05.

$$R_i = R_t = 2k_t[\mathrm{P}^\bullet]^2 \qquad (1.05)$$

In a conventional radical polymerization the steady state equilibrium is set up because the rate of termination is dependent on the [P$^\bullet$], which is governed by R_i, and will continue until the initiator is used up. Insertion of Equation 1.01 into 1.05 provides Equation 1.06 from which [P$^\bullet$] can be determined by rearrangement to Equation 1.07.

$$2fk_{dec}[\mathrm{I}] = 2k_t[\mathrm{P}^\bullet]^2 \qquad (1.06)$$

$$[\mathrm{P}^\bullet] = \sqrt{(2fk_{dec}[\mathrm{I}]/2k_t)} \qquad (1.07)$$

Propagation involves a large number of monomer molecules per chain, whereas initiation consumes only one, therefore R_p, for all practical purposes is equivalent to the rate of polymerization. Insertion of Equation 1.07 into Equation 1.03 yields the fundamental expression for the rate of a radical polymerization under steady state conditions (Equation 1.08).

$$R_p = k_p \sqrt{\left(\frac{2fk_{dec}[\mathrm{I}]}{2k_t}\right)}[\mathrm{M}] \qquad (1.08)$$

As R_p is equivalent to the rate of monomer consumption under steady state conditions a linear first order plot of monomer consumption ($\ln([\mathrm{M}]_0/[\mathrm{M}])$ versus time signifies that $[\mathrm{P}^\bullet]$ is remaining constant during the polymerization.

In the absence of chain transfer events the instantaneous maximum attainable average degree of polymerization (*DP*) for RP is determined by the number of monomer units incorporated into each chain before termination occurs and is approximately equal to $\delta(R_p/R_i)$ (where δ represcents the contribution of disproportionation to the overall termination process and is calculated by $\delta = k_{td}/k_{td} + k_{tc}$) which is represented in Equation 1.09.

$$DP = \frac{2}{(1+\delta)}\frac{R_p}{R_i} = \frac{k_p[\mathrm{M}]}{(1+\delta)k_t[\mathrm{P}^\bullet]} \qquad (1.09)$$

Chain transfer is a reaction involving the transfer of the polymer active radical ($\mathrm{P}^\bullet$) to another molecule or chain transfer agent (CTA) to yield a dead polymer and a small radical capable of initiating a new polymer chain, Scheme 1.07. Where, k_{tr} and k_{ri} are the rate coefficients for chain transfer and re-initiation respectively.

$$\mathrm{P}_n^\bullet + \mathrm{CTA\text{-}H} \xrightarrow{k_{tr}} \mathrm{P}_n\text{-H} + \mathrm{CTA}^\bullet$$

$$\mathrm{CTA}^\bullet + \mathrm{M} \xrightarrow{k_{ri}} \mathrm{P}^\bullet$$

Scheme 1.07: Chain transfer

Chain transfer can occur to most reactants in a polymerization via hydrogen abstraction (e.g. solvent, monomer, initiator, polymer or added CTA). It can be inherent of the

system or introduced intentionally to control average MW or introduce polymer end-functionality. Chain transfer does not change [P$^{\bullet}$], so the rate of polymerization (monomer consumption) remains the same. For chain transfer to low MW species, the polymer chain length is reduced, while chain transfer to polymer will result in polymer branching and a higher MW polymer. For ideal chain transfer, the kinetic chain length (υ), defined as being the number of molecules of monomer consumed by an initiator radical, should be identical in the presence and absence of a transfer agent. For steady state polymerization $R_i = R_t$ and υ can be expressed in Equation 1.10.[29]

$$\upsilon = \frac{R_p}{R_i} = \frac{R_p}{R_t} \qquad (1.10)$$

In the absence of transfer reactions, *DP* will be equal to υ assuming termination by disproportionation only and twice υ assuming termination by combination only. Where chains generated by transfer must be taken into account, the average chain length will be reduced and *DP* can be calculated using Equation 1.11.

$$DP = \frac{R_p}{(R_{td} + R_{tc}/2) + R_{tr,M} + R_{tr,I} + R_{tr,s} + R_{tr,CTA}} \qquad (1.11)$$

Where $R_{tr,M}$, $R_{tr,I}$, $R_{tr,S}$ and $R_{tr,CTA}$ are the rates of chain transfer to monomer, initiator, solvent and added chain transfer agent respectively.

1.3 Controlled/Living Radical Polymerizations (CLRPs)

1.3.1 Introduction

The term living polymerization is defined as the removal of all chain breaking reactions such as termination and chain transfer, allowing living polymers to continue to grow provided monomer is available. This was first coined for an anionic polymerization by Szwarc.[30] The living characteristic refers to end-group control and facilitates the production of block copolymers, but does not indicate any specific control over MW or formation of narrow molecular weight distribution (MWD) polymer. Living ionic polymerizations usually require the rigorous purification of reagents, low temperatures, and exclusion of water. Since the early 1990s ionic polymerizations have been superseded by the more versatile controlled/living radical polymerization (CLRP) techniques. In conventional RP the process of initiation, propagating and termination takes place for each $P^{\bullet}$ typically in the order of less than 1 s, thus it is impossible to get narrow MWD polymer. CLRPs are more controllable since the life time of propagating radicals is much longer, usually hours, allowing targeted MW and narrow MWDs to be achieved, as well as chain extension to give block copolymers.

CLRP techniques achieve controlled/living character by establishing an activation-deactivation equilibrium by rapid reversible deactivation of propagating radicals ($P^{\bullet}$), which is required to minimize the contribution of irreversible bimolecular termination. Common features of CLRP include:

- *First order kinetics with respect to monomer*

  The natural logarithmic function of monomer concentration, $\ln([M]_0/[M])$, is a linear function with time. This is a general function of steady state kinetics. In CLRP it depends on condition that initiation is fast, with all chains beginning to grow at close to t_0 and a lack of termination allowing $[P^{\bullet}]$ to remain constant.

- *Linear increase of M_n or degree of polymerization (DP) with conversion*

  This indicates a constant number of propagating chains are generated at sufficient speed that all chains begin to grow simultaneously and no chain transfer occurs. Monomer consumption is directly proportional to M_n.

- *Narrow MWD*

While this is desired, narrow MWD is not a prerequisite of a living polymerization, but is a requirement for CLRP. Four conditions must be met to achieve a narrow MWD

- The rate of initiation is greater than or equal to the rate of propagation. This allows simultaneous growth of all polymer chains.
- The activation, deactivation reactions of the mediating species is faster than propagation. This ensures an equal probability of all active chains to react with monomer.
- There must be no significant chain transfer or termination.
- The rate of de-propagation is substantially lower than propagation i.e. polymerization is irreversible.

$$I_p = \frac{DP_w}{DP_n} = \frac{M_w}{M_n} = 1 + \frac{DP_n}{(DP_n + 1)^2} \qquad (1.12)$$

Equation 1.12[31, 32] shows that the polydispersity index (I_p) decreases as the polymer chain length increases.

- *Long lived polymer chains with preserved end-functionality.*

A living polymerization is achieved by the elimination of irreversible chain transfer and termination. Consequently, all the chains retain their active centres after the full consumption of the monomer. Propagation can be resumed upon introduction of additional monomer to form block copolymers.

CLRPs are based on dissociation-combination, atom transfer and degenerative chain transfer mechanisms/techniques. The most widely used CLRPs using the first two techniques are nitroxide-mediated polymerization (NMP) [33, 34] and atom transfer radical polymerization (ATRP) [35, 36] respectively. The most common degenerative transfer methodologies are reversible addition-fragmentation chain transfer (RAFT) [37, 38] and macromolecular design via the interchange of xanthate (MADIX).[39]

By definition all CLRP methods are not entirely living systems because termination to some degree inevitably occurs. It has been argued that although these systems do not produce 100% living polymer they do result in a substantial proportion

of the product being living and capable of chain extension. The use of the term "living" should be applicable to a process which succeeds in producing living polymer and not be concerned with the fraction of living chains that might be present.[40]

The International Union of Pure and Applied Chemistry (IUPAC) have offered guidelines for alternative terminology to be used for these processes.[41] Reversible deactivation radical polymerization (RDRP) has been recommended in place of CLRP. Aminoxyl-mediated radical polymerization (AMRP) is the term proposed in place of NMP, as the term nitroxide is discouraged. While their recommendations may become standard terminology in the future, they are currently not used to any visible degree and all use of the term controlled/living within this text denotes polymerization reactions that take on much of the character of living polymerizations, even though some termination unavoidably takes place.

1.3.2 Nitroxide-Mediated Radical Polymerization (NMP)

Nitroxides are *N,N*-disubstituted NO persistent radicals with a delocalized unpaired electron, resonance stabilized between the N and O atoms as shown in Scheme 1.08.

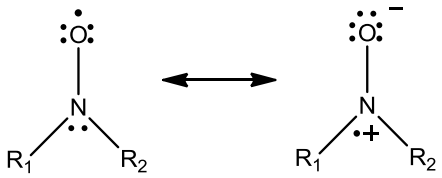

Scheme 1.08: Nitroxide: resonance structures.

Nitroxides ($T^{\bullet}$) act as effective traps for carbon-centered radicals and can control radical polymerization by trapping $P^{\bullet}$ to form the corresponding dormant alkoxyamine (P-T), as outlined in scheme 1.09, which becomes reversible at elevated temperatures.

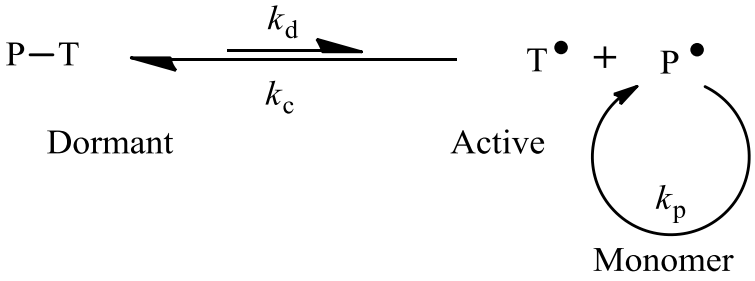

Scheme 1.09: Reversible dissociation of polymeric alkoxyamine (P-T)

At a suitably high temperature, the formed P-T bond becomes sufficiently labile with a rate constant for dissociation (k_d). In the dissociated or active state the polymeric radical can propagate by addition of monomer but is invariably trapped or recombined with the $T^{\bullet}$ to give back the dormant species, P-T. The rate constant of combination (k_c) is several orders of magnitude greater than k_d leading to large equilibrium constants, K in Equation 1.13. The K value defines the established relationship between active and dormant states, whereby P-T is in a higher concentration than $P^{\bullet}$. A low population of active propagating chains is maintained throughout the polymerization, thus immensely reducing (ideally eliminating) the probability of irreversible termination reactions occurring. In this thesis, control/living character is achieved in the presence of an excess of $T^{\bullet}$ that ensures the equilibrium resides towards the dormant state.

$$K = \frac{k_d}{k_c} = \frac{[P^{\bullet}][T^{\bullet}]}{[P-T]_0} \qquad (1.13)$$

TEMPO (2,2,6,6-tetramethylpiperidine-1-oxyl, Figure 1.01) was the first nitroxide used to establish a controlled/living NMP.[42] TEMPO can however only efficiently control the polymerization of styrene based monomers and some styrene copolymerizations.[42-44] TEMPO is inadequate at controlling the polymerization of other vinyl monomers such as, acrylates, acrylamides and acrylonitrile.[1, 33, 45] The incompatibility is mainly due to the relatively strong covalent bond in the derived alkoxyamine, giving a low $[P^{\bullet}]$ and an early build up of $T^{\bullet}$ due to termination reactions being highest in propensity at the start. In the case of styrene, the thermal self-initiated polymerization produces new $P^{\bullet}$ throughout the polymerization to reduce the [TEMPO] allowing a slow polymerization to continue and reach high conversions.[15, 43, 46] The rate of thermal self-initiation ($R_{i,th}$) of St is expressed by Equation 1.14,

$$R_{i,th} = k_{i,th}[St]^3 \qquad (1.14)$$

where $k_{i,th}$ is the rate for thermal self-initiation (at 120 °C $k_{i,th}$ (St) = 1.10 x 10^{-10} M^{-2} s^{-1}). The styrene self-initiation mechanism involves three monomer molecules and is generally accepted to be a third order reaction with respect to monomer concentration as demonstrated by Hui and Hamielec[47] and Ito[48] (see Scheme 1.04). Stationary kinetics applies almost immediately for a TEMPO-mediated controlled/living polymerization

because of the small *K* value of the styrene/TEMPO system. The steady state is determined by the balance of thermal initiation and termination rates. The R_p value for a TEMPO system is equal to that of the thermal (nitroxide-free) system, according to Equation 1.15, which is derived by inserting the steady state approximation of $P^{\bullet}$ by thermal initiation into the rate expression.

$$R_p = k_p[P^{\bullet}][M] = k_p\sqrt{\left(\frac{R_{i,th}}{k_t}\right)}[M] \qquad (1.15)$$

Georges et al, early work achieved low polydispersity polystyrene from a TEMPO-mediated bulk polymerization at 130 °C. These polymerizations required long times (≈ 70 h) to achieve high conversions (> 85%). Under similar conditions using TEMPO as mediating agent the controlled polymerization of acrylates could not be achieved. A 4-oxo-TEMPO derivative was used in the XEROX group to control the polymerization of *n*-butyl acrylate at 145 °C. The achieved polydispersities of 1.40-1.67 at ≈ 60% conversion leaves uncertainty as to the effectiveness of the claimed control/livingness of the produced polymer. Other cyclic nitroxides have been used to successfully control the polymerization of styrene at 125-145 °C and butyl acrylate at 145-155 °C.[33, 49-52]

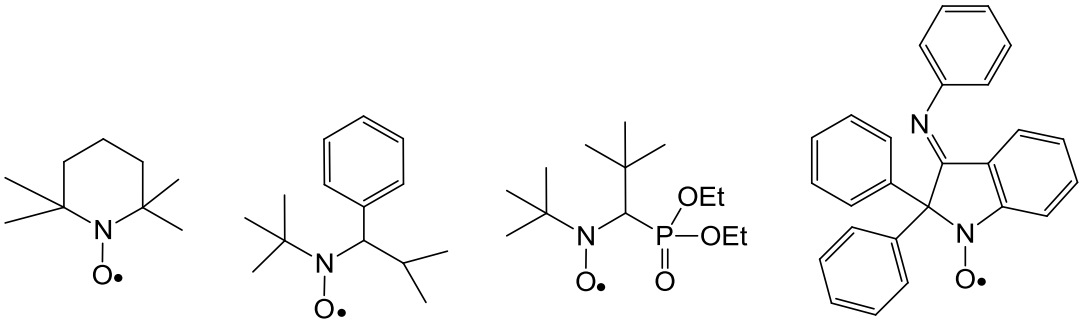

TEMPO TIPNO SG1 DPAIO

Figure 1.01: Most widely used nitroxides for NMP and DPAIO used with MMA

Following the initial control achieved using TEMPO and other first generation cyclic nitroxides, new second generation acyclic nitroxides were introduced, in order to extend the range of monomers amenable to NMP such as acrylates[53-56] and acrylamides[54, 57-59]. Second generation nitroxides, 2,2,5-trimethyl-4-phenyl-3-azahexane-3-aminoxyl (TIPNO; Figure 1.01)[54] and *N*-*tert*-butyl-*N*-[1-

diethylphosphono-(2,2-dimethylpropyl)] nitroxide (SG1, also known as DEPN, Figure 1.01)[53] are the most widely used and versatile acyclic nitroxides in this class. TIPNO[54] and SG1[53, 55, 60, 61] can control the polymerization of a wider range of monomers than TEMPO because of the more highly sterically hindered nature of the alicyclic nitroxide and the presence of an α-hydrogen adjacent to the nitroxide moiety. The α-hydrogen makes these nitroxides more labile than TEMPO, so they can degrade during NMPs. This can influence the rate and control of polymerizations, particularly with long polymerization times associated with some nitroxide-mediated polymerizations.[62, 63]

Nitroxide	K(M)	k_d (s^{-1})	k_c (M^{-1} s^{-1})
TEMPO	2.1×10^{-12}	5.2×10^{-4}	2.5×10^{8}
SG1	1.0×10^{-9}	5.3×10^{-3}	4.6×10^{6}
TIPNO	4.0×10^{-10}	3.3×10^{-3}	8.2×10^{6}

Table 1.02: Equilibrium constant (K), rate constant of dissociation (k_d) and rate constant of combination (k_c)[64] for the alkoxyamines, 1-phenylethyl-TEMPO, 1-phenylethyl-SG1 and 1-phenylethyl-TIPNO at 120 °C (Figure 1.02).

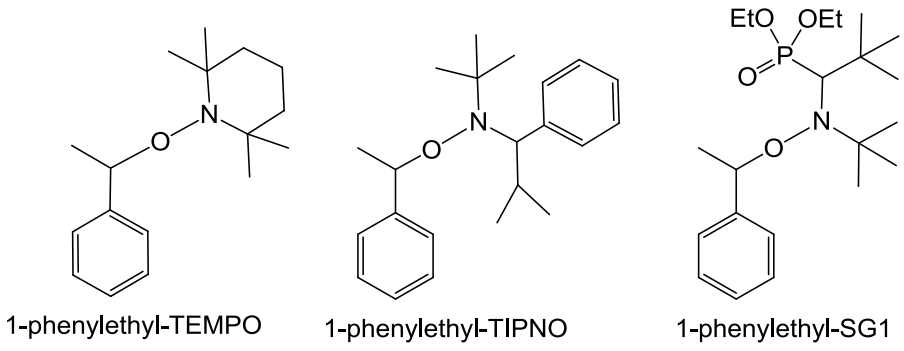

1-phenylethyl-TEMPO 1-phenylethyl-TIPNO 1-phenylethyl-SG1

Figure 1.02: Alkoxyamines used for NMP

The K values for SG1 and TIPNO alkoxyamines are similar in magnitude with larger k_d and smaller k_c values than the corresponding TEMPO alkoxyamines (Table: 1.02). The relatively large K value for SG1 compared to TEMPO is due mainly to its particularly low k_c value, resulting predominantly from the extent of steric hindrance around the NO moiety. The large K value can result in SG1-mediated polymerizations taking a relatively long time to reach a steady state (8.3 h, for styrene polymerization).

When NMPs are initiated by a SG1-alkoxyamine with no added nitroxide at $t = 0$ the rate of polymerization follows power-law kinetics expressed by Equation 1.16.[45]

$$\ln\left(\frac{[\mathrm{M}]_0}{[\mathrm{M}]}\right) = \left(\frac{3k_p}{2}\right)\left(\frac{K[\mathrm{PT}]_0}{6k_t}\right)^{\frac{1}{3}} t^{\frac{2}{3}} \qquad (1.16)$$

From Equation 1.16 it is clear that rate of monomer conversion shows a 2/3 order dependence on time and a 1/3 order dependence on alkoxyamine concentration, provided external (thermal or conventional initiator) initiation is negligible. In contrast, if the system includes a large excess of $[\mathrm{T}^\bullet]_0$, ($[\mathrm{T}^\bullet]_0 >> (3k_tK^2[\mathrm{P\text{-}T}]_0^2t)^{1/3}$), Equation 1.17 can now be applied, with $\ln[\mathrm{M}]_0/[\mathrm{M}]$ first-order with respect to t as in a stationary-state system. According to Equation 1.17, R_p is independent of [P-T] and $[\mathrm{T}^\bullet]$ for a given ratio of $[\mathrm{P\text{-}T}]/[\mathrm{T}^\bullet]$.

$$\ln\left(\frac{[\mathrm{M}]_0}{[\mathrm{M}]}\right) = \left(\frac{k_pK[\mathrm{PT}]_0}{[\mathrm{T}^\bullet]_0}\right)t \qquad (1.17)$$

The addition of a large excess of free nitroxide for a NMP with large K value greatly reduces the time required to reach a stationary state of $\mathrm{T}^\bullet$ and by extension $\mathrm{P}^\bullet$.[45] The use of these second generation nitroxides has resulted in the controlled polymerization of a wide range of monomers, including St, [54-56, 65-69] acrylates, [53-56, 63, 70] acrylic acid,[71] acrylonitrile,[54, 72] 1,3-dienes[73] and acrylamides.[54, 57-59, 62, 74-79]

A notable obstacle of NMP is the control of the polymerization of methacrylic monomers such as methyl methacrylate (MMA). These polymerizations undergo significant disproportionation reactions between a nitroxide radical and the propagating methacrylic radicals. The extent of the disproportionation reaction is highly dependent on $[\mathrm{T}^\bullet]$.[80, 81] Alkoxyamines based on the heavily conjugated nitroxide, 2,2-diphenyl-3-phenylimino-2,3-dihydroindol-1-iloxyl (DPAIO) has been reported to mediate the NMP of MMA up to 80% conversion with $M_w/M_n \approx 1.4$ at 100 °C.[82] The poly(MMA)-DPAIO system has increased k_d and decreased k_c values compared to SG1, but the greatly reduced K is incompatible with other vinyl monomers (e.g. styrene, acrylates). The lack of disproportionation is probably due to a deactivated nitroxyl radical in conjugation with the adjacent benzene moiety of DPAIO. Alternatively Charleux et al

controlled the NMP of MMA using a SG1 based alkoxyamine with a small amount (2.2-8.8 mol %) of a suitable co-monomer.[83, 84] The inclusion of a co-monomer with a low *K* value (such as St or acrylonitrile) greatly reduced the overall *K* for the system, leading to a high proportion of living polymer with MMA-comonomer-SG1 chain-end structure.[83-85]

1.3.3 Atom transfer radical polymerization (ATRP)

In 1995, Matyjaszewski[86] and Sawamoto[87] independently reported a new CLRP method called ATRP, shown in Scheme 1.10. ATRP has been successfully used to control an wide array of monomers, including styrenes, (meth)acrylates, (meth)acrylamides, acrylonitrile and 1,3-dienes.[1]

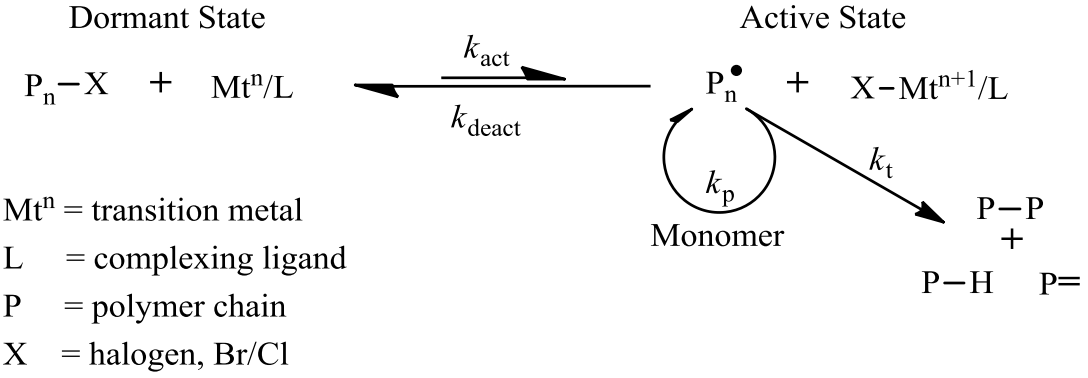

Scheme 1.10: General mechanism for ATRP

ATRP is a multi-component system incorporating, monomer, initiator (with a transferable (pseudo) halogen) and a catalyst (a transition metal species with a suitable ligand). The initiator usually a labile alkyl halide undergoes fast homolytic fission upon reduction by the metal species capable of increasing its oxidation number and complexing with ligand (L). The formed metal complex (X-Mt^{n+1}-L) is then reversibly deactivated upon reduction with $P^\bullet$.[88, 89] The $P^\bullet$ can as per conventional radical polymerization propagate with vinyl monomer or undergo a termination reaction with another $P^\bullet$, alternatively it can also reversibly deactivate to form a dormant halide capped polymer chain (P-X) and the original metal complex (Mt^n-L). *DP* is determined by the concentration of alkyl halide initiator relative to monomer, Equation 1.18.

$$DP = \frac{\alpha[\mathrm{M}]}{[\text{Alkyl halide}]_0} \qquad (1.18)$$

Teodorescu and Matyjaszewski reported the polymerization of various acrylamides (i.e. *N*,*N*-dimethylacrylamide (DMA), *N*-*tert*-butylacrylamide (TBAM) and *N*-(2-hydroxypropyl)methacrylamide (HPMA)) by ATRP using CuBr. Conversions remained low for all monomers after long polymerization times (45 h) at temperatures of 90 °C and 110 °C.[90] Higher conversions but uncontrolled polymerizations indicated by M_n being much greater than $M_{n,th}$ and high polydispersities were obtained at 90 °C, when using 1,4,8,11-tetramethyl-1,4,8,11-tetraazacyclotetradecane (Me_4Cyclam) as the ligand. ATRP of (meth)acrylamides is thus not a controlled process, although using the Me_4Cyclam-based catalyst system and macroinitiators prepared by ATRP, poly(methyl acrylate-*b*-*N*,*N*-dimethylacrylamide) (M_n = 48,600, M_w/M_n = 1.33) and poly(butyl acrylate-*b*-*N*-(2-hydroxypropyl)methacrylamide) (M_n = 34,000, M_w/M_n = 1.69) block copolymers were synthesized.

Another major limitation for ATRP is the stoichiometric amounts of metal catalyst required to sufficiently control polymerizations and their subsequent removal from the polymer product. More recently, atom transfer techniques that reduce the amount of metal salt catalyst used, called initiators for continuous activator regeneration (ICAR), [91] activators regenerated by electron transfer (ARGET), [92] and single-electron transfer living radical polymerization (SET-LRP), [93] have been popularised. ICAR works by using conventional radical initiators to slowly and continually reduce and regenerate the metal activators that accumulate in the reaction due to irreversible termination.[91] This increases the rate of polymerization and lowers the amount of necessary metal catalyst required under normal conditions to <50 ppm, while maintaining control over MW and MWD. ARGET employs a large excess of a carefully selected reducing agent relative to metal compound to continually generate the activating agent, minimising the amount of catalyst required.[92] In SET-LRP it is proposed that elemental copper ($Cu^{(0)}$) is oxidised to a $Cu^{(I)}$ intermediate activating the polymerization.[93] Spontaneous disproportionation of the intermediate in dipolar aprotic solvents e.g. water, alcohols, [94] generates $Cu^{(II)}$ which is needed to deactivate the propagating chain, completing the polymerization cycle. The $Cu^{(0)}$ species used in SET-LRP is significantly more reactive than the $Cu^{(I)}$ used in other techniques that it is only required in ppm amounts.

1.3.4 Reversible addition-fragmentation chain transfer (RAFT)

RAFT[37] was first developed by CSIRO[95] in 1998, making it the youngest of the 3 major CLRP techniques. Macromolecular design via interchange of xanthate (MADIX) is a specific type of process which differs from RAFT only by the type of mediator used. MADIX was reported by Zard et al [96] at almost the same time as RAFT. Since MADIX and RAFT are based on the same mechanism, except the former uses xanthates, RAFT will be used throughout this thesis to describe both techniques. RAFT is similar to NMP and ATRP in that it works by reversible deactivation of propagating radicals and formation of equilibria between active and dormant states, but the mechanism operates under very different principles. In theory if the selected RAFT agent behaves as an ideal chain transfer agent the reaction kinetics will be comparable to those of a conventional radical polymerization, determined simply by the equilibrium between initiation and termination. Control is achieved by inclusion of a suitable thiocarbonylthio compound (RAFT agent Figure 1.03) into a conventional RP mixture. After conventional initiation the propagating radical adds to the RAFT agent, followed by fragmentation of the leaving group (R), giving rise to a polymeric macro-RAFT and a new radical ($R^{\bullet}$) (Scheme 1.11).

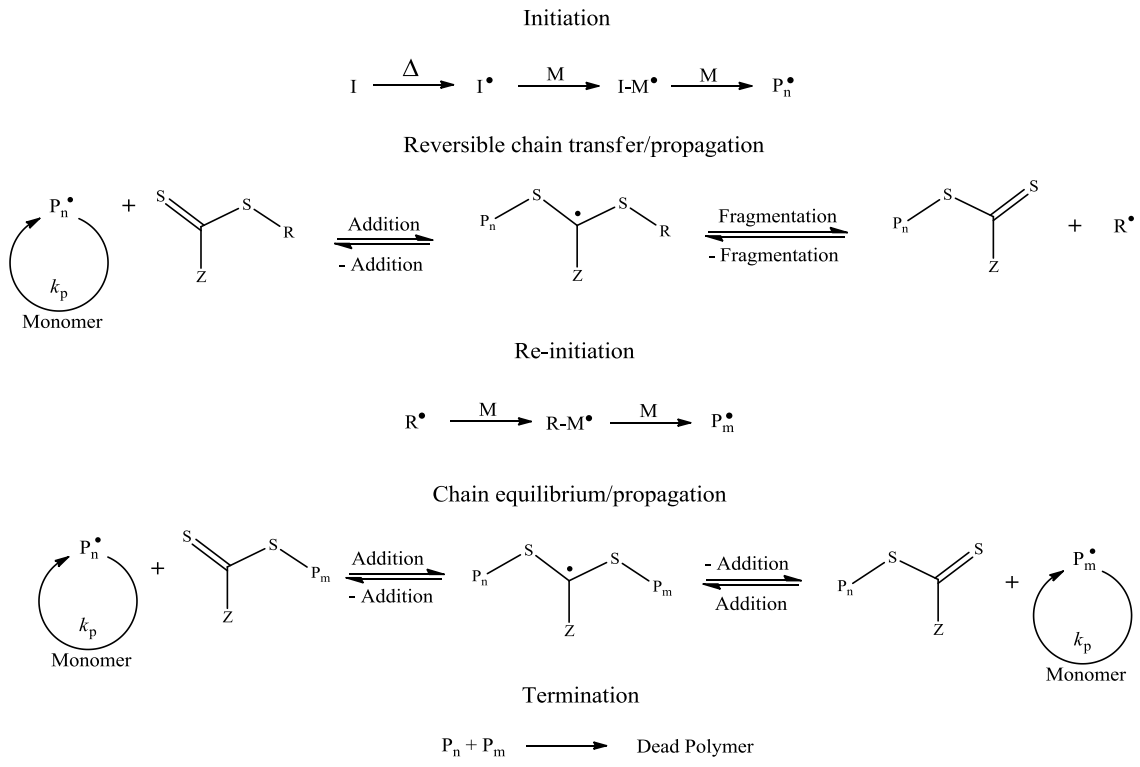

Scheme 1.11: General mechanism for RAFT polymerization

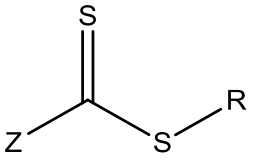

RAFT Agent	Z	R	Monomers
dithioesters	Ph	$C(Me)_2Ph$	MA, methacrylamide
trithiocarbonates	S(ME)	$HC(Ph)CO_2H$	St, acrylamide, acrylate
dithiocarbamates	$N(Et)_2$	CH_2Ph	VAc, vinyl amide
xanthate	OEt	$C(Me)_2CN$	VAc

Figure 1.03: Different examples of RAFT (and MADIX) agents

The unique characteristic of a RAFT polymerization compared to conventional RP is the sequence of addition and fragmentation equilibria achieved. The rate of addition of the propagating chain to the RAFT agent is influenced by the nature of Z, which can activate or deactivate the thiocarbonyl double bond to radical addition. The rate is increased when Z = Ph (dithioesters) or S(Me) (trithiocarbonates) and lower when Z = OEt (xanthates) or $N(Et)_2$ (dithiocarbamates).[97] Canonical forms of xanthate and dithiocarbamate (Figure 1.04) help to explain the lower activity of the thiocarbonyl double bond, through delocalization of the lone pairs on O and N. This lowers the rate of addition onto the sulfur atom, which forms an un-stabilized tertiary radical intermediate leading to rates of β-fragmentation which compete with higher monomer k_p. This makes them suitable for the polymerization of deactivated monomers such as VAc.[97, 98] The R group must also be a good radical leaving group relative to the attacking polymeric chain and capable of initiating a new polymer chain.

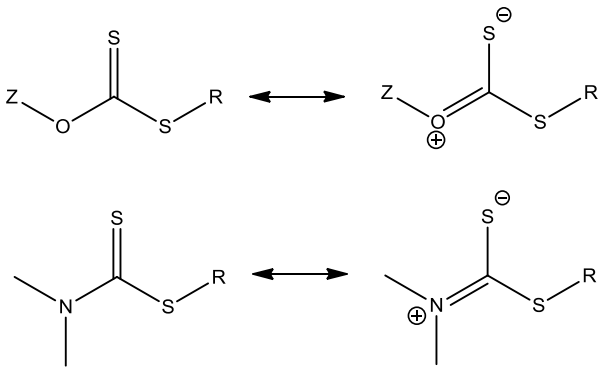

Figure 1.04: Canonical forms of xanthate and dithiocarbamate

The equilibrium between the active propagating species and the dormant polymeric RAFT agent must be established rapidly at the start of polymerization to provide all chains an equal probability to grow (Scheme 1.11). The living macro-RAFT agents are retained at the end of the polymerization and can continue to polymerize with new monomer. Block copolymers can be prepared by sequential polymerization of different monomer but the order in which the individual blocks are produced is very important. The monomer with the highest transfer rates towards the RAFT agent must be polymerized first to completion, to avoid inefficient blocking when chain extended with monomers with lower transfer rates. E.g. To make a block copolymer of MMA and St the MMA block must be made first. Equation 1.19, shows the relationship between *DP* and the concentration of the RAFT agent ([RAFT]), where α is the fractional conversion of monomer.

$$DP = \frac{\alpha[\mathrm{M}]}{[\mathrm{RAFT\ Agent}]} \qquad (1.19)$$

RAFT polymerization is possibly the most versatile of CLRP methods because it can effectively polymerize a large number of vinyl monomers (e.g. with a range of functional groups OH, NR_2, COOH, $CONR_2$, SO_3H). However each polymerization system requires very careful design/selection of RAFT agent and more than one agent may be required for block copolymer synthesis.[98]

1.4 Significance of Supercritical Carbon Dioxide ($ScCO_2$)

A supercritical fluid (SCF) is defined as a substance above its critical pressure and temperature (critical point, Figure 1.05). Above its critical point CO_2 demonstrates gas-like diffusivity, with liquid-like density. $ScCO_2$ has a more accessible critical point of 31.1 °C and 7.38 MPa compared to other SCF. Water would be a safe alternative but its critical point is far from ideal at 374.2 °C and 22.05 MPa.[99] A widely utilised industrial application of $scCO_2$ is in the dry cleaning industry [100, 101] and for the decaffeination of coffee;[102, 103] more than a hundred thousand tons of decaffeinated coffee are produced per year in the world using $scCO_2$.

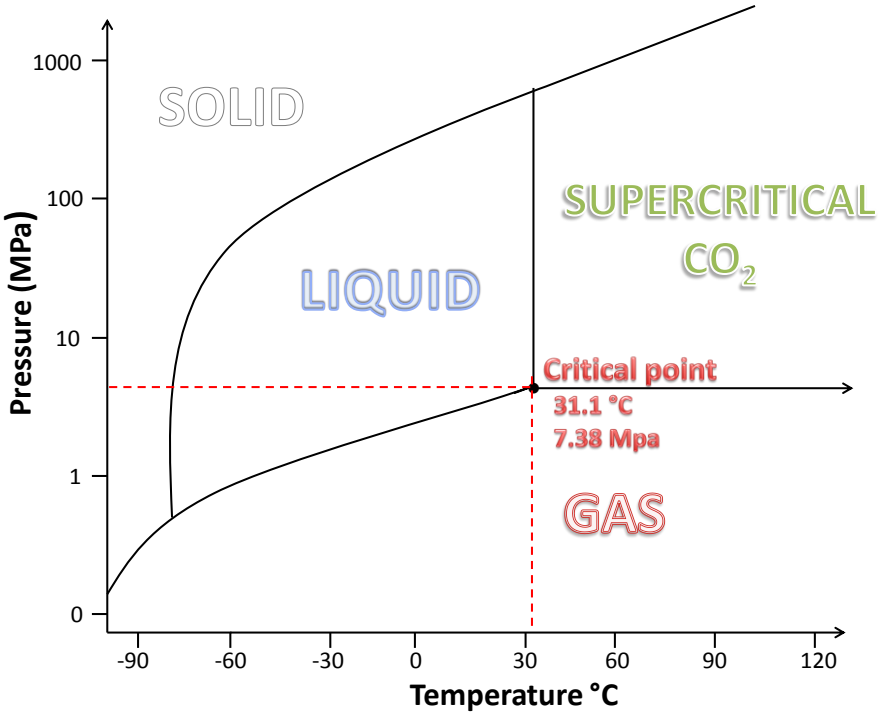

Figure 1.05: Phase Diagram for Carbon Dioxide

CO_2 is an inert symmetrical linear molecule with a zero dipole moment, in the supercritical state it has been shown to be marginally non-linear giving it an induced dipole and a significant quadrapole moment capable of taking part in quadrapole dipole interactions.[104] This gives $scCO_2$ the ability to dissolve an appreciable number of organic molecules, with the surface tension and viscosity remaining comparable to that of a gas. The fluid density and solvating power is easily tuneable with small changes to temperature and pressure. CO_2 is an inert, non-toxic (biocompatible), non-flammable, inexpensive substance, which is readily available and recyclable. It is also inert towards

polymer-based radicals and cannot undergo chain transfer reactions, making it ideally suited to radical initiated polymerizations. DeSimone and co-workers carried out pioneering homogenous radical polymerizations in $scCO_2$, with polytetrafluoroethylene (TEFLON) commercially produced in $scCO_2$.[105, 106]

Another crucial property of $scCO_2$ in polymer synthesis is its sorption into the polymers making them swell, resulting in changes in the polymers mechanical and physical properties. The most important alteration to the polymer is a lowering of the glass transition temperature (T_g).[107, 108] This effect is called plasticization and is significant in both polymerisation and processing.[109] The consequence of plasticization is an increase of polymer chain mobility at significantly lower temperatures than at atmospheric pressure, [110] brought about by CO_2 molecules interacting with the basic sites in the polymer units, in a Lewis acid-base type interaction.[111] Superior diffusion rates in the polymer matrix allows easier extraction of monomer or other species for purification in polymer processing, producing products that are virtually free of residual organic or aqueous contaminants. Conversely an impregnation protocol of small molecules into polymers for drug delivery applications is also enhanced by the plasticization effect. This has also proven beneficial for CLRP processes by reducing the onset of the gel effect resulting in higher monomer conversion and improved control.[112-114] [115]

Several types of polymerization processes can be carried out in $scCO_2$: solution[105], suspension[116, 117] and (mini)emulsion.[118-120] Apart from the formation of fluoropolymers and polysiloxanes, most polymerizations in $scCO_2$ are heterogeneous in nature. Heterogeneous systems include suspension and emulsion polymerizations, which are heterogeneous from the start. Conventional radical suspension polymerization of divinylbenzene[116, 117] and the emulsion radical polymerizations of acrylate[119] and acrylamide[118] have been reported in $scCO_2$. Precipitation[121, 122] and dispersion[123, 124] (with added surfactant) are examples of heterogeneous polymerizations where the mixture of monomer and initiator are soluble at the onset of the polymerization, but the resultant polymer is insoluble. DeSimone and Canelas used poly(styrene-*b*-dimethylsiloxane), as stabilizer to achieve a dispersion polymerization of styrene in $scCO_2$.[125]

1.4.1 Heterogeneous CLRP in $ScCO_2$

The three major CLRP techniques have all utilized $scCO_2$ as a polymerization medium to achieve a heterogeneous polymerization. The most straight forward heterogeneous CLRP in $scCO_2$ is precipitation polymerization. For conventional radical precipitation polymerizations in $scCO_2$, heterogenicity is more or less immediate as high MW polymer is produced very quickly (< 1s). The use of NMP has allowed our group to determine the point at which particle nucleation or precipitation occurs, known as the critical degree of polymerization, denoted as J_{crit}.[67, 114, 126] The slow linear build up in MW with conversion for a CLRP allows all chains to reach J_{crit} at approximately the same time and the precipitation can be visually observed. A 2009 review summarised a decade of research activity into heterogeneous CLRP in $scCO_2$.[127] At the start of this PhD only NMP had been investigated as a precipitation polymerization in $scCO_2$, with dispersion polymerizations being the focus of ATRP [128-131] and RAFT.[132, 133] A summary of NMP heterogeneous polymerizations in $scCO_2$ now follows:

Odell and Hamer in 1996 carried out a NMP in $scCO_2$, which is now believed to be a precipitation due to the low monomer loading and high conversion achieved.[134] Our group has extensively investigated the precipitation and dispersion polymerizations of St in $scCO_2$, using SG1 as the mediating agent.[17, 67, 114, 126, 135, 136] Precipitation polymerizations carried out at 40% w/v monomer loading and relatively high excess of SG1 (100% excess) at 110 °C and ≈ 42 MPa, achieved good control (M_w/M_n = 1.11-1.32) up to high conversion (92%).[17] A high excess of SG1 is required in precipitation and dispersion polymerizations due to nitroxide partitioning away from the locus of polymerization after particle nucleation, which may contribute to poor control/livingness.[17, 67] At high conversions the poly(St) was isolated as a powder with SEM images showing hemispherical cavities on the particle surface attributed to the expulsion of CO_2 from the polymer phase on de-pressurization. Despite the narrow MWDs obtained, low MW tailing was observed and shown to be due to an increase in the total number of chains with conversion. This was thought to be predominantly due to chain transfer to the Diels-Alder induced dimer of styrene (see Scheme 1.04). As dimer formation is monomer concentration dependent, the controlled/living precipitation polymerization in $scCO_2$ is similar to bulk after J_{crit}, and the corresponding bulk St polymerization had a similar increase in the total number of new chains produced. This is further backed up with less new chains being produced in earlier studied solution polymerizations.[67] Previously conducted, conventional precipitation

polymerizations of St in $scCO_2$ at 65 °C reported limiting low conversions.[125, 137] To investigate this, conventional radical polymerizations of St were conducted at the same temperature as the NMPs (110 °C) and almost quantitative conversion (~95%) was reached in 48h. This suggested that temperature and not the controlled/living nature is the important factor for these improved conversions to be achieved in precipitation polymerizations in $scCO_2$. In a subsequent paper, it was revealed that control superior to an analogous controlled/living solution NMP of St can be achieved in $scCO_2$ when high monomer loadings (70% w/v) are used, leading to greater monomer conversion before particle nucleation occurs (high J_{crit}).[114] For St polymerizations at high monomer loadings in $scCO_2$ both TIPNO and SG1 achieved better control with a slower R_p than in their corresponding solution polymerizations.[114, 126] A slightly broader MWD for TIPNO-mediated precipitation polymerizations in $scCO_2$ was attributed to greater partitioning of TIPNO towards the $scCO_2$ continuous phase, due to it having a greater predicted solubility in the $scCO_2$ phase than SG1.[126] While the difference in R_p was due to the partitioning of monomer away from the locus of polymerization, which would result in less monomer units being incorporated into each polymer chain per activation-deactivation cycle. This rationalizes the improved control in $scCO_2$ compared to solution as the number of activation-deactivation cycles would be increased in $scCO_2$.

The first dispersion NMP in $scCO_2$ was carried out on St with SG1 as nitroxide using a commercially available azo-initiator (VPS-0501) (Figure 1.06) and a SG1-poly(St)-*b*-poly(DMS)-b-poly(St)-SG1 alkoxyamine generated *in situ*, to achieve simultaneous initiation and stabilization (inistab[138]).[135] Inistab methodology was earlier developed by Okubo and co-workers for the dispersion ATRP of MMA in $scCO_2$.[139]

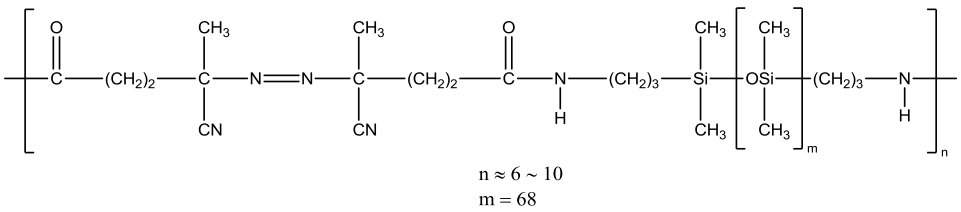

Figure 1.06: VPS-0501.

Initial attempts with the commercially available VPS-0501 as inistab, produced a polymer with a very broad and bimodal MWD. The bimodality was due to chains

growing from one or both ends of the VPS-0501. The inclusion of AIBN and reduction of VPS-0501 from 3.5 to 1.5 wt % relative to St resulted in much narrower MWDs but conversion was limited to 40% due to inadequate stabilization. Using 20 wt % of a bifunctional inistab (heat treated VPS-0501, which had an estimated two azo-moieties remaining per chain) relative to monomer achieved control with lower polydispersity (M_w/M_n = 1.56) at high conversion (89%). The increased conversion indicated better stabilization, but the formed polymer particles were irregular in shape (non-spherical) and showed coagulation, signifying imperfect stabilization.[135] Stabilization in this case was reduced by a significant proportion of the stabilizer chains having both (poly(St)) ends anchored in the particles and the CO_2 philic mid-section unable to extended freely into the continuous phase reducing the thickness of the colloidal protective layer. Improved stabilization and control for an inistab system was then reported using the a mono-functional poly(DMS)-*b*-poly(St)-SG1[140] inistab MI, which grows from only one-end. This was tailor made by a combination of ATRP followed by low temperature nitroxide trapping (Scheme 1.12).[141] The dispersion polymerizations were carried out using this inistab at 40 % w/v St with 10% excess SG1. High MW poly(St) with low polydispersity was obtained up to high M_n (M_n = 44,300 g mol^{-1}, M_w/M_n = 1.36) although R_p was relatively slow (60% conv. in 72 h). Uniform spherical particles were seen by Transmission electron micrograph (TEM) indicating good colloidal stabilization.[140] A similar dispersion polymerization was carried out using a separate initiator/stabilizer system.[67] A commercially available stabilizer (Poly(DMS)-*b*-Poly(MMA), 7.5 wt % relative to monomer), with AIBN as initiator were used for a 40% w/v St loading dispersion polymerization in scCO_2 with [SG1]/[AIBN] = 3.3 at 110 °C. Good controlled/livingness (M_w/M_n <1.4) was achieved up to high conversion (85%), when a sufficient concentration of stabilizer was used. TEM of the recovered dry poly(St) powder showed stabilized colloidal particles with a number-average particle diameter of ~150 nm.

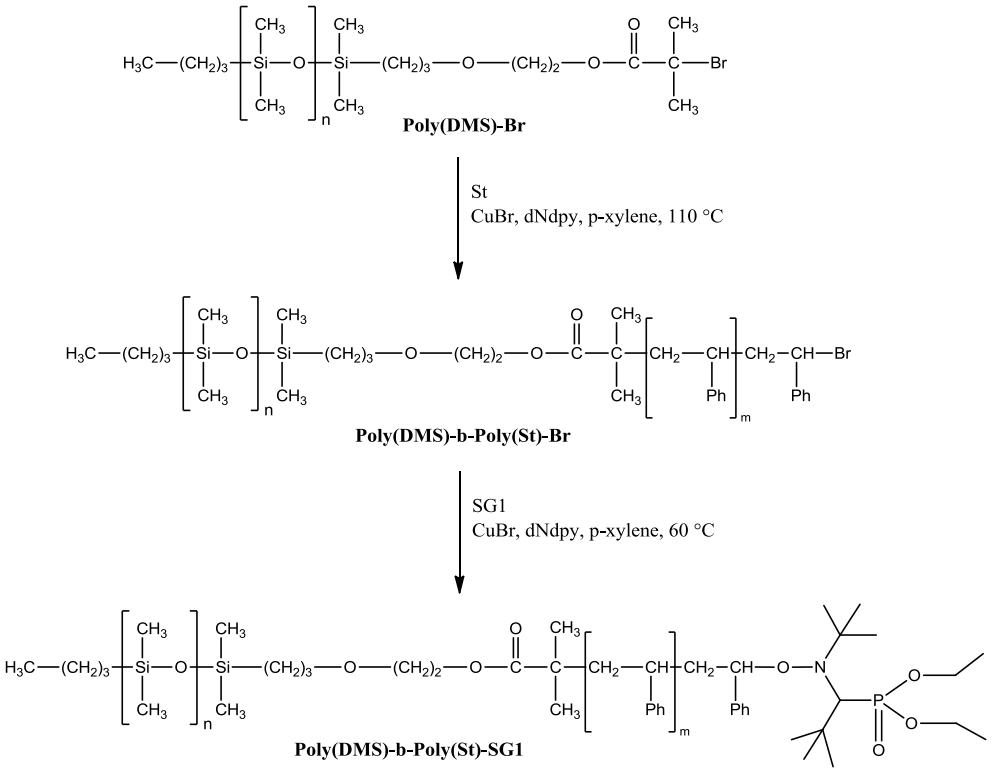

Scheme 1.12: Synthesis of Poly(DMS-b-Poly(St)-SG1 (n ≈49, m ≈ 41).
Where; dNdpy = 4,4′-dinonyl-2,2′-dipyridyl

Grignard et al published a communication in 2010 on the dispersion NMP of MMA in $scCO_2$.[142] They used the method for NMP of MMA developed by Charleux's group using a small amount of styrene (8.8 mol%),[84] to achieve good control/livingness, as well as the use of an *in situ* prepared stabilizer for dispersion polymerizations similar to the inistab approach (above). Grignard used the commercially available SG1 based alkoxyamine (blockbuilder®) and a SG1-terminated poly(heptadecafluorodecyl acrylate, FDA – "the inistab"[135]) for initiation. The CO_2-philic MI formed a poly(FDA)-*b*-poly(MMA) stabilizer by chain extension with MMA helping it to anchor to the polymer particles, affording stabilization. These reactions resulted in good control over MWD (M_w/M_n = 1.26-1.31). At high conversion with 10% wt stabilizer a white free flowing powder was obtained consisting of well-defined microspheres (16 ± 2 μm).

1.5 Thesis Aims and Objectives

Chapter 2:

I. To investigate the effects of varying initial monomer loading, monomer to initiator ratio ($M_{n,th}$) and pressure on the point of particle nucleation (J_{crit}) for heterogeneous NMP in $scCO_2$.
II. To devise a working model for the prediction of J_{crit} as a function of, initial monomer loading and targeted molecular weight.

Chapter 3:

I. To investigate the effect of chain transfer to solvent in both conventional and NMPs of NIPAM and to determine the upper limit of obtainable molecular weight in the radical polymerization of NIPAM in DMF at 120 °C.
II. To calculate the $C_{tr,S}$ to DMF using a variety of analytical equations and experimental techniques (Mayo plot), and compare the obtained $C_{tr,S}$ value with the experimental data from conventional RP and NMPs.
III. To investigate the production of new chains with conversion due to chain transfer to solvent, thermal self-initiation and mid-chain radical formation, and determine its effect on MWD and livingness in NMP.

Chapter 4:

I. To develop a method for the nitroxide-mediated polymerization of the $scCO_2$ insoluble monomer NIPAM. Representing the first dispersed phase CLRP polymerization of any monomer in $scCO_2$.
II. To produce controlled/living poly(NIPAM) in $scCO_2$ free from the use of volatile organic solvents in both polymerization and purification.

Chapter 5:

I. To devise a new protocol for the efficient preparation of poly(NIPAM) block copolymers, utilizing successive nitroxide-mediated precipitation and inverse suspension heterogeneous polymerizations in $scCO_2$.
II. To investigate the effect block copolymer composition and block length on the aqueous cloud point temperatures of the NIPAM-containing copolymers.

CHAPTER 2

Effect of Monomer Loading and Pressure on Particle Formation in Nitroxide-Mediated Precipitation Polymerization in Supercritical Carbon Dioxide

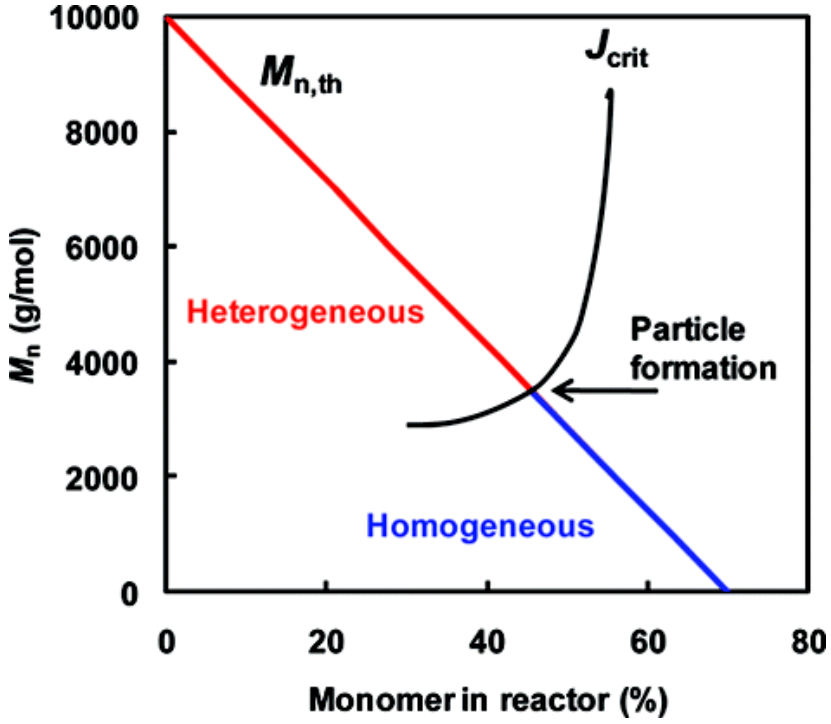

2.1 Introduction

Supercritical carbon dioxide ($scCO_2$) is a benign reaction solvent well-suited for heterogeneous radical polymerizations, because most organic small molecules (incl. monomer, initiator) are soluble in the medium, but the resulting high molecular weight (MW) polymers are insoluble.[127, 143] Polymer chains are soluble in the medium up to a certain critical degree of polymerization (J_{crit}) when chains become insoluble and precipitate, resulting in particle formation. At J_{crit}, the polymerization changes from a homogeneous phase in $scCO_2$ to a heterogeneous system. Dispersion polymerizations contain a colloidal stabilizer to prevent coagulation of particles giving polymer of narrow particle size distributions and more well-defined particles (d ≈ 100 nm to 15 μm).[127, 143, 144]

Over the past 20 years, controlled/living radical polymerization (CLRP) has revolutionized polymer chemistry, allowing the synthesis of narrow molecular weight distribution (MWD) polymer, as well as complex architectures under less stringent polymerization conditions than ionic methods.[1] Although initially most CLRPs were carried out under homogeneous conditions, many have since been carried out using commercially important heterogeneous techniques.[145, 146] The three most widely used CLRPs, nitroxide-mediated radical polymerization (NMP),[17, 67, 114, 126, 135, 136] atom transfer radical polymerization (ATRP),[128-131, 147, 148] and reversible addition-fragmentation chain transfer (RAFT)[132, 133, 149, 150] have all been successfully implemented as heterogeneous polymerizations in $scCO_2$. However, only NMP has thus far been shown to proceed in a controlled/living manner to high conversion using the stabilizer-free precipitation system.[17, 114, 126] Furthermore, under certain conditions (70% w/v monomer, $[SG1]_0/[AIBN]_0$ = 1.99, 110 °C, 30 MPa, where the nitroxide is SG1 = *N*-*tert*-butyl-*N*-[1-diethylphosphono(2,2-dimethylpropyl)]oxy and AIBN = 2,2′-azobisbutyronitrile), it has been shown that the precipitation NMP of styrene (St) can proceed with better control over the MWD than the corresponding solution polymerization.[114, 126]

The slow build up in MW in a CLRP by virtue of the equilibrium between active (propagating radicals) and dormant polymer chains allows measurement of J_{crit} by estimating via visual observation of the conversion (and thus the MW) at which the reaction mixture changes from transparent to opaque (the cloud point). In a conventional nonliving polymerization, the system would immediately become

heterogeneous because of the instantaneous formation of high MW polymer. The value of J_{crit} would change with conversion as the composition of the continuous phase changes because chains are continuously initiated and grow to reach J_{crit} throughout the polymerization. However, in CLRP, the initial stoichiometry dictates the conversion at J_{crit}, and a single J_{crit} value applies to a given polymerization system. This technique has been employed to estimate J_{crit} for precipitation/dispersion NMP of St in $scCO_2$.[67, 114]

To date, only the NMP of St in $scCO_2$ has been studied, and no information on controlled/living character at low conversion (before J_{crit}), when the reaction is homogeneous, has been obtained. The NMP of St and *tert*-butyl acrylate (*t*-BA) in $scCO_2$ before and after J_{crit} is now presented. The detailed effects of composition and pressure on J_{crit} and the associated controlled/living character are examined. This has led us to develop a simple graphical approach to predicting J_{crit} as a function of both target MW ($[monomer]_0/[initiator]_0$) and initial monomer loading based on a data set of J_{crit} versus initial monomer loading. These findings will enable future optimization of heterogeneous (precipitation and dispersion) CLRPs in $scCO_2$.

2.2 Experimental

2.2.1 Materials

St (Aldrich, >99%) and *t*-BA (Aldrich, 98%) were distilled under reduced pressure before use. AIBN (DuPont Chemical Solution Enterprise) was recrystallised from methanol before use. SG1 (also known as DEPN) was prepared according to the literature[151] with purity (96%) determined using ^1H NMR spectroscopy from the reaction of SG1 radical with pentafluorophenylhydrazine (Aldrich). Reagent grade toluene (Aldrich, ≥ 99.7%), methanol (Corcoran Chemicals, 99.9%), dichloromethane (DCM, Corcoran Chemicals, 99.9%), and CO_2 (BOC, 99.8%) were used as received. Macroinitiator (MI) (poly(St)-T, where, T = SG1, M_n = 4,250 g mol^{-1}, M_w/M_n = 1.18) was obtained from the J_{crit} measurement experiment at 55% monomer loading (see Table 2.01).

2.2.2 Equipment and Measurements.

All NMP in $scCO_2$ were conducted in a 100 ml stainless steel Thar reactor with 180° in-line sapphire windows, and overhead Magdrive stirrer with maximum programmable operating pressure and temperature of 41.4 MPa and 120 °C, respectively. The pressure was produced and maintained by a Thar P-50 series high pressure pump to within ±0.2 MPa. The temperature was regulated by a Thar CN6 controller to within ±1 °C. The reactor is connected to a Thar Automated Back Pressure Regulator (ABPR, a computer controlled-needle valve) for controlled venting.

M_n and polydispersity (M_w/M_n) were determined using a gel permeation chromatography (GPC) system consisting of a Viscotek DM 400 data manager, a Viscotek VE 3580 refractive-index detector and two Viscotek Viscogel GMH_{HR}-M columns. Measurements were carried out using tetrahydrofuran (THF) at a flow rate of 1.0 mL min^{-1} at 35 °C with columns calibrated using twelve linear poly(St) standards (M_n = 162 - 6,035,000). M_n and M_w/M_n values for poly(*t*-BA) are not accurate due to calibration against poly(St) standards. However our primary focus is trends as well as shape and relative position of MWDs. M_n is given in grams per mole (g mol^{-1}) throughout, to the nearest 50 g mol^{-1}.

2.2.3 Polymerization of St in $scCO_2$

The reactor was loaded with St (58.320 g, 0.56 mol), poly(St)-T (1.680 g, 0.40 mmol) (60% w/v includes St + poly(St)-T), and SG1 (47 mg, 0.16 mmol). The reactor was sealed with the magnetically coupled stirring lid (Magdrive). The mixture was purged for 15 min by bubbling gaseous CO_2 through the mixture to remove air. Liquid CO_2 (~5 MPa) was added, and the temperature was raised to the reaction temperature of 110 °C, followed by the pressure to the reaction pressure (in this case 30 MPa) by the addition of CO_2. The transparent reaction mixture was stirred at ~1000 rpm throughout and monitored through the inline sapphire windows, and if J_{crit} was required, stopped when the reaction mixture became opaque. Heating was stopped, and rapid external cooling using dry ice was carried out (this caused the temperature of the reactor to drop to ~80 °C in 10 min). The CO_2 was vented slowly from the reactor (when at approximately room temperature after 40 min of cooling) through a suitable solvent (methanol) to prevent the loss of polymer and opened using the ABPR, and the reaction mixture pipetted directly from the reactor. The polymer was precipitated from excess methanol, filtered, and dried prior to conversion measurement by gravimetry.

2.2.4 Polymerization of *t*-BA in $scCO_2$

t-BA (50.0 g, 0.39 mol, 50% w/v), AIBN (0.124 g , 0.76 mmol) and SG1 (0.550 g, 1.87 mmol) were heated at 118 °C and 30 MPa using the polymerization procedure above. The polymer was precipitated from a 3:2 water/methanol mixture, filtered and dried prior to conversion measurement by gravimetry.

2.2.5 Measurement of J_{crit} in $scCO_2$

For the 70% w/v initial St loading and $M_{n,th}$ at 100% conversion = 40,000 (Equation 2.01): St (70.0 g, 0.67 mol), AIBN (0.173 g, 1.05 mmol) and SG1 (0.620 g, 2.11 mmol) were heated at 110 °C and 30 MPa and the polymerization stopped at J_{crit} (see procedure above). The theoretical value of M_n ($M_{n,th}$) is calculated via Equation 2.01:

$$M_{n,th} = \frac{\alpha[M]_0 MW_{mon}}{2f[AIBN]_0} \qquad (2.01)$$

where f is the AIBN initiator efficiency, α is the fractional conversion of monomer, $[M]_0$ is the initial monomer concentration and MW_{mon} is the molecular weight of the monomer. The value of f in $scCO_2$ at 59.4 ºC has been estimated as 0.83 by DeSimone and co-workers.[152] In the present study f was estimated by fitting the initial portion of the M_n vs conversion plots of the polymerization data to yield f = 0.83 (St) and 1.23 (*t*-BA). $M_{n,th}$ values were computed throughout this work using Equation 2.01 in connection with these f-estimates. A value of f greater than unity, as obtained for *t*-BA, is of course not physically meaningful, this is most likely a result of accumulated error primarily due to inaccuracy caused by the use of poly(St) standards. The initiator efficiency of the MI poly(St)-T is taken as 1.

2.2.6 Chain Extension of Poly(*t*-BA) with Bulk St

Poly(*t*-BA)-T MI from the 70% w/v initial loading experiment (Figure. 2.04, Table 2.02) (0.4270 g, 0.025 mmol), St (2 g, 19.20 mmol) and SG1 (1.5 mg, 5.10 μmol) were charged in a glass ampoule. Air was removed by several freeze thaw degas cycles before sealing. It was then placed in an aluminium heating block at 120 °C for 24 h. The polymerization was quenched by immersing the ampoule into an ice-water bath. Subsequently the mixture was dissolved in DCM and poured into an excess of 3:2 water/methanol to precipitate the formed polymer. After filtration and drying, the conversion was obtained from the increase in weight of polymeric material.

Table 2.01: Results for Measurement of J_{crit} for Poly(styrene) using Different Monomer Loadings and Pressures at 110 °C

$[M]_0$ (% w/v)[a]	Pressure (MPa)	Time at J_{crit} (min)	Conv (%)	M_n	$M_{n,th}$	M_w/M_n	J_{crit}
80	30	272	32.8	13450	13100	1.13	129
70	30	227	22.0	8550	8800	1.15	82
60	30	119	14.1	5000	5650	1.17	48
55	30	96	10.3	4250	4100	1.18	41
50	30	71	8.4	3450	3400	1.17	33
40	30	51	3.9	3000	1550	1.18	29
35	30	44	1.8	2950	700	1.19	28
30	30	35	0.9	2800	350	1.35	27
70	23	264	21.9	7600	8750	1.20	73
70	15	175	16.0	6100	6400	1.22	59
70	10	140	16.8	5400	6700	1.21	52

(a) Initial monomer loading.

Table 2.02: Results for Measurement of J_{crit} for Poly(*tert*-butyl acrylate) using Different Monomer Loadings and Pressures at 118 °C

$[M]_0$ (% w/v)[a]	Pressure (MPa)	Time at J_{crit} (min)	Conv (%)	M_n	$M_{n,th}$	M_w/M_n	J_{crit}
70	30	1159	66.0	17100	17750	1.44	133
60	30	960	51.8	12650	13950	1.37	99
50	30	720	38.8	10500	10500	1.28	82
30	30	225	10.0	3900	2700	1.29	30
60	23	576	43.1	11100	11600	1.35	87
60	15	428	29.6	9500	8000	1.29	74
60	10	335	24.7	7750	6650	1.23	61

[(a)] Initial monomer loading.

2.3 Results and Discussion

2.3.1 NMP of St and *t*-BA in $scCO_2$

Conversion, time and MWD data for NMP of St (60% w/v) in $scCO_2$ initiated by a soluble MI (poly(St)-SG1, with 40 mol% free SG1 relative to [MI]; the addition of free SG1 is primarily to alleviate partitioning effects[67] anticipated after J_{crit}) at 110 °C and 30 MPa are displayed in Figures 2.01 and 2.02. The polymerization proceeded to intermediate conversion with no sign of having reached a limiting conversion (Figure 2.01), and the MWDs shifted to higher MW with increasing conversion (Figure 2.02).

The value of J_{crit} was obtained by visual monitoring of the polymerization via the reactor in-line sapphire windows. The polymerization was stopped at the point when the mixture changed from transparent to opaque. Subsequent measurement of M_n yielded J_{crit} = 110 (M_n = 11,440) at 7.3% conversion. Because of the inherent polydispersity of the polymer (despite the CLRP process), this value of J_{crit} is to an extent an underestimate of the true J_{crit}. This is because the chains of the highest MW of the MWD will be the ones that first precipitate, whereas the obtained J_{crit} corresponds to the full MWD. The values of M_w/M_n increased with conversion in the range 1.16-1.18 before J_{crit} and 1.23-1.56 after J_{crit} (Figure 2.02), indicating good control/livingness in agreement with our previously reported SG1/AIBN-initiated precipitation polymerizations.[17, 114, 126]

Conversion-time and MWD data for NMP of *t*-BA (50% w/v) in $scCO_2$ initiated by AIBN and controlled using an excess of nitroxide, $[SG1]_0/[AIBN]_0$ = 2.5, at 118 °C and 30 MPa are displayed in Figures 2.01 and 2.02. Similarly to the St NMP above, M_n increased linearly with conversion, indicative of good controlled/living character, and J_{crit} = 82 (M_n = 10,510) was recorded at 38.8% conversion. M_w/M_n increased dramatically after J_{crit} (1.28-1.35 before J_{crit} and 1.66 after J_{crit}), which is probably the consequence of a lowering in the free [SG1] at the locus of polymerization due to partitioning towards the $scCO_2$ continuous phase (the particle phase is the main locus of polymerization after J_{crit}),[114, 127] although partial loss of control of NMP would be expected at high conversions.

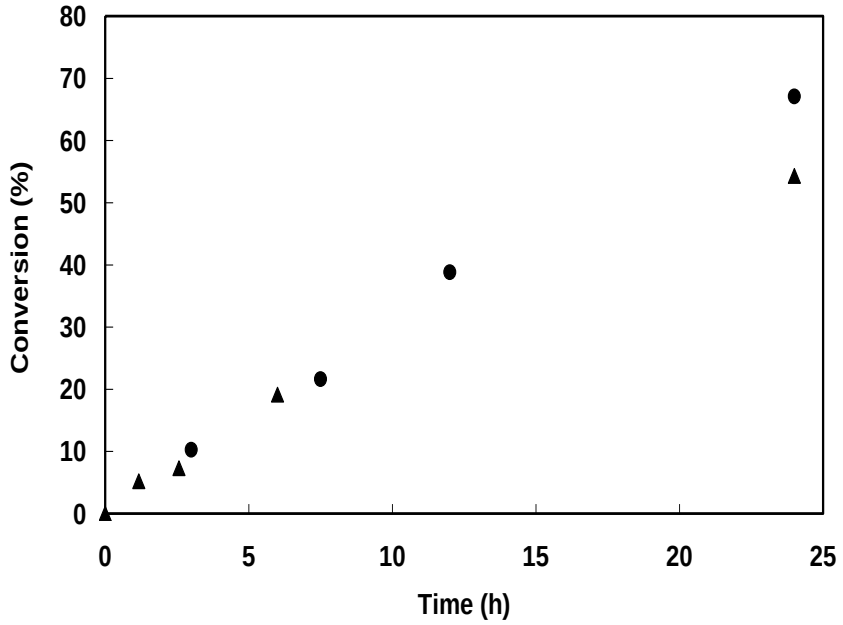

Figure 2.01: Conversion versus time for the SG1-mediated polymerization of St (▲, 60% w/v) at 110 °C (initiated by poly(St)-SG1 MI in the presence of 40 mol% free SG1) and *t*-BA (●, 50% w/v) at 118 °C ($[SG1]_0/[AIBN]_0 = 2.5$) in $scCO_2$ at 30 MPa. J_{crit} is at 7.3% and 38.8% conversion for St and *t*-BA, respectively.

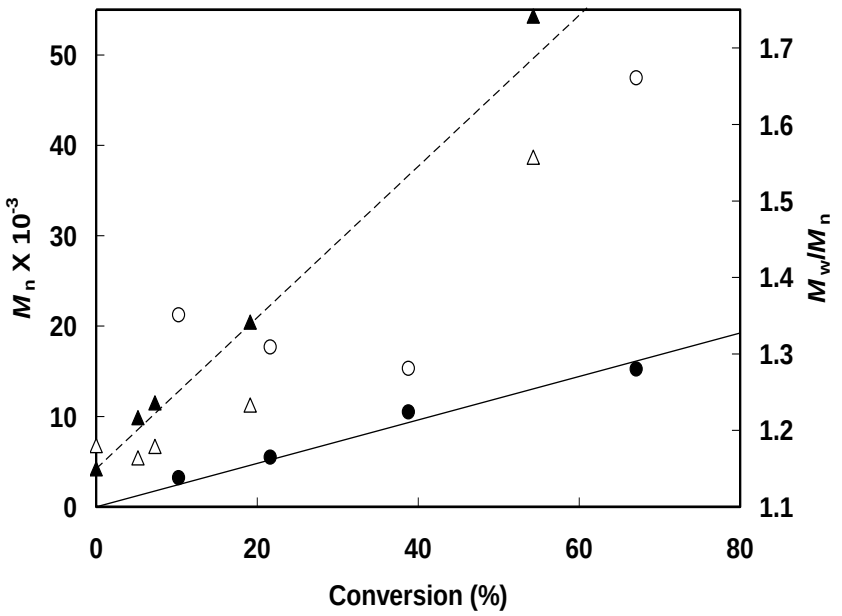

Figure 2.02: M_n (closed symbols) and M_w/M_n (open symbols) versus conversion for the SG1-mediated polymerization of St (▲, △, 60% w/v) at 110 °C (initiated by Poly(St)-SG1, MI in the presence of 40 mol% free SG1) and *t*-BA (●, ○, 50% w/v) at 118 °C ($[SG1]_0/[AIBN]_0$ = 2.5) in $scCO_2$ at 30 MPa. Dashed and continuous lines represent $M_{n,th}$ for St and *t*-BA polymerizations, respectively. J_{crit} is at 7.3% and 38.8% conversion for St and *t*-BA, respectively.

2.3.2 Effect of Monomer Loading on J_{crit}

Values of J_{crit} were estimated for the NMP of St in $scCO_2$ at a range of different initial monomer loadings of 30-80% w/v using $[SG1]_0/[AIBN]_0 = 2.0$ ($M_{n,th}$ = 40,000 at 100% conversion) at 110 °C and 30 MPa (Figure 2.03, Table 2.01). As expected, J_{crit} increased with monomer loading due to increased solubility of the polymer in the increasingly monomer rich continuous phase. However, J_{crit} increased only slightly from 27 (conv. = 0.9%) to 33 (conv. = 8.4%) as the initial loading was increased from 30 to 50% w/v. As the monomer loading was increased further to 55% w/v (J_{crit} = 41, conv. = 10.3%), the values of J_{crit} increased more dramatically to reach 129 (conv. = 32.8%) at 80% w/v.

Considering that the ratio $[St]_0/[AIBN]_0$ was the same in all polymerizations, one would expect that M_n vs conversion of these polymerizations would give a straight line (provided that f does not change significantly with monomer loading), that is J_{crit} versus conversion at J_{crit} should give a straight line. It is however apparent from Figure 2.03 (and Table 2.01) that at low monomer loadings, this is not the case, J_{crit} is higher than expected considering the conversions at J_{crit}. Because of the short polymerization times required to reach J_{crit} (35-51 min at 30-40% w/v St, Table 2.01), some fraction of AIBN remains undecomposed at J_{crit}, thus giving $M_n > M_{n,th}$. Estimation of apparent f values based on Equation 2.01 gives $f \approx 0.1$, 0.4 and 0.78 at 30, 40 and 50% w/v St, respectively, with $M_n \approx M_{nth}$ at 50% w/v St. This hypothesis was confirmed by taking a 35% w/v initial loading polymerization of St (under the same conditions as that used for the J_{crit} measurement, where apparent $f = 0.2$) to well-beyond J_{crit} (15 h), which gave M_n = 13,700 ($M_w/M_n = 1.33$) at 31.3% conversion. This approached the $M_{n,th}$ = 12,500, with apparent $f \approx 0.76$ which is close to the literature value of 0.83.[152]

Values of J_{crit} were estimated for the NMP of *t*-BA in $scCO_2$ at a range of different initial monomer loadings of 30-70% w/v using [SG1]/[AIBN] = 2.5 ($M_{n,th}$ = 26,900 at 100% conversion) at 118 °C and 30 MPa (Figure 2.04, Table 2.02). J_{crit} and the conversion at J_{crit} increased almost linearly with initial monomer loading from J_{crit} = 30 at 10.0% to 133 at 66.0% conversion, indicative of increased polymer solubility in the continuous phase. The J_{crit} (and conversion at J_{crit}) values for *t*-BA (for a given monomer loading) are considerably higher than those for St, indicating a greater solubility of poly(*t*-BA) compared to poly(St) in $scCO_2$ at the respective temperatures and pressures, St and *t*-BA polymerizations resulted in similar M_n vs conversion plots (Table 2.01 and 2.02); that is similar M_n values were reached at a given conversion, thus

making direct comparison meaningful in this sense. It has been reported that the solubility of poly(butyl acrylate) in neat $scCO_2$ is higher than that of poly(St), mainly as a result of the higher glass transition temperature of poly(St).[153]

Longer polymerization times were required to reach J_{crit} for *t*-BA than St (Tables 2.01 and 2.02) and the temperature was higher for *t*-BA (118 ºC vs 110 ºC), therefore partial decomposition of AIBN at J_{crit} at low monomer loadings was not an issue for *t*-BA (i.e. J_{crit} increases close to linearly with conversion at J_{crit}). Controlled/living character was maintained up to high conversion, as indicated by M_n = 17,100 remaining close to $M_{n,th}$ = 17,750 at 66.0% conversion (Table 2.02), and confirmed by efficient chain extension of this sample with bulk St (Figure 2.05).

The J_{crit} values for St appear to be consistent with the work of Vana and co-workers, who reported homogeneous RAFT polymerizations of St in $scCO_2$ at 80 °C and 30 MPa using 78% vol% St for $M_n < 29800$.[154]

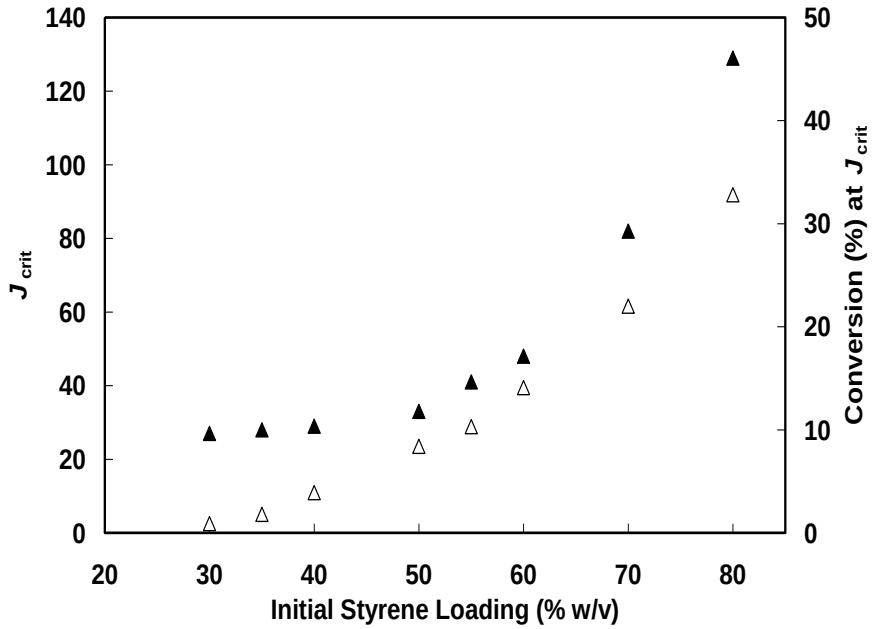

Figure 2.03: J_{crit} (▲) and conversion at J_{crit} (△) versus initial St loading for the SG1-mediated polymerization of St in $scCO_2$ at 110 °C and 30 MPa ($[SG1]_0/[AIBN]_0$ = 2.0, and theoretical M_n at 100% conversion ($M_{n,th}$) = 40,000).

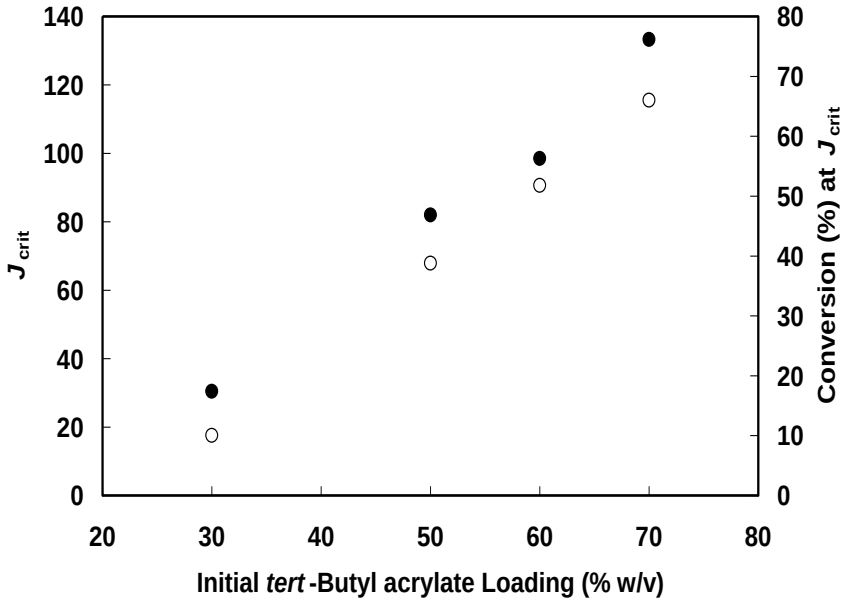

Figure 2.04: J_{crit} (●) and conversion at J_{crit} (○) versus initial *t*-BA loading for the SG1-mediated polymerization of *t*-BA in $scCO_2$ at 118 °C and 30 MPa ($[SG1]_0/[AIBN]_0$ = 2.5).

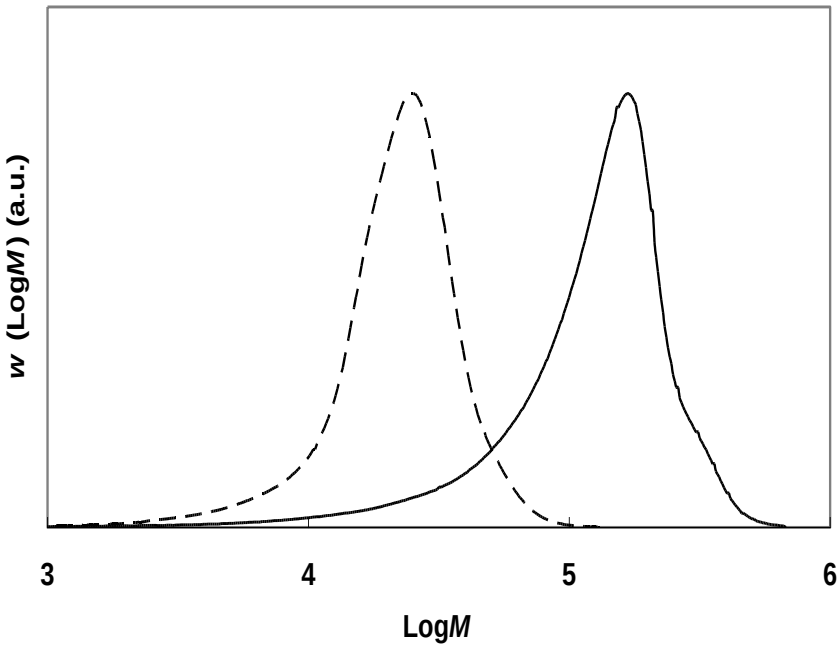

Figure 2.05: MWDs (normalized to peak height) of the chain extension of Poly(*t*-BA) (from 70% w/v initial monomer loading experiment (Table 2.02) M_n = 17,100, M_w/M_n = 1.44) with bulk St at 120 °C to give Poly(*t*-BA)-*b*-Poly(St); M_n = 65,200, M_w/M_n = 2.23, Conv. = 91.1%.

2.3.3 Predicting J_{crit}

The J_{crit} data described above for St and *t*-BA can be employed to predict J_{crit} under different experimental conditions, in terms of the targeted molecular weight ($M_{n,th}$ at 100% conversion) and the initial monomer loading, for the systems investigated (i.e. same temperature and pressure). For example, if the ratio of monomer to AIBN is altered (i.e. different $M_{n,th}$) but the initial monomer loading is the same, how does J_{crit} change? To this end, the J_{crit} data are presented graphically in Figures 2.06 and 2.07 in the form of a plot of J_{crit} versus the monomer content (as % w/v) of the mixture at J_{crit} (readily calculated from the monomer conversion at J_{crit}). The J_{crit} value can be predicted graphically by constructing theoretical lines of $M_{n,th}$ from the initial monomer loading, based on Equation 2.01. The theoretical lines describe how the degree of polymerization changes with the % w/v monomer remaining when the polymerization proceeds in accordance with Equation 2.01. J_{crit} of the "new" system corresponds to the point of intersection of the straight $M_{n,th}$ line and the J_{crit} curve. In the case of St (Figure 2.06, Table 2.03), using 70% w/v initial St loading and $M_{n,th}$ = 20,000 and 50,000 (at 100% conv.), the predictive graphical approach resulted in J_{crit} = 50 and 110 (at the intersections), respectively, remarkably close to the experimentally (in independent experiments) obtained values of J_{crit} = 47 and 113. Varying the initial St monomer loadings, 50% and 60% w/v, with $M_{n,th}$ = 100,000 and 60,000 (at 100% conv.), respectively, gave predicted J_{crit} = 38 and 65, which were also close to those obtained experimentally at J_{crit} = 44 and 72. Also in the case of *t*-BA (Figure 2.07 and Table 2.03), excellent agreement was obtained between the prediction (J_{crit} = 55) and experiment (J_{crit} = 58) for 45% w/v *t*-BA and $M_{n,th}$ = 20,000 (at 100% conv.).

The success of this predictive approach demonstrates how J_{crit} is governed by the dependence of M_n on conversion as well as the initial monomer loading. A change in $M_{n,th}$ at a fixed initial monomer loading affects J_{crit} because it alters the composition of the continuous medium at a given M_n. For example, an increase in $M_{n,th}$ by a factor of two means that a given M_n will be reached at half the conversion of the original recipe. In other words, at this value of M_n, the remaining monomer content will be higher than for the original recipe. This understanding, as well as the predictive approach developed, are expected to also apply equally well to other CLRP systems such as ATRP and RAFT, as well as non-scCO_2 media (e.g. alcohols/water). Moreover, the above is not restricted to precipitation polymerizations, but also applies to dispersion (stabilized heterogeneous) polymerizations.

The J_{crit} curves in Figures 2.06 and 2.07 are shaped in such a way that at higher initial monomer loadings, the monomer content (% w/v) of the mixture (or monomer remaining) is lower than the monomer content of the mixture at lower initial monomer loadings, i.e. the curve exhibits a negative gradient ("goes back on itself"). The reason is that at a high initial monomer loading, J_{crit} is so high that very significant monomer consumption is required to reach this degree of polymerization, and hence the amount of remaining monomer becomes very low. This effect is particularly strong for *t*-BA, which (under the present conditions), exhibits higher J_{crit} than St. If the $M_{n,th}$ line crosses the J_{crit} curve twice, then it is the first intersection that corresponds to J_{crit}.

Table 2.03: Results for Prediction of J_{crit} for Poly(Styrene) at 110 °C and Poly(*tert*-butyl acrylate) at 118 °C using Different Monomer Loadings and Targeted $M_{n,th}$

Monomer	$[M]_0$ (% w/v)[a]	Conv (%)	M_n	$M_{n,th}$	M_w/M_n	Expt J_{crit}	Predicted J_{crit}[b]
St	70	24.5	11800	12250	1.15	113	110
St	70	27.6	4900	5500	1.13	47	50
St	60	12.6	7500	7500	1.19	72	65
St	50	3.6	4550	3550	1.33	44	38
t-BA	45	34.8	7450	6950	1.30	58	55

[a] Initial monomer loading. [b] Predicted J_{crit} is from the intersection of the theoretical $M_{n,th}$ line and the curve.

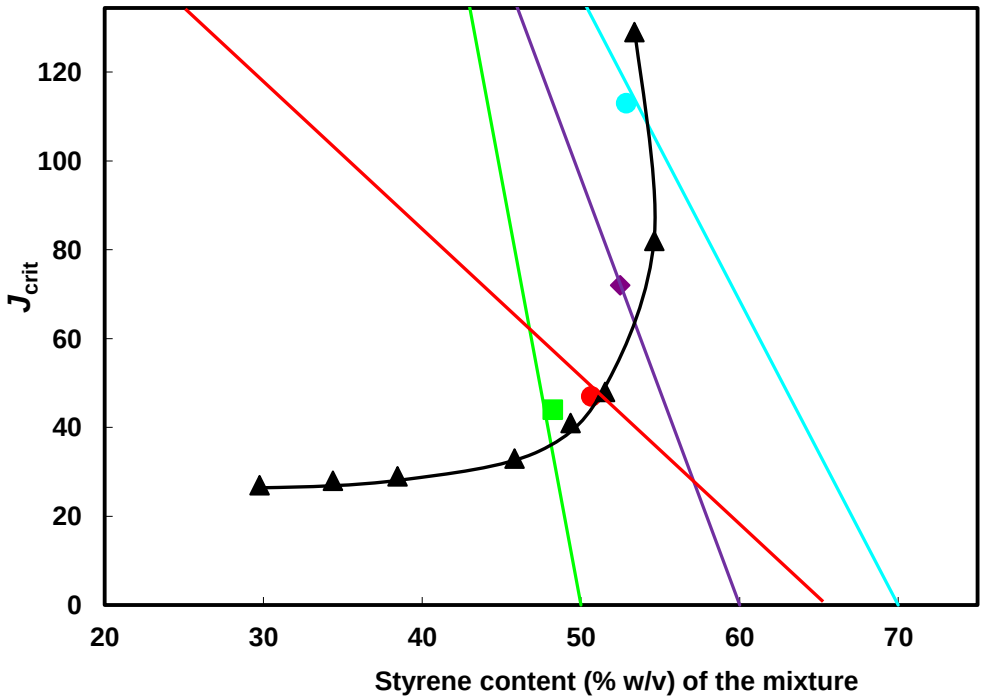

Figure 2.06: Plot of J_{crit} versus St content of the mixture at J_{crit} (▲) for the SG1-mediated polymerization of St in $scCO_2$ at 110 °C and 30 MPa ($[SG1]_0/[AIBN]_0$ = 2.0; $M_{n,th}$ (100% conv.) = 40,000). The straight lines (colours), each representing a given set of conditions in terms of initial monomer loading and $M_{n,th}$, describe how the degree of polymerization (symbols) changes with the % w/v monomer content when the polymerization proceeds in accordance with Equation 2.01. $M_{n,th}$ lines: 70% w/v St, $M_{n,th}$ = 20,000 (●; red), 70% w/v St, $M_{n,th}$ = 50,000 (●; blue), 60% w/v St, $M_{n,th}$ = 60,000 (◆; purple) and 50% w/v St, $M_{n,th}$ = 100,000 (■; green). $M_{n,th}$ values in legend refer to 100% conversion and the symbols represent individual experiments carried out using these conditions.

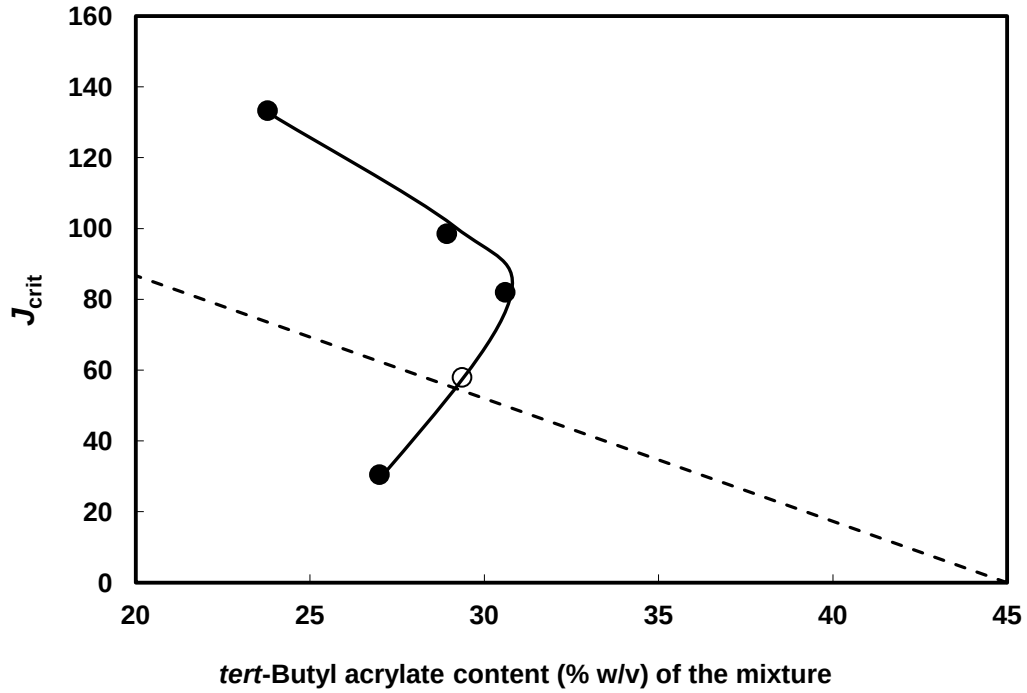

Figure 2.07: Plot of J_{crit} versus *t*-BA content of the mixture at J_{crit} (●) for the SG1-mediated polymerization of *t*-BA in $scCO_2$ at 118 °C and 30 MPa ($[SG1]_0/[AIBN]_0$ = 2.5, $M_{n,th}$ (100% conv.) = 26,900). The straight dotted line represents a given set of conditions in terms of initial monomer loading and $M_{n,th}$, and describe how the degree of polymerization changes with the % w/v monomer content when the polymerization proceeds in accordance with Equation 2.01. $M_{n,th}$ line: 45% w/v *t*-BA, $M_{n,th}$ = 20,000 at 100% conversion and (o) represents the J_{crit} experiment using these conditions.

2.3.4 Effect of Pressure on J_{crit}

Attention was next turned to how pressure influences J_{crit} during precipitation NMP in $scCO_2$. Polymer solubility in $scCO_2$ increases with increasing pressure as a result of the increase in CO_2 density,[153, 155] and thus solvent power. One would therefore anticipate J_{crit} to increase with increasing pressure. Figure 2.08 shows J_{crit} versus pressure for SG1-mediated polymerizations in $scCO_2$ of St 70% w/v at 110 °C ($[SG1]_0/[AIBN]_0$ = 2.0, $M_{n,th}$ = 40,000 at 100% conv.) and *t*-BA 60% w/v at 118 °C ($[SG1]_0/[AIBN]_0$ = 2.5, $M_{n,th}$ = 26,900 at 100% conv.). For both monomers, there is a close to linear increase in J_{crit} with increasing pressure. The increase is quite pronounced in the case of *t*-BA, an increase in pressure from 10 to 30 MPa leads to an increase in J_{crit} from 61 to 99. In terms of conversion at J_{crit}, this means that the system is homogeneous to 24.7 and 51.8% conversion at 10 and 30 MPa, respectively. In both cases controlled/living character is confirmed by M_n values that are reasonably close to $M_{n,th}$, and low M_w/M_n of 1.15-1.22 and 1.23-1.37 for St and *t*-BA, respectively (Tables 2.01 and 2.02).

McHugh and co-workers attributed the lower solubility of poly(St) relative to poly(acrylates) to its higher T_g, and a very high hindrance potential for chain segment rotations giving a higher entropy penalty for CO_2 to dissolve poly(St) compared to poly(acrylates).[153] There is an overall increase in J_{crit} of 30 between 10 and 30 MPa for St, with the latter polymerization giving excellent control/living character, M_n (8550) close to $M_{n,th}$ (8800) and low M_w/M_n (1.15). At 70-80% w/v initial St loadings and the highest pressure used (30 MPa), the reaction is homogeneous over the widest conversion range (also J_{crit} is highest), which favours optimal controlled/living character at J_{crit} and beyond (as indicated by our earlier high conversion NMP precipitation polymerizations[114, 126]).

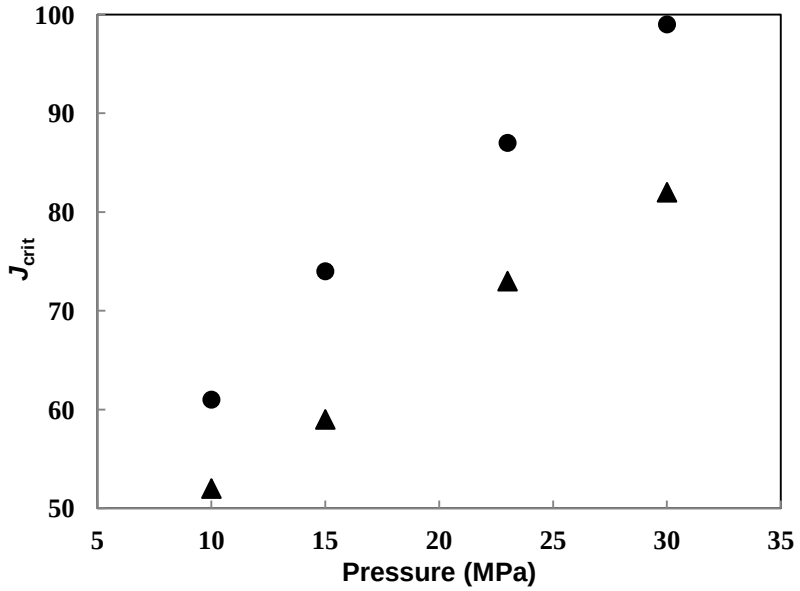

Figure 2.08: Plot of J_{crit} versus pressure (± 0.2 MPa) for the SG1-mediated precipitation polymerization in $scCO_2$ of 70% w/v St (▲) at 110 °C (using [SG1]/[AIBN] = 2.0, $M_{n,th}$ = 40,000 at 100% conv.) and 60% w/v *t*-BA (●) at 118 °C (using [SG1]/[AIBN] = 2.5, $M_{n,th}$ = 26,900 at 100% conv.).

2.4 Conclusions

SG1-mediated polymerizations of St (110 °C) and *t*-BA (118 °C) were shown to proceed in a controlled/living manner from low (homogeneous) to high (heterogeneous) conversion in $scCO_2$ at 30 MPa. The influence of monomer to initiator ratio, initial monomer loading and pressure on the critical degree of polymerization (J_{crit}) in $scCO_2$ has been determined. J_{crit} represents the point where the polymerization becomes heterogeneous or polymer chains become insoluble in the continuous medium, and particle formation begins. J_{crit} increased close to linearly with increasing initial monomer loading (50 to 80% w/v and 30 to 70% w/v for St and *t*-BA, respectively) and pressure (10 to 30 MPa) for both monomers. A simple graphical approach to predict J_{crit} as a function of initial monomer loading and targeted $M_{n,th}$ ($[monomer]_0/[initiator]_0$) is presented. This predictive approach will equally apply to other CLRP systems such as ATRP and RAFT, as well as non-$scCO_2$ media (e.g. alcohols/water). Moreover, the above is not restricted to precipitation polymerizations, but also applies to dispersion polymerizations.

CHAPTER 3

Chain Transfer to Solvent in the Radical Polymerization of *N*-Isopropylacrylamide

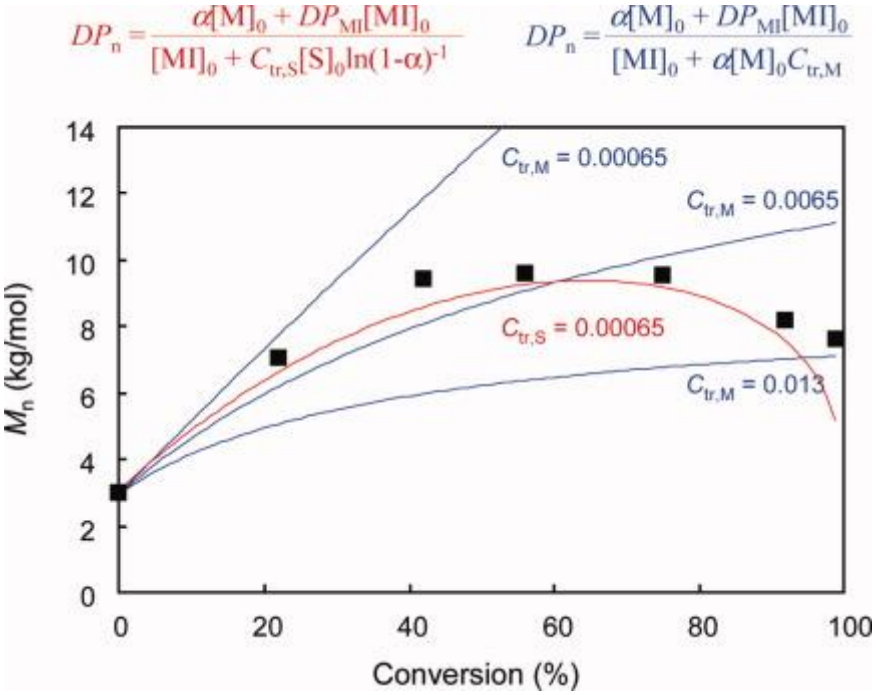

3.1 Introduction

Poly(*N*-isopropylacrylamide, NIPAM) is a well-known temperature-sensitive polymer with a lower critical solution temperature (LCST) in water of about 33 °C.[156-158] The proximity of the LCST to physiological temperature has led to intense research into biological/medical applications.[159, 160] There are numerous reports of homo- and co-polymerizations of NIPAM under conventional (nonliving) radical and controlled/living radical polymerization (CLRP) conditions. CLRP of NIPAM has been reported using nitroxide-mediated radical polymerization (NMP),[59, 76, 77, 79, 161-163] atom transfer radical polymerization (ATRP),[161, 164, 165] reversible addition-fragmentation chain transfer (RAFT) polymerization,[161, 166-176] organotellurium-mediated radical polymerization,[177] and single electron transfer living radical polymerization.[178] NIPAM is a solid at room temperature (mp = 60-63 °C), and is most commonly polymerized in solution, using benzene,[163, 166, 179] alcohols,[164, 178, 180] 1,4-dioxane,[166, 167, 172, 173, 176] *N*,*N*-dimethylformamide (DMF),[59, 76, 77, 162, 169, 177] anisole,[161, 165] or water[174, 175] as solvents.

Chain transfer to monomer or solvent can play an important role in radical polymerization under certain conditions. Ultimately, for a given set of conditions, chain transfer to monomer or solvent dictates an upper limit in accessible molecular weight (MW), which may influence both a conventional radical polymerization (RP) and CLRP.[181] In CLRP, significant occurrence of such chain transfer events does not only influence the accessible MW but also compromises both control over the molecular weight distribution (MWD) and livingness (end functionality). For example, it has been reported that chain transfer to solvent (DMF, anisole, and p-xylene) in the NMP of *tert*-butyl acrylate caused the number average molecular weight (M_n) to deviate downward from the theoretical M_n ($M_{n,th}$) with increasing conversion and even go through a maximum.[182] It has also been shown that chain transfer to monomer in NMP may cause a similar, but less pronounced, deviation from $M_{n,th}$.[68, 71] However, poor performance of a CLRP may be due to a number of reasons, and it can often be difficult to ascribe deviations from ideal controlled/living behaviour specifically to chain transfer events.

In the present study, chain transfer to solvent has been analyzed in detail in both the conventional RP and CLRP of NIPAM in DMF. As far as we are aware, chain transfer to solvent constants ($C_{tr,S}$) for this important monomer have to date not been

reported for any solvent. It is shown that significant chain transfer to solvent occurs, and that these chain transfer reactions preclude synthesis of high molecular weight poly(NIPAM) by NMP in DMF. Various analytical equations are used to show that the same values of $C_{tr,S}$ (within experimental error) can accurately describe the chain transfer events observed in both conventional RP and CLRP of NIPAM.

The author of this thesis carried out experiments 3.2.4, 3.2.5 and 3.2.7.

3.2 Experimental

3.2.1 Materials

tert-Butyl acrylate (*t*-BA, Aldrich, 98%) and *N*-isopropylacrylamide (NIPAM, Aldrich, 97%) were purified by distillation under reduced pressure and recrystallization from 3:2 benzene:hexane, respectively. 2,2′-Azobisisobutyronitrile (DuPont Chemical Solution Enterprise) was recrystallized twice from methanol, and *t*-butyl peroxide (TBP, Aldrich, 98%) was used as received. *N*-tert-Butyl-*N*-[1-diethylphosphono(2,2-dimethylpropyl)]oxy (SG1) was prepared according to the literature,[56] Poly(*t*-BA)-SG1 macroinitiator (MI) with M_n = 3,000 g mol^{-1} and M_w/M_n = 1.17 g mol^{-1} was prepared by precipitation NMP in supercritical carbon dioxide, according to the procedure in chapter 2.[183] HPLC grade solvents were used throughout, and lithium bromide (LiBr) was used as received.

3.2.2 Measurements

M_n and M_w/M_n were determined using a gel permeation chromatography (GPC) system described in chapter 2. Measurements were carried out at 60 °C at a flow rate of 1.0 mL min^{-1} using HPLC-grade DMF containing 0.01 M LiBr as the eluent.[184, 185] The columns were calibrated using six poly(St) standards (M_n = 376–2,570,000 g mol^{-1}). The present GPC methodology for poly(NIPAM) has previously been adopted in NIPAM CLRP studies.[59, 168, 170, 177] To the best of our knowledge, Mark–Houwink-Sakurada parameters are not available for poly(NIPAM)/DMF/LiBr/Poly(St). Work by Ganachaud et al.[166] has indicated that the error in M_n values estimated by GPC analysis of poly(NIPAM) relative to poly(St) standards using THF as eluent is approximately 5% on average (depending on the molecular weight), and it is expected that the GPC error in this work is of similar order. The GPC analysis is further complicated by the fact that the polymers prepared by NMP are block copolymers of *t*-BA and NIPAM. ^{1}H

NMR spectra were recorded using a Joel GXFT 400 MHz instrument equipped with a DEC AXP 300 computer workstation.

3.2.3 General Polymerization Details

All reaction mixtures were added to Pyrex ampoules and subjected to several freeze-thaw degas cycles before sealing under vacuum. The ampoules were heated in an aluminium heating block at the designated temperature for various times. Polymerizations were stopped by placing ampoules in an ice-bath. GPC measurements were carried out on the non-precipitated reaction mixtures. Conversions were estimated using ^{1}H NMR by comparing the integration of the polymer peak at 3.85 ppm [$CH(Me)_2$] with NIPAM monomer at 4.01 ppm [$CH(Me)_2$].

3.2.4 Conventional Radical Polymerization

Stock solutions containing 0.41, 1.37 and 4.1 mM TBP were made up in DMF. The obtained stock solution (4 mL) was added to NIPAM (0.91 g, 8.00 mmol) in a Pyrex ampoule. Evacuated ampoules were heated at 120 °C for various times.

3.2.5 Chain Transfer to Solvent (Mayo Plot)

DMF stock solution (4 mL) containing 0.41 mM of TBP was added to NIPAM (0.29 g, 2.56 mmol; 0.39 g, 3.45 mmol; 0.58 g, 5.12 mmol; and 1.17 g, 10.34 mmol) in a Pyrex ampoule. Evacuated ampoules were heated at 120 °C for various times. Conversions were less than 5% in all cases.

3.2.6 Nitroxide-Mediated Polymerizations (Performed by Yusuke Sugihara)

The following polymerizations in DMF (4 mL) were carried out $[NIPAM]_0/[poly(t\text{-}BA)\text{-}SG1]_0$ = 100 (a), 200 (b), and 300 (c); (a) NIPAM (0.91 g, 8.00 mmol), poly(*t*-BA)-SG1 (0.24 g, 8.00 x 10^{-2} mmol), and SG1 (5.89 mg, 2.00 x 10^{-2} mmol); (b) NIPAM (0.91 g, 8.00 mmol), poly(*t*-BA)-SG1 (0.12 g, 4.00 x 10^{-2} mmol), and SG1 (2.94 mg, 1.00 x 10^{-2} mmol); (c) NIPAM (0.91 g, 8.00 mmol), poly(*t*-BA)-SG1 (0.080 g, 2.67 x 10^{-2} mmol), and SG1 (1.96 mg, 0.67 x 10^{-2} mmol).

3.2.7 Thermal Polymerization in the Absence of Initiator and Nitroxide

Evacuated ampoules containing NIPAM (0.91 g, 8.00 mmol) in DMF (4 mL) were heated at 120 °C for various times.

3.3 Results and Discussion

3.3.1 Limiting Molecular Weight

Under normal conditions of conventional (nonliving) radical polymerization in the absence of a chain transfer agent, the main end-forming event is bimolecular termination. However, when the rate of initiation in a bulk polymerization is sufficiently low, the propagating radical concentration becomes so low that the bimolecular termination rate is reduced to the point that chain transfer to monomer becomes the main end-forming event.[181] The ratio $k_p/k_{tr,M}$ (=1/$C_{tr,M}$; k_p is the propagation rate coefficient, $k_{tr,M}$ the rate coefficient for chain transfer to monomer) dictates the maximum attainable number-average degree of polymerization (DP_n) for a given monomer. In a solution polymerization, the chain transfer to monomer limit is only reached if the rate of chain transfer to solvent is negligible relative to the rate of chain transfer to monomer. If chain transfer to solvent is the main end-forming event, $DP_n = k_p[M]/k_{tr,S}[S]$ (= $[M]/C_{tr,S}[S]$) ($k_{tr,S}$ is the rate coefficient for chain transfer to solvent, [M] and [S] are the monomer and solvent concentrations, respectively).

3.3.2 Conventional Radical Polymerization in DMF

By performing a series of radical polymerizations with decreasing initiator concentration, DP_n will increase with decreasing initiator concentration until the maximum DP_n is reached, corresponding to either the chain transfer to monomer or solvent limit. Polymerizations of NIPAM in DMF were carried out at 120 °C (relevant to NMP) using three different low concentrations of the high-temperature initiator, TBP. All MWDs are very similar (Figure. 3.01; M_n = 20,100 g mol^{-1} ($[TBP]_0$ = 4.1 mM), 17,600 g mol^{-1} ($[TBP]_0$ = 1.4 mM), 21,100 g mol^{-1} ($[TBP]_0$ = 0.41 mM), and 21,600 g mol^{-1} ($[TBP]_0$ = 0), consistent with the majority of propagating radicals being transformed to dead chains and new propagating radicals by chain transfer to monomer or solvent.

3.3.3 Nitroxide-Mediated Radical polymerization

NMP can be a useful mechanistic tool in radical polymerization, because, ideally, the number of chains is constant throughout the polymerization. Moreover, if one initiates the polymerization with a MI of relatively high molecular weight, chain transfer events to low molecular weight species like monomer and solvent are likely to be readily detected in the MWDs.[68] The concept of a maximum molecular weight imposed by chain transfer to monomer or solvent applies to both conventional RP and CLRP (including NMP).

Figure 3.02 shows conversion versus time data for NMP of NIPAM in DMF at 120 °C initiated by three different concentrations of poly(*t*-BA)-SG1 (MI), revealing that R_p is (within experimental error) independent of the MI concentration to high conversion. Such behaviour is observed if the polymerization proceeds in the stationary state with respect to the propagating radical concentration, for example, styrene/ TEMPO/125 °C.[43, 45] A somewhat more special case where R_p is independent of the MI concentration is when the rate of spontaneous radical initiation (from monomer or adventitious impurities) is close to zero in the presence of an excess amount of free nitroxide.[45, 67] Because of the uncertainties in rate coefficients of the present system, further speculation on this topic will not be made. The MWDs shift to higher molecular weights with increasing conversion, but significant low molecular weight tailing is visible (Figure 3.03), consistent with chain transfer to monomer or solvent. Figure 3.04 shows M_n versus conversion, revealing how M_n initially increases with conversion but then reaches a maximum value and decreases at high conversion. The values of M_w/M_n gradually increase with increasing conversion (Figure 3.04).

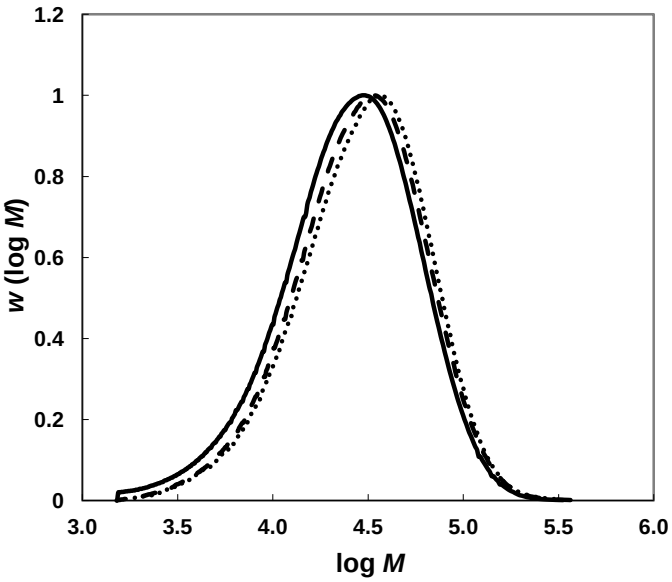

Figure 3.01: MWDs for the conventional radical polymerization of NIPAM (2 M) in DMF initiated by TBP at 120 °C for initiator concentrations of 0.41 (13%, dotted), 1.4 (33%, continuous) and 4.1 mM (22%, dashed), with monomer conversions as indicated.

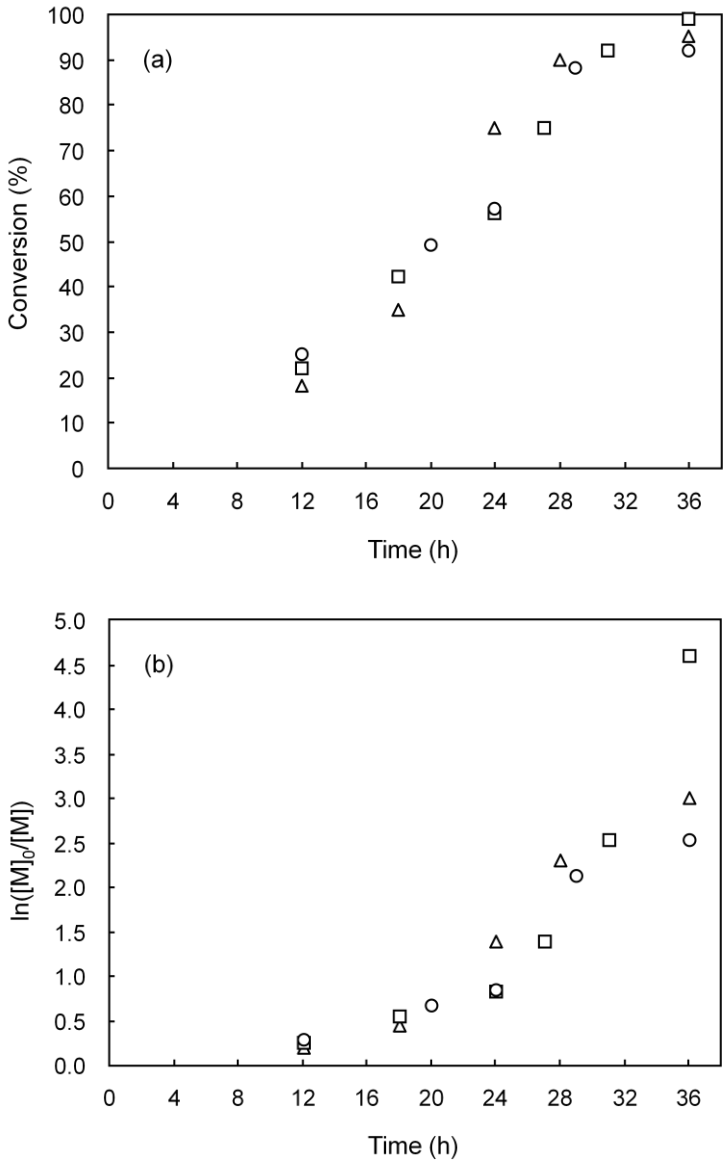

Figure 3.02: Conversion vs. time data (a) and first-order plot (b) for NMP of NIPAM in DMF (2 M) using Poly(*t*-BA)-SG1 as MI with 25 mol% free SG1 relative to MI at 120 °C with $[M]_0/[MI]_0$ = 100 (○), 200 (□), and 300 (Δ).

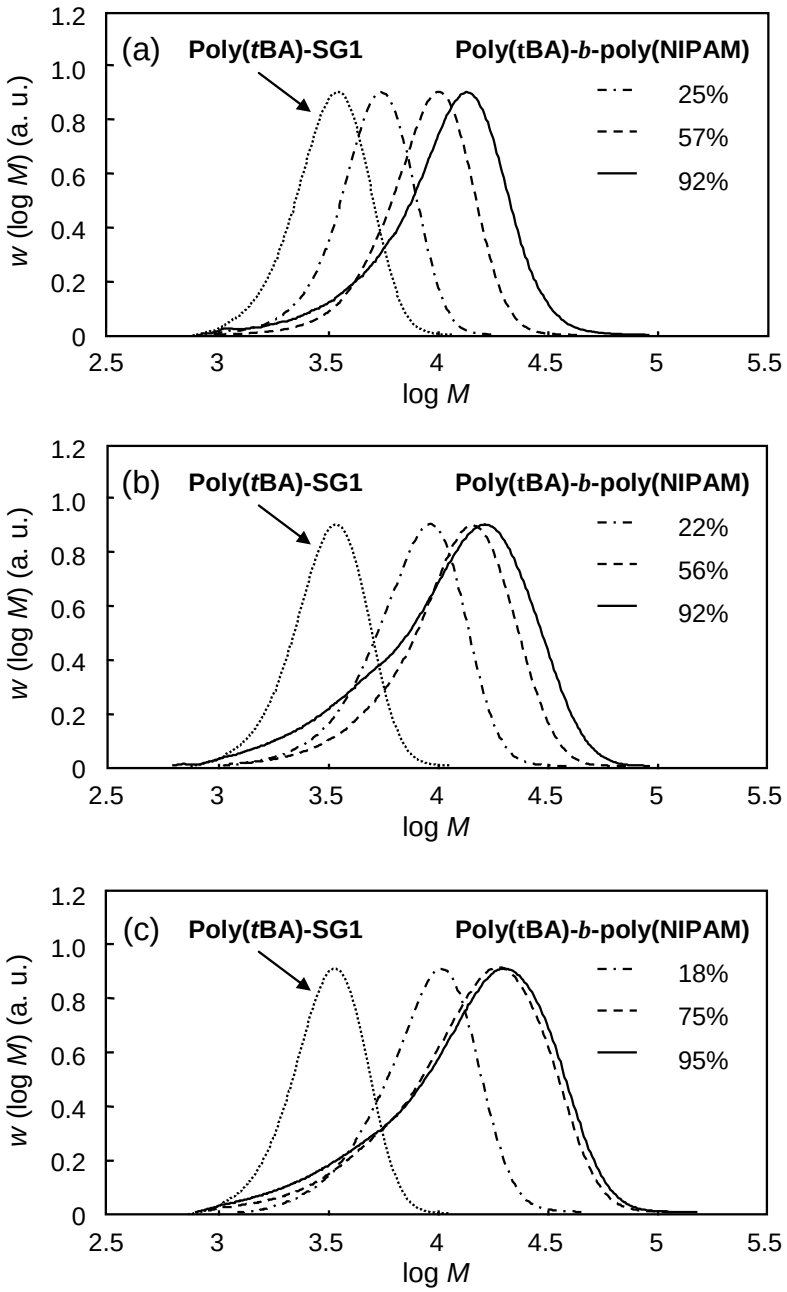

Figure 3.03: MWDs of poly(*t*-BA)-*b*-poly(NIPAM) and original poly(*t*-BA)-SG1 for $[M]_0/[MI]_0$ = 100 (a), 200 (b), 300 (c) with NIPAM conversions as indicated.

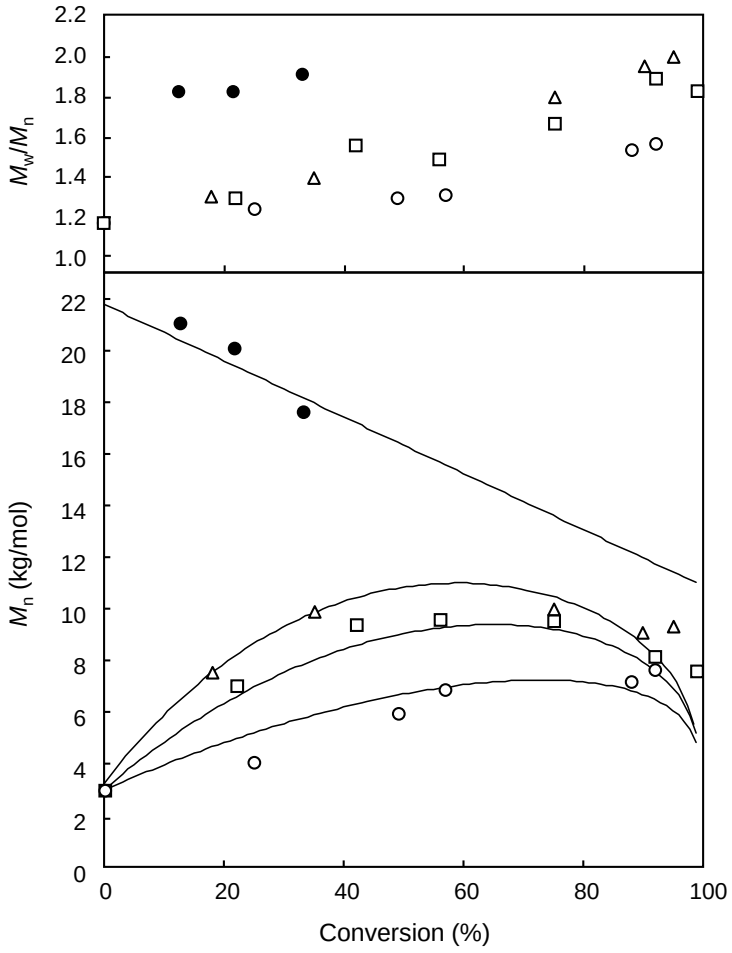

Figure 3.04: M_w/M_n (top) and M_n (bottom) vs conversion plots for NMP of NIPAM in DMF (2 M) at 120 °C with poly(*t*-BA)-SG1 as MI with 25 mol% free SG1 relative to MI and $[M]_0/[MI]_0$ = 100 (○), 200 (□), and 300 (Δ), and conventional RP of NIPAM (2 M) in DMF at 120 °C with various concentrations of TBP as initiator (•) in DMF at 120 °C (each data point corresponding to a different $[TBP]_0$). The full lines are theoretical M_n using Equation 3.04 and 3.07 with $C_{tr,S}$ = 0.00065 (NMP) and 0.0008 (conventional radical polymerization). Theoretical lines were modelled by A/Prof Per B. Zetterlund.

3.3.4 Chain Transfer to Solvent/Monomer

The concept of instantaneous DP_n is not applicable to CLRP because chains grow throughout the polymerization. The value of DP_n as a function of conversion is equal to the concentration of reacted monomer plus the concentration of monomeric units in the MI, divided by the total number of chains. The latter equals the MI concentration plus the concentration of chains generated during the course of the polymerization. Thus, in the case of new chain generation by chain transfer, DP_n is given as a function of [M] by Equation 3.01 and 3.02.

$$DP_n = \frac{\alpha[M]_0 + DP_{MI}[MI]_0}{[MI]_0 + [chains]_{new}} \tag{3.01}$$

$$[chains]_{new} = -\int_{[M]_0}^{[M]} \left(\frac{\sum_i C_{tr,i}\,[X]_i}{[M]} \right) d[M] \tag{3.02}$$

where α denotes monomer conversion, $[X_i]$ is the concentration of a low molecular weight species to which chain transfer occurs (where i denotes monomer, solvent, chain transfer agent, etc.), and [MI] is the macroinitiator concentration. In the case of chain transfer to monomer only (where $C_{tr,M}$ is the chain transfer to monomer constant), we obtain:

$$DP_n = \frac{\alpha[M]_0 + DP_{MI}[MI]_0}{[MI]_0 + \alpha[M]_0 C_{tr,M}} \tag{3.03}$$

In the case of chain transfer to solvent only, assuming also that [S] is constant, we can write:[186]

$$DP_n = \frac{\alpha[M]_0 + DP_{MI}[MI]_0}{[MI]_0 + C_{tr,S}[S]_0 \ln(1-\alpha)^{-1}} \tag{3.04}$$

Figure 3.05 shows M_n vs conversion computed from Equation 3.03, for various values of $C_{tr,M}$ for $[M]_0/[MI]_0$ = 200. It is immediately obvious that regardless of the

value of $C_{tr,M}$, the agreement with the experimental data is not satisfactory. A maximum in M_n vs conversion cannot be explained by chain transfer to monomer, regardless of the value of $C_{tr,M}$. Figure 3.04 shows experimental data of M_n vs conversion for three different $[M]_0/[MI]_0$ overlaid with predictions from Equation 3.04, using $C_{tr,S}$ = 6.5 x 10^{-4}. The agreement between the model and the experimental data is very good and it is noted how Equation 3.04 correctly predicts the maximum observed experimentally. Moreover, the data sets corresponding to all three MI concentrations can be successfully fitted with the same value of $C_{tr,S}$. The maximum M_n reached in the NMPs are all markedly lower than the maximum M_n as dictated by the expression $k_p[M]_0/k_{tr,S}[S]_0$ (≈ 27,000 g mol^{-1} based on $C_{tr,S}$ = 6.5 x 10^{-4}, not considering M_n of the macroinitiator; see Section 3.2.1). The reason is that in NMP (and any CLRP), each chain transfer to solvent event generates a new living chain, thus reducing the number of chains over which the remaining monomer units are to be distributed (this is accounted for in Equation 3.04).

We have very recently reported [79] (see chapter 4) that nitroxide-mediated (SG1) radical polymerization of NIPAM in supercritical carbon dioxide (as an inverse suspension polymerization, i.e. in the absence of solvent capable of undergoing chain transfer) proceeds to M_n ≈ 11,000 g mol^{-1} with M_n vs conversion being a straight line close to $M_{n,th}$, thus providing strong evidence that chain transfer to monomer is not occurring to any significant extent in the present study either.

Chain-stopping events specific to NMP in general include (polymeric) alkoxyamine decomposition [187] and hydrogen transfer from hydroxylamine (formed by hydrogen abstraction by nitroxide) to propagating radicals.[188] The rates of these reactions in the case of SG1 and NIPAM under the present conditions are not known. However, these reactions do not alter the number of chains and therefore M_n is not expected to be affected. The fact that very similar chain transfer to solvent constants were obtained for conventional radical polymerization and NMP in the present work suggest that any influence of such side reactions is very minor at most.

In the case of conventional radical polymerization, the instantaneous DP_n is equal to $[M]/(\Sigma C_{tr,i}[X_i]) + DP_{n,0}$ (where $DP_{n,0}$ is DP_n in the absence of transfer) as given by the Mayo equation. The Mayo equation can be formulated as a function of [M] and the cumulative DP_n at a given conversion (i.e. the overall DP_n of the polymer formed between zero and a given conversion) as shown by Equation 3.05.

$$DP_{\mathrm{n}} = \frac{1}{[\mathrm{M}] - [\mathrm{M}]_0} \int_{[\mathrm{M}]_0}^{[\mathrm{M}]} \left(\frac{k_{\mathrm{p}}[\mathrm{M}]}{\sum_i k_{tr,i}\,[\mathrm{X_i}] + (k_{\mathrm{t}} + k_{\mathrm{td}})[\mathrm{P}^\bullet]} \right) d[\mathrm{M}] \qquad (3.05)$$

where k_t is the overall termination rate coefficient, k_{td} is the rate coefficient for termination by disproportionation, and $k_{tr,i}$ is the rate coefficient for chain transfer to species X_i. Assuming that all end-forming events are chain transfer to monomer (Equation 3.06) or solvent (Equation 3.07), with the additional assumption of a constant [S], DP_n can be expressed as functions of conversion.

$$DP_n = \frac{1}{C_{\mathrm{tr,M}}} \qquad (3.06)$$

$$DP_n = \frac{[\mathrm{M}]_0(2-\alpha)}{2[\mathrm{S}]_0 C_{\mathrm{tr,S}}} \qquad (3.07)$$

Even if chain transfer to monomer or solvent is the predominant end-forming event, some fraction of propagating radicals will inevitably undergo bimolecular termination, which will cause deviation from DP_n as given by Equations 3.06 and 3.07. Note that Equation 3.06 shows that the cumulative DP_n is the same as the instantaneous DP_n when chain transfer to monomer is the end-forming event. In the case of chain transfer to solvent being the end-forming event, Equation 3.07 reveals that the cumulative DP_n decreases with conversion.

The conventional data at three different (low) initiator concentrations at 120 ºC in DMF (from Figure 3.01) were plotted as M_n vs conv. in Figure 3.04. Equation 3.07 was subsequently fitted to this data, resulting in good agreement with $C_{tr,S} = 8.0 \times 10^{-4}$. This value of $C_{tr,S}$ is very close to the value derived by fitting Equation 3.04 to the NMP experiments ($C_{tr,S} = 6.5 \times 10^{-4}$). The somewhat higher value of $C_{tr,S}$ obtained in the case of conventional radical polymerization may be a result of bimolecular termination reactions between propagating radicals (which would cause propagating radicals to stop growing prior to reaching the chain transfer to solvent limit). Bimolecular termination would of course also occur to some minor extent in the NMP system, but the extent of such termination reactions in an NMP system without transfer reactions would obviously be much lower than in a conventional radical polymerization without chain transfer (in the latter case, all propagating radicals would undergo bimolecular

termination). The data nicely illustrate how the same $C_{tr,S}$ (within experimental error, and allowing for the "error" due to termination in the conventional radical polymerization) can be employed to (and also that $C_{tr,M}$ cannot) rationalize the polymerization behaviour of NIPAM in DMF with regards to chain transfer to solvent both in controlled/living (NMP) and conventional RP.

The four different scenarios, i.e. chain transfer to monomer or solvent in conventional radical polymerization and NMP, are plotted in Figure 3.06. Conventional radical polymerization: In the case of chain transfer to monomer, theory predicts DP_n to remain constant with conversion, whereas in the case of chain transfer to solvent, DP_n decreases with conversion. CLRP: In the case of chain transfer to monomer, DP_n gradually deviates downward from the theoretical values (i.e. a straight line), whereas in the case of chain transfer to solvent, DP_n goes through a maximum.

3.3.5 Estimation of $C_{tr,S}$ via Mayo Plot

The value of $C_{tr,S}$ in the conventional radical polymerization of NIPAM in DMF at 120 °C was also estimated based on the classical Mayo treatment:

$$\frac{1}{DP_n} = \frac{1}{DP_{n,0}} + C_{tr,S}\frac{[S]}{[M]} \qquad (3.08)$$

where $DP_{n,0}$ is DP_n when [S] = 0. The slope of the straight line obtained by plotting $1/DP_n$ vs [S]/[M] (Figure 3.07) yields $C_{tr,S}$ = 9.2 x 10^{-4}, which is in relatively good agreement with $C_{tr,S}$ = 8.0 x 10^{-4} (Equation 3.07) and 6.5 x 10^{-4} (Equation 3.04) (Table 3.01).

$C_{tr,S}$ from Mayo plot (Conventional RP)	$C_{tr,S}$ from Equation 3.07 (Conventional RP)	$C_{tr,S}$ from Equation 3.04 (NMP)
9.2 x 10^{-4}	8.0 x 10^{-4}	6.5 x 10^{-4}

Table 3.01: Values of $C_{tr,S}$ for RP of NIPAM in DMF at 120 °C estimated in the present work.

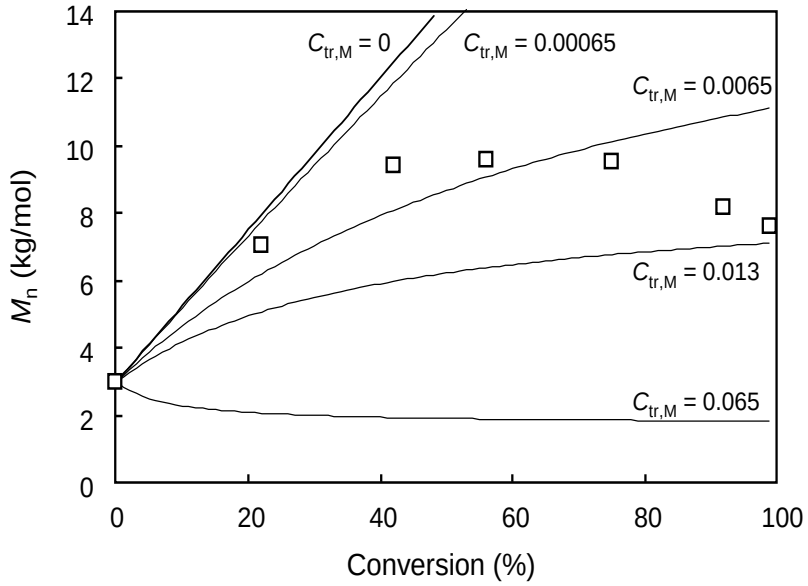

Figure 3.05: M_n vs conversion plots for NMP of NIPAM in DMF (2 M) at 120 °C with poly(*t*-BA)-SG1 as MI with 25 mol% free SG1 relative to MI and $[M]_0/[MI]_0$ = 200. Solid lines are computed from Equation 3.03 with various $C_{tr,M}$. Theoretical lines were modelled by A/Prof Per B. Zetterlund.

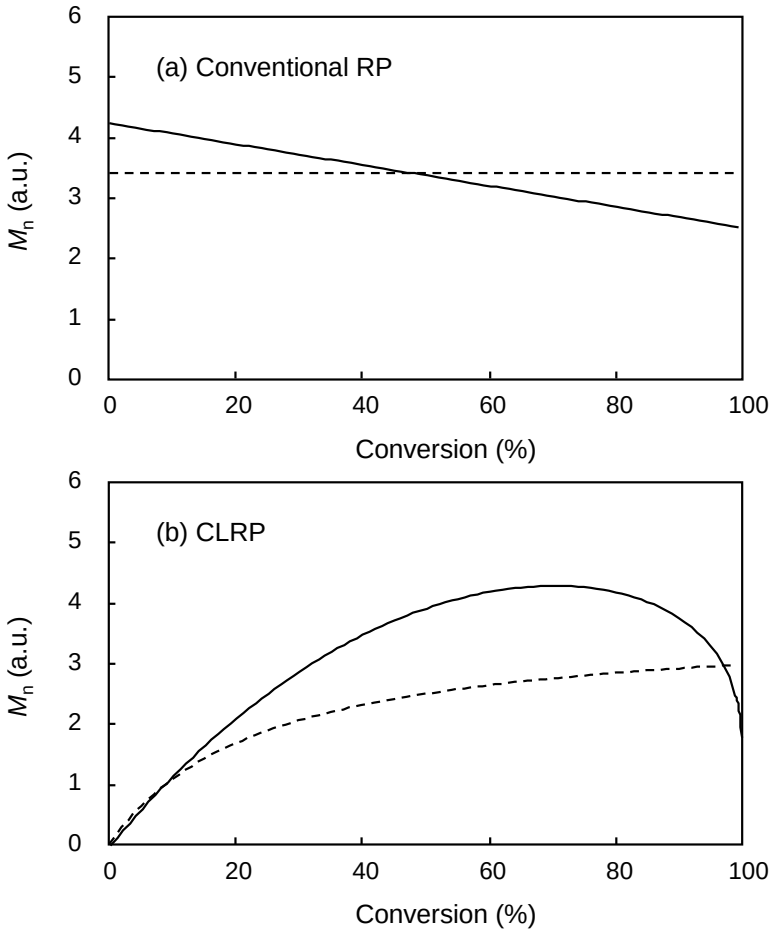

Figure 3.06: Typical traces of M_n against conversion in conventional radical polymerization (a) and controlled/living radical polymerization (b) with chain transfer to monomer (broken line) and chain transfer to solvent (solid line). Theoretical lines were modelled by A/Prof Per B. Zetterlund.

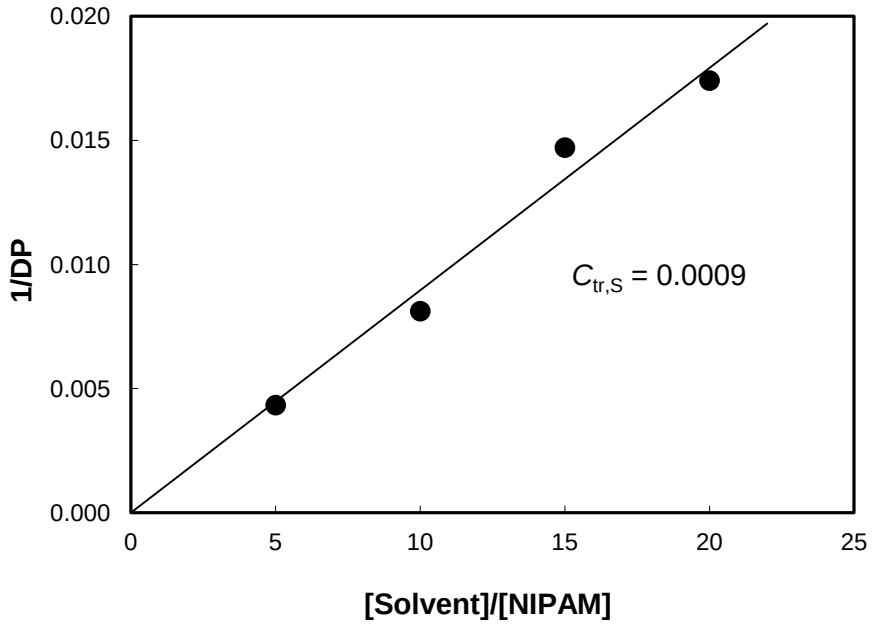

Figure 3.07: Mayo plot of NIPAM in DMF initiated by TBP at 120 °C for initiator concentrations of 0.41 mM. Solid lines correspond to $1/DP_n = (1/DP_{n,0}) + C_{tr,S}[S]_0/[M]_0$

3.3.6 Number of New Chains

Alternatively, the effects of chain transfer in NMP can be discussed based on the number of new chains generated as a function of conversion. Experimental values of the concentrations of new chains ($[\text{chains}]_{new}$) can be readily calculated from Equation 3.09.

$$[\text{chains}]_{\text{new}} = [\text{MI}]_0 \left(\left(\frac{DP_{Max}}{DP} \right) - 1 \right) \qquad (3.09)$$

Figure 3.08 shows the experimental $[\text{chains}]_{new}$ from Equation 3.09 as well as theoretical predictions based on chain transfer to monomer ($[\text{chains}]_{tr,M} = \alpha[\text{M}]_0 C_{tr,M}$) for $[\text{M}]_0/[\text{MI}]_0 = 200$, revealing that the theoretical prediction is in disagreement with the experimental data regardless of the value of $C_{tr,M}$. However, the concentration of new chains based on chain transfer to solvent ($[\text{chains}]_{tr,S} = C_{tr,S}[\text{S}]_0 \ln(1-\alpha)^{-1}$; Figure 3.09), the data for all three [MI] are in good agreement with theory for $C_{tr,S} = 6.5 \times 10^{-4}$ (the value obtained from fitting M_n vs conversion). One single master curve is formed for all [MI], because the number of new chains is a function of the total number of propagation steps and thus independent of $[\text{MI}]_0$ (as apparent from Equation 3.04).

3.3.7 Molecular Weight Distribution

A plot of M_w/M_n vs $[\text{chains}]_{tot}/[\text{MI}]_0$ (i.e. the total number of chains relative to the initial number of chains as given by the initial [MI]; Figure 3.10) for all three [MI] shows clearly how the generation of new chains is an important factor causing a gradual loss of control with increasing conversion. Interestingly, the data points for all three [MI] fall on the same master curve in this particular case. The effect of new chain generation on the MWD increases in magnitude with increasing $M_{n,th}$ (i.e. decreasing [MI], Figure 3.04). The NMP data in Figure 3.04 reveal that M_n begins to deviate downwards from $M_{n,th}$ with increasing conversion, consistent with chain transfer to solvent becoming increasingly significant. The newly generated radicals would have the same probability of propagation as longer living radical chains and the low MW tail observed in the MWDs would thus mainly consist of living chains from chain transfer to solvent shifting to higher MW with conversion (Figure 3.03). Consequently, even in the event of fairly significant chain transfer to solvent, the livingness may still be reasonable (especially considering the excess of free SG1 used in the present work).

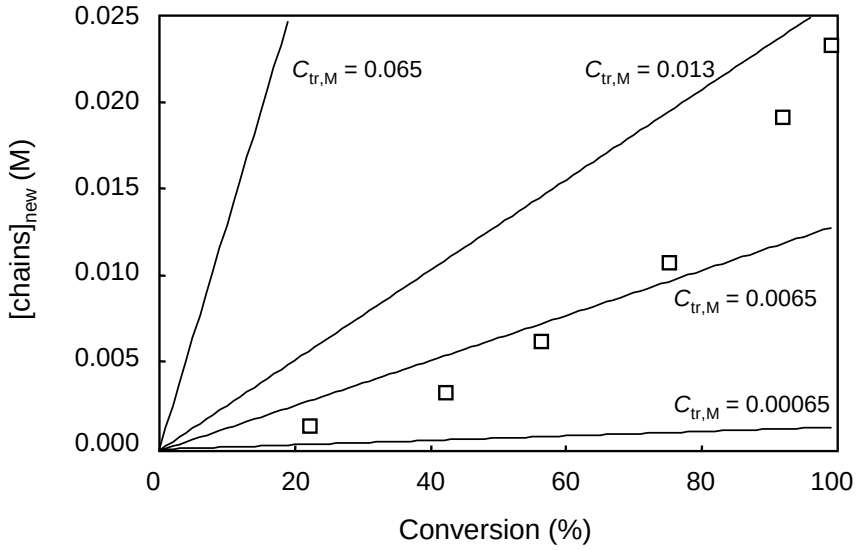

Figure 3.08: $[chains]_{new}$ vs conversion plots for NMP of NIPAM in DMF (2 M) at 120 °C using poly(*t*-BA)-SG1 as MI with 25 mol% free SG1 relative to MI and $[M]_0/[MI]_0$ = 200. Solid lines correspond to $[chains]_{tr,M} = \alpha[M]_0 C_{tr,M}$ (see Equation 3.03). Theoretical lines were modelled by A/Prof Per B. Zetterlund.

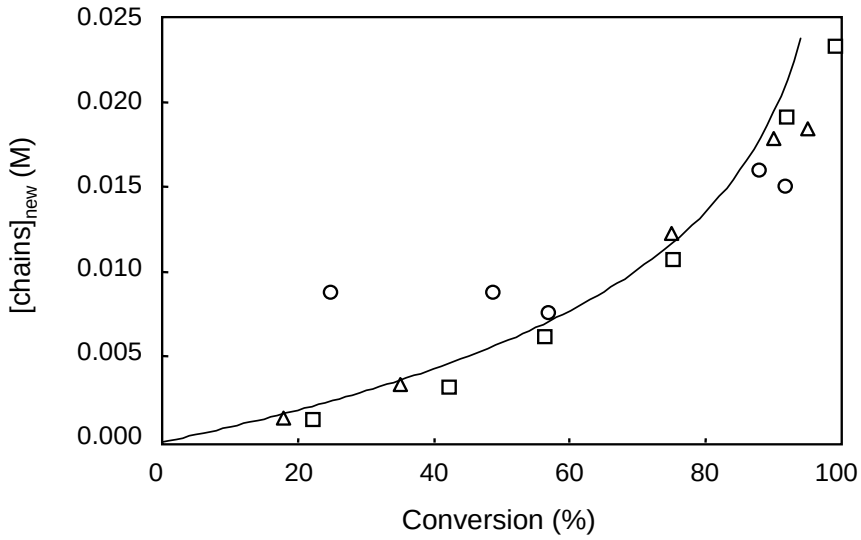

Figure 3.09: $[chains]_{new}$ versus conversion plots for NMP of NIPAM in DMF (2 M) at 120 °C using poly(*t*-BA)-SG1 as MI with 25 mol% free SG1 relative to MI with $[M]_0/[MI]_0$ = 100 (○), 200 (□) and 300 (Δ). The line represents $[chains]_{tr,S} = C_{tr,S}[S]_0\ln(1-\alpha)^{-1}$ (see Equation 3.04) for $C_{tr,S} = 6.5 \times 10^{-4}$. Theoretical line was modelled by A/Prof Per B. Zetterlund.

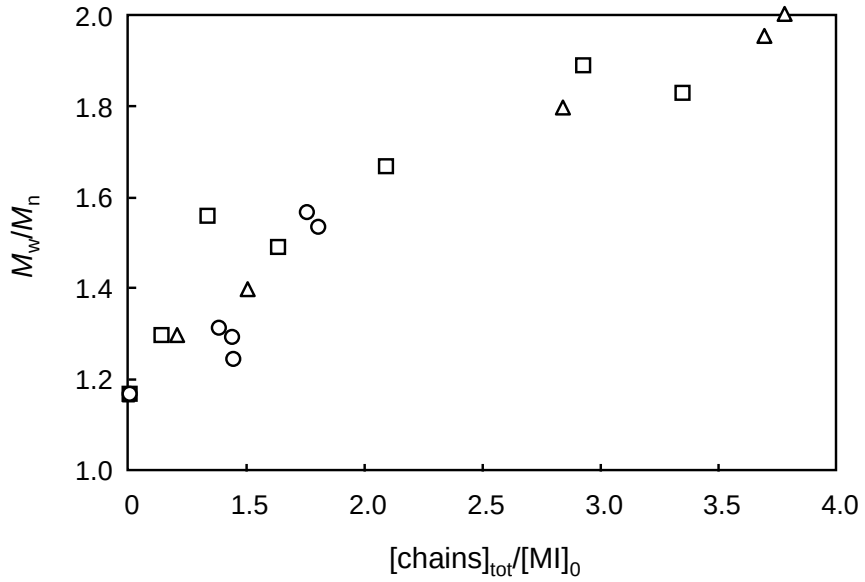

Figure 3.10: M_w/M_n vs $[chains]_{tot}/[MI]_0$ for NMP of NIPAM in DMF (2 M) at 120 °C using poly(*t*-BA)-SG1 as MI with 25 mol% free SG1 relative to MI with $[M]_0/[MI]_0$ = 100 (○), 200 (□), and 300 (Δ).

3.3.8 Effect of Poly(acrylate) Macroinitiator

Acrylate polymerization is complicated by the formation of mid-chain radicals (MCRs) that are formed by intra- (backbiting) or intermolecular chain transfer reactions.[189-191] It has been reported recently that the extent of branch formation via MCRs is significantly lower in CLRP than conventional radical polymerization.[192] However, it is conceivable that MCRs may form during NMP due to the presence of the poly(acrylate) MI, and subsequent fragmentation of MCR would result in an increase in the number of chains and thus a decrease in M_n. However, if this occurred to any significant extent, the master curve of $[chains]_{new}$ vs conversion Figure 3.09 would not be observed, and furthermore, it would not be possible to fit all data (NMP for three different [MI] and conventional RP) with one single value of $C_{tr,S}$ (Figures 3.04 and 3.09). It can thus be concluded that MCR formation followed by fragmentation is not a significant mechanism with regards to generation of new chains.

3.3.9 Spontaneous Initiation

Spontaneous (thermal) initiation (i.e. no initiator present) has been previously reported in the polymerization of acrylates and acrylamides.[193-195] In order to estimate the extent of thermal generation of chains, polymerizations of NIPAM (2 M) in the absence of initiator and nitroxide were carried out in DMF at 120 ºC. The rate of thermal initiation ($R_{i,th}$) can be estimated from the slope of a first-order plot (Figure 3.11) according to Equation 3.10:

$$Slope = k_p[P^\bullet] = k_p\sqrt{\frac{R_{i,th}}{2k_t}}$$

Based on a slope of 3.19 x 10^{-6} and a literature value for $k_p/k_t^{0.5}$ = 0.24 $M^{0.5}$ $s^{0.5}$ in DMF at 65° C,[196] a $R_{i,th}$ = 1.8 x 10^{-10} s^{-1} was calculated. Assuming that $R_{i,th}$ is independent of conversion, the concentration of chains generated by spontaneous initiation is equal to $R_{i,th}$ multiplied by the polymerization time (longest time = 36 h), which gives 2.3 x 10^{-5} M. Considering that the [MI] is 6.7 x 10^{-3} M or higher, it can be safely concluded that the contribution of spontaneous initiation to the overall number of chains in the system is insignificant (especially considering that the value of $k_p/k_t^{0.5}$ will be higher at 120 °C than at 65 °C).

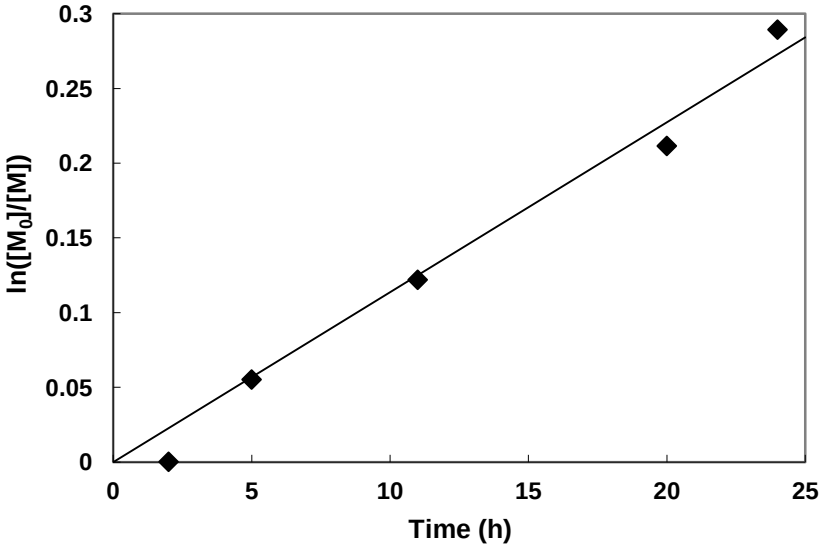

Figure 3.11: First–order plot of spontaneous polymerization (in the absence of initiator or nitroxide) of NIPAM (2 M) in DMF at 120 °C (the solid line is a best fit).

3.3.10 Comparison with Literature

Table 3.01 lists the values of $C_{tr,S}$ estimated in this work based on Equation 3.04 (NMP) and 3.07 (conventional RP). $C_{tr,S}$ for NIPAM have to date not been reported for any solvent. Min et al, [197] studied the conventional radical polymerization of NIPAM initiated by γ-radiation in a wide range of solvents, reporting strong solvent effects on the molecular weights obtained and speculated that this may be caused by differences in the extents of chain transfer to solvent. Of the solvents investigated, the highest molecular weight was obtained for water and the lowest for THF (DMF was not investigated). McCormick and co-workers [198] reported RAFT of NIPAM in DMF at 25 °C, obtaining close to linear M_n vs conversion plots with M_n as high as 44,500 g mol^{-1} with excellent control over the MWD. The absence of any apparent influence of chain transfer to DMF is most likely a result of the low polymerization temperature ($C_{tr,S}$ increases with temperature) as well as the higher ratio [monomer]/[solvent] in their work. In the nitroxide-mediated stabilizer-free inverse suspension polymerization of NIPAM in $scCO_2$ (discussed in chapter 4) M_n did not deviate significantly from $M_{n,th}$ with increasing conversion, consistent with chain transfer to CO_2 being negligible (as well as chain transfer to monomer), and thus supporting the present results.[79]

Conventional RP of St (60 °C) and *t*-BA (115 °C) in DMF have been reported to proceed with $C_{tr,S} = 4 \times 10^{-4}$ [199] and 8.6×10^{-4}, respectively, [200] with a similar value of, $C_{tr,S} = 6.0 \times 10^{-4}$ for the NMP of acrylic acid in 1,4-dioxane.[71] The $C_{tr,S}$ values for these monomers are similar to $C_{tr,S}$ for NIPAM/DMF observed in the present work. Downward deviations of M_n from $M_{n,th}$ with increasing conversion ($M_n < M_{n,th}$) have also been reported for other CLRPs in DMF, including the SG1-mediated polymerizations of *t*-BA [200] and RAFT polymerizations of hydrophobic acrylamides, [201] consistent with chain transfer to solvent. Thus, chain transfer seems to be more significant to DMF than to other common polymerization solvents, possibly due to the greater stability of the DMF adduct radical. There are nevertheless scant reports of DMF generating radicals in small molecule reactions, [202] and DMF has continued to be widely used in the conventional RP and CLRP of NIPAM[198, 203-208] and other monomers.[195, 201, 203, 209-212] The wide literature use of NIPAM/DMF probably stems from its good solvent properties, our preliminary studies showed poly(NIPAM) to be poorly soluble (precipitates to form heterogeneous mixtures in NMPs) in benzene, anisole and *m*-xylene under the polymerization conditions of the present paper.

3.4 CONCLUSIONS

Chain transfer to solvent can be a significant factor in limiting the maximum attainable molecular weight in both conventional RP and NMP of NIPAM. Based on a theoretical treatment, it has been demonstrated that the same value of $C_{tr,S}$ (within experimental error) can be invoked to quantitatively rationalize experimental molecular weight data both in conventional RP and NMP in DMF at 120 °C under conditions where chain transfer to solvent is a significant end-forming event. The extent of chain transfer to solvent can have deleterious effects on both the control over the MWD (higher M_w/M_n) and the maximum attainable molecular weight in NMP (which is normally carried out at elevated temperatures). Chain transfer to solvent in NMP (or any controlled/living radical polymerization technique) may lead to M_n going through a maximum with increasing conversion. This is distinctly different from the case of chain transfer to monomer, in which case M_n also deviates downward from $M_{n,th}$, but never goes through a maximum regardless of the extent of chain transfer to monomer.

CHAPTER 4

Nitroxide-mediated inverse suspension polymerization of *N*-isopropylacrylamide in supercritical carbon dioxide

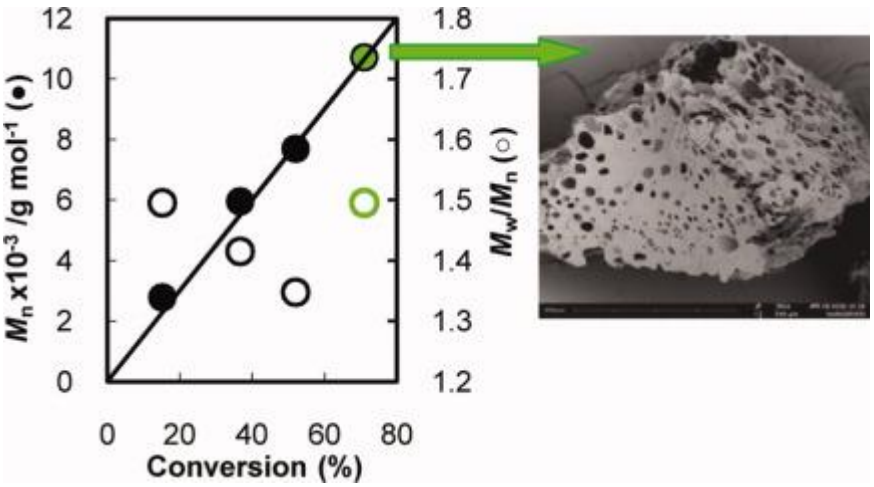

4.1 Introduction

In recent years, benign supercritical carbon dioxide ($scCO_2$) has been widely used to perform heterogeneous (precipitation and dispersion) [143, 213, 214] controlled/living radical polymerization (CLRP) including nitroxide-mediated radical polymerization (NMP), atom transfer radical polymerization (ATRP), and reversible addition-fragmentation chain transfer (RAFT) polymerization.[70, 127, 142, 144] These heterogeneous polymerizations rely upon the solubility of the monomer, initiator, and control agent in $scCO_2$, and the precipitation of polymer chains at a certain critical degree of polymerization (J_{crit}).[70, 127] Beyond J_{crit}, the polymerization continues towards high conversion mainly in the monomer rich particle phase. A dispersion polymerization contains a stabilizer to prevent particle coagulation.

Poly(*N*-isopropylacrylamide, NIPAM) exhibits a phase transition at ~32 °C in water, which is known as the lower critical solution temperature (LCST). The proximity of the LCST to room and physiological temperature has resulted in extensive biotechnological and biomedical applications (including tissue engineering, biomolecule separation and drug delivery).[157, 159, 160] NIPAM is a solid (mp = 60–63 °C), and is most commonly polymerized in solution of alcohols, dioxane, water, or DMF (*N*,*N*-dimethylformamide). The resultant polymer is usually isolated by precipitation from hydrophobic volatile organic compounds (VOC), including petroleum ether and diethyl ether, as non-solvent for poly(NIPAM). CLRP of NIPAM in solution using NMP, [76, 77, 163] ATRP, [164] RAFT, [167-170, 175, 215-219] TERP, [177] (organotellurium-mediated controlled radical polymerization), and SET-LRP (single-electron transfer living radical polymerization) [178] have been carried out, but CLRP of NIPAM in $scCO_2$ has to date not been reported. Low temperature (and microwave assisted) controlled/living aqueous homogeneous polymerizations of water soluble monomers, including acrylamides, have been reported using NMP.[75, 220-222] It is noteworthy that aqueous CLRP of NIPAM relies on precipitation from VOC for polymer isolation [175, 216-219] and non-living aqueous precipitation and interfacial polymerizations use intensive dialysis (water exchange) and centrifugation, respectively, for purifying crosslinked poly(NIPAM) particles.[223, 224] Recently it has been reported (see chapter 3) that the polymerization of NIPAM in VOC is prone to significant chain transfer to solvent (depending on the solvent) limiting the maximum attainable molecular weight.[78]

Literature precipitation and dispersion conventional (nonliving) radical homo- and co-polymerizations of NIPAM (sparingly soluble) in $scCO_2$ use low monomer loadings to ensure that the monomer is initially soluble in the continuous phase.[225-228] In this chapter it is now shown that CLRP of NIPAM can be carried out to high conversion using initial loadings of monomer, where the NIPAM is dispersed in $scCO_2$. NMP[229, 230] is carried out in the absence of stabilizer (which is often expensive or requires prior synthesis) giving poly(NIPAM) as a dry powder and circumventing the requirement for environmentally damaging VOC for polymerization and polymer isolation. It represents the first controlled/living dispersed phase polymerization or non-stabilized suspension polymerization in $scCO_2$.[116]

4.2 Experimental

4.2.1 Materials

N-Isopropylacrylamide (NIPAM, Aldrich 97%) was recrystallized from a mixture of 3:2 benzene/hexane before use. 2,2'- Azobisisobutyronitrile (AIBN, DuPont Chemical Solution Enterprise) was recrystallized from methanol. *N*-*tert*-butyl-*N*-[1-diethylphosphono-(2,2-dimethylpropyl)]nitroxide SG1 (also known as DEPN) was synthesized according to the literature[56] with purity 96% determined using ^{1}H NMR spectroscopy from the reaction of the SG1 radical with pentafluorophenylhydrazine (Aldrich 97%). *N*,*N*-Dimethlyformamide (DMF, Aldrich, HPLC grade), anhydrous lithium bromide (LiBr, BDH), methanol (Corcoran Chemicals 99.9%), hexane (Fisher Scientific, reagent grade), benzene (BDH, reagent grade) and CO_2 (BOC, 99.8%) were all used as received.

4.2.2 Equipment and Measurements

All polymerizations were carried out in a 100 mL stainless steel Thar reactor described in chapter 2. All GPC measurements were obtained on polymerization mixtures prior to purification by dissolving the samples in DMF. M_n and polydispersity (M_w/M_n) were determined using a gel permeation chromatography (GPC) system consisting of a Viscotek DM 400 data manager, a Viscotek VE 3580 refractive-index detector, and two Viscotek Viscogel GMHHR-M columns. Measurements were carried out at 60 °C at a flow rate of 1.0 mL/min using HPLC grade DMF containing 0.01 M LiBr as the eluent. The columns were calibrated using six linear polystyrene standards (Mn = 376–2,570,000 g/mol). M_n measurements are not accurate. Control/livingness is assessed using MWD relative shifts, trends and shapes. Similar GPC conditions for the analysis of control/livingness of NIPAM polymerizations have been used by others in the literature.[168, 170, 177, 184, 185] Conversions were measured by weighing the dry polymeric product after careful removal of any remaining monomer. The theoretical number-average molecular weights ($M_{n,th}$) were calculated according to Equation 4.01:

$$M_{n,th} = \left(\frac{n_{\text{NIPAM}}}{2fn_{\text{AIBN}}}\right) \alpha \, MW_{NIPAM} \qquad (4.01)$$

where *n* denotes the numbers of moles, *f* is the AIBN initiator efficiency, α is fractional monomer conversion, and MW_{NIPAM} is the molecular weight of NIPAM.

^{1}H-NMR spectra were recorded on a JEOL 400 MHz model ECX-400. Tetramethylsilane was used as internal standard, with all chemical shifts quoted in parts per million (ppm). All poly(NIPAM) NMR's were carried out in $CDCl_3$. Scanning Electron Microscopy (SEM) images were obtained using a FEI Phenom SEM with light optical magnification fixed at 20 times, electron optical magnification 120-20,000 times, and digital zoom of 12 times.

4.2.3 Polymerization of NIPAM in $ScCO_2$

The reactor was loaded with NIPAM (e.g. 10.0 g, 88.4 mmol, equivalent to 10% w/v), AIBN (80 mg, 0.49 mmol) and SG1 (0.36 g, 1.22 mmol), $[SG1]_0/[AIBN]_0 = 2.5$ in all experiments. The reactor was sealed with the magnetically coupled stirring lid (Magdrive). The mixture was purged for 15 minutes by passing gaseous CO_2 through the mixture to remove air. Liquid CO_2 (~5 MPa) was added, and the temperature was raised to the reaction temperature of 120 °C, followed by the pressure to the desired reaction pressure by the addition of CO_2. The opaque reaction mixture was stirred at ~1200 rpm throughout. At the desired times, heating was stopped, and rapid external cooling using dry ice was carried out (this caused the temperature of the reactor to drop to ~80 °C in 10 minutes). The CO_2 was vented slowly from the reactor (when at approximately room temperature after 30 minutes of cooling) through methanol to prevent the loss of polymer and opened using the ABPR. Upon opening the reactor, at low conversion the polymerization mixture appeared as a gel (which hardens with time), which was dissolved in methanol and the polymer precipitated from excess hexane. At 71% and higher conversion, a white crystalline powder containing polymer and non-reacted monomer was obtained.

4.2.4 Polymer Purification using $scCO_2$

High conversion (>71%) NIPAM polymerizations were purified in-situ by up to three, fresh $scCO_2$ washings. After the initial venting of CO_2 any required samples were collected. The reactor was then resealed and the temperature and pressure increased to 50 °C and 30 MPa respectively. The mixture was stirred for up to 30 min before the CO_2 was re-vented. The expelled CO_2 was bubbled through methanol, which was evaporated to dryness under vacuum, and the resultant solid analysed by ^{1}H NMR spectroscopy.

4.3 Results and Discussion

4.3.1 Solubility of NIPAM in $scCO_2$

The sapphire windows allowed us to visually observe the polymerizations. At the start of reactions the solid NIPAM monomer (mp = 60-63 °C) was gently stirred in the reactor as the temperature and pressure were increased. It was noticed that the monomer melted at a reduced temperature of ≈ 50 – 55 °C at ≈ 10 MPa. The crystalline NIPAM behaves similar to water (ice) where the mp decreases under elevated pressure as the system moves to reduce the pressure by lowering its volume. The initial monomer solubility of NIPAM in $scCO_2$ was also investigated, with less than 5% w/v NIPAM becoming soluble at approximately 120 °C and 27 MPa. At loadings greater than 5% w/v a whitish emulsion was formed in $scCO_2$ at 120 °C and 10-30 MPa. It follows that for a 10% w/v NIPAM, approximately half the monomer will form large droplets suspended in $scCO_2$. We believe that this process is best described as an inverse suspension polymerization, as the liquid monomer droplets are predominantly suspended in the reaction medium. The term inverse is used because it is contrary to a traditional suspension polymerizations, which employ oil-soluble monomers (acrylics or styrenics) suspended in an aqueous medium; in this case the water-soluble monomer (NIPAM) is suspended in a hydrophobic continuous phase ($scCO_2$). Further evidence of a suspension is discussed below.

4.3.2 Effect of Pressure

NMP was carried out at three different pressures, 10, 20 and 30 MPa for 24 h (Figure 4.01). The 10 MPa reaction reached 70% conversion in 24 h but with very poor control obtained, as signified by the broad MWD (M_w/M_n = 2.03), which was not resolved from monomer in the GPC trace. Polymerizations carried out at 20 and 30 MPa had lower polymerization rates reaching 32 % and 37 % conversion with narrower MWDs observed (M_w/M_n = 1.42 and 1.38) respectively. The polymerization at 30 MPa offered marginally better control, and was more efficient in terms of apparent initiator efficiency compared to that at 20 MPa, signified by a lower, controlled M_n at higher conversion for the 30 MPa reaction (Figure 4.01). The change in pressure influences the partitioning of reactants between the two phases, as well as the monomer solubility in

$scCO_2$.[106] Apparent initiator efficiency (f_{app}) was calculated from Equation 4.03: based on a comparison of an obtained M_n with the expected $M_{n,th}$ for that specific conversion.

$$\frac{M_{n,th}}{M_n} = f_{app} \qquad (4.03)$$

For a given conversion $M_{n,th}$ is calculated, assuming an initiator efficiency f = 1, using Equation 4.01: The 20 and 30 MPa polymerizations gave f_{app} of 0.47 and 0.63 respectively showing that the higher pressure allows for better initiation of the NMP of NIPAM in $scCO_2$.

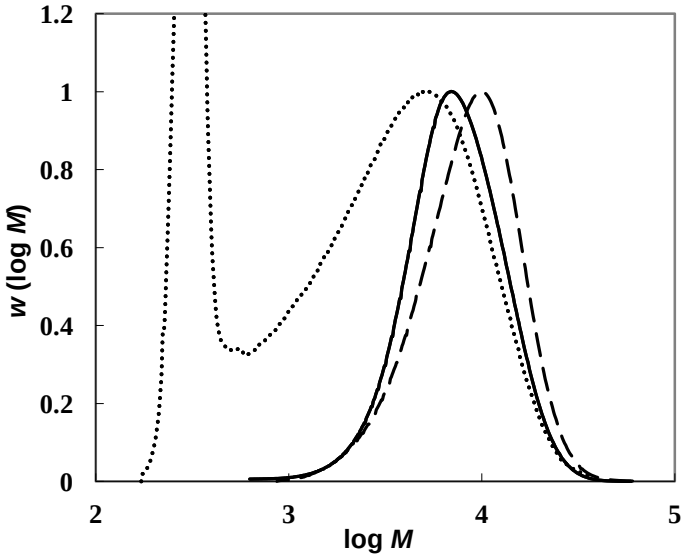

FIGURE 4.01: Influence of pressure on MWDs (normalised to peak height) for the NMP of 10% w/v NIPAM in $scCO_2$ at 120 °C for 24 h with $[SG1]_0/[AIBN]_0$ = 2.5. Dotted line = 10 MPa (not resolved from monomer), Conv. = 70%; Dashed line = 20 MPa, M_n = 7000 g mol^{-1}, M_w/M_n = 1.42, Conv. = 32%; Solid line = 30 MPa, M_n = 6000 g mol^{-1}, M_w/M_n = 1.39, Conv. = 37%.

4.3.3 Influence of Monomer Loading

To evaluate the effect of initial monomer loading, polymerizations were carried at 5, 10, 20 and 40% w/v initial NIPAM loading at 120 °C and 30 MPa for 24 h. The GPC traces from these reactions overlap very closely with each other and conversions were very similar (Figure 4.02). Therefore control and polymerization rate did not vary significantly with monomer loading (10-40% w/v) at 30 MPa (Figure 4.02), this is consistent with (but does not prove) a suspension polymerization, whereby each monomer droplet essentially behaves as a "mini-bulk" system.

The 40% w/v loading NMP has a similar polydispersity as the other loadings but reached the highest conversion (42%) with a slightly decreased M_n. This suggests that the initiator efficiency could be increased at higher loading. At higher loading there is physically less space for $scCO_2$ in the reactor and the apparent increase in initiator efficiency at higher monomer loading is most likely a consequence of less partitioning of the AIBN into the continuous phase away from the monomer/polymer droplets. In the case of 5% w/v NIPAM in $scCO_2$, the system initially appeared homogeneous and the polymerization proceeded as a precipitation polymerization with similar polymerization rate, but somewhat less control, than the inverse suspension polymerizations.

4.3.4 Inverse Suspension NMP of NIPAM in $scCO_2$

The polymerization of 10% w/v NIPAM at 30 MPa was carried out over a range of conversions, they proceeded with controlled/living character to high conversion (~70%) as indicated by MWDs remaining relatively narrow throughout (M_w/M_n = 1.35-1.50) and shifting to higher molecular weights with increasing conversion (Figure 4.03). There is a clear linear increase in M_n with conversion, without any downward deviation from the $M_{n,th}$ line indicating that chain transfer to solvent is not occuring in this system. With chain transfer to solvent eliminated (no chain transfer to CO_2), it would become easier to observe the consequences of chain transfer to monomer, particularly in a suspension (bulk-like) system. Chain transfer to monomer is not a major chain end-forming event, shown by a lack of deviation from linearity (Figure 4.03 (b)) in the inverse suspension NMP of NIPAM in $scCO_2$, but this topic was not deliberately studied.

Significant coagulation was visible at 71% conversion (36 h), but the polymer and non-reacted monomer were nonetheless isolated as a dry crystalline white powder

upon venting (depressurization) of CO_2. At 82% conversion, there was a significant loss in control/livingness, as evidenced by a broad MWD (M_w/M_n = 2.1), although there is no obvious evidence of a limiting M_n (= 12,100 g mol^{-1}), which remains close to $M_{n,th}$ = 12,300 g mol^{-1} (using f = 0.68). SEM images taken of the nonpurified polymer did not show well-defined particles. Coagulation of the particle matter lead to large masses of polymer which were too large to enable particle size and particle size distribution data to be obtained.

4.3.5 $ScCO_2$ washing

Despite the monomer being a solid under ambient conditions, it can be washed away from the poly(NIPAM) by purging the isolated polymer powder with $scCO_2$ two or three times at 50 °C (Figures 4.04, 4.05 and 4.06). The temperature must be kept sufficiently low not to reinitiate the polymerization. Removal of the NIPAM monomer was confirmed by ^{1}H NMR spectroscopy, before (Figure 4.05) and after (Figure 4.06) purification. The absence of low molecular weight polymer in the CO_2 eluent was confirmed by venting the CO_2 into methanol followed by ^{1}H NMR analysis of the solid obtained upon evaporation of the methanol.

The use of $scCO_2$ to purify poly(NIPAM) based materials prepared in (non-living) conventional radical precipitation polymerizations has been reported by others.[227, 228] The cavities in the polymer shown in SEM image (Figure 4.04) are attributed to expulsion of monomer by CO_2 upon venting. Thus the technique circumvents the requirement for VOC, and avoids the loss of low molecular weight polymer, which often occurs with traditional precipitation methods using VOC.

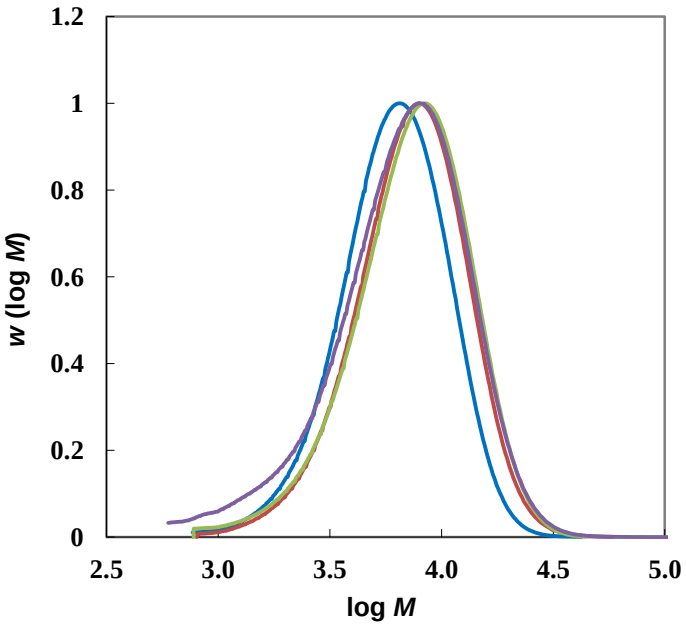

FIGURE 4.02: Influence of monomer loading on MWDs (normalised to peak height) for the NMP of NIPAM using 5% (purple line; M_n = 5600 g mol^{-1}, M_w/M_n = 1.59, Conv. = 37%) , 10% (green line; M_n = 6000 g mol^{-1} , M_w/M_n = 1.39, Conv. = 37%), 20% (red line; M_n = 6900 g mol^{-1}, M_w/M_n = 1.34, Conv. = 39%) and 40% (blue line; M_n = 5150 g mol^{-1}, M_w/M_n = 1.35, Conv. = 42%) w/v of NIPAM in scCO$_2$ for 24 h at 120 °C and 30 MPa using $[SG1]_0/[AIBN]_0$ = 2.5.

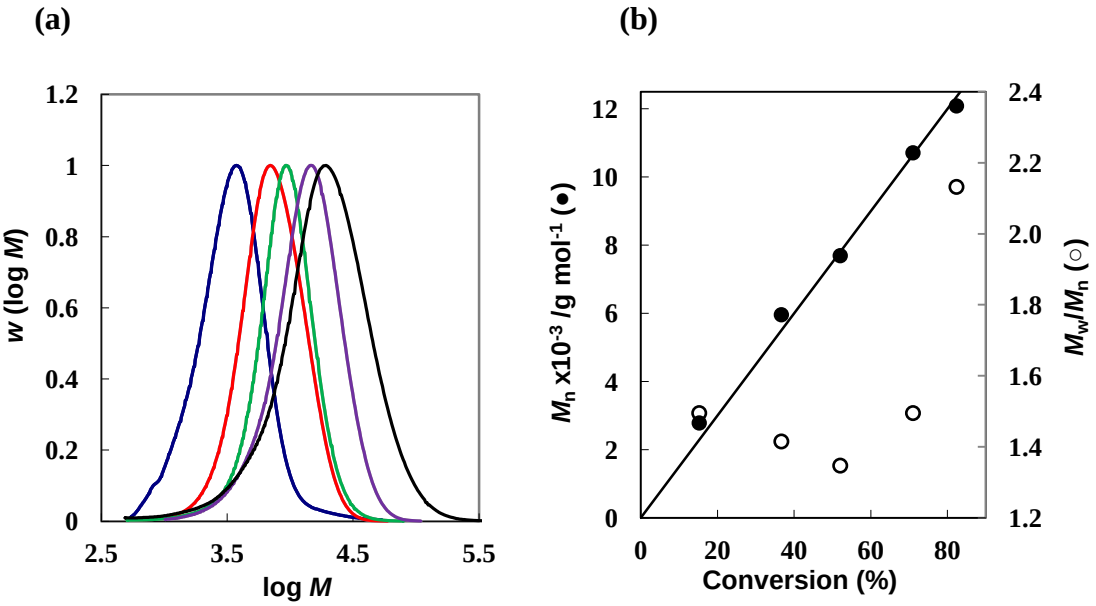

FIGURE 4.03: NMP of 10% w/v NIPAM in $scCO_2$ at 120 °C and 30 MPa (polymerization times are given within the brackets): **(a)** MWDs normalised to peak height corresponding to 15% (blue, 12 h), 37% (red, 24 h), 52% (green, 30 h), 71% (purple, 36 h) and 82% (black, 48 h) conversion and **(b)** M_n (●) and M_w/M_n (○) versus conversion. Line = M_{nth} based on initiator efficiency (f) = 0.68 obtained from the line of best fit ($M_{n,th}$ = 15000 g mol^{-1}at 100% conv).

FIGURE 4.04: Photograph (left) and SEM image (right; scale bar is 270 µm) of purified poly(NIPAM) obtained at 71% conversion.

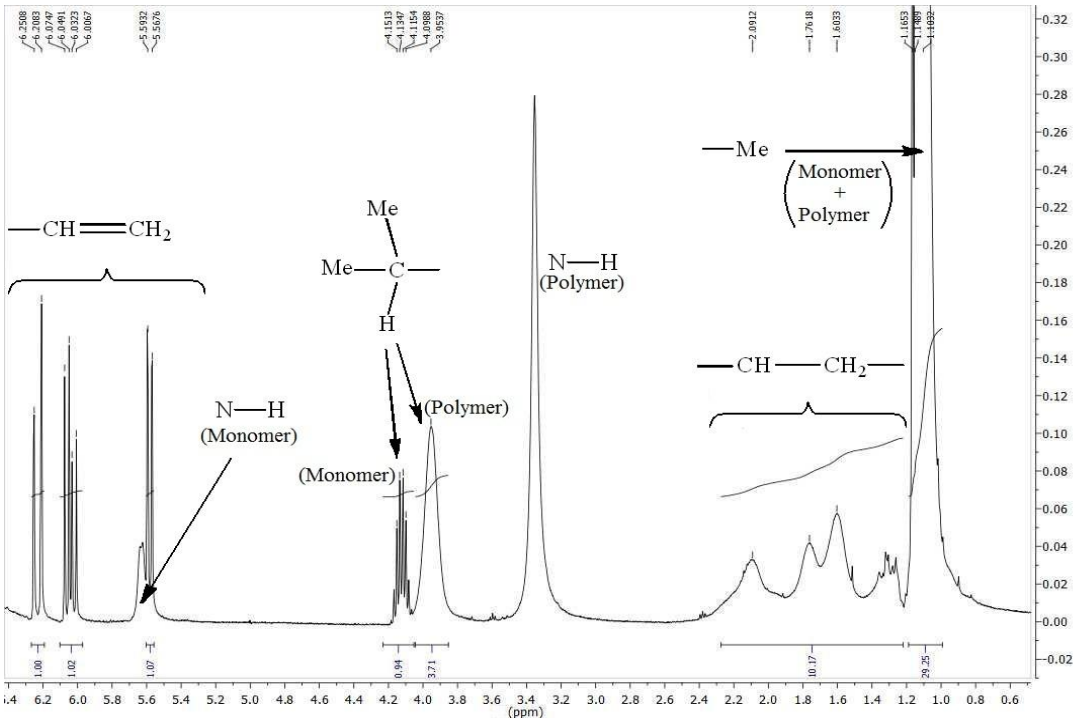

FIGURE 4.05: ^{1}H NMR spectra of dry polymer powder (71% Conv.) isolated from the NMP of 10% w/v NIPAM in $scCO_2$ at 120 °C and 30 MPa: before purification (note that some monomer has been lost during venting)

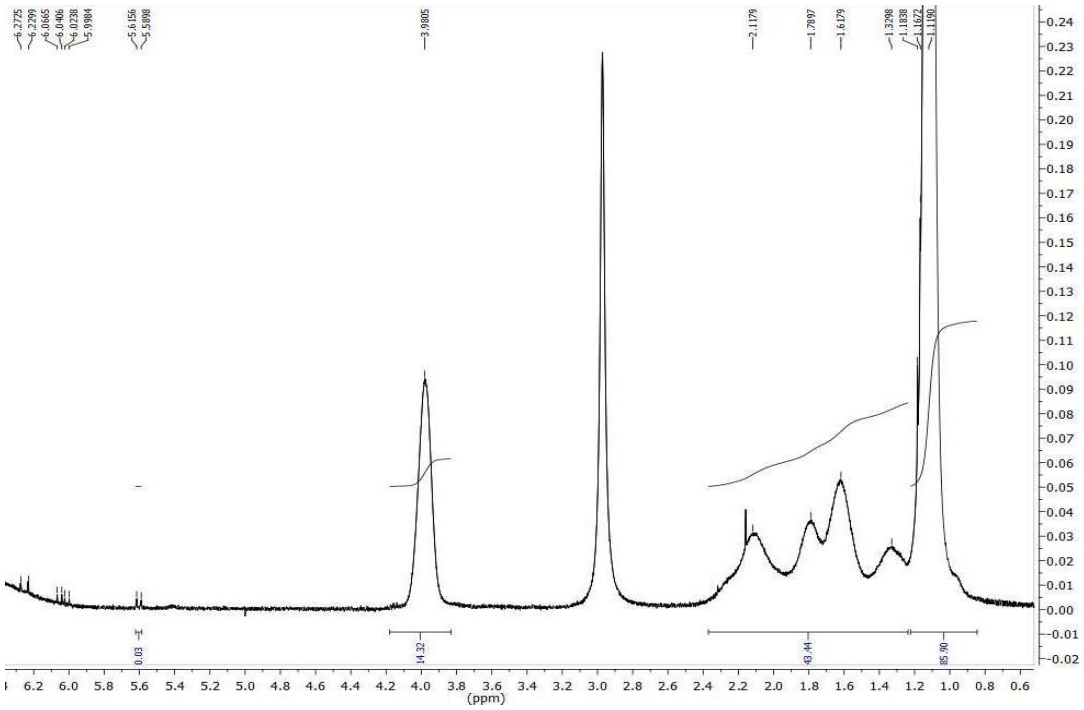

FIGURE 4.06: ^{1}H NMR spectra of dry polymer powder (71% Conv.) isolated from the NMP of 10% w/v NIPAM in $scCO_2$ at 120 °C and 30 MPa: after washing the sample 3 times with fresh $scCO_2$ at 50 °C and 30 MPa.

4.4 Conclusions

Nitroxide-mediated stabilizer-free inverse suspension polymerization of NIPAM has been performed successfully in $scCO_2$, this is the first report of an inverse dispersed phase CLRP in $scCO_2$. This new heterogeneous polymerization technique using benign $scCO_2$ offers significant advantages from a technical, commercial as well as an environmental perspective. Controlled/living character could be maintained up to high conversion, with $M_n \approx M_{n,th}$, the high conversion poly(NIPAM) could be obtained as a dry crystalline powder and further purified using CO_2. The system appears to be free of unwanted chain transfer reactions. There is a loss of control at conversions > 70% but this is due to agglomeration of the poly(NIPAM) particles and is not an effect of the NMP. Consequently our group are currently pursuing a stabilized controlled/living polymerization of NIPAM in $scCO_2$, which would sterically stabilize the monomer/polymer particles which is anticipated to yield small spherical particles as well as preventing agglomeration at high conversion allowing control to be maintained.

CHAPTER 5

Facile synthesis of thermoresponsive block copolymers of *N*-isopropylacrylamide using heterogeneous controlled/living nitroxide-mediated polymerizations in supercritical carbon dioxide

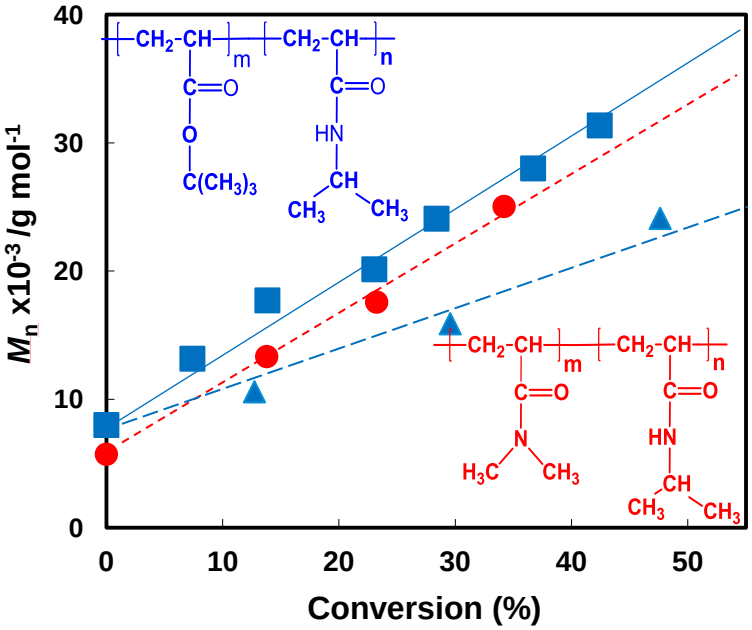

5.1 Introduction

The first preparation of well-defined block copolymers using controlled/living chain growth polymerizations that minimise termination and transfer reactions is attributed to Szwarc et al by means of living anionic polymerizations and date back to the 1950s.[30, 231] Since the early 1990s the more versatile controlled/living radical polymerization (CLRP) techniques have largely superseded living ionic polymerizations for forming block copolymers and other well-defined polymers with narrow molecular weight distributions (MWDs) and various topologies. Poly(NIPAM) is a thermoresponsive polymer exhibiting a lower critical solution temperature (LCST) in water of ~ 32 °C leading to biomedical and drug delivery applications.[157, 159, 160] The manipulation of the polymer's LCST by incorporating additional monomers has attracted much interest with block copolymers prepared by a variety of CLRPs, including solution NMPs of NIPAM.[59, 78, 162, 232] Block copolymers of NIPAM and acrylic acid (AA) have attracted much interest, because they form thermo- and pH-responsive micelles, useful in drug-delivery.[171, 233-236] The combination of NIPAM with the hydrophilic monomer *N*,*N*-dimethylacrylamide (DMA) gives copolymers with elevated LCST, [237-243] which may be closer to physiological temperature of ~ 37 °C.

Supercritical carbon dioxide ($scCO_2$) is a benign reaction medium which has been shown to circumvent the requirement for toxic and hazardous volatile organic compound (VOC). Its physical and chemical properties make $scCO_2$ a useful medium for industrially important heterogeneous polymerizations that allow the synthesis of sub-micron sized polymer particles.[145, 146] Controlled/living precipitation NMPs, [17, 70, 114, 126] and dispersion (with added stabilizer) NMPs, [67, 135, 140, 142, 244] in $scCO_2$ have been reported, as well as dispersion polymerizations using ATRP, [128-131, 148] and RAFT, [132, 133, 149] in $scCO_2$. The dispersion CLRP allows simultaneous control over particle size distribution and MWD of polymers.[127, 144]

Using the NMP of styrene (St) and *tert*-butyl acrylate (*t*-BA) in $scCO_2$ (chapter 2), polymer chains have been shown to be soluble up to a certain critical degree of polymerization (J_{crit}) prior to precipitation, after which the polymerization continues in the monomer rich particle phase.[70] J_{crit} or the particle nucleation step can be predicted based on the targeted molecular weight and initial monomer loading and J_{crit} or polymer solubility can be increased approximately linearly with pressure. However it is not possible to carry out precipitation or dispersion polymerizations of NIPAM in $scCO_2$ at higher loadings than approximately 5% w/v because of the poor solubility of the

monomer (chapter 4).[79] Nevertheless the inverse suspension NMP of NIPAM at loadings 10 – 40% w/v using the AIBN/SG1 system in $scCO_2$ was achieved with good control/living character established up to high conversion. Amongst the benefits of using $scCO_2$ include elimination of chain transfer to solvent (chapter 3).[78] Chain transfer to solvent (*N*,*N*-dimethylformamide, DMF) has been shown to be significant in the polymerizations of NIPAM. Chain transfer to solvent gives a maximum attainable MW for a given set of conditions in both conventional radical polymerization and CLRP. In CLRPs chain transfer to solvent or monomer impedes control by leading to low MW tailing in MWDs at high conversions because of the accumulation of shorter chains.[17, 62, 68]

Presently we report the facile preparation of various well-defined thermoresponsive block copolymers through controlled/living radical inverse suspension NMP of NIPAM in $scCO_2$. The polymeric alkoxyamines or macroinitiators (MI) are prepared by precipitation NMP in $scCO_2$ and a first report of the controlled/living polymerization of DMA in $scCO_2$ is described. There are in fact few heterogeneous controlled/living polymerizations of DMA, with only inverse microemulsion RAFT polymerizations reported.[245, 246] Further the thermal responsive properties of the block copolymers prepared using heterogeneous polymerizations in $scCO_2$; poly(DMA)-*b*-poly(NIPAM), poly(*t*-BA)-*b*-poly(NIPAM), poly(AA)-*b*-poly(NIPAM), and poly(St)-*b*-poly(NIPAM) are examined.

5.2 Experimental

5.2.1 Materials

NIPAM (98% TCI) was recrystallized from a mixture of 3:2 benzene/hexane before use. St (Aldrich, >99%), *t*-BA (Aldrich, 98%) and *N*,*N*-dimethylacrylamide (DMA, TCI, >99%) were distilled under reduced pressure before use. AIBN (DuPont Chemical Solution Enterprise) was recrystallized twice from methanol. SG1 was synthesized according to the literature.[56] Macroinitiators (MI) of poly(*t*-BA)-SG1(M_n = 8000 g mol^{-1}, M_w/M_n = 1.17) and poly(St)-SG1 (M_n = 6450 g mol^{-1}, M_w/M_n = 1.13) were prepared by precipitation NMP in $scCO_2$ as outlined in chapter 2. Sodium hydroxide (Aldrich ≥ 97%), DMF (Fisher, GPC grade), THF (Aldrich, 99.9%), dichloromethane (DCM, Aldrich 99%), MeOH (Corcoran Chemicals 99.9%), acetone (Corcoran Chemicals 99.5%), hexane (Fisher Scientific, reagent grade), benzene (BDH, reagent grade), diethyl ether (Aldrich, reagent grade), trifluoroacetic acid (TFA, Aldrich, 99%), (trimethylsilyl)diazomethane solution in 2.0 M hexanes (Aldrich), LiBr (BDH, >97%), and CO_2 (BOC, 99.8%) were all used as received.

5.2.2 Equipment and Measurements

All polymerizations were carried out in a 100 mL stainless steel Thar reactor described in chapter 2. The GPC system and all M_n and polydispersity (M_w/M_n) measurement conditions are described in chapter 3. The columns were calibrated using six linear poly(St) standards (M_n = 376-2570,000). The M_n(GPC) values are given as grams per mole (g mol^{-1}) throughout, and are not absolute, but relative to linear poly(St) standards. Theoretical M_n ($M_{n,th}$) are not quoted due to the use of relative M_n(GPC) values and uncertainties in initiator efficiencies. Control/livingness is assessed using MWD relative shifts, trends and shapes. All GPC data corresponds to polymer before purification, unless otherwise stated.

^{1}H NMR spectra were obtained using a JEOL 400 MHz spectrometer. Samples containing poly(acrylic acid, AA) were recorded in $(CD_3)_2SO$, and all other samples were analysed in $CDCl_3$ with Me_4Si used as the internal standard. M_n(NMR) of purified block copolymers is calculated according to Equation 5.01: where $DP_{n(MI)}$ is the average degree of polymerization of each MI obtained from M_n(GPC) = $M_{n(MI)}$ divided by the MW of the constituent monomer; x is the ratio of poly(NIPAM) relative to MI incorporated in the block copolymer obtained from integration of poly(NIPAM)

N—C—H (δ_H ~ 3.8–4.1 ppm, 1H) resonance, and resonances at δ_H ~ 1.0–2.4 ppm due to each individual incorporated MI plus poly(NIPAM) (see Figures 5.11-5.13). E.g. In the case of poly(DMA)-*b*-poly(NIPAM), δ_H 0.90–2.0 ppm represents 3H (CH-CH_2) of poly(DMA) plus 9H (CH-CH_2 and 2 X Me) of poly(NIPAM) (Figure 5.11). $MW_{[NIPAM]}$ is the molecular weight of NIPAM monomer.

$$M_n(NMR) = \{DP_{n(MI)} \times x\} \times MW_{[NIPAM]} + M_{n(MI)} \qquad (5.01)$$

Aqueous cloud point measurements were carried out using a Cary 100 UV-Vis spectrophotometer at 500 nm, with temperature ramping at 0.1 °C/min.

5.2.3 Precipitation NMP of DMA in $scCO_2$

DMA (20.0 g, 0.20 mol), AIBN (66 mg, 0.40 mmol) and SG1 (0.393 g, 1.33 mmol) were loaded into the $scCO_2$ reactor. The reactor was sealed and the mixture was purged for 15 min by passing gaseous CO_2 through the mixture to remove oxygen. Liquid CO_2 (~5 MPa) was added and the temperature was raised to the reaction temperature of 120 °C followed by the pressure to the reaction pressure (in this case 30 MPa) by the addition of CO_2. The reaction mixture was stirred at ~1200 rpm throughout and monitored through the inline sapphire windows. At the start the viewing window indicated a transparent solution, which became opaque at J_{crit} or the particle nucleation stage. Heating was stopped and rapid external cooling using a cooling fan applied (this caused the temperature of the reactor to drop to ~80 °C in 10 min). When at approximately room temperature the CO_2 was vented slowly from the reactor through DCM to prevent the loss of polymer and opened using the ABPR. The reaction mixture was pipetted directly from the reactor. The polymer was precipitated into excess hexane, filtered and dried prior to conversion measurement by gravimetry. Polymerizations were then carried out to higher conversions beyond J_{crit}.

5.2.4 Test for livingness: chain extension of Macroinitiator (MI) with bulk St

MI (0.025 mmol, based on the M_n of the purified polymer), St (2.0 g, 19.2 mmol), and SG1 (5.2 mg, 17.7 μmol) were charged in glass ampoules and subjected to several freeze/thaw degas cycles. After sealing under vacuum, the ampoules were heated at 110 °C in an aluminium heating block for 15 h. The polymerizations were quenched by

immersing the ampoule into an ice-water bath. Each polymer was precipitated into an excess of methanol, filtered and dried prior to conversion measurement by gravimetry. Conversion was obtained from the increase in weight of polymeric material.

5.2.5 MI-initiated inverse suspension NMP of NIPAM in $scCO_2$

NIPAM (10.0 g, 88.4 mmol), MI (0.14 mmol, based on the M_n of the purified polymer; e.g. poly(*t*-BA)-SG1= 1.12 g) and SG1 (20.6 mg, 0.07 mmol) were loaded into the reactor. Poly(St)-SG1 initiated polymerization was carried out at 20% w/v NIPAM loading (20.0 g, 0.177 mol) using poly(St)-SG1 (1.81 g, 0.28 mmol) and SG1 (61.8 mg, 0.21 mmol). The polymerizations were carried out as above at 120 °C and 30 MPa and stopped at various times. Poly(*t*-BA)-*b*-poly(NIPAM) and poly(St)-*b*-poly(NIPAM) were dissolved in MeOH and acetone respectively and precipitated into excess petroleum ether and poly(DMA)-*b*-poly(NIPAM) was dissolved in DCM and precipitated into excess hexane. All copolymer samples were filtered and dried prior to conversion measurement by gravimetry.

5.2.6 Hydrolysis of poly(*t*-BA)-*b*-poly(NIPAM)

Poly(*t*-BA)-*b*-poly(NIPAM) (1.5 g) was dissolved in DCM (15 mL) and a tenfold molar excess of TFA was added and the mixture stirred at room temperature for 24 h. The reaction was evaporated to dryness and the solid dissolved in methanol. The polymer was precipitated into excess diethyl ether, filtered and dried under vacuum. ^{1}H NMR spectra verified the hydrolysis of the *tert*-butyl groups (~1.4 ppm) had occurred quantitatively (see Figure 5.12).

5.2.7 Aqueous cloud point measurements of block copolymers (Measurements performed by Rongbing Yang)

Polymers solutions (0.1% w/v) were prepared in Millipore water. NaOH solutions were used to adjust the pH of samples containing poly(AA) blocks. Samples were allowed to equilibrate for several hours before analysis. Commercial poly(NIPAM) with $M_n \approx$ 56,000 and $M_w/M_n \approx 2.70$ using the above GPC conditions, was used as reference.

5.3 Results and Discussion

5.3.1 Precipitation NMP of *N,N*-dimethylacrylamide (DMA) in $scCO_2$

DMA has a large propagation rate constant (k_p), and NMP with good control/living character is reported with bulk monomer in the presence of an excess of the nitroxide, SG1.[57, 58] For precipitation and dispersion NMP of St in $scCO_2$, a larger amount of free nitroxide is necessary compared to the solution or bulk polymerization of St because of the partitioning of some of the mediating nitroxide away from the locus of polymerization upon precipitation of the propagating radical from the continuous phase.[17, 67, 126] Polymerizations of 20% w/v DMA in $scCO_2$ with initial ratios of $[SG1]_0/[AIBN]_0$ = 2.5, 3.0 and 3.3 were carried out at 120 °C and 30 MPa, in order to give an optimal ratio required to achieve control/living character, as well as reasonable polymerization rates (Figure 5.01). The highest ratio of $[SG1]_0/[AIBN]_0$ was found to give the narrowest MWD with negligible effect on rate and was used in subsequent polymerizations. The solubility of DMA in $scCO_2$ using these polymerization conditions was deciphered by observation of the reaction through the inline sapphire windows. The monomer was found to be soluble beyond 40% w/v loading and thus amenable to a precipitation polymerization. At 20% w/v monomer loading, precipitation occurred after 37 min at the above conditions with J_{crit} occurring at 6% conversion (M_n = 1600 g/mol and M_w/M_n = 1.22). Poly(DMA) has comparable solubility to poly(*t*-BA) in $scCO_2$, which has been shown to be more soluble than poly(St) under similar conditions (chapter 2).[70] A series of polymerizations were then performed to high conversion and despite the large excess of nitroxide used, the NMP remained relatively fast reaching 66% conversion in about 12 h (Figure 5.02). Controlled/living character is demonstrated by uniform MWDs remaining relatively narrow throughout (1.22 – 1.37) and M_n increasing linearly with conversion. It is interesting that the polydispersity index also increases approximately linearly with conversion (over this narrow range) with the initial rise in M_w/M_n presumably because of the partitioning of the nitroxide between the continuous and particle phase causing a small depreciation in control. Livingness was assessed by chain extension of the isolated poly(DMA)-SG1 at 24% conversion with bulk St (Figure 5.03). After conversion of the chain extended GPC trace, to its number distribution curve (P(*M*) *vs. M*, Figure 5.03b), [67, 68, 247] and integration of the distinctive low MW peak (non-extended chains, M_n < ~ 5700 g/mol) relative to the overall distribution, it is calculated that 82% of poly(DMA) chains contain the SG1 end-group.

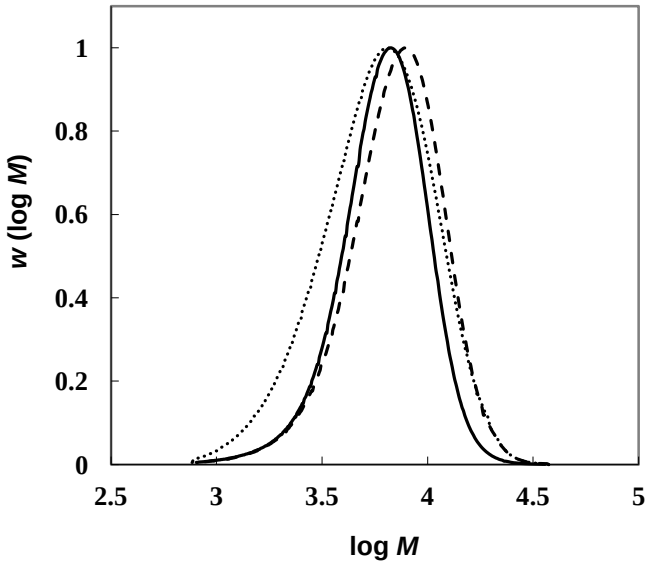

Figure 5.01: Influence of initial nitroxide concentration on MWDs (normalized to peak height) for the precipitation NMPs of 20% w/v initial loading of DMA in $scCO_2$ at 120 °C and 30 MPa. $[SG1]_0/[AIBN]_0$ = 2.5 (dotted line), 3.0 (dashed line) and 3.3 (continuous line), where M_n = 4750 g/mol, M_w/M_n = 1.45, 16% conversion; M_n= 6100 g/mol, M_w/M_n = 1.32, 28% conversion; and M_n= 5450 g/mol, M_w/M_n = 1.26, 24% conversion; respectively.

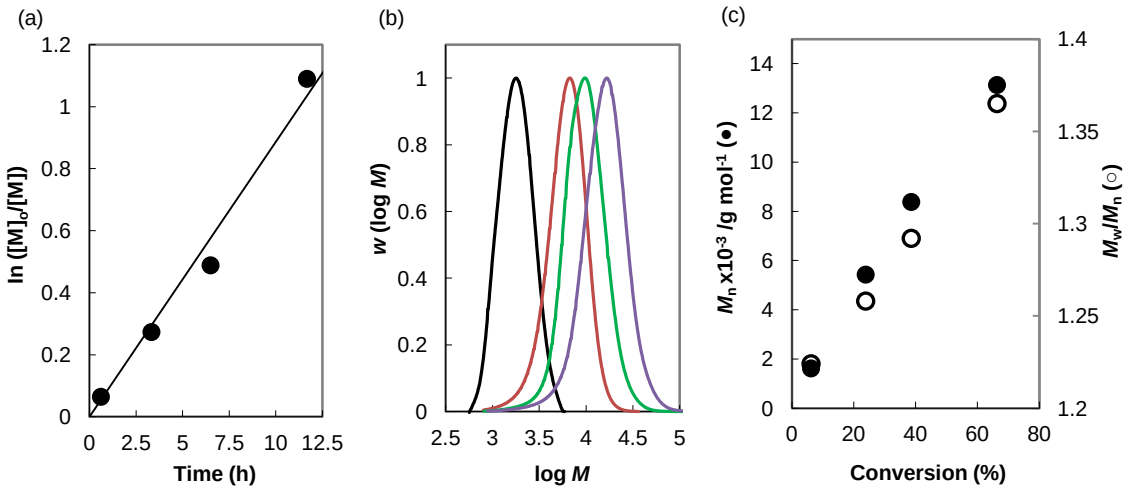

Figure 5.02: Precipitation NMPs of 20% w/v initial loading of DMA in $scCO_2$ at 120 °C and 30 MPa, where $[SG1]_0/[AIBN]_0$= 3.3. (a) First order rate plot (b) MWDs (normalized to peak height) and (c) GPC M_n (●) and M_w/M_n (○) versus conversion plots. J_{crit} is at 6% conversion.

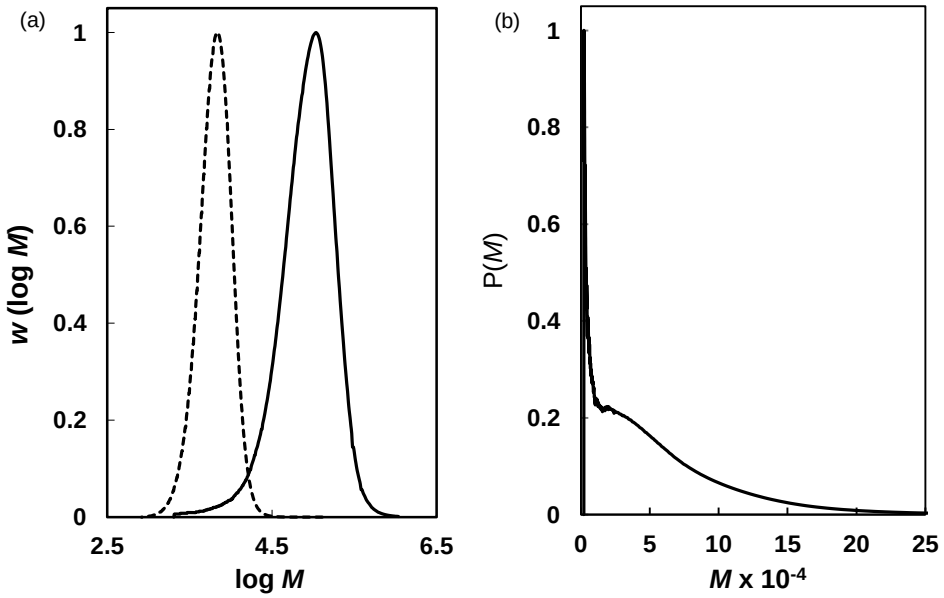

Figure 5.03: Chain extension of poly(DMA)-SG1 with bulk St at 110 °C for 15 h: (a) GPC traces of MI (dashed line) from precipitation NMP of DMA in $scCO_2$ at 24% conversion (see Figure 5.02), M_n = 5700 g/mol, M_w/M_n = 1.23 and chain extension in bulk St in the presence of 100 % free SG1 (solid line) M_n = 60,250 g/mol, M_w/M_n = 1.78 and (b) P*(M) vs M* (number distribution curve) of the chain extended polymer. All peaks normalized to peak height.

5.3.2 MI-initiated inverse suspension polymerizations of *N*-isopropylacrylamide (NIPAM) in $scCO_2$

The block copolymers were prepared by inverse suspension NMP of NIPAM in $scCO_2$ at 120 °C and 30 MPa. The poly(DMA)-SG1 sample at 24% conversion in Figure 5.02 was used as MI, and the poly(*t*-BA)-SG1 MI synthesis is previously reported. Since the MIs were obtained using precipitation NMPs in $scCO_2$, it follows that the polymeric initiators would be expected to have a lower solubility in the continuous phase, and would be located in the monomer-rich suspended droplets at the start of the polymerization. NMP of 10% w/v NIPAM was initiated by the MIs in the presence of a 50 mol% excess of free SG1 (Figure 5.04). There is an induction period in the polymerizations using two different concentrations of poly(*t*-BA)-SG1, which is absent when using poly(DMA)-SG1, as MI (Figure 5.04a). This however is not be due to the dispersed nature of the polymerization mixture, but is a feature of the kinetics of this particular NMP, given that a similar ~12 h delay in polymerization was observed in the solution NMP of NIPAM in DMF using a similar poly(*t*-BA)-SG1 MI (with 25% excess free SG1, shown in chapter 3, Figure 3.02). This may be attributed to the dissociation rate constant (k_d) of the MI, which is likely to be about two times greater for poly(DMA)-SG1 compared to poly(*t*-BA)-SG1, based on literature k_d data available for analogous small molecule alkoxyamines of SG1 at 120 °C.[248] It is thus expected that in the polymerizations initiated by poly(*t*-BA)-SG1, there is a greater tendency for the initiation equilibrium to lie towards the dormant state (i.e. non-dissociated MI). Halving the ratio of $[NIPAM]_0/[poly(t\text{-BA})\text{-}SG1]_0$ by doubling the number of initiated chains, with the $[MI]_0/[\text{free SG1}]_0$ ratio maintained, gives no increase in the rate of polymerization (Figure 5.04a). This indicates that stationary state kinetics apply, whereby the $[P^\bullet]$ is not affected by $[MI]_0$.[45] The rate of spontaneous thermal initiation is negligible in this system, (shown in chapter 3) and rate which is proportional to $[P^\bullet]$ (evidenced by the linear first order plot) will be dictated by the high excess of free nitroxide available for a given $[MI]_0/[SG1]_0$.[17, 67, 126] It is also evident from the identical rates of polymerization for the two different $[poly(t\text{-BA})\text{-}SG1]_0$ initiated polymerizations that the level of partitioning of SG1 between phases is proportionate. Figure 5.04b shows the increase in the poly(*t*-BA)-SG1 concentration by a factor of two resulted in a decrease in M_n by close to a factor of two, as expected for a controlled/living system. This increase in $[MI]_0$ has however no effect on the rate of monomer consumption because of an increase in the average number of activation-

deactivation cycles for the higher $[MI]_0$ is accompanied by a proportional decrease in the number of monomer units incorporated into each living polymer chain per cycle, in accordance with ideal CLRP kinetics.[45] The monomodal MWDs demonstrated that the polymerizations took place exclusively in the suspended particles and that no polymerization occurred in the $scCO_2$ phase (see Figures 5.05-5.07). Therefore the polymerizations initiated by poly(DMA)-SG1 and poly(*t*-BA)-SG1 (at two different $[MI]_0$) proceeded with good controlled/living character, since M_n increases linearly with conversion starting from each $M_{n(MI)}$. Polydispersities remain reasonably low, although some broadening occurs up to intermediate conversion especially for the poly(DMA)-SG1 initiated system.

The initial inverse suspension polymerization of NIPAM in $scCO_2$ initiated by poly(St)-SG1 was carried out using the same conditions that proved successful using the polyamide and polyacrylate MIs (shown above). However poor control/livingness was obtained, as indicated by a prominent low MW shoulder corresponding to non-extended MI (Figure 5.08a). Simultaneous doubling of the monomer loading, concentration of MI, and an increase in the excess free SG1 (Figure 5.08b) gave a clear shift in the MWD of MI (at M_n = 6450 and M_w/M_n = 1.13) to higher MW block copolymer (at M_n = 30,700 and M_w/M_n = 1.63). The minor low MW tail in Figure 5.08b is attributed to mainly dead poly(St) chains that did not initiate the polymerization of NIPAM, based on a 70% calculation of livingness of the MI (Figure 5.09).

Prior to aqueous cloud point analysis of block copolymers, any traces of unreacted MI and NIPAM were removed by selective precipitation procedures using an anti-solvent for the block copolymers, which dissolved monomer and any non-extended MI (see Experimental). M_n(GPC) of purified block copolymers are in reasonable agreement with M_n(NMR) in Table 5.01, indicating good accuracy in the estimation of the average degrees of polymerization of block copolymers (^{1}H NMR spectra of block copolymers are given in Figures 5.11-5.13).

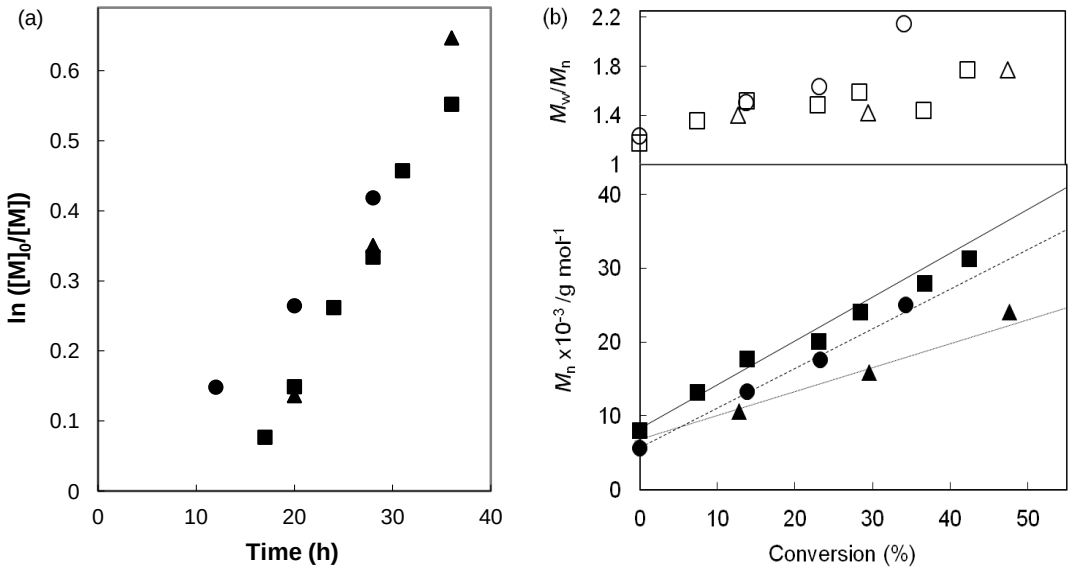

Figure 5.04: Inverse suspension NMPs of 10% w/v initial loading of NIPAM in $scCO_2$ at 120 °C and 30 MPa initiated by poly(*t*-BA-SG1) = 0.14 mmol (■, □), poly(*t*-BA-SG1) = 0.28 mmol (▲,Δ) and poly(DMA-SG1) = 0.14 mmol (●, ○) in the presence of 50 mol% free SG1. (a) First order rate plot and (b) GPC M_n (closed symbols with trend lines) and M_w/M_n (open symbols) versus conversion plots.

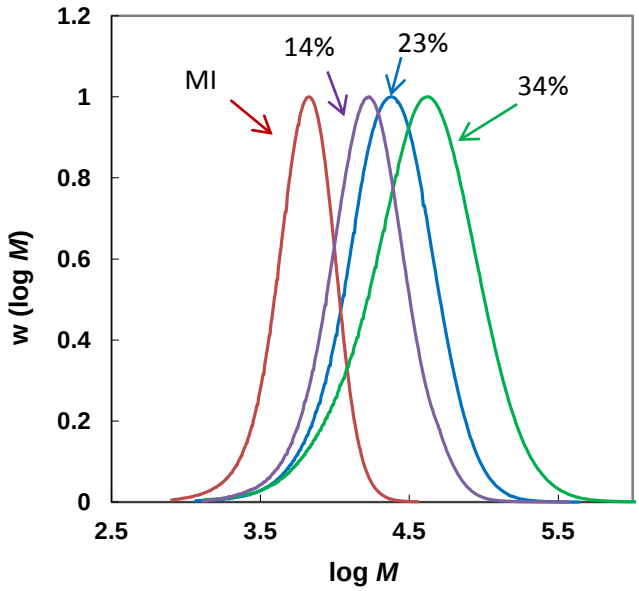

Figure 5.05: Inverse suspension NMP at 10% w/v initial loading of NIPAM in $scCO_2$ at 120 °C and 30 MPa initiated by poly(DMA)-SG1 = 0.14 mmol in the presence of 50 mol% free SG1. MWDs are normalized to peak height with conversions of NIPAM given within the figure.

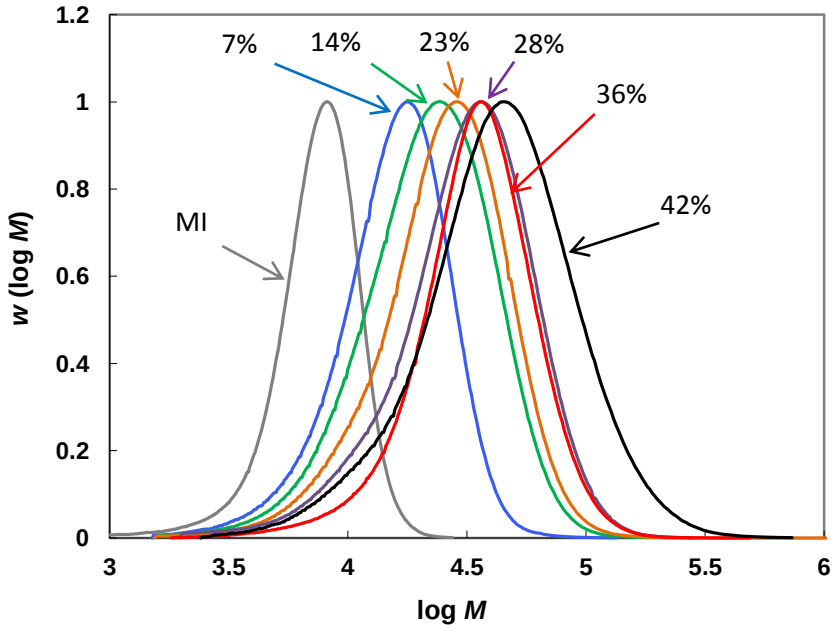

Figure 5.06: Inverse suspension NMP at 10% w/v initial loading of NIPAM in $scCO_2$ at 120 °C and 30 MPa initiated by poly(*t*-BA)-SG1 = 0.14 mmol of in the presence of 50 mol% free SG1. MWDs are normalized to peak height with conversions of NIPAM given within the figure.

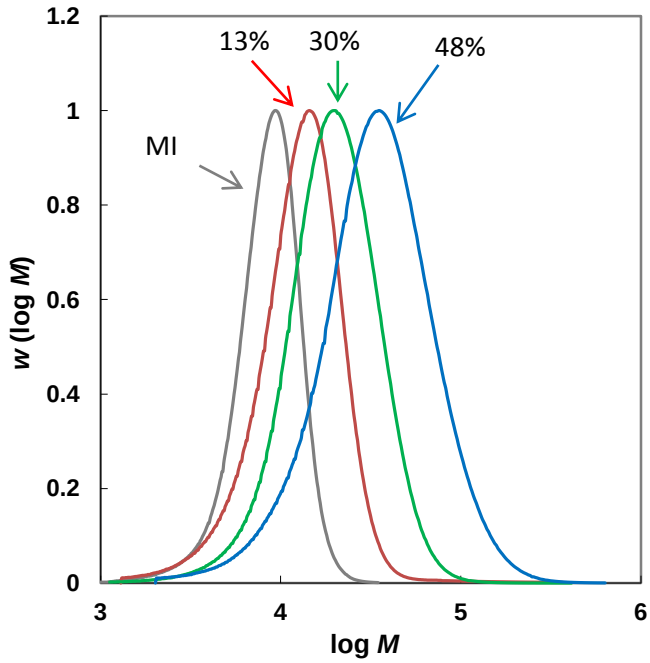

Figure 5.07: Inverse suspension NMP at 10% w/v initial loading of NIPAM in $scCO_2$ at 120 °C and 30 MPa initiated by poly(*t*-BA)-SG1 = 0.28 mmol of in the presence of 50 mol% free SG1. MWDs are normalized to peak height with conversions of NIPAM given within the figure.

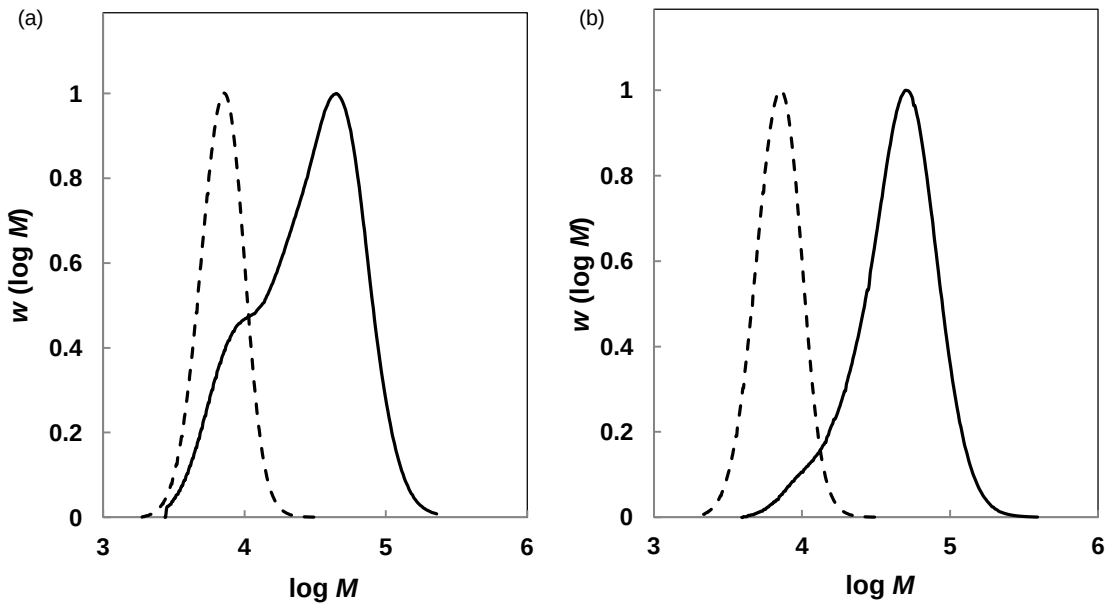

Figure 5.08: Inverse suspension NMPs of NIPAM in $scCO_2$ at 120 °C and 30 MPa initiated by (a) 0.14 mmol and (b) 0.28 mmol poly(St)-SG1 (dashed lines, M_n = 6450, M_w/M_n = 1.13). MWDs for (a) 10% w/v initial monomer loading with 50 mol% free SG1 (solid line, M_n = 18450, M_w/M_n = 2.00, 14% conv.) and (b) 20% w/v initial monomer loading with 75 mol% free SG1 (solid line, M_n = 30700, M_w/M_n = 1.63, 51% conv.). All peaks normalized to peak height.

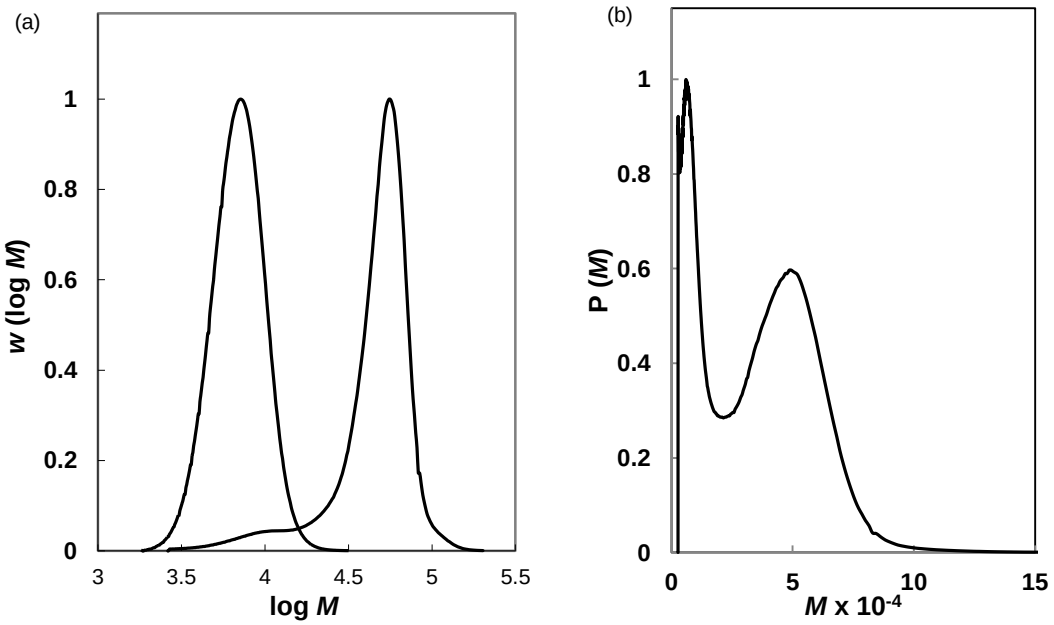

Figure 5.09: Chain extension of poly(St)-SG1 with bulk St at 110 °C for 15 h: (a) GPC traces of MI (dashed line) from precipitation NMP of St in $scCO_2$ at 13% conversion, M_n = 6450 g/mol, M_w/M_n = 1.13 and chain extension in bulk St in the presence of 75 % free SG1 (solid line) M_n = 36,500 g/mol, M_w/M_n = 1.38 (b) P*(M) vs M* (number distribution curve) of the chain extended polymer. All peaks normalized to peak height.

Table 5.01:

Poly(NIPAM) containing block co-polymers used in aqueous cloud point analysis

Block copolymers[a]	M_n(GPC)	(M_w/M_n) [b]	M_n (NMR) [c]
Poly(DMA)$_{(58)}$-*b*-Poly(NIPAM)$_{(82)}$	13400	(1.48)	15000
Poly(DMA)$_{(58)}$-*b*-Poly(NIPAM)$_{(117)}$	21400	(1.55)	18950
Poly(DMA)$_{(58)}$-*b*-Poly(NIPAM)$_{(217)}$	29250	(2.07)	30250
Poly(*t*-BA)$_{(62)}$-*b*-Poly(NIPAM)$_{(81)}$	20600	(1.42)	17200
Poly(*t*-BA)$_{(62)}$-*b*-Poly(NIPAM)$_{(192)}$	30750	(1.33)	29700
Poly(*t*-BA)$_{(62)}$-*b*-Poly(NIPAM)$_{(254)}$	34550	(1.31)	36750
Poly(St)$_{(62)}$-*b*-Poly(NIPAM)$_{(266)}$	34200	(1.51)	36500

[a] DP_n is calculated from M_n(GPC) for the first block relative to overall M_n(NMR) of the block copolymer [b] after purification [c] Calculated from ^{1}H NMR according to Equation 5.01.

5.3.3 Hydrolysis of Poly(*t*-BA)-*b*-Poly(NIPAM)

The required pH-sensitive thermal response polymer, poly(AA)-*b*-poly(NIPAM) was obtained through hydrolysis of the *tert*-butyl groups of poly(*t*-BA)-*b*-poly(NIPAM) with an excess of TFA (Figure 5.12). The poly(AA) copolymer was then methylated using $Me_3SiCH=N_2$, and its MWD shown to be similar to that of the poly*(t*-BA) precursor before hydrolysis, indicating both negligible loss of polymer chains, and decomposition of the poly(NIPAM) part during the hydrolysis process (Figure 5.10). The average degrees of polymerization for each poly(AA)-*b*-poly(NIPAM) are assumed to be the same as the *t*-BA precursor prior to hydrolysis (Table 5.01).

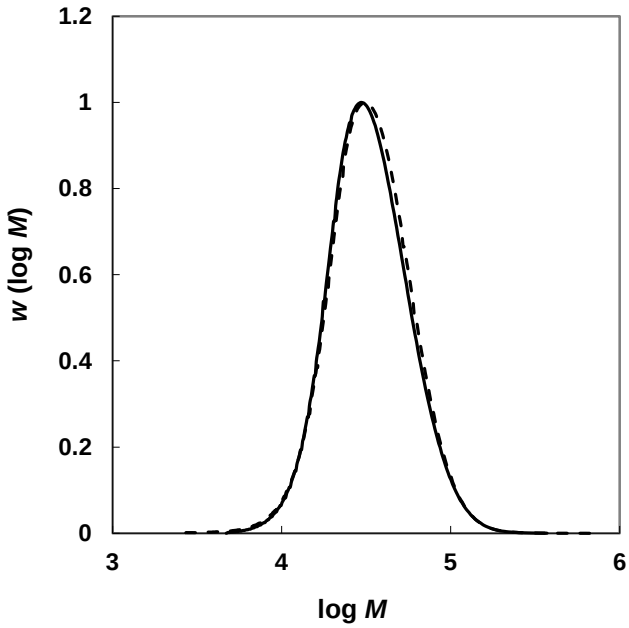

Figure 5.10: Hydrolysis of poly(*t*-BA)-*b*-poly(NIPAM) (dashed line, M_n = 30,750 g/mol, M_w/M_n = 1.34) with TFA giving poly(AA)-*b*-poly(NIPAM) (continuous line, M_n = 29,300 g/mol, M_w/M_n = 1.35) after methylation of the latter acid functionality using $Me_3SiCH=N_2$. MWDs normalized to peak height.

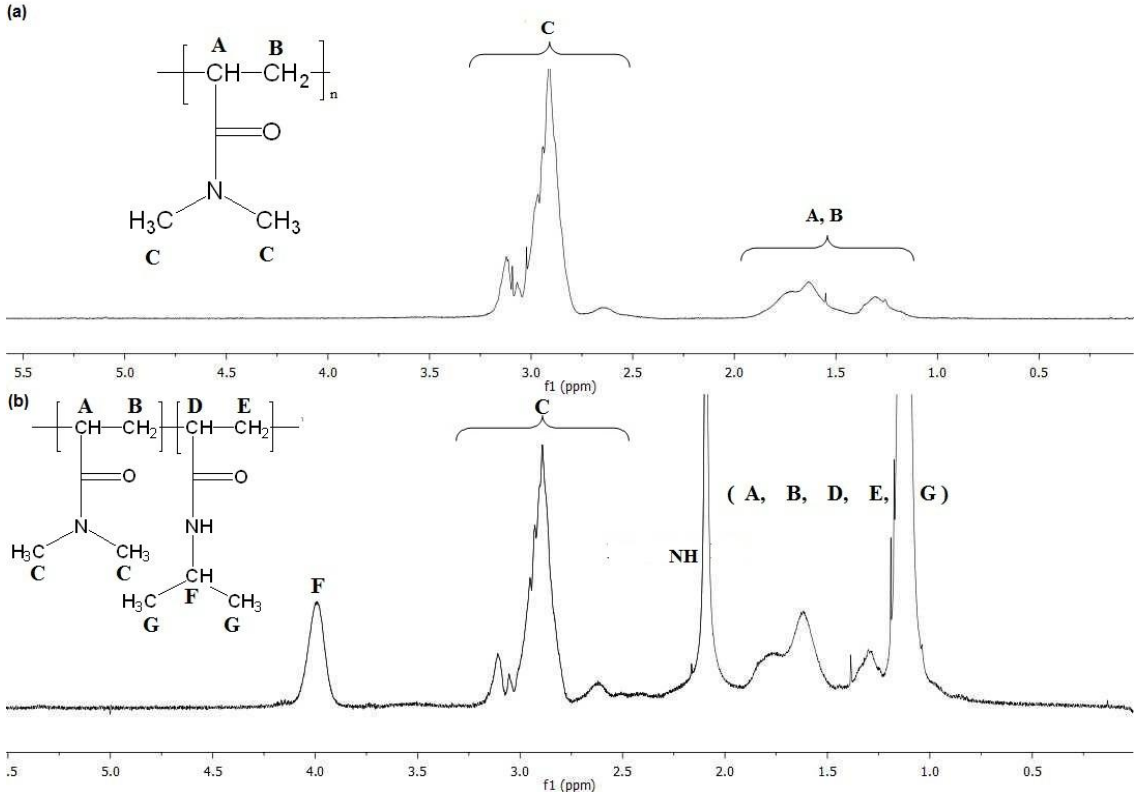

Figure 5.11: ^{1}H NMR spectra in $CDCl_3$ of the MI (poly(DMA)-SG1) and derived block copolymer at 23% conversion of NIPAM, after purification. (a) Poly(DMA)-SG1 and (b) poly(DMA)-*b*-poly(NIPAM). SG1 end-group is not visible.

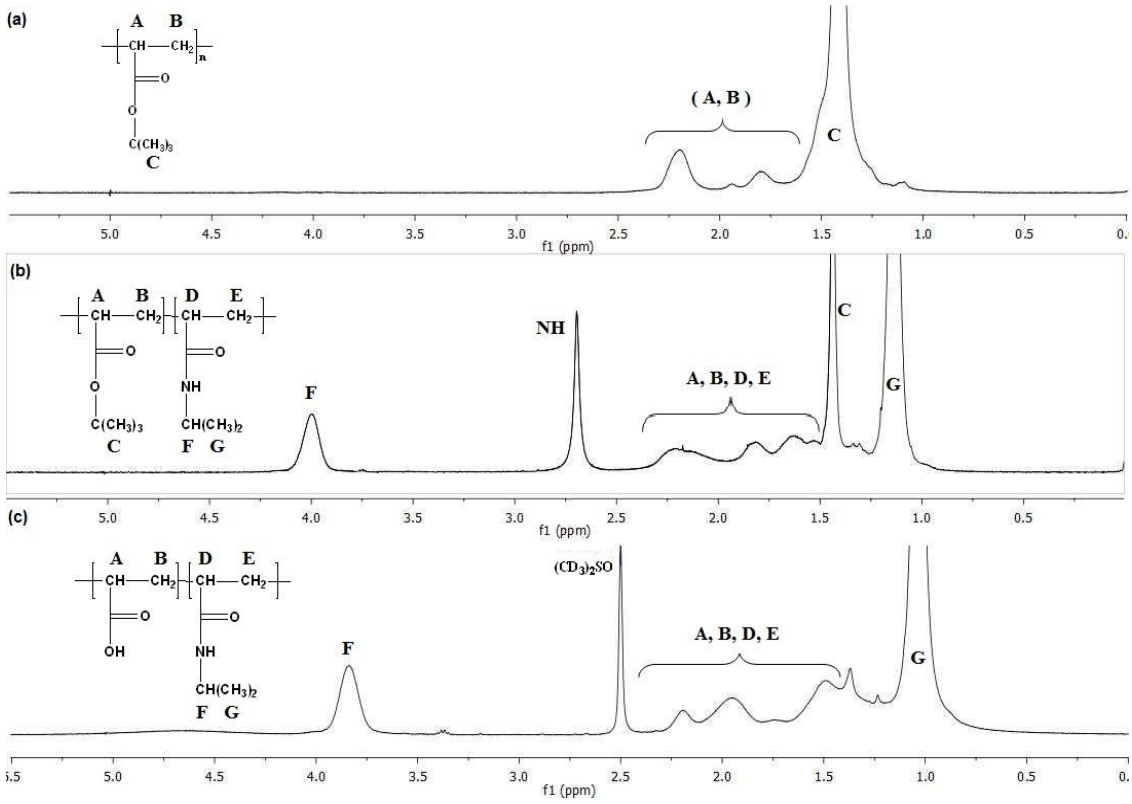

Figure 5.12: ^{1}H NMR spectra: (a) poly(*t*-BA)-SG1 (MI) in $CDCl_3$; (b) poly(*t*-BA)-*b*-poly(NIPAM) in $CDCl_3$ at 28% conversion of NIPAM and after purification; (c) poly(AA)-*b*-poly(NIPAM) in $(CD_3)_2SO$. SG1 end-group and OH of poly(AA) are not visible.

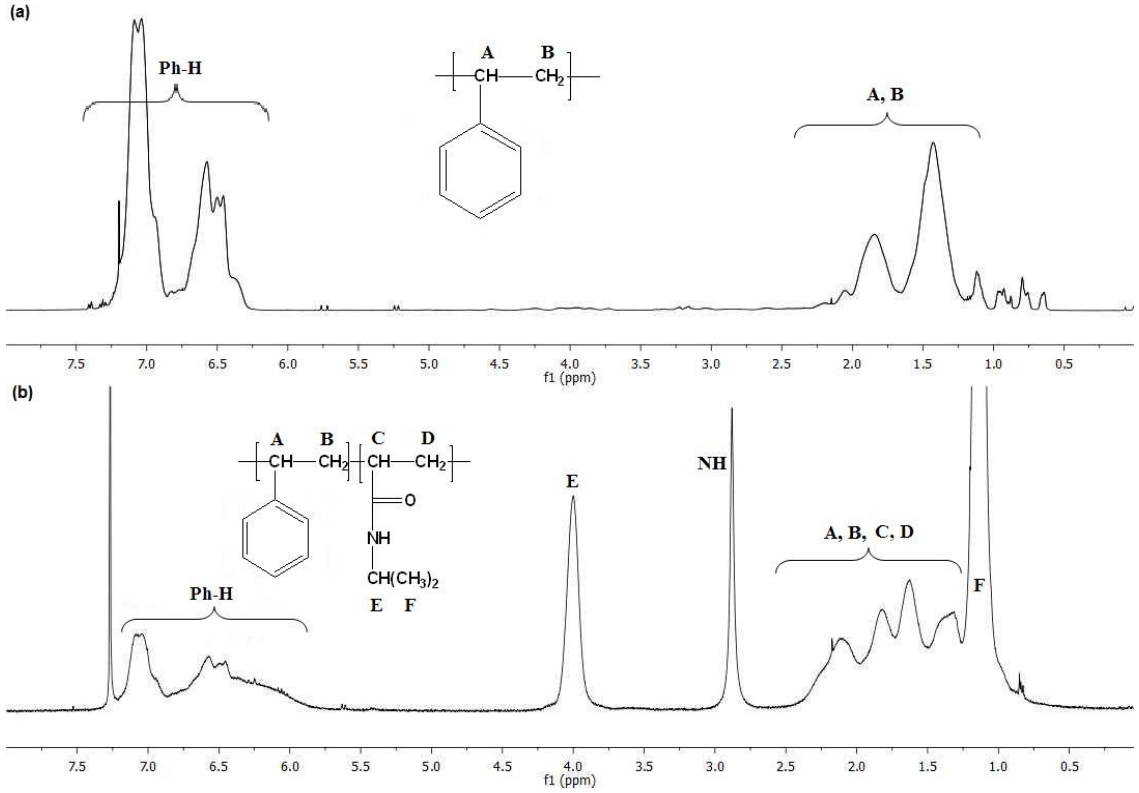

Figure 5.13: ^{1}H NMR spectra in $CDCl_3$ of the MI (poly(St)-SG1) and derived block copolymer at 51% conversion of NIPAM, after purification. (a) Poly(St)-SG1 and (b) poly(St)-*b*-poly(NIPAM). SG1 end-group is not visible.

5.3.4 Aqueous cloud point analysis of block copolymers

This involved the preparation of purified and dried block copolymer samples (0.1% w/v) in de-ionized water. Upon heating at pH 7, the solutions became turbid above the LCST, which corresponds to 50% transmittance on the heating curves in Figures 5.14-5.16, with commercially available high MW polydisperse poly(NIPAM) (LCST = 31.7 °C) used as a reference. Our study assumes negligible end-group influences and similar relative GPC error for all samples (see Experimental). The MI incorporated part of the AB poly(NIPAM) block copolymer is of similar length in each case. Figure 5.14 shows the block copolymer solutions containing a hydrophobic poly(St) and poly(*t*-BA) parts become turbid at lower temperatures than those block copolymers incorporating hydrophilic poly(AA) and poly(DMA) parts. The controlled/living polymerization technique allowed us to analyze the effect of extending the poly(NIPAM) block length, while maintaining identical MI incorporated block sizes. Figures 5.15a and 5.15b respectively show this for the poly(DMA) and poly(AA) containing block copolymers. As a greater number of NIPAM monomeric units are incorporated in each case, the copolymers reach the cloud point at temperatures closer to that of commercial poly(NIPAM). The differences in polydispersity have less effect on cloud points, as indicated upon examination of Table 5.01. Strong decreases in the phase transition temperature with increasing MW of poly(NIPAM) have been reported by Stöver and co-workers for narrow dispersity homopolymers prepared using room temperature ATRP.[164] Poly(AA)-*b*-poly(NIPAM) is a well-studied dual responsive copolymer, [171, 234-236] and it is now observed that the cloud point is lowered significantly at pH 4 close to the pK_a (≈ 4.5 – 5.0) of the poly(AA) part, where it is the most hydrophobic (Figure 5.16). This is in agreement with the findings of Kulkarni et al [233] with the dependence of cloud point measurements on pH being small once the p*K*a is exceeded.

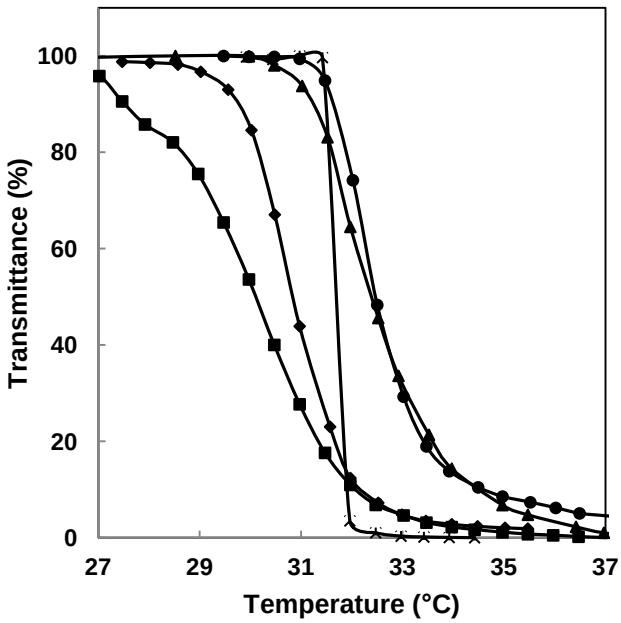

Figure 5.14: Light transmittance as a function of temperature of 0.1% w/v aqueous solutions at pH 7 of commercial poly(NIPAM) (x), poly(DMA)$_{(58)}$-*b*-poly(NIPAM)$_{(217)}$ (●), poly(*t*-BA)$_{(62)}$-*b*-poly(NIPAM)$_{(192)}$ (■), poly(AA)$_{(62)}$-*b*-poly(NIPAM)$_{(192)}$ (▲), and poly(St)$_{(62)}$-*b*-poly(NIPAM)$_{(266)}$ (♦).

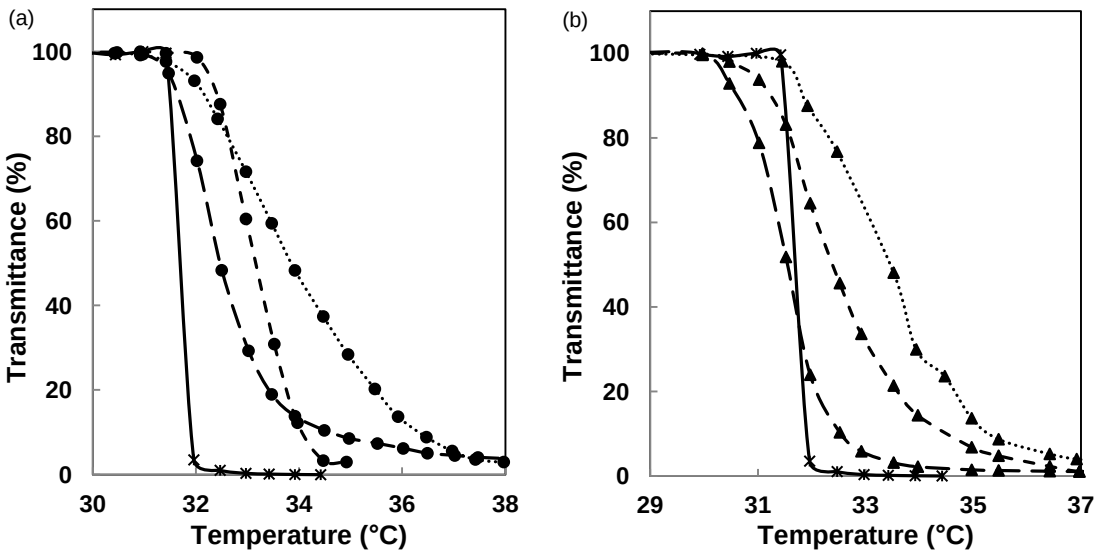

Figure 5.15: Light transmittance as a function of temperature of 0.1% w/v aqueous solution at pH 7 of (a) commercial poly(NIPAM) (continuous line), poly(DMA)$_{(58)}$-*b*-poly(NIPAM)$_{(82)}$ (dotted line), poly(DMA)$_{(58)}$-*b*-poly(NIPAM)$_{(117)}$ (dashed line) and poly(DMA)$_{(58)}$-*b*-poly(NIPAM)$_{(217)}$ (long dashed line) and (b) commercial poly(NIPAM) (continuous line), poly(AA)$_{(62)}$-*b*-poly(NIPAM)$_{(81)}$ (dotted line), poly(AA)$_{(62)}$-*b*-poly(NIPAM)$_{(192)}$ (dashed line) and poly(AA)$_{(62)}$-*b*-poly(NIPAM)$_{(254)}$ (long dashed line).

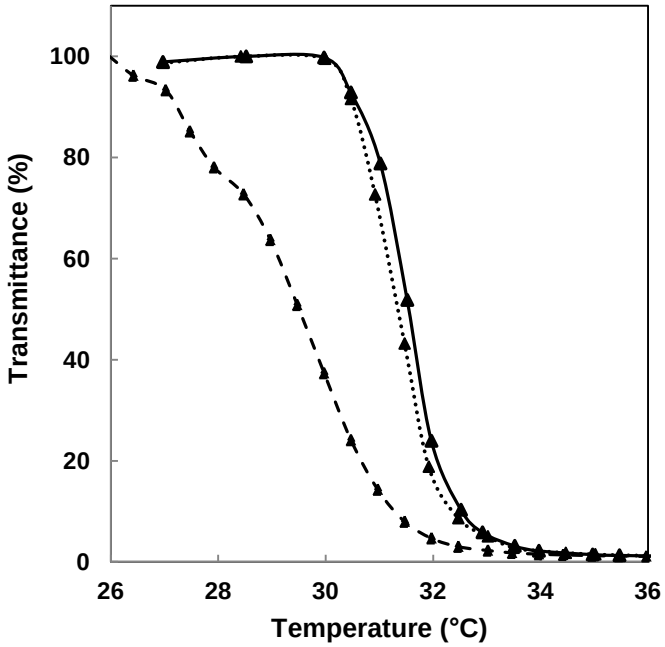

Figure 5.16: Light transmittance as a function of temperature of 0.1% w/v aqueous solution of poly(AA)$_{(62)}$-*b*-poly(NIPAM)$_{(254)}$, at pH = 4 (dashed line), pH = 7 (dotted line), and pH = 10 (continuous line).

5.4 Conclusions

DMA is found to be appreciably soluble in $scCO_2$ and amenable to a precipitation polymerization. Precipitation NMP of 20% w/v DMA was carried out in $scCO_2$ at 120 °C and 30 MPa with good control/living character demonstrated. Under these conditions the polymer becomes insoluble at the critical degree of polymerization (J_{crit}) at 6% conversion, M_n = 1600 g/mol and M_w/M_n = 1.22. This indicates a similar solubility to polyacrylates in $scCO_2$. Poly(DMA) at 24% conversion was used as MI, which was estimated to contain ≈ 82% living chains based on chain extension with bulk styrene. Inverse suspension NMP of 10% w/v NIPAM in $scCO_2$ using various MIs (prepared by precipitation NMPs) was then carried out with controlled/living stationary state kinetics observed, when using poly(*t*-BA)-SG1 (at two different $[MI]_0$). Different conditions were required to establish control for poly(St)-SG1 initiated inverse suspension polymerization of NIPAM in $scCO_2$, in comparison to poly(DMA)-SG1 and poly(*t*-BA)-SG1 initiated polymerizations. The MIs incorporated are shown to greatly influence the aqueous cloud point temperature, and cloud points approach commercial polydisperse high MW poly(NIPAM) as a greater number of NIPAM units are incorporated.

Bibliography

[1]. Braunecker, W. A.; Matyjaszewski, K. *Prog. Polym. Sci.* **2007,** 32, 93-146.
[2]. Uhrig, D.; Mays, J. W. *J. Polym. Sci. Part A Polym. Chem.* **2005,** 43, 6179-6222.
[3]. Aldabbagh, F.; Gibbons, O. *Sci. Synthesis* **2010,** 45b, 723-744.
[4]. Ito, M.; Ishizone, T. *Des. Monomers Polym.* **2004,** 7, 11-24.
[5]. Carraher, C. E.; Seymour, R. B., *Carraher's polymer chemistry*. CRC Press: Boca Raton, FL, 2011.
[6]. Aldabbagh, F.; Bowman, W. R.; Storey, J. M. D., Investigation of Reactions Involving Radical Intermediates. In *The Investigation of Organic Reactions and their Mechanisms*, Maskill, H., Ed. Blackwell: Oxford, 2006; pp 261-292.
[7]. Ayrey, G.; Evans, K. L.; Wong, D. J. D. *Eur. Polym. J.* **1973,** 9, 1347-1353.
[8]. Dixon, K., Decomposition Rates of Organic Free Radical Initiators. In *Polymer Handbook*, 4th ed.; Brandrup, J.; Immergut, E. H.; Grulke, E. A., Eds. John Wiley & Sons: New York, 1999; p 1.
[9]. Moad, G.; Solomon, D. H., *The Chemistry of Radical Polymerization*. 2nd ed.; Elsevier: Oxford, 2006.
[10]. Asikoglu, B.; Kilic, S.; Baysal, B. M. *J. Polym. Sci., Polym. Chem. Ed.* **1985,** 23, 1017-29.
[11]. Ryan, J.; Aldabbagh, F.; Zetterlund, P. B.; Yamada, B. *Macromol. Rapid Comm.* **2004,** 25, 930-934.
[12]. Rantow, F. S.; Soroush, M.; Grady, M. C.; Kalfas, G. A. *Polymer* **2006,** 47, 1423-1435.
[13]. Lehrle, R. S.; Shortland, A. *Eur. Polym. J.* **1988,** 24, 425-429.
[14]. Odian, G. G., *Principles of polymerization*. Wiley-Interscience: 2004.
[15]. Mayo, F. R. *J. Amer. Chem. Soc.* **1968,** 90, 1289-95.
[16]. Mayo, F. R. *J. Am. Chem. Soc.* **1953,** 75, 6133-41.
[17]. McHale, R.; Aldabbagh, F.; Zetterlund, P. B.; Okubo, M. *Macromol. Chem. Phys.* **2007,** 208, 1813-1822.
[18]. Kamachi, M.; Yamada, B., Propagation and Termination Constants in Free Radical Polymerization. In *Polymer Handbook*, 4th ed.; Brandrup, J.; Immergut, E. H.; Grulke, E. A., Eds. John Wiley & Sons: New York, 1999; p 77.
[19]. O'Driscoll, K. F.; Mahabadi, H. K. *J. Polym. Sci., Pol. Chem. Ed.* **1976,** 14, 869-881.
[20]. Yamada, B.; Kageoka, M.; Otsu, T. *Polym. Bull.* **1992,** 28, 75-80.
[21]. Olaj, O. F.; Bitai, I.; Hinkelmann, F. *Makromol. Chem.* **1987,** 188, 1689-702.
[22]. Buback, M.; Gilbert, R. G.; Hutchinson, R. A.; Klumperman, B.; Kuchta, F.-D.; Manders, B. G.; O'Driscoll, K. F.; Russell, G. T.; Schweer, J. *Macromol. Chem. Phys.* **1995,** 196, 3267-80.
[23]. Dervaux, B.; Junkers, T.; Schneider-Baumann, M.; Du Prez, F. E.; Barner-Kowollik, C. *Journal of Polymer Science Part A: Polymer Chemistry* **2009,** 47, 6641-6654.
[24]. Ganachaud, F.; Balic, R.; Monteiro, M. J.; Gilbert, R. G. *Macromolecules* **2000,** 33, 8589-8596.
[25]. Pascal, P.; Winnik, M. A.; Napper, D. H.; Gilbert, R. G. *Macromolecules* **1993,** 26, 4572-4576.
[26]. Zammit, M. D.; Davis, T. P.; Haddleton, D. M.; Suddaby, K. G. *Macromolecules* **1997,** 30, 1915-1920.
[27]. Bevington, J. C.; Eaves, D. E. *Trans. Faraday Soc.* **1959,** 55, 1777-82.
[28]. Ayrey, G.; Humphrey, M. J.; Poller, R. C. *Polymer* **1977,** 18, 840-4.

[29]. Yamada, B.; Zetterlund, P. B., General Chemistry of Radical Polymerization. In *Handbook of Radical Polymerization*, Matyjaszewski, K.; Davis, T. P., Eds. John Wiley and Sons, Inc.: Hoboken, 2002; pp 117-186.
[30]. Szwarc, M. *Nature* **1956,** 178, 1168-9.
[31]. Litvinenko, G.; Müller, A. H. E. *Macromolecules* **1997,** 30, 1253-1266.
[32]. Qiu, J.; Charleux, B.; Matyjaszewski, K. *Prog. Polym. Sci.* **2001,** 26, 2083-2134.
[33]. Hawker, C. J.; Bosman, A. W.; Harth, E. *Chem. Rev.* **2001,** 101, 3661-3688.
[34]. Grubbs, R. B. *Polym. Rev.* **2011,** 51, 104-137.
[35]. Matyjaszewski, K.; Xia, J. *Chem. Rev.* **2001,** 101, 2921-2990.
[36]. Ayres, N. *Polym. Rev.* **2011,** 51, 138-162.
[37]. Moad, G.; Rizzardo, E.; Thang, S. H. *Aust. J. Chem.* **2009,** 62, 1402-1472.
[38]. Destarac, M. *Polym. Rev.* **2011,** 51, 163-187.
[39]. Perrier, S.; Takolpuckdee, P. *J. Polym. Sci. Part A Polym. Chem.* **2005,** 43, 5347-5393.
[40]. Darling, T. R.; Davis, T. P.; Fryd, M.; Gridnev, A. A.; Haddleton, D. M.; Ittel, S. D.; Matheson, R. R.; Moad, G.; Rizzardo, E. *J. Polym. Sci. Part A Polym. Chem.* **2000,** 38, 1706-1708.
[41]. Jenkins, A. D.; Jones, R. G.; Moad, G. *Pure Appl. Chem.* **2010,** 82, 483-491.
[42]. Georges, M. K.; Veregin, R. P. N.; Kazmaier, P. M.; Hamer, G. K. *Macromolecules* **1993,** 26, 2987-8.
[43]. Fukuda, T.; Terauchi, T.; Goto, A.; Ohno, K.; Tsujii, Y.; Miyamoto, T.; Kobatake, S.; Yamada, B. *Macromolecules* **1996,** 29, 6393-6398.
[44]. Goto, A.; Fukuda, T. *Macromolecules* **1997,** 30, 5183-5186.
[45]. Goto, A.; Fukuda, T. *Prog. Polym. Sci.* **2004,** 29, 329-385.
[46]. Fukuda, T.; Terauchi, T. *Chem. Lett.* **1996**, 293-4.
[47]. Hui, A. W.; Hamielec, A. E. *J. Appl. Polym. Sci.* **1972,** 16, 749-769.
[48]. Ito, K. *Polym. J.* **1986,** 18, 877-9.
[49]. Georges, M. K.; Veregin, R. P. N.; Kazmaier, P. M.; Hamer, G. K.; Saban, M. *Macromolecules* **1994,** 27, 7228-9.
[50]. Miura, Y.; Nakamura, N.; Taniguchi, I. *Macromolecules* **2001,** 34, 447-455.
[51]. Dervan, P.; Aldabbagh, F.; Zetterlund, P. B.; Yamada, B. *J. Polym. Sci. Part A Polym. Chem.* **2003,** 41, 327-334.
[52]. Keoshkerian, B.; Georges, M.; Quinlan, M.; Veregin, R.; Goodbrand, B. *Macromolecules* **1998,** 31, 7559-7561.
[53]. Benoit, D.; Grimaldi, S.; Finet, J.-P.; Tordo, P.; Fontanille, M.; Gnanou, Y. *Polymer Preprints* **1997,** 38, 729-730.
[54]. Benoit, D.; Chaplinski, V.; Braslau, R.; Hawker, C. J. *J. Am. Chem. Soc.* **1999,** 121, 3904-3920.
[55]. Benoit, D.; Grimaldi, S.; Robin, S.; Finet, J.-P.; Tordo, P.; Gnanou, Y. *J. Am. Chem. Soc.* **2000,** 122, 5929-5939.
[56]. Cuervo-Rodriguez, R.; Bordegé, V.; Fernández-Monreal, M. C.; Fernández-García, M.; Madruga, E. L. *J. Polym. Sci. Part A Polym. Chem.* **2004,** 42, 4168-4176.
[57]. Diaz, T.; Fischer, A.; Jonquières, A.; Brembilla, A.; Lochon, P. *Macromolecules* **2003,** 36, 2235-2241.
[58]. Schierholz, K.; Givehchi, M.; Fabre, P.; Nallet, F.; Papon, E.; Guerret, O.; Gnanou, Y. *Macromolecules* **2003,** 36, 5995-5999.
[59]. Gibbons, O.; Carroll, W. M.; Aldabbagh, F.; Yamada, B. *J. Polym. Sci. Part A Polym. Chem.* **2006,** 44, 6410-6418.
[60]. Grimaldi, S.; Finet, J.-P.; Moigne, F. L.; Zeghdaoui, A.; Tordo, P.; Benoit, D.; Fontanille, M.; Gnanou, Y. *Macromolecules* **2000,** 33, 1141-1147.

[61]. Benoit, D.; Grimaldi, S.; Robin, S.; Finet, J.-P.; Tordo, P.; Gnanou, Y. *J. Am. Chem. Soc.* **2000,** 122, 5929.
[62]. Gibbons, O.; Carroll, W. M.; Aldabbagh, F.; Zetterlund, P. B.; Yamada, B. *Macromol. Chem. Phys.* **2008,** 209, 2434-2444.
[63]. Lacroix-Desmazes, P.; Lutz, J.-F.; Chauvin, F.; Severac, R.; Boutevin, B. *Macromolecules* **2001,** 34, 8866-8871.
[64]. Sobek, J.; Martschke, R.; Fischer, H. *J. Am. Chem. Soc.* **2001,** 123, 2849-2857.
[65]. Benoit, D.; Grimaldi, S.; Finet, J.-P.; Tordo, P.; Fontanille, M.; Gnanou, Y. *Polym. Prepr., ACS Polym. Div.* **1997,** 38, 729.
[66]. Lacroix-Desmazes, P.; Lutz, J.-F.; Boutevin, B. *Macromol. Chem. Phys.* **2000,** 201, 662-669.
[67]. McHale, R.; Aldabbagh, F.; Zetterlund, P. B.; Minami, H.; Okubo, M. *Macromolecules* **2006,** 39, 6853-6860.
[68]. Zetterlund, P. B.; Saka, Y.; McHale, R.; Nakamura, T.; Aldabbagh, F.; Okubo, M. *Polymer* **2006,** 47, 7900-7908.
[69]. Ryan, J.; Aldabbagh, F.; Zetterlund, P.; Yamada, B. *React. Funct. Polym.* **2008,** 68, 692-700.
[70]. O'Connor, P.; Zetterlund, P. B.; Aldabbagh, F. *Macromolecules* **2010,** 43, 914-919.
[71]. Couvreur, L.; Lefay, C.; Belleney, J.; Charleux, B.; Guerret, O.; Magnet, S. *Macromolecules* **2003,** 36, 8260-8267.
[72]. Tang, C.; Kowalewski, T.; Matyjaszewski, K. *Macromolecules* **2003,** 36, 1465.
[73]. Benoit, D.; Harth, E.; Fox, P.; Waymouth, R. M.; Hawker, C. J. *Macromolecules* **2000,** 33, 363.
[74]. Grassl, B.; Clisson, G.; Khoukh, A.; Billon, L. *Eur. Polym. J.* **2008,** 44, 50.
[75]. Phan, T. N. T.; Bertin, D. *Macromolecules* **2008,** 41, 1886-1895.
[76]. Bosman, A. W.; Vestberg, R.; Heumann, A.; Fréchet, J. M. J.; Hawker, C. J. *J. Am. Chem. Soc.* **2003,** 125, 715-728.
[77]. Binder, W. H.; Gloger, D.; Weinstabl, H.; Allmaier, G.; Pittenauer, E. *Macromolecules* **2007,** 40, 3097-3107.
[78]. Sugihara, Y.; O'Connor, P.; Zetterlund, P. B.; Aldabbagh, F. *J. Polym. Sci. Part A Polym. Chem.* **2011,** 49, 1856-1864.
[79]. O'Connor, P.; Zetterlund, P. B.; Aldabbagh, F. *J. Polym. Sci. Part A Polym. Chem.* **2011,** 49, 1719-1723.
[80]. McHale, R.; Aldabbagh, F.; Zetterlund, P. B. *J. Polym. Sci. Part A Polym. Chem.* **2007,** 45, 2194-2203.
[81]. Charleux, B.; Nicolas, J.; Guerret, O. *Macromolecules* **2005,** 38, 5485-5492.
[82]. Guillaneuf, Y.; Gigmes, D.; Marque, S. R. A.; Astolfi, P.; Greci, L.; Tordo, P.; Bertin, D. *Macromolecules* **2007,** 40, 3108-3114.
[83]. Nicolas, J.; Brusseau, S. g. n.; Charleux, B. *J. Polym. Sci. Part A Polym. Chem.* **2010,** 48, 34-47.
[84]. Nicolas, J.; Dire, C.; Mueller, L.; Belleney, J.; Charleux, B.; Marque, S. R. A.; Bertin, D.; Magnet, S.; Couvreur, L. *Macromolecules* **2006,** 39, 8274-8282.
[85]. Nicolas, J.; Mueller, L.; Dire, C.; Matyjaszewski, K.; Charleux, B. *Macromolecules* **2009,** 42, 4470-4478.
[86]. Wang, J.-S.; Matyjaszewki, K. *J. Am. Chem. Soc.* **1995,** 117, 5614-5615.
[87]. Kato, M.; Kamigaito, M.; Sawamoto, M.; Higashimura, T. *Macromolecules* **1995,** 28, 1721-1723.
[88]. Matyjaszewski, K.; Xia, Y. *Chem. Rev.* **2001,** 101, 2921.
[89]. Kamigaito, M.; Ando, T.; Sawamoto, M. *Chem. Rev.* **2001,** 101, 3689-3746.

[90]. Teodorescu, M.; Matyjaszewski, K. *Macromolecules* **1999,** 32, 4826-4831.
[91]. Matyjaszewski, K.; Jakubowski, W.; Min, K.; Tang, W.; Huang, J.; Braunecker, W. A.; Tsarevsky, N. V. *Proc. Natl. Acad. Sci. U. S. A.* **2006,** 103, 15309-15314.
[92]. Jakubowski, W.; Min, K.; Matyjaszewski, K. *Macromolecules* **2005,** 39, 39-45.
[93]. Rosen, B. M.; Percec, V. *Chem. Rev.* **2009,** 109, 5069-5119.
[94]. Lligadas, G.; Rosen, B. M.; Monteiro, M. J.; Percec, V. *Macromolecules* **2008,** 41, 8360-8364.
[95]. Chiefari, J.; Chong, Y. K.; Ercole, F.; Krstina, J.; Jeffery, J.; Le, T. P. T.; Mayadunne, R. T. A.; Meijs, G. F.; Moad, C. L.; Moad, G.; Rizzardo, E.; Thang, S. H. *Macromolecules* **1998,** 31, 5559-5562.
[96]. Corpart, P.; Charmot, D.; Biadatti, T.; Zard, S.; Michelet, D. WO9858974, 1998.
[97]. Moad, G.; Rizzardo, E.; Thang, S. H. *Aust. J. Chem.* **2005,** 58, 379-410.
[98]. Moad, G.; Rizzardo, E.; Thang, S. H. *Strem Chem.* **2011,** 25, 2-10.
[99]. Ajzenberg, N.; Trabelsi, F.; Recasens, F. *Chem. Eng. Technol.* **2000,** 23, 829-839.
[100]. McCoy, M. *Chem. Eng. News* **2006,** 84, 27.
[101]. McCoy, M. *Chem. Eng. News* **1999,** 77, 10.
[102]. Zosel, K. *Angew. Chem.* **1978,** 17, 702-709.
[103]. McHugh, M. A.; Krukonis, V. J., *Supercritical Fluid Extraction: Principles and Practice*. Butterworth-Heinemann: Boston, 1994.
[104]. Saharay, M.; Balasubramanian, S. *Chemphyschem* **2004,** 5, 1442-5.
[105]. DeSimone, J. M.; Guan, Z.; Elsbernd, C. S. *Science* **1992,** 257, 945-947.
[106]. Guan, Z.; Combes, J. R.; Menceloglu, Y. Z.; DeSimone, J. M. *Macromolecules* **1993,** 26, 2663-2669.
[107]. Alessi, P.; Cortesi, A.; Kikic, I.; Vecchione, F. *J. Appl. Polym. Sci.* **2003,** 88, 2189-2193.
[108]. Smith, P. B.; Moll, D. J. *Macromolecules* **1990,** 23, 3250-6.
[109]. Fleming, O. S.; Kazarian, S. G., Polymer Processing with Supercritical Fluids. In *Supercritical Carbon Dioxide*, Wiley-VCH Verlag GmbH & Co. KGaA: 2006; pp 205-238.
[110]. Kazarian, S. G.; Brantley, N. H.; West, B. L.; Vincent, M. F.; Eckert, C. A. *Appl. Spectrosc.* **1997,** 51, 491-494.
[111]. Kazarian, S. G.; Vincent, M. F.; Bright, F. V.; Liotta, C. L.; Eckert, C. A. *J. Am. Chem. Soc.* **1996,** 118, 1729-1736.
[112]. Monteiro, M. J.; Bussels, R.; Beuermann, S.; Buback, M. *Aust. J. Chem.* **2002,** 55, 433-437.
[113]. Arita, T.; Buback, M.; Janssen, O.; Vana, P. *Macromol. Rapid Comm.* **2004,** 25, 1376-1381.
[114]. Aldabbagh, F.; Zetterlund, P. B.; Okubo, M. *Macromolecules* **2008,** 41, 2732-2734.
[115]. Buback, M.; Morick, J. *Polym. Prepr.* **2008,** 49, 109-110.
[116]. Cooper, A. I.; Hems, W. P.; Holmes, A. B. *Macromol. Rapid Comm.* **1998,** 19, 353-357.
[117]. Wood, C. D.; Cooper, A. I. *Macromolecules* **2000,** 34, 5-8.
[118]. Adamsky, F. A.; Beckman, E. J. *Macromolecules* **1994,** 27, 312-14.
[119]. O'Neill, M. L.; Yates, M. Z.; Harrison, K. L.; Johnston, K. P.; Canelas, D. A.; Betts, D. E.; DeSimone, J. M.; Wilkinson, S. P. *Macromolecules* **1997,** 30, 5050-5059.
[120]. Ye, W.; DeSimone, J. M. *Macromolecules* **2005,** 38, 2180-2190.
[121]. Romack, T. J.; Combes, J. R.; DeSimone, J. M. *Macromolecules* **1995,** 28, 1724-6.

[122]. Okubo, M.; Fujii, S.; Maenaka, H.; Minami, H. *Colloid Polym. Sci.* **2003,** 281, 964-972.
[123]. DeSimone, J. M.; Maury, E. E.; Menceloglu, Y. Z.; McClain, J. B.; Romack, T. J.; Combes, J. R. *Science* **1994,** 265, 356-359.
[124]. Shaffer, K. A.; Jones, T. A.; Canelas, D. A.; DeSimone, J. M.; Wilkinson, S. P. *Macromolecules* **1996,** 29, 2704-2706.
[125]. Canelas, D. A.; DeSimone, J. M. *Macromolecules* **1997,** 30, 5673-5682.
[126]. Aldabbagh, F.; Zetterlund, P. B.; Okubo, M. *Eur. Polym. J.* **2008,** 44, 4037-4046.
[127]. Zetterlund, P. B.; Aldabbagh, F.; Okubo, M. *J. Polym. Sci. Part A Polym. Chem.* **2009,** 47, 3711-3728.
[128]. Xia, J.; Johnson, T.; Gaynor, S. G.; Matyjaszewski, K.; DeSimone, J. *Macromolecules* **1999,** 32, 4802-4805.
[129]. Minami, H.; Kagawa, Y.; Kuwahara, S.; Shigematsu, J.; Fujii, S.; Okubo, M. *Des. Monomers Polym.* **2004,** 7, 553-562.
[130]. Grignard, B.; Jérôme, C.; Calberg, C.; Jérôme, R.; Wang, W.; Howdle, S. M.; Detrembleur, C. *Chem. Commun.* **2008**, 314-316.
[131]. Grignard, B.; Jérôme, C.; Calberg, C.; Jérôme, R.; Detrembleur, C. *Eur. Polym. J.* **2008,** 44, 861-871.
[132]. Thurecht, K. J.; Gregory, A. M.; Wang, W.; Howdle, S. M. *Macromolecules* **2007,** 40, 2965-2967.
[133]. Gregory, A. M.; Thurecht, K. J.; Howdle, S. M. *Macromolecules* **2008,** 41, 1215-1222.
[134]. Odell, P. G.; Hamer, G. K. *Polym. Mater. Sci. Eng.* **1996,** 74, 404-5.
[135]. Ryan, J.; Aldabbagh, F.; Zetterlund, P. B.; Okubo, M. *Polymer* **2005,** 46, 9769-9777.
[136]. McHale, R.; Aldabbagh, F.; Zetterlund, P. B.; Okubo, M. *Macromol. Rapid Comm.* **2006,** 27, 1465-1471.
[137]. Canelas, D. A.; Betts, D. E.; DeSimone, J. M. *Macromolecules* **1996,** 29, 2818-2821.
[138]. Okubo, M.; Fujii, S.; Maenaka, H.; Minami, H. *Colloid Polym. Sci.* **2002,** 280, 183-187.
[139]. Minami, H.; Kagawa, Y.; Kuwahara, S.; Shigematsu, J.; Fujii, S.; Okubo, M. *Des. Monom. Polym.* **2004,** 7, 553-562.
[140]. McHale, R.; Aldabbagh, F.; Zetterlund, P. B.; Okubo, M. *Macromol. Rapid Commun.* **2006,** 27, 1465-1471.
[141]. Matyjaszewski, K.; Woodworth, B. E.; Zhang, X.; Gaynor, S. G.; Metzner, Z. *Macromolecules* **1998,** 31, 5955-5957.
[142]. Grignard, B.; Phan, T.; Bertin, D.; Gigmes, D.; Jérôme, C.; Detrembleur, C. *Polym. Chem.* **2010,** 1, 837-840.
[143]. Kendall, J. L.; Canelas, D. A.; Young, J. L.; DeSimone, J. M. *Chem. Rev.* **1999,** 99, 543-564.
[144]. Thurecht, K. J.; Howdle, S. M. *Aust. J. Chem.* **2009,** 62, 786-789.
[145]. Zetterlund, P. B.; Kagawa, Y.; Okubo, M. *Chem. Rev.* **2008,** 108, 3747-3794.
[146]. Cunningham, M. F. *Prog. Polym. Sci.* **2008,** 33, 365-398.
[147]. Grignard, B.; Calberg, C.; Jérôme, C.; Wang, W.; Howdle, S.; Detrembleur, C. *Chem. Commun.* **2008**, 5803-5805.
[148]. Grignard, B.; Jérôme, C.; Calberg, C. d.; Jérôme, R.; Wang, W.; Howdle, S. M.; Detrembleur, C. *Macromolecules* **2008,** 41, 8575-8583.

[149]. Zong, M.; Thurecht, K. J.; Howdle, S. M. *Chem. Commun.* **2008,** 45, 5942-5944.
[150]. Lee, H.; Terry, E.; Zong, M.; Arrowsmith, N.; Perrier, S. b.; Thurecht, K. J.; Howdle, S. M. *J. Am. Chem. Soc.* **2008,** 130, 12242-12243.
[151]. Cuervo-Rodriguez, R.; Bordegé, V.; Fernández-Monreal, M. C.; Fernández-García, M.; Madruga, E. L. *J. Polym. Sci.; Part A: Polym. Chem.* **2004,** 42, 4168-4176.
[152]. Guan, Z.; Combes, J. R.; Menceloglu, Y. Z.; DeSimone, J. M. *Macromolecules* **1993,** 26, 2663-2669.
[153]. Rindfleisch, F.; DiNoia, T. P.; McHugh, M. A. *J. Phys. Chem.* **1996,** 100, 15581-15587.
[154]. Arita, T.; Beuermann, S.; Buback, M.; Vana, P. *e-Polym.* **2004,** 003, 1-14.
[155]. Sadowski, G., Phase behaviour of polymer systems in high-pressure carbon dioxide In *Supercritical carbon dioxide in polymer reaction engineering*, Kemmere, M. F.; Meyer, T., Eds. Wiley-VCH: Weinheim, Germany, 2005; pp 15-35.
[156]. Heskins, M.; Guillet, J. E. *J. Macromol. Sci. Part A Chem.* **1968,** 2, 1441-1455.
[157]. Schild, H. G. *Prog. Polym. Sci.* **1992,** 17, 163-249.
[158]. Cho, E. C.; Lee, J.; Cho, K. *Macromolecules* **2003,** 36, 9929-9934.
[159]. Kikuchi, A.; Okano, T. *J. Control. Release* **2005,** 101, 69-84.
[160]. Wei, H.; Cheng, S.-X.; Zhang, X.-Z.; Zhuo, R.-X. *Prog. Polym. Sci.* **2009,** 34, 893-910.
[161]. Savariar, E. N.; Thayumanavan, S. *J. Polym. Sci. Part A Polym. Chem.* **2004,** 42, 6340-6345.
[162]. Kuroda, K.; Swager, T. M. *Macromolecules* **2004,** 37, 716-724.
[163]. Schulte, T.; Siegenthaler, K. O.; Luftmann, H.; Letzel, M.; Studer, A. *Macromolecules* **2005,** 38, 6833-6840.
[164]. Xia, Y.; Yin, X.; Burke, N. A. D.; Stöver, H. D. H. *Macromolecules* **2005,** 38, 5937-5943.
[165]. Rathfon, J. M.; Tew, G. N. *Polymer* **2008,** 49, 1761-1769.
[166]. Ganachaud, F.; Monteiro, M. J.; Gilbert, R. G.; Dourges, M. A.; Thang, S. H.; Rizzardo, E. *Macromolecules* **2000,** 33, 6738-6745.
[167]. Schilli, C.; Lanzendörfer, M. G.; Müller, A. H. E. *Macromolecules* **2002,** 35, 6819-6827.
[168]. Ray, B.; Isobe, Y.; Morioka, K.; Habaue, S.; Okamoto, Y.; Kamigaito, M.; Sawamoto, M. *Macromolecules* **2003,** 36, 543-545.
[169]. Convertine, A. J.; Ayres, N.; Scales, C. W.; Lowe, A. B.; McCormick, C. L. *Biomacromolecules* **2004,** 5, 1177-1180.
[170]. Ray, B.; Isobe, Y.; Matsumoto, K.; Habaue, S.; Okamoto, Y.; Kamigaito, M.; Sawamoto, M. *Macromolecules* **2004,** 37, 1702-1710.
[171]. Schilli, C. M.; Zhang, M.; Rizzardo, E.; Thang, S. H.; Chong, Y. K.; Edwards, K.; Karlsson, G.; Müller, A. H. E. *Macromolecules* **2004,** 37, 7861-7866.
[172]. Liu, B.; Perrier, S. *J. Polym. Sci. Part A Polym. Chem.* **2005,** 43, 3643-3654.
[173]. Carter, S.; Hunt, B.; Rimmer, S. *Macromolecules* **2005,** 38, 4595-4603.
[174]. Smith, A. E.; Xu, X.; Kirkland-York, S. E.; Savin, D. A.; McCormick, C. L. *Macromolecules* **2010,** 43, 1210-1217.
[175]. Millard, P.-E.; Barner, L.; Reinhardt, J.; Buchmeiser, M. R.; Barner-Kowollik, C.; Müller, A. H. E. *Polymer* **2010,** 51, 4319-4328.
[176]. Nuopponen, M.; Ojala, J.; Tenhu, H. *Polymer* **2004,** 45, 3643-3650.
[177]. Yusa, S.-i.; Yamago, S.; Sugahara, M.; Morikawa, S.; Yamamoto, T.; Morishima, Y. *Macromolecules* **2007,** 40, 5907-5915.

[178]. Nguyen, N. H.; Rosen, B. M.; Percec, V. *J. Polym. Sci. Part A Polym. Chem.* **2010,** 48, 1752-1763.
[179]. Zhou, S.; Fan, S.; Au-yeung, S. C. F.; Wu, C. *Polymer* **1995,** 36, 1341-1346.
[180]. Yu, T. L.; Lu, W.-C.; Liu, W.-H.; Lin, H.-L.; Chiu, C.-H. *Polymer* **2004,** 45, 5579-5589.
[181]. Kukulj, D.; Davis, T. P.; Gilbert, R. G. *Macromolecules* **1998,** 31, 994-999.
[182]. Lessard, B.; Tervo, C.; Maric, M. *Macromol. React. Eng.* **2009,** 3, 245-256.
[183]. O'Connor, P.; Zetterlund, P. B.; Aldabbagh, F. *Macromolecules* **2010,** 43, 914-919.
[184]. Ishizone, T.; Ito, M. *J. Polym. Sci. Part A Polym. Chem.* **2002,** 40, 4328-4332.
[185]. Ito, M.; Ishizone, T. *J. Polym. Sci. Part A Polym. Chem.* **2006,** 44, 4832-4845.
[186]. Loiseau, J.; Doerr, N.; Suau, J. M.; Egraz, J. B.; Llauro, M. F.; Ladaviere, C. *Macromolecules* **2003,** 36, 3066-3077.
[187]. Goto, A.; Kwak, Y.; Yoshikawa, C.; Tsujii, Y.; Sugiura, Y.; Fukuda, T. *Macromolecules* **2002,** 35, 3520-3525.
[188]. Gridnev, A. A. *Macromolecules* **1997,** 30, 7651-7654.
[189]. Sato, E.; Emoto, T.; Zetterlund, P. B.; Yamada, B. *Macromol. Chem. Phys.* **2004,** 205, 1829-1839.
[190]. Yamada, B.; Zetterlund, P. B.; Sato, E. *Prog. Polym. Sci.* **2006,** 31, 835-877.
[191]. Junkers, T.; Barner-Kowollik, C. *J. Polym. Sci.; Part A: Polym. Chem.* **2008,** 46, 7585-7605.
[192]. Ahmad, N. M.; Charleux, B.; Farcet, C.; Ferguson, C. J.; Gaynor, S. G.; Hawkett, B. S.; Heatley, F.; Klumperman, B.; Konkolewicz, D.; Lovell, P. A.; Matyjaszewski, K.; Venkatesh, R. *Macromol. Rapid Commun.* **2009,** 30, 2002-2021.
[193]. Ryan, J.; Aldabbagh, F.; Zetterlund, P. B.; Yamada, B. *Macromol. Rapid Commun.* **2004,** 25, 930-934.
[194]. Moad, G.; Solomon, D. H., *The Chemistry of Radical Polymerization*. Elsevier: Oxford, 2006; p p. 107.
[195]. Gibbons, O.; Carroll, W. M.; Aldabbagh, F.; Zetterlund, P. B.; Yamada, B. *Macromol. Chem. Phys.* **2008,** 209, 2434-2444.
[196]. Costioli, M. D.; Berdat, D.; Freitag, R.; Andre, X.; Muller, A. H. E. *Macromolecules* **2005,** 38, 3630-3637.
[197]. Min, Y.; Jun, L.; Hongfei, H. *Radiat. Phys. Chem.* **1995,** 46, 855-858.
[198]. Convertine, A. J.; Ayres, N.; Scales, C. W.; Lowe, A. B.; McCormick, C. L. *Biomacromolecules* **2004,** 5, 1177-1180.
[199]. Ueda, A.; Nagai, S., Transfer constants to monomers, polymers, catalysts and initiators, solvents and additives, and sulfur compounds in free radical polymerization. In *Polymer Handbook*, Brandrup, J.; Immergut, E. H.; Grulke, E. A., Eds. Wiley: New York, 1999; Vol. 4th ed, p II/97.
[200]. Lessard, B.; Tervo, C.; Maric, M. *Macromol. React. Eng.* **2009,** 3, 245-256.
[201]. de Lambert, B.; Charreyre, M. T.; Chaix, C.; Pichot, C. *Polymer* **2005,** 46, 623-637.
[202]. Opstad, C. L.; Melo, T. B.; Sliwka, H. R.; Partali, V. *Tetrahedron* **2009,** 65, 7616-7619.
[203]. Binder, W. H.; Gloger, D.; Weinstabl, H.; Allmaier, G.; Pittenauer, E. *Macromolecules* **2007,** 40, 3097-3107.
[204]. Yusa, S.; Yamago, S.; Sugahara, M.; Morikawa, S.; Yamamoto, T.; Morishima, Y. *Macromolecules* **2007,** 40, 5907-5915.
[205]. Carter, S.; Hunt, B.; Rimmer, S. *Macromolecules* **2005,** 38, 4595-4603.

[206]. Gibbons, O.; Carroll, W. M.; Aldabbagh, F.; Yamada, B. *J. Polym. Sci.; Part A: Polym. Chem.* **2006,** 44, 6410-6418.
[207]. Bosman, A. W.; Vestberg, R.; Heumann, A.; Frechet, J. M. J.; Hawker, C. J. *J. Am. Chem. Soc.* **2003,** 125, 715-728.
[208]. Kuroda, K.; Swager, T. M. *Macromolecules* **2004,** 37, 716-724.
[209]. Gotz, H.; Harth, E.; Schiller, S. M.; Frank, C. W.; Knoll, W.; Hawker, C. J. *J. Polym. Sci.; Part A: Polym. Chem.* **2002,** 40, 3379-3391.
[210]. Xu, W. J.; Zhu, X. L.; Cheng, Z. P.; Chen, J. Y.; Lu, J. M. *Macromolecular Research* **2004,** 12, 32-37.
[211]. Gonzalez, N.; Elvira, C.; Roman, J. S. *Macromolecules* **2005,** 38, 9298-9303.
[212]. Eggenhuisen, T. M.; Becer, C. R.; Fijten, M. W. M.; Eckardt, R.; Hoogenboom, R.; Schubert, U. S. *Macromolecules* **2008,** 41, 5132-5140.
[213]. Cooper, A. I. *J. Mater. Chem.* **2000,** 10, 207-234.
[214]. Firetto, V.; Scialdone, O.; Silvestri, G.; Spinella, A.; Galia, A. *J. Polym. Sci. Part A Polym. Chem.* **2010,** 48, 109-121.
[215]. Ganachaud, F.; Monteiro, M. J.; Gilbert, R. G.; Dourges, M.-A.; Thang, S. H.; Rizzardo, E. *Macromolecules* **2000,** 33, 6738-6745.
[216]. Millard, P. E.; Barner, L.; Stenzel, M. H.; Davis, T. P.; Barner-Kowollik, C.; Müller, A. H. E. *Macromol. Rapid Comm.* **2006,** 27, 821-828.
[217]. Boyer, C.; Bulmus, V.; Liu, J.; Davis, T. P.; Stenzel, M. H.; Barner-Kowollik, C. *J. Am. Chem. Soc.* **2007,** 129, 7145-7154.
[218]. Bai, W.; Zhang, L.; Bai, R.; Zhang, G. *Macromol. Rapid Comm.* **2008,** 29, 562-566.
[219]. Alidedeoglu, A. H.; York, A. W.; McCormick, C. L.; Morgan, S. E. *J. Polym. Sci. Part A Polym. Chem.* **2009,** 47, 5405-5415.
[220]. Nicolaÿ, R.; Marx, L.; Hémery, P.; Matyjaszewski, K. *Macromolecules* **2007,** 40, 6067-6075.
[221]. Rigolini, J.; Grassl, B.; Billon, L.; Reynaud, S.; Donard, O. F. X. *J. Polym. Sci. Part A Polym. Chem.* **2009,** 47, 6919-6931.
[222]. Rigolini, J.; Grassl, B.; Reynaud, S.; Billon, L. *J. Polym. Sci. Part A Polym. Chem.* **2010,** 48, 5775-5782.
[223]. Karg, M.; Lu, Y.; Carbó-Argibay, E.; Pastoriza-Santos, I.; Pérez-Juste, J.; Liz-Marzán, L. M.; Hellweg, T. *Langmuir* **2009,** 25, 3163-3167.
[224]. Sánchez-Iglesias, A.; Grzelczak, M.; Rodríguez-González, B.; Guardia-Girós, P.; Pastoriza-Santos, I.; Pérez-Juste, J.; Prato, M.; Liz-Marzán, L. M. *ACS Nano* **2009,** 3, 3184-3190.
[225]. Temtem, M. r.; Casimiro, T.; Mano, J. o. F.; Aguiar-Ricardo, A. *Green Chem.* **2007,** 9, 75.
[226]. Hu, Y.; Cao, L.; Xiao, F.; Wang, J. *Polym. Advan. Technol.* **2010,** 21, 386-391.
[227]. Cao, L.; Chen, L.; Lai, W. *J. Polym. Sci. Part A Polym. Chem.* **2007,** 45, 955-962.
[228]. Wang, C.; Wang, J.; Gao, W.; Jiao, J.; Feng, H.; Liu, X.; Chen, L. *J. Colloid Interf. Sci.* **2010,** 343, 141-148.
[229]. Pu, D. W.; Lucien, F. P.; Zetterlund, P. B. *J. Polym. Sci. Part A Polym. Chem.* **2010,** 48, 5636-5641.
[230]. Edeleva, M. V.; Kirilyuk, I. A.; Zubenko, D. P.; Zhurko, I. F.; Marque, S. R. A.; Gigmes, D.; Guillaneuf, Y.; Bagryanskaya, E. G. *J. Polym. Sci. Part A Polym. Chem.* **2009,** 47, 6579-6595.
[231]. Szwarc, M.; Levy, M.; Milkovich, R. *J. Am. Chem. Soc.* **1956,** 78, 2656-7.

[232]. Harth, E.; Bosman, A.; Benoit, D.; Helms, B.; Fréchet, J. M. J.; Hawker, C. J. *Macromol. Symp.* **2001,** 174, 85-92.
[233]. Kulkarni, S.; Schilli, C.; Grin, B.; Müller, A. H. E.; Hoffman, A. S.; Stayton, P. S. *Biomacromolecules* **2006,** 7, 2736-2741.
[234]. Li, G.; Shi, L.; An, Y.; Zhang, W.; Ma, R. *Polymer* **2006,** 47, 4581-4587.
[235]. Li, G.; Shi, L.; Ma, R.; An, Y.; Huang, N. *Angew. Chem. Int. Ed.* **2006,** 45, 4959-4962.
[236]. Li, G.; Song, S.; Guo, L.; Ma, S. *J. Polym. Sci. Part A Polym. Chem.* **2008,** 46, 5028-5035.
[237]. Masci, G.; Giacomelli, L.; Crescenzi, V. *Macromol. Rapid Commun.* **2004,** 25, 559-564.
[238]. Convertine, A. J.; Lokitz, B. S.; Vasileva, Y.; Myrick, L. J.; Scales, C. W.; Lowe, A. B.; McCormick, C. L. *Macromolecules* **2006,** 39, 1724-1730.
[239]. Li, Y.; Lokitz, B. S.; McCormick, C. L. *Macromolecules* **2006,** 39, 81-89.
[240]. An, Z.; Shi, Q.; Tang, W.; Tsung, C.-K.; Hawker, C. J.; Stucky, G. D. *J. Am. Chem. Soc.* **2007,** 129, 14493-14499.
[241]. Xie, D.; Ye, X.; Ding, Y.; Zhang, G.; Zhao, N.; Wu, K.; Cao, Y.; Zhu, X. X. *Macromolecules* **2009,** 42, 2715-2720.
[242]. Sun, X.-L.; He, W.-D.; Li, J.; Li, L.-Y.; Zhang, B.-Y.; Pan, T.-T. *J. Polym. Sci. Part A Polym. Chem.* **2009,** 47, 6863-6872.
[243]. Li, K.; Cao, Y. *Soft Matter.* **2010,** 8, 226-238.
[244]. Ramírez-Wong, D. G.; Posada-Vélez, C. A.; Saldívar-Guerra, E.; Luna-Bárcenas, J. G.; Ott, C.; Schubert, U. S. *Macromol. Symp.* **2009,** 283–284, 120-129.
[245]. Sogabe, A.; McCormick, C. L. *Macromolecules* **2009,** 42, 5043-5052.
[246]. Sogabe, A.; Flores, J. D.; McCormick, C. L. *Macromolecules* **2010,** 43, 6599-6607.
[247]. Gilbert, R. G. *Trends Polym. Sci.* **1995,** 3, 222-6.
[248]. Bertin, D.; Dufils, P.-E.; Durand, I.; Gigmes, D.; Giovanetti, B.; Guillaneuf, Y.; Marque, S. R. A.; Phan, T.; Tordo, P. *Macromol. Chem. Phys.* **2008,** 209, 220-224.

Peer-Reviewed Publications

Effect of Monomer Loading and Pressure on Particle Formation in Nitroxide-Mediated Precipitation Polymerization in Supercritical Carbon Dioxide.

Pádraig O'Connor, Per B. Zetterlund, Fawaz Aldabbagh, *Macromolecules*, **2010**, 43, 914-919.

Chain Transfer to Solvent in the Radical Polymerization of *N*-Isopropylacrylamide.

Yusuke Sugihara, Pádraig O'Connor, Per B. Zetterlund, Fawaz Aldabbagh, *J. Polym. Sci. Part A: Polym. Chem.*, **2011**, 49, 1856-1864.

Nitroxide-Mediated Stabilizer-Free Inverse Suspension Polymerization of *N*-Isopropylacrylamide in Supercritical Carbon Dioxide.

Pádraig O'Connor, Per B. Zetterlund, Fawaz Aldabbagh, *J. Polym. Sci. Part A: Polym. Chem.*, **2011,** 49, 1719-1723.

Facile Synthesis of Thermoresponsive Block Copolymers of *N*-Isopropylacrylamide using Heterogeneous Controlled/Living Nitroxide-Mediated Polymerizations in Supercritical Carbon Dioxide.

Pádraig O'Connor, Rongbing Yang, William M. Carroll, Yury Rochev, Fawaz Aldabbagh. *Eur. Poly. J.* **2012**, in press *doi.org/10.1016/j.eurpolymj.2012.04.011*

Conference Proceedings

Nitroxide-mediated precipitation polymerization in supercritical carbon dioxide: Effects of monomer loading and pressure

Pádraig O'Connor, Fawaz Aldabbagh, Per B Zetterlund. **Macro2010: 43rd IUPAC World Polymer Congress 11th-16th July 2010, SECC, Glasgow, UK.**

Heterogeneous Nitroxide-Mediated Controlled / Living Radical Polymerizations in Supercritical Carbon Dioxide

Pádraig O'Connor, Fawaz Aldabbagh, Per B Zetterlund. **Eli Lilly Chemistry Symposium, 30th Nov. 2010, NUI Galway.**

Nitroxide-Mediated Controlled/Living Radical Precipitation and Suspension Polymerizations in Supercritical Carbon Dioxide

Pádraig O'Connor, Per B Zetterlund, Fawaz Aldabbagh. **63rd Irish Universities Chemistry Research Colloquium 23rd-24th June 2011, UCD Dublin**

DOI: 10.1021/ma9022179

Macromolecules
ARTICLE

Effect of Monomer Loading and Pressure on Particle Formation in Nitroxide-Mediated Precipitation Polymerization in Supercritical Carbon Dioxide

Padraig O'Connor,[†] Per B. Zetterlund,*[,‡] and Fawaz Aldabbagh*[,†]

[†]*School of Chemistry, National University of Ireland, Galway, Ireland, and* [‡]*Centre for Advanced Macromolecular Design (CAMD), School of Chemical Sciences and Engineering, The University of New South Wales, Sydney NSW 2052, Australia*

Received October 6, 2009; Revised Manuscript Received November 6, 2009

ABSTRACT: The critical degree of polymerization (J_{crit}) at which polymer chains become insoluble in the continuous medium and particle formation commences has been estimated under a variety of experimental conditions for the nitroxide-mediated precipitation polymerizations of styrene (St) at 110 °C and *tert*-butyl acrylate (*t*-BA) at 118 °C in supercritical carbon dioxide ($scCO_2$) mediated by *N*-*tert*-butyl-*N*-[1-diethylphosphono(2,2-dimethylpropyl)]oxy (SG1). The value of J_{crit} increases with increasing target molecular weight, initial monomer loading, and pressure. Under the conditions investigated, J_{crit} for *t*-BA is higher than that for St, which is consistent with greater solubility of poly(acrylates) in neat $scCO_2$. A simple graphical approach has been developed and successfully employed, whereby J_{crit} can be predicted as a function of both target molecular weight and initial monomer loading on the basis of a data set of J_{crit} versus initial monomer loading.

Introduction

Supercritical carbon dioxide ($scCO_2$) is a benign reaction solvent well-suited for heterogeneous radical polymerizations because most organic small molecules (incl. monomer, initiator) are soluble in the medium, but the resulting high molecular weight (MW) polymers are insoluble.[1,2] Polymer chains are soluble in the medium up to a certain critical degree of polymerization (J_{crit}) when chains become insoluble and precipitate, resulting in particle formation. At J_{crit}, the polymerization changes from a homogeneous phase in $scCO_2$ to a heterogeneous system. Dispersion polymerizations contain a colloidal stabilizer to prevent coagulation of particles giving polymer of narrow particle size distributions and more well-defined particles ($d \approx$ 100 nm to 15 μm).[1−3]

Over the past 20 years, controlled/living radical polymerization (CLRP) has revolutionized polymer chemistry, allowing the synthesis of narrow molecular weight distribution (MWD) polymer, as well as complex architectures under less stringent polymerization conditions than ionic methods.[4] Although initially most CLRPs were carried out under homogeneous conditions, many have since been carried out using commercially important heterogeneous techniques.[5,6] The three most widely used CLRPs, nitroxide-mediated radical polymerization (NMP),[7−12] atom transfer radical polymerization (ATRP),[13−18] and reversible addition−fragmentation chain transfer (RAFT)[19−22] have all been successfully implemented as heterogeneous polymerizations in $scCO_2$. However, only NMP has thus far been shown to proceed in a controlled/living manner to high conversion using the stabilizer-free precipitation system.[10−12] Furthermore, under certain conditions (70% w/v monomer, $[SG1]_0/[AIBN]_0 = 1.99$, 110 °C, 30 MPa, where the nitroxide is SG1 = *N*-*tert*-butyl-*N*-[1-diethylphosphono(2,2-dimethylpropyl)]oxy and AIBN = 2,2′-azobisbutyronitrile), we showed that the precipitation NMP of styrene (St) can proceed with better control over the MWD than the corresponding solution polymerization.[11,12]

The slow build up in MW in a CLRP by virtue of the equilibrium between active (propagating radicals) and dormant polymer chains allows measurement of J_{crit} by estimating via visual observation the conversion (and thus the MW) at which the reaction mixture changes from transparent to opaque (the cloud point). In a conventional nonliving polymerization, the system would immediately become heterogeneous because of the instantaneous formation of high MW polymer. The value of J_{crit} would change with conversion as the composition of the continuous phase changes because chains are continuously initiated and grow to reach J_{crit} throughout the polymerization. However, in CLRP, the initial stoichiometry dictates the conversion at J_{crit}, and a single J_{crit} value applies to a given polymerization system. This technique has been employed to estimate J_{crit} for precipitation/dispersion NMP of St in $scCO_2$.[8,11]

To date, only the NMP of St in $scCO_2$ has been studied, and no information on controlled/living character at low conversion (before J_{crit}), when the reaction is homogeneous, has been obtained. The NMP of St and *tert*-butyl acrylate (*t*-BA) in $scCO_2$ before and after J_{crit} is now presented. The detailed effects of composition and pressure on J_{crit} and the associated controlled/living character are examined. This has led us to develop a simple graphical approach to predicting J_{crit} as a function of both target MW ($[monomer]_0/[initiator]_0$) and initial monomer loading based on a data set of J_{crit} versus initial monomer loading. These findings will enable future optimization of heterogeneous (precipitation and dispersion) CLRPs in $scCO_2$.

Experimental Section

Materials. St (Aldrich, >99%) and *t*-BA (Aldrich, 98%) were distilled under reduced pressure before use. AIBN (DuPont

*Corresponding authors. (P.B.Z.) Tel: +61-2-9385 4331. Fax:+61-2-9385 6250. E-mail: p.zetterlund@unsw.edu.au. (F.A.) Tel: +353-91-493120. Fax: +353-91-525700. E-mail: fawaz.aldabbagh@nuigalway.ie.

 Published on Web 11/18/2009

Table 1. Results for Measurement of J_{crit} for Poly(styrene) using Different Monomer Loadings and Pressures at 110 °C

$[M]_0$ (% w/v)[a]	pressure (MPa)	time at J_{crit} (min)	conv. (%)	M_n	$M_{n,th}$	M_w/M_n	J_{crit}
80	30	272	32.8	13 450	13 100	1.13	129
70	30	227	22.0	8550	8800	1.15	82
60	30	119	14.1	5000	5650	1.17	48
55	30	96	10.3	4250	4100	1.18	41
50	30	71	8.4	3450	3400	1.17	33
40	30	51	3.9	3000	1550	1.18	29
35	30	44	1.8	2950	700	1.19	28
30	30	35	0.9	2800	350	1.35	27
70	23	264	21.9	7600	8750	1.20	73
70	15	175	16.0	6100	6400	1.22	59
70	10	140	16.8	5400	6700	1.21	52

[a] Initial monomer loading.

Chemical Solution Enterprise) was recrystallized from methanol before use. SG1 (also known as DEPN) was prepared according to the literature[23] with purity (96%) determined using ^{1}H NMR spectroscopy from the reaction of SG1 radical with pentafluorophenylhydrazine (Aldrich). Reagent grade toluene (Aldrich, ≥ 99.7%), methanol (Corcoran Chemicals, 99.9%), dichloromethane (Corcoran Chemicals, 99.9%), and CO_2 (BOC, 99.8%) were used as received. Macroinitiator (poly(St)-T, PSt-T: where, T = SG1, M_n = 4250 g mol^{-1}, M_w/M_n = 1.18) was obtained from the J_{crit} measurement experiment at 55% monomer loading. (See Table 1.)

Equipment and Measurements. All NMP in $scCO_2$ were conducted in a 100 mL stainless steel Thar reactor with 180° inline sapphire windows and overhead Magdrive stirrer with maximum programmable operating pressure and temperature of 41.4 MPa and 120 °C, respectively. The pressure was produced and maintained by a Thar P-50 series high-pressure pump to within ±0.2 MPa. The temperature was regulated by a Thar CN6 controller to within ±1 °C. The reactor is connected to a Thar automated back pressure regulator (ABPR, a computer-controlled needle valve) for controlled venting.

M_n and polydispersity (M_w/M_n) were determined using a gel permeation chromatography (GPC) system consisting of a Viscotek DM 400 data manager, a Viscotek VE 3580 refractive-index detector, and two Viscotek Viscogel GMH_{HR}-M columns. Measurements were carried out using tetrahydrofuran (THF) at a flow rate of 1.0 mL·min^{-1} at 35 °C with columns calibrated using 12 linear poly(St) standards (M_n = 162−6 035 000). M_n and M_w/M_n values for poly(*t*-BA) (P*t*-BA) are not accurate because of the calibration against PSt standards. However, our primary focus is trends as well as shape and relative position of MWDs. M_n is given in grams per mole (g·mol^{-1}) throughout to the nearest 50 g·mol^{-1}.

Polymerization of St in $scCO_2$. The reactor was loaded with St (58.320 g, 0.56 mol), PSt-T (1.680 g, 0.40 mmol) (60% w/v includes St + PSt-T), and SG1 (47 mg, 0.16 mmol). The reactor was sealed with the magnetically coupled stirring lid (Magdrive). The mixture was purged for 15 min by bubbling gaseous CO_2 through the mixture to remove air. Liquid CO_2 (~5 MPa) was added, and the temperature was raised to the reaction temperature of 110 °C, followed by the pressure to the reaction pressure (in this case 30 MPa) by the addition of CO_2. The transparent reaction mixture was stirred at ~1000 rpm throughout and monitored through the inline sapphire windows, and if J_{crit} was required, stopped when the reaction mixture became opaque. Heating was stopped, and rapid external cooling using dry ice was carried out (this caused the temperature of the reactor to drop to ~80 °C in 10 min). The CO_2 was vented slowly from the reactor (when at approximately room temperature after 40 min of cooling) through a suitable solvent (methanol) to prevent the loss of polymer and opened using the ABPR, and the reaction mixture pipetted directly from the reactor. The polymer was precipitated from excess methanol, filtered, and dried prior to conversion measurement by gravimetry.

Table 2. Results for Measurement of J_{crit} for Poly(*tert*-butyl acrylate) using Different Monomer Loadings and Pressures at 118 °C

$[M]_0$ (% w/v)[a]	pressure (MPa)	time at J_{crit} (min)	conv. (%)	M_n	$M_{n,th}$	M_w/M_n	J_{crit}
70	30	1159	66.0	17100	17750	1.44	133
60	30	960	51.8	12650	13950	1.37	99
50	30	720	38.8	10500	10500	1.28	82
30	30	225	10.0	3900	2700	1.29	30
60	23	576	43.1	11100	11600	1.35	87
60	15	428	29.6	9500	8000	1.29	74
60	10	335	24.7	7750	6650	1.23	61

[a] Initial monomer loading.

Polymerization of *t*-BA in $scCO_2$. *t*-BA (50.000 g, 0.39 mol, 50% w/v), AIBN (0.124 g, 0.76 mmol) and SG1 (0.550 g, 1.87 mmol) were heated at 118 °C and 30 MPa using the polymerization procedure above. The polymer was precipitated from a 3:2 water/methanol mixture, filtered, and dried prior to conversion measurement by gravimetry.

Measurement of J_{crit} in $scCO_2$. For the 70% w/v initial St loading and $M_{n,th}$ at 100% conversion = 40 000 (eq 1), St (70.000 g, 0.67 mol), AIBN (0.173 g, 1.05 mmol), and SG1 (0.620 g, 2.11 mmol) were heated at 110 °C and 30 MPa, and the polymerization stopped at J_{crit} (see procedure above). The theoretical value of M_n ($M_{n,th}$) is calculated via eq 1

$$M_{n,\,th} = \frac{\alpha[M]_0 MW_{mon}}{2f[AIBN]_0} \quad (1)$$

where f is the AIBN initiator efficiency, α is the fractional conversion of monomer, $[M]_0$ is the initial monomer concentration, and MW_{mon} is the molecular weight of the monomer. The value of f in $scCO_2$ at 59.4 °C has been estimated to be 0.83 by DeSimone and coworkers.[24] In the present study, f was estimated by fitting the initial portion of the M_n versus conversion plots of the polymerization data to yield f = 0.83 (St) and 1.23 (*t*-BA). $M_{n,th}$ values were computed throughout this work using eq 1 in connection with these f-estimates. A value of f greater than unity, as obtained for *t*-BA, is of course not physically meaningful; this is most likely a result of accumulated error primarily due to inaccuracy caused by the use of linear PSt standards. The initiator efficiency of the macroinitiator PSt-T is taken as 1.

Chain Extension of P*t*-BA with Bulk St. P*t*-BA macroinitiator from 70% w/v initial loading experiment (Table 2) (0.4270 g, 0.025 mmol), St (2 g, 19.20 mmol), and SG1 (1.5 mg, 5.10 μmol) were charged in a glass ampule. Air was removed by several freeze−thaw degas cycles before the ampule was sealed. It was then placed in an aluminum heating block at 120 °C for 24 h. The polymerization was quenched by immersing the ampule into an ice−water bath. Subsequently, the mixture was dissolved in dichloromethane and poured into an excess of 3:2 water/methanol to precipitate the formed polymer. After filtration and drying, the conversion was obtained from the increase in weight of polymeric material.

Results and Discussion

NMP of St and *t*-BA in $scCO_2$. Conversion−time and MWD data for NMP of St (60% w/v) in $scCO_2$ initiated by a soluble macroinitiator (PSt-T, where T = SG1, with 40 mol % free SG1 relative to PSt-T; the addition of free SG1 is primarily to alleviate partitioning effects[8] anticipated after J_{crit}) at 110 °C and 30 MPa are displayed in Figures 1 and 2. The polymerization proceeded to intermediate conversion with no sign of having reached a limiting conversion (Figure 1), and the MWDs shifted to higher MW with increasing conversion (Figure 2).

We obtained the value of J_{crit} by visually monitoring the polymerization via the reactor inline sapphire windows. The

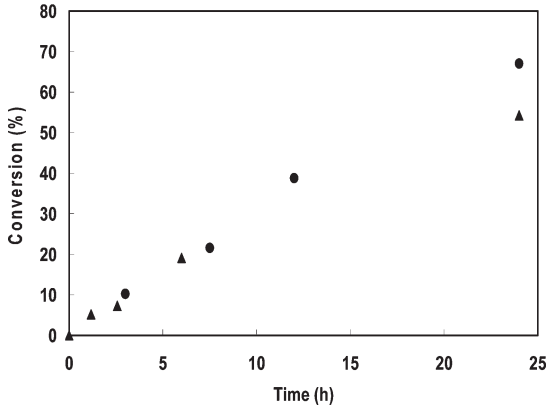

Figure 1. Conversion versus time for the SG1-mediated polymerization of St (▲, 60% w/v) at 110 °C (initiated by PSt-T macroinitiator in the presence of 40 mol % free SG1) and *t*-BA (●, 50% w/v) at 118 °C ($[SG1]_0/[AIBN]_0 = 2.5$) in $scCO_2$ at 30 MPa. J_{crit} is at 7.3 and 38.8% conversion for St and *t*-BA, respectively.

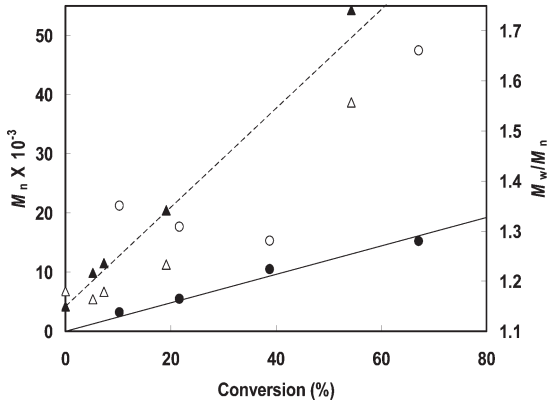

Figure 2. M_n (closed symbols) and M_w/M_n (open symbols) versus conversion for the SG1-mediated polymerization of St (▲, △, 60% w/v) at 110 °C (initiated by PSt-T macroinitiator in the presence of 40 mol % free SG1) and *t*-BA (●, ○, 50% w/v) at 118 °C ($[SG1]_0/[AIBN]_0 = 2.5$) in $scCO_2$ at 30 MPa. Dashed and continuous lines represent $M_{n,th}$ for St and *t*-BA polymerizations, respectively. J_{crit} is at 7.3 and 38.8% conversion for St and *t*-BA, respectively.

polymerization was stopped at the point when the mixture changed from transparent to opaque. Subsequent measurement of M_n yielded $J_{crit} = 110$ ($M_n = 11\,450$) at 7.3% conversion. Because of the inherent polydispersity of the polymer (despite the CLRP process), this value of J_{crit} is to an extent an underestimate of the true J_{crit}. This is because the chains of the highest MW of the MWD will be the ones that first precipitate, whereas the obtained J_{crit} corresponds to the full MWD. The values of M_w/M_n increased with conversion in the range of 1.16 to 1.18 before J_{crit} and 1.23 to 1.56 after J_{crit} (Figure 2), indicating good control/livingness in agreement with our previously reported SG1/AIBN-initiated precipitation polymerizations.[10−12]

Conversion−time and MWD data for NMP of *t*-BA (50% w/v) in $scCO_2$ initiated by AIBN and controlled using an excess of nitroxide, $[SG1]_0/[AIBN]_0 = 2.5$, at 118 °C and 30 MPa are displayed in Figures 1 and 2. Similarly to the St NMP above, M_n increased linearly with conversion, which is indicative of good controlled/living character, and $J_{crit} = 82$ ($M_n = 10\,510$) was recorded at 38.8% conversion. M_w/M_n increased dramatically after J_{crit} (1.28 to 1.35 before J_{crit} and 1.66 after J_{crit}), which is probably the consequence of a lowering in the free [SG1] at the locus of polymerization due to partitioning toward the $scCO_2$ continuous phase

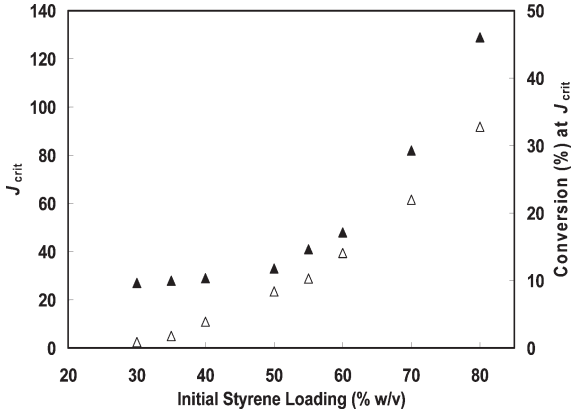

Figure 3. J_{crit} (▲) and conversion at J_{crit} (△) versus initial St loading for the SG1-mediated polymerization of St in $scCO_2$ at 110 °C and 30 MPa ($[SG1]_0/[AIBN]_0 = 2.0$, theoretical M_n at 100% conversion ($M_{n,th}$) = 40 000).

(the particle phase is the main locus of polymerization after J_{crit}),[2,12] although partial loss of control of NMP would be expected at high conversions.

Effect of Monomer Loading on J_{crit}. Values of J_{crit} were estimated for the NMP of St in $scCO_2$ at a range of different initial monomer loadings of 30−80% w/v using $[SG1]_0/[AIBN]_0 = 2.0$ ($M_{n,th} = 40\,000$ at 100% conversion) at 110 °C and 30 MPa (Figure 3, Table 1). As expected, J_{crit} increased with monomer loading because of the increased solubility of the polymer in the increasingly monomer-rich continuous phase. However, J_{crit} increased only slightly from 27 (conv. = 0.9%) to 33 (conv. = 8.4%) as the initial loading was increased from 30 to 50% w/v. As the monomer loading was increased further to 55% w/v ($J_{crit} = 41$, conv. = 10.3%), the values of J_{crit} increased more dramatically to reach 129 (conv. = 32.8%) at 80% w/v.

Considering that the ratio $[St]_0/[AIBN]_0$ was the same in all polymerizations, one would expect that M_n versus conversion of these polymerizations would give a straight line (provided that *f* does not change significantly with monomer loading); that is, J_{crit} versus conversion at J_{crit} should give a straight line. It is, however, apparent from Figure 3 (and Table 1) that at low monomer loadings, this is not the case; J_{crit} is higher than expected considering the conversions at J_{crit}. Because of the short polymerization times required to reach J_{crit} (35−51 min at 30−40% w/v St, Table 1), some fraction of AIBN remains undecomposed at J_{crit}, thus giving $M_n > M_{n,th}$. Estimation of apparent *f* values based on eq 1 gives $f \approx 0.1$, 0.4, and 0.78 at 30, 40, and 50% w/v St, respectively, with $M_n \approx M_{nth}$ at 50% w/v St. This hypothesis was confirmed by taking a 35% w/v initial loading polymerization of St (under the same conditions as that used for the J_{crit} measurement, where apparent $f = 0.2$) to well beyond J_{crit} (15 h), which gave $M_n = 13\,700$ ($M_w/M_n = 1.33$) at 31.3% conversion. This approached the $M_{n,th} = 12\,500$ with apparent $f \approx 0.76$, which is close to the literature value of 0.83.[24]

Values of J_{crit} were estimated for the NMP of *t*-BA in $scCO_2$ at a range of different initial monomer loadings of 30−70% w/v using $[SG1]/[AIBN] = 2.5$ ($M_{n,th} = 26{,}900$ at 100% conversion) at 118 °C and 30 MPa (Figure 4, Table 2). J_{crit} and the conversion at J_{crit} increased almost linearly with initial monomer loading from $J_{crit} = 30$ at 10.0% to 133 at 66.0% conversion, which is indicative of increased polymer solubility in the continuous phase. The J_{crit} (and conversion at J_{crit}) values for *t*-BA (for a given monomer loading) are considerably higher than those for St, indicating greater

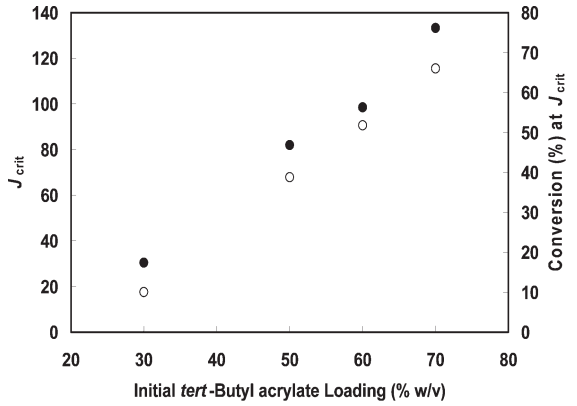

Figure 4. J_{crit} (●) and conversion at J_{crit} (○) versus initial *t*-BA loading for the SG1-mediated polymerization of *t*-BA in $scCO_2$ at 118 °C and 30 MPa ($[SG1]_0/[AIBN]_0$ = 2.5, theoretical M_n at 100% conversion ($M_{n,th}$) = 26 900).

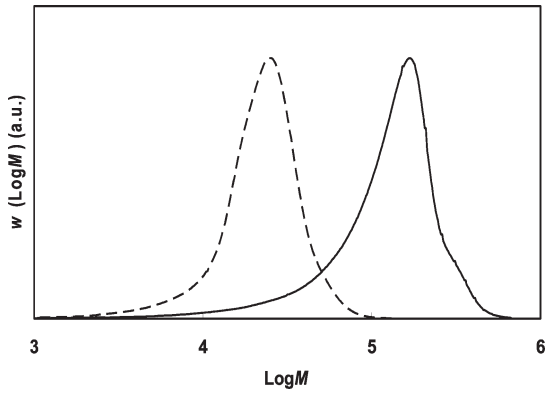

Figure 5. MWDs (normalized to peak height) of the chain extension of P*t*-BA (from 70% w/v initial monomer loading experiment (Table 2) M_n = 17 100, M_w/M_n = 1.44) with bulk St at 120 °C to give P*t*-BA-*b*-PSt; M_n = 65 200, M_w/M_n = 2.23, Conv. = 91.1%.

solubility of P*t*-BA compared with PSt in $scCO_2$ at the respective temperatures and pressures. The St and *t*-BA polymerizations resulted in similar M_n vs conversion plots (Table 1 and 2); that is, similar M_n values were reached at a given conversion, thus making direct comparison meaningful in this sense. It has been reported that the solubility of poly(butyl acrylate) in neat $scCO_2$ is higher than that of PSt, mainly as a result of the higher glass-transition temperature of PSt.[25]

Longer polymerization times were required to reach J_{crit} for *t*-BA than St (Tables 1 and 2) and the temperature was higher for *t*-BA (118 vs 110 °C); therefore, partial decomposition of AIBN at J_{crit} at low monomer loadings was not an issue for *t*-BA (i.e., J_{crit} increases close to linearly with conversion at J_{crit}). Controlled/living character was maintained up to high conversion, as indicated by M_n = 17 100 remaining close to $M_{n,th}$ = 17 750 at 66.0% conversion (Table 2) and confirmed by efficient chain extension of this sample with bulk St (Figure 5).

The J_{crit} values for St appear to be consistent with the work of Vana and coworkers, who reported homogeneous RAFT polymerizations of St in $scCO_2$ at 80 °C and 30 MPa using 78% vol % St for M_n < 29 800.[26]

Predicting J_{crit}. The J_{crit} data described above for St and *t*-BA can be employed to predict J_{crit} under different experimental conditions in terms of the targeted MW ($M_{n,th}$ at 100% conversion) and the initial monomer loading for the systems investigated (i.e., same temperature and pressure).

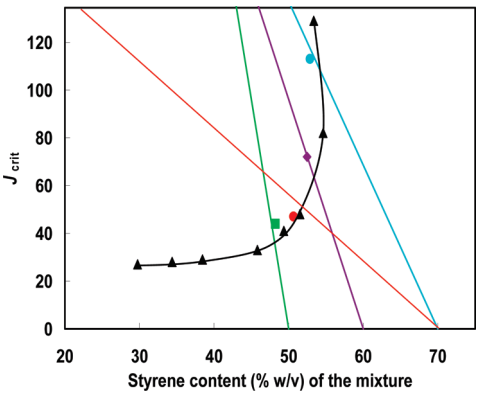

Figure 6. Plot of J_{crit} versus St content of the mixture at J_{crit} (▲) for the SG1-mediated polymerization of St in $scCO_2$ at 110 °C and 30 MPa ($[SG1]_0/[AIBN]_0$ = 2.0; $M_{n,th}$ (100% conv.) = 40 000). The straight lines (colors), each represent a given set of conditions in terms of initial monomer loading and $M_{n,th}$, describing how the degree of polymerization changes with the % w/v monomer content when the polymerization proceeds in accordance with eq 1. $M_{n,th}$ lines: 70% w/v St, $M_{n,th}$ = 20 000 (●; red), 70% w/v St, $M_{n,th}$ = 50 000 (●; blue), 60% w/v St, $M_{n,th}$ = 60 000 (◆; purple), and 50% w/v St, $M_{n,th}$ = 100 000 (■; green). $M_{n,th}$ values in the legend refer to 100% conversion, and symbols represent individual experiments carried out using these conditions.

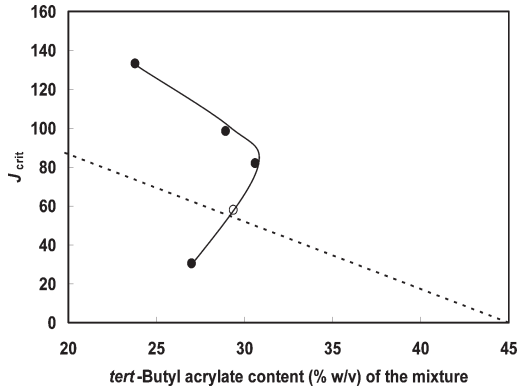

Figure 7. Plot of J_{crit} versus *t*-BA content of the mixture at J_{crit} (●) for the SG1-mediated polymerization of *t*-BA in $scCO_2$ at 118 °C and 30 MPa ($[SG1]_0/[AIBN]_0$ = 2.5, $M_{n,th}$ (100% conv.) = 26 900). The straight dotted line represents a given set of conditions in terms of initial monomer loading and $M_{n,th}$ and describes how the degree of polymerization changes with the % w/v monomer content when the polymerization proceeds in accordance with eq 1. $M_{n,th}$ line: 45% w/v *t*-BA, $M_{n,th}$ = 20 000 at 100% conversion, and (○) represents the J_{crit} experiment using these conditions.

For example, if the ratio of monomer to AIBN is altered (i.e., different $M_{n,th}$) but the initial monomer loading is the same, then how does J_{crit} change? To this end, the J_{crit} data are presented graphically in Figures 6 and 7 in the form of a plot of J_{crit} versus the monomer content (as % w/v) of the mixture at J_{crit} (readily calculated from the monomer conversion at J_{crit}). The J_{crit} value can be graphically predicted by constructing theoretical lines of $M_{n,th}$ from the initial monomer loading based on eq 1. The theoretical lines describe how the degree of polymerization changes with the % w/v monomer remaining when the polymerization proceeds in accordance with eq 1. J_{crit} of the "new" system corresponds to the point of intersection of the straight $M_{n,th}$ line and the J_{crit} curve. In the case of St (Figure 6, Table 3), using 70% w/v initial St loading and $M_{n,th}$ = 20 000 and 50 000 (at 100% conv.), the predictive graphical approach resulted in J_{crit} = 50 and 110 (at the intersections), respectively, which are remarkably close to the experimentally (in independent experiments)

Table 3. Results for Prediction of J_{crit} for Poly(styrene) at 110 °C and Poly(*tert*-butyl acrylate) at 118 °C using Different Monomer Loadings and Targeted $M_{n,th}$

monomer	$[M]_0$ (% w/v)[a]	conv. (%)	M_n	$M_{n,th}$	M_w/M_n	expt J_{crit}	predicted J_{crit}[b]
St	70	24.5	11 800	12 250	1.15	113	110
St	70	27.6	4900	5500	1.13	47	50
St	60	12.6	7500	7500	1.19	72	65
St	50	3.6	4550	3550	1.33	44	38
t-BA	45	34.8	7450	6950	1.30	58	55

[a] Initial monomer loading. [b] Predicted J_{crit} is from the intersection of the theoretical $M_{n,th}$ line and the curve.

obtained values of J_{crit} = 47 and 113. Varying the initial St monomer loadings, 50 and 60% w/v, with $M_{n,th}$ = 100 000 and 60 000 (at 100% conv.), respectively, gave predicted J_{crit} = 38 and 65, which were also close to those obtained experimentally at J_{crit} = 44 and 72. Also, in the case of *t*-BA (Figure 7 and Table 3), excellent agreement was obtained between the prediction (J_{crit} = 55) and experiment (J_{crit} = 58) for 45% w/v *t*-BA and $M_{n,th}$ = 20 000 (at 100% conv.).

The success of this predictive approach demonstrates how J_{crit} is governed by the dependence of M_n on conversion as well as the initial monomer loading. A change in $M_{n,th}$ at a fixed initial monomer loading affects J_{crit} because it alters the composition of the continuous medium at a given M_n. For example, an increase in $M_{n,th}$ by a factor of two means that a given M_n will be reached at half the conversion of the original recipe. In other words, at this value of M_n, the remaining monomer content will be higher than that for the original recipe. This understanding, as well as the predictive approach developed, is also expected to apply equally well to other CLRP systems such as ATRP and RAFT as well as non-$scCO_2$ media (e.g., alcohols/water). Moreover, the above is not restricted to precipitation polymerizations but also applies to dispersion (stabilized heterogeneous) polymerizations.

The J_{crit} curves in Figures 6 and 7 are shaped in such a way that at higher initial monomer loadings, the monomer content (% w/v) of the mixture (or monomer remaining) is lower than the monomer content of the mixture at lower initial monomer loadings; that is, the curve exhibits a negative gradient ("goes back on itself"). The reason is that at a high initial monomer loading, J_{crit} is so high that very significant monomer consumption is required to reach this degree of polymerization and hence the amount of remaining monomer becomes very low. This effect is particularly strong for *t*-BA, which (under the present conditions), exhibits higher J_{crit} than St. If the $M_{n,th}$ line crosses the J_{crit} curve twice, then it is the first intersection that corresponds to J_{crit}.

Effect of Pressure on J_{crit}. Attention was next turned to how pressure influences J_{crit} during precipitation NMP in $scCO_2$. Polymer solubility in $scCO_2$ increases with increasing pressure as a result of the increase in CO_2 density[25,27] and thus solvent power. One would therefore anticipate J_{crit} to increase with increasing pressure. Figure 8 shows J_{crit} versus pressure for SG1-mediated polymerizations in $scCO_2$ of St 70% w/v at 110 °C ($[SG1]_0/[AIBN]_0$ = 2.0, $M_{n,th}$ = 40 000 at 100% conv.) and *t*-BA 60% w/v at 118 °C ($[SG1]_0/[AIBN]_0$ = 2.5, $M_{n,th}$ = 26 900 at 100% conv.). For both monomers, there is a close-to-linear increase in J_{crit} with increasing pressure. The increase is quite pronounced: in the case of *t*-BA, an increase in pressure from 10 to 30 MPa leads to an increase in J_{crit} from 61 to 99. In terms of conversions at J_{crit}, this means that the system is homogeneous to 24.7 and 51.8% conversion at 10 and 30 MPa, respectively. In both cases, controlled/living character is confirmed by M_n values

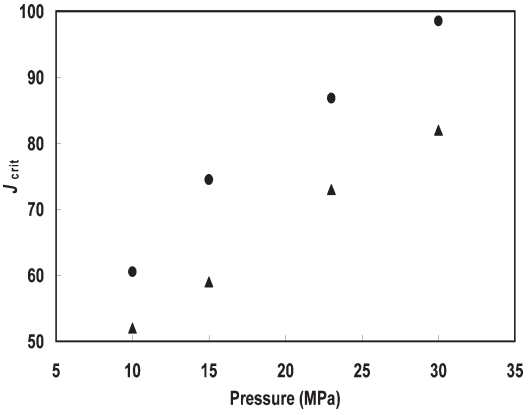

Figure 8. Plot of J_{crit} versus pressure (±0.2 MPa) for the SG1-mediated precipitation polymerization in $scCO_2$ of 70% w/v St (▲) at 110 °C (using [SG1]/[AIBN] = 2.0, $M_{n,th}$ = 40 000 at 100% conv.) and 60% w/v *t*-BA (●) at 118 °C (using [SG1]/[AIBN] = 2.5, $M_{n,th}$ = 26 900 at 100% conv.).

that are reasonably close to $M_{n,th}$ and low M_w/M_n of 1.15 to 1.22 and 1.23 to 1.37 for St and *t*-BA, respectively (Tables 1 and 2).

McHugh and coworkers attributed the lower solubility of PSt relative to poly(acrylates) to its higher T_g and a very high hindrance potential for chain segment rotations giving a higher entropy penalty for CO_2 to dissolve PSt compared to poly(acrylates).[25] There is an overall increase in J_{crit} of 30 between 10 and 30 MPa for St, with the latter polymerization giving excellent control/living character, M_n (8550) close to $M_{n,th}$ (8800), and low M_w/M_n (1.15). At 70−80% w/v initial St loadings and the highest pressure used (30 MPa), the reaction is homogeneous over the widest conversion range (also J_{crit} is highest), which favors optimal controlled/living character at J_{crit} and beyond (as indicated by our earlier high conversion NMP precipitation polymerizations[11,12]).

Conclusions

SG1-mediated polymerizations of St (110 °C) and *t*-BA (118 °C) were shown to proceed in a controlled/living manner from low (homogeneous) to high (heterogeneous) conversion in $scCO_2$ at 30 MPa. The influence of monomer-to-initiator ratio, initial monomer loading, and pressure on the critical degree of polymerization (J_{crit}) in $scCO_2$ has been determined. J_{crit} represents the point at which the polymerization becomes heterogeneous or polymer chains become insoluble in the continuous medium, and particle formation begins. J_{crit} increased close to linearly with increasing initial monomer loading (50 to 80% w/v and 30 to 70% w/v for St and *t*-BA, respectively) and pressure (10 to 30 MPa) for both monomers. A simple graphical approach to predict J_{crit} as a function of initial monomer loading and targeted $M_{n,th}$ ($[monomer]_0/[initiator]_0$) is presented. This predictive approach will equally apply to other CLRP systems such as ATRP and RAFT as well as non-$scCO_2$ media (e.g., alcohols/water). Moreover, the above is not restricted to precipitation polymerizations but also applies to dispersion polymerizations.

Acknowledgment. This publication has emanated from research work conducted with financial support from Science Foundation Ireland (08/RFP/MTR1201).

References and Notes

(1) Kendall, J. L.; Canelas, D. A.; Young, J. L.; DeSimone, J. M. *Chem. Rev.* **1999**, *99*, 543–563.
(2) Zetterlund, P. B.; Aldabbagh, F.; Okubo, M. *J. Polym. Sci., Part A: Polym. Chem.* **2009**, *47*, 3711–3728.

(3) Thurecht, K. J.; Howdle, S. M. *Aust. J. Chem.* **2009**, *62*, 786–789.
(4) Braunecker, W. A.; Matyjaszewski, K. *Prog. Polym. Sci.* **2007**, *32*, 93–146.
(5) Zetterlund, P. B.; Kagawa, Y.; Okubo, M. *Chem. Rev.* **2008**, *108*, 3747–3794.
(6) Cunningham, M. F. *Prog. Polym. Sci.* **2008**, *33*, 365–398.
(7) Ryan, J.; Aldabbagh, F.; Zetterlund, P. B.; Okubo, M. *Polymer* **2005**, *46*, 9769–9777.
(8) McHale, R.; Aldabbagh, F.; Zetterlund, P. B.; Minami, H.; Okubo, M. *Macromolecules* **2006**, *39*, 6853–6860.
(9) McHale, R.; Aldabbagh, F.; Zetterlund, P. B.; Okubo, M. *Macromol. Rapid Commun.* **2006**, *27*, 1465–1471.
(10) McHale, R.; Aldabbagh, F.; Zetterlund, P. B.; Okubo, M. *Macromol. Chem. Phys.* **2007**, *208*, 1813–1822.
(11) Aldabbagh, F.; Zetterlund, P. B.; Okubo, M. *Macromolecules* **2008**, *41*, 2732–2734.
(12) Aldabbagh, F.; Zetterlund, P. B.; Okubo, M. *Eur. Polym. J.* **2008**, *44*, 4037–4046.
(13) Xia, J.; Johnson, T.; Gaynor, S. G.; Matyjaszewski, K.; DeSimone, J. M. *Macromolecules* **1999**, *32*, 4802–4805.
(14) Minami, H.; Kagawa, Y.; Kuwahara, S.; Shigematsu, J.; Fujii, S.; Okubo, M. *Des. Monomers Polym.* **2004**, *7*, 553–562.
(15) Grignard, B.; Jerome, C.; Calberg, C.; Jerome, R.; Detrembleur, C. *Eur. Polym. J.* **2008**, *44*, 861–871.
(16) Grignard, B.; Jerome, C.; Calberg, C.; Jerome, R.; Wang, W.; Howdle, S. M.; Detrembleur, C. *Chem. Commun.* **2008**, 314–316.
(17) Grignard, B.; Calberg, C.; Jerome, C.; Wang, W. X.; Howdle, S.; Detrembleur, C. *Chem. Commun.* **2008**, *44*, 5803–5805.
(18) Grignard, B.; Jérôme, C.; Calberg, C.; Jérôme, R.; Wang, W.; Howdle, S. M.; Detrembleur, C. *Macromolecules* **2008**, *41*, 8575–8583.
(19) Thurecht, K. J.; Gregory, A. M.; Wang, W.; Howdle, S. M. *Macromolecules* **2007**, *40*, 2965–2967.
(20) Gregory, A. M.; Thurecht, K. J.; Howdle, S. M. *Macromolecules* **2008**, *41*, 1215–1222.
(21) Zong, M. M.; Thurecht, K. J.; Howdle, S. M. *Chem. Commun.* **2008**, *45*, 5942–5944.
(22) Lee, H.; Terry, E.; Zong, M.; Arrowsmith, N.; Perrier, S.; Thurecht, K. J.; Howdle, S. M. *J. Am. Chem. Soc.* **2008**, *130*, 12242–12243.
(23) Cuervo-Rodriguez, R.; Bordegé, V.; Fernández-Monreal, M. C.; Fernández-García, M.; Madruga, E. L. *J. Polym. Sci., Part A: Polym. Chem.* **2004**, *42*, 4168–4176.
(24) Guan, Z.; Combes, J. R.; Menceloglu, Y. Z.; DeSimone, J. M. *Macromolecules* **1993**, *26*, 2663–2669.
(25) Rindfleisch, F.; DiNoia, T. P.; McHugh, M. A. *J. Phys. Chem.* **1996**, *100*, 15581–15587.
(26) Arita, T.; Beuermann, S.; Buback, M.; Vana, P. *e-Polym.* **2004**, *003*, 1–14.
(27) Sadowski, G. Phase Behaviour of Polymer Systems in High-Pressure Carbon Dioxide. In *Supercritical Carbon Dioxide in Polymer Reaction Engineering*, Kemmere, M. F., Meyer, T., Eds.; Wiley-VCH: Weinheim, Germany, 2005; pp 15−35.

Chain Transfer to Solvent in the Radical Polymerization of *N*-Isopropylacrylamide

YUSUKE SUGIHARA,[1,2] PADRAIG O'CONNOR,[1] PER B. ZETTERLUND,[2] FAWAZ ALDABBAGH[1]

[1]School of Chemistry, National University of Ireland Galway, University Road, Galway, Ireland

[2]Centre for Advanced Macromolecular Design (CAMD), School of Chemical Engineering, The University of New South Wales, Sydney, NSW 2052, Australia

Received 11 November 2010; accepted 29 January 2011
DOI: 10.1002/pola.24612
Published online 1 March 2011 in Wiley Online Library (wileyonlinelibrary.com).

ABSTRACT: Chain transfer to solvent has been investigated in the conventional radical polymerization and nitroxide-mediated radical polymerization (NMP) of *N*-isopropylacrylamide (NIPAM) in *N*,*N*-dimethylformamide (DMF) at 120 °C. The extent of chain transfer to DMF can significantly impact the maximum attainable molecular weight in both systems. Based on a theoretical treatment, it has been shown that the same value of chain transfer to solvent constant, $C_{tr,S}$, in DMF at 120 °C (within experimental error) can account for experimental molecular weight data for both conventional radical polymerization and NMP under conditions where chain transfer to solvent is a significant end-forming event. In NMP (and other controlled/living radical polymerization systems), chain transfer to solvent is manifested as the number-average molecular weight (M_n) going through a maximum value with increasing monomer conversion. © 2011 Wiley Periodicals, Inc. J Polym Sci Part A: Polym Chem 49: 1856–1864, 2011

KEYWORDS: kinetics (polym.); living radical polymerization (LRP); molecular weight distribution/molar mass distribution; radical polymerization

INTRODUCTION Poly(*N*-isopropylacrylamide, NIPAM) is a well-known temperature-sensitive polymer with a lower critical solution temperature (LCST) in water of about 33 °C.[1–3] The proximity of the LCST to physiological temperature has led to intense research into biological/medical applications.[4,5] There are numerous reports of homo- and co-polymerizations of NIPAM under conventional (nonliving) radical and controlled/living radical polymerization (CLRP) conditions. CLRP of NIPAM has been reported using nitroxide-mediated radical polymerization (NMP),[6–12] atom transfer radical polymerization (ATRP),[7,13,14] reversible addition-fragmentation chain transfer (RAFT) polymerization,[7,15–25] organotellurium-mediated radical polymerization,[26] and single electron transfer living radical polymerization.[27] NIPAM is a solid at room temperature (mp = 60−63 °C), and is most commonly polymerized in solution, using benzene,[9,15,28] alcohols,[13,27,29] 1,4-dioxane,[15,16,21,22,25] *N*,*N*-dimethylformamide (DMF),[6,8,10,11,18,26] anisole,[7,14] or water[23,24] as solvents.

Chain transfer to monomer or solvent can play an important role in radical polymerization under certain conditions. Ultimately, for a given set of conditions, chain transfer to monomer or solvent dictates an upper limit in accessible molecular weight, which may influence both a conventional radical polymerization and CLRP.[30] In CLRP, significant occurrence of such chain transfer events does not only influence the accessible molecular weight but also compromises both control over the molecular weight distribution (MWD) and livingness (end functionality). For example, it has been reported that chain transfer to solvent (DMF, anisole, and *p*-xylene) in the NMP of *tert*-butyl acrylate caused the number-average molecular weight (M_n) to deviate downward from the theoretical M_n ($M_{n,th}$) with increasing conversion, and even go through a maximum.[31] It has also been shown that chain transfer to monomer in NMP may cause a similar, but less pronounced, deviation from $M_{n,th}$.[32] However, poor performance of a CLRP may be due to a number of reasons, and it can often be difficult to ascribe deviations from ideal controlled/living behavior specifically to chain transfer events.

In the present contribution, chain transfer to solvent has been analyzed in detail in both the conventional radical polymerization and CLRP of NIPAM in DMF. As far as we are aware, chain transfer to solvent constants ($C_{tr,S}$) for this important monomer have to date not been reported for any solvent. It is shown that significant chain transfer to solvent occurs, and that these chain transfer reactions preclude synthesis of high molecular weight poly(NIPAM) by NMP in DMF. Various analytical equations are used to show that the same values of $C_{tr,S}$ (within experimental error) can accurately describe the chain transfer events observed in both conventional radical polymerization and CLRP of NIPAM.

Correspondence to: P. B. Zetterlund (E-mail: p.zetterlund@unsw.edu.au) or F. Aldabbagh (E-mail: fawaz.aldabbagh@nuigalway.ie)
Journal of Polymer Science Part A: Polymer Chemistry, Vol. 49, 1856–1864 (2011) © 2011 Wiley Periodicals, Inc.

EXPERIMENTAL

Materials

tert-Butyl acrylate (*t*-BA, Aldrich, 98%) and NIPAM (Aldrich, 97%) were purified by distillation under reduced pressure and recrystallization from 3:2 benzene:hexane, respectively. 2,2′-Azobisisobutyronitrile (DuPont Chemical Solution Enterprise) was recrystallized twice from methanol, and *t*-butyl peroxide (TBP, Aldrich, 98%) was used as received. *N*-*tert*-Butyl-*N*-[1-diethylphosphono(2,2-dimethylpropyl)]oxy (SG1) was prepared according to the literature,[33] and purified by column chromatography with purity (96%) determined using ^{1}H NMR spectroscopy from the reaction of SG1 radical with pentafluorophenylhydrazine (Aldrich). Poly(*t*-BA)-SG1 macroinitiator (MI) with M_n = 3000 g mol^{-1} and M_w/M_n = 1.17 g mol^{-1} was prepared by precipitation NMP in supercritical carbon dioxide, according to our published procedure.[34] HPLC grade solvents were used throughout, and lithium bromide (LiBr) was used as received.

Measurements

Number-average molecular weight (M_n) and polydispersity (M_w/M_n) were determined using a gel permeation chromatography (GPC) system consisting of a Viscotek DM 400 data manager, a Viscotek VE 3580 refractive-index detector, and two Viscotek Viscogel GMH$_{HR}$-M columns. Measurements were carried out at 60 °C at a flow rate of 1.0 mL min^{-1} using HPLC-grade DMF containing 0.01 M LiBr as the eluent.[35,36] The columns were calibrated using six poly(styrene, St) standards (M_n = 376–2,570,000 g mol^{-1}), and M_n is given in grams per mole (g mol^{-1}) throughout. The present GPC methodology for poly(NIPAM) has previously been adopted in NIPAM CLRP studies.[10,17,19,26] To the best of our knowledge, Mark–Houwink-Sakurada parameters are not available for poly(NIPAM)/DMF/LiBr/PSt. Work by Ganachaud et al.[15] has indicated that the error in M_n values estimated by GPC analysis of poly(NIPAM) relative to polystyrene standards using THF as eluent is only approximately 5% on average (depending on the molecular weight), and it is expected that the GPC error in this work is of similar order. The GPC analysis is further complicated by the fact that the polymers prepared by NMP are block copolymers of *t*BA and NIPAM.

^{1}H NMR spectra were recorded using a Joel GXFT 400 MHz instrument equipped with a DEC AXP 300 computer workstation.

General Polymerization Details

All reaction mixtures were added to Pyrex ampoules and subjected to several freeze-thaw degas cycles before sealing under vacuum. The ampoules were heated in an aluminium heating block at the designated temperature for various times. Polymerizations were stopped by placing ampoules in an ice-bath. GPC measurements were carried out on the non-precipitated reaction mixtures. Conversions were estimated using ^{1}H NMR by comparing the integration of the polymer peak at 3.85 ppm [C*H*(Me)$_2$] with NIPAM monomer at 4.01 ppm [C*H*(Me)$_2$].

Conventional Radical Polymerization

Stock solutions containing 0.41, 1.37, and 4.1 mM TBP were made up in DMF. The obtained stock solution (4 mL) was added to NIPAM (0.91 g, 8.00 mmol) in a Pyrex ampoule. Evacuated ampoules were heated at 120 °C for various times.

Chain Transfer to Solvent (Mayo Plot)

DMF stock solution (4 mL) containing 0.41 mM of TBP was added to NIPAM (0.29 g, 2.56 mmol; 0.39 g, 3.45 mmol; 0.58 g, 5.12 mmol; and 1.17 g, 10.34 mmol) in a Pyrex ampoule. Evacuated ampoules were heated at 120 °C for various times. Conversions were less than 5% in all cases.

Nitroxide-Mediated Polymerizations

The following polymerizations in DMF (4 mL) were carried out [NIPAM]$_0$/[poly(*t*-BA)-SG1]$_0$ = 100 (a), 200 (b), and 300 (c); (a) NIPAM (0.91 g, 8.00 mmol), poly(*t*-BA)-SG1 (0.24 g, 8.00 × 10^{-2} mmol), and SG1 (5.89 mg, 2.00 × 10^{-2} mmol); (b) NIPAM (0.91 g, 8.00 mmol), poly(*t*-BA)-SG1 (0.12 g, 4.00 × 10^{-2} mmol), and SG1 (2.94 mg, 1.00 × 10^{-2} mmol); (c) NIPAM (0.91 g, 8.00 mmol), poly(*t*-BA)-SG1 (0.080 g, 2.67 × 10^{-2} mmol), and SG1 (1.96 mg, 0.67 × 10^{-2} mmol).

Thermal Polymerization in the Absence of Initiator and Nitroxide

Evacuated ampoules containing NIPAM (0.91 g, 8.00 mmol) in DMF (4 mL) were heated at 120 °C for various times.

RESULTS AND DISCUSSION

Limiting Molecular Weight

Under normal conditions of conventional (nonliving) radical polymerization in the absence of a chain transfer agent, the main end-forming event is bimolecular termination. However, when the rate of initiation in a bulk polymerization is sufficiently low, the propagating radical concentration becomes so low that the bimolecular termination rate is reduced to the point that chain transfer to monomer becomes the main end-forming event.[30] The ratio $k_p/k_{tr,M}$ (=$1/C_{tr,M}$; k_p is the propagation rate coefficient, $k_{tr,M}$ the rate coefficient for chain transfer to monomer) dictates the maximum attainable number-average degree of polymerization (DP_n) for a given monomer. In a solution polymerization, the chain transfer to monomer limit is only reached if the rate of chain transfer to solvent is negligible relative to the rate of chain transfer to monomer. If chain transfer to solvent is the main end-forming event, $DP_n = k_p[M]/k_{tr,S}[S]$ (= $[M]/C_{tr,S}[S]$) ($k_{tr,S}$ is the rate coefficient for chain transfer to solvent, [M] and [S] are the monomer and solvent concentrations, respectively).

Conventional Radical Polymerization in DMF

If one performs a series of radical polymerizations with decreasing initiator concentration, DP_n will increase with decreasing initiator concentration until the maximum DP_n is reached, corresponding to either the chain transfer to monomer or solvent limit. Polymerizations of NIPAM in DMF were carried out at 120 °C (relevant to NMP) using three different low concentrations of the high-temperature initiator TBP. All MWDs are very similar (Fig. 1; M_n = 20,100 ([TBP]$_0$ = 4.1 mM), 17,600 ([TBP]$_0$ = 1.4 mM), 21,100 ([TBP]$_0$ = 0.41

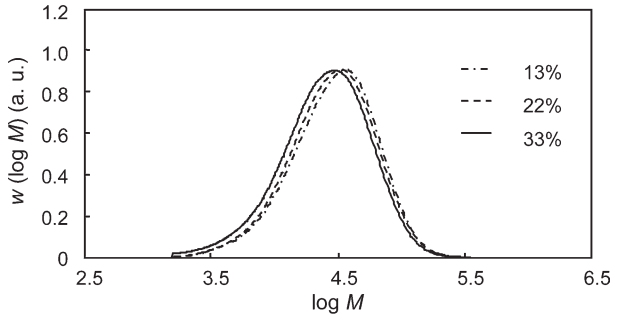

FIGURE 1 MWDs for the conventional radical polymerization of NIPAM (2 M) in DMF initiated by TBP at 120 °C for initiator concentrations of 0.41 (13%), 1.4 (33%), and 4.1 mM (22%), with monomer conversions as indicated.

mM), and 21,600 g mol^{-1} ([TBP]$_0$ = 0), consistent with the majority of propagating radicals being transformed to dead chains and new propagating radicals by chain transfer to monomer or solvent.

Nitroxide-Mediated Radical Polymerization

NMP can be a useful mechanistic tool in radical polymerization, because, ideally, the number of chains is constant throughout the polymerization. Moreover, if one initiates the polymerization with a MI of relatively high molecular weight, chain transfer events to low molecular weight species like monomer and solvent are likely to be readily detected in the MWDs.[32] The concept of a maximum molecular weight imposed by chain transfer to monomer or solvent applies to both conventional radical polymerization and CLRP (including NMP).

Figure 2 shows conversion versus time data for NMP of NIPAM in DMF at 120 °C initiated by three different concentrations of poly(*t*-BA)-SG1 (MI), revealing that R_p is (within experimental error) independent of the MI concentration to high conversion. Such behavior is observed if the polymerization proceeds in the stationary state with respect to the propagating radical concentration, for example, styrene/TEMPO/125 °C.[37,38] A somewhat more special case where R_p is independent of the MI concentration is when the rate of spontaneous radical initiation (from monomer or adventitious impurities) is close to zero in the presence of an excess amount of free nitroxide.[38,39] Because of the uncertainties in rate coefficients of the present system, we refrain from further speculation on this topic. The MWDs shift to higher molecular weights with increasing conversion, but significant low molecular weight tailing is visible (Fig. 3), consistent with chain transfer to monomer or solvent. Figure 4 shows M_n versus conversion, revealing how M_n initially increases with conversion but then reaches a maximum value and decreases at high conversion. The values of M_w/M_n gradually increase with increasing conversion (Fig. 4).

Chain Transfer to Solvent/Monomer

The concept of instantaneous DP_n is not applicable to CLRP because chains grow throughout the polymerization. The value of DP_n as a function of conversion is equal to the concentration of reacted monomer plus the concentration of monomeric units in the MI, divided by the total number of chains. The latter equals the MI concentration plus the concentration of chains generated during the course of the polymerization. Thus, in the case of new chain generation by chain transfer, DP_n is given as a function of [M] by:

$$DP_n = \frac{\alpha[M]_0 + DP_{MI}[MI]_0}{[MI]_0 + [chains]_{new}} \quad (1)$$

$$[chains]_{new} = -\int_{[M]_0}^{[M]} \left(\frac{\sum_i C_{tr,i}[X_i]}{[M]} \right) d[M] \quad (2)$$

where α denotes monomer conversion, [X$_i$] is the concentration of a low molecular weight species to which chain transfer occurs (where i denotes monomer, solvent, chain transfer agent, etc.), and [MI] is the MI concentration. In the case of chain transfer to monomer only (where $C_{tr,M}$ is the chain transfer to monomer constant), we obtain:

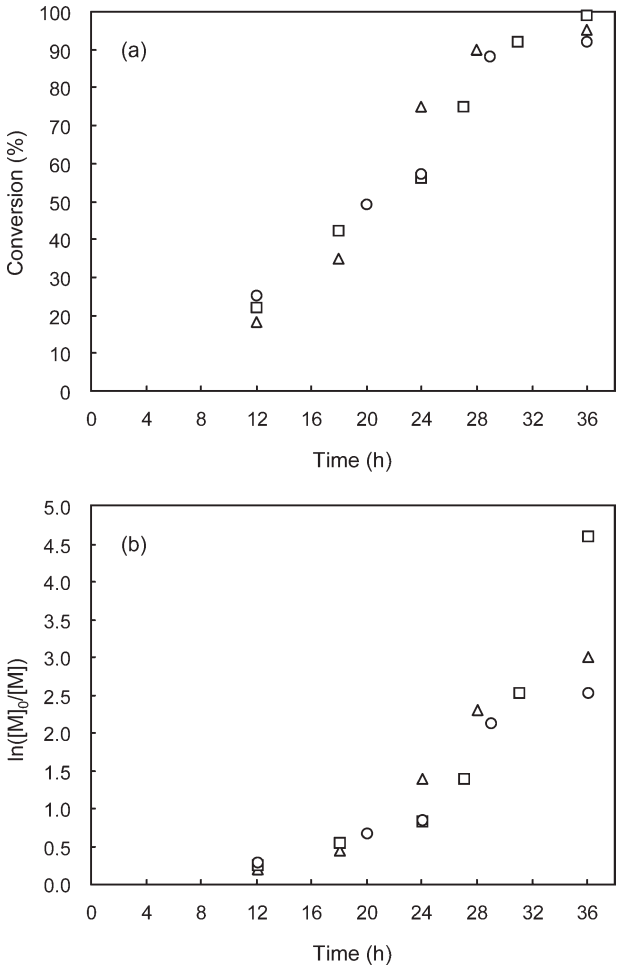

FIGURE 2 Conversion versus time data (a) and first-order plot (b) for NMP of NIPAM in DMF (2 M) using poly(*t*BA)-SG1 as macroinitiator with 25 mol % free SG1 relative to macroinitiator at 120 °C with [M]$_0$/[MI]$_0$ = 100 (○), 200 (□), and 300 (△).

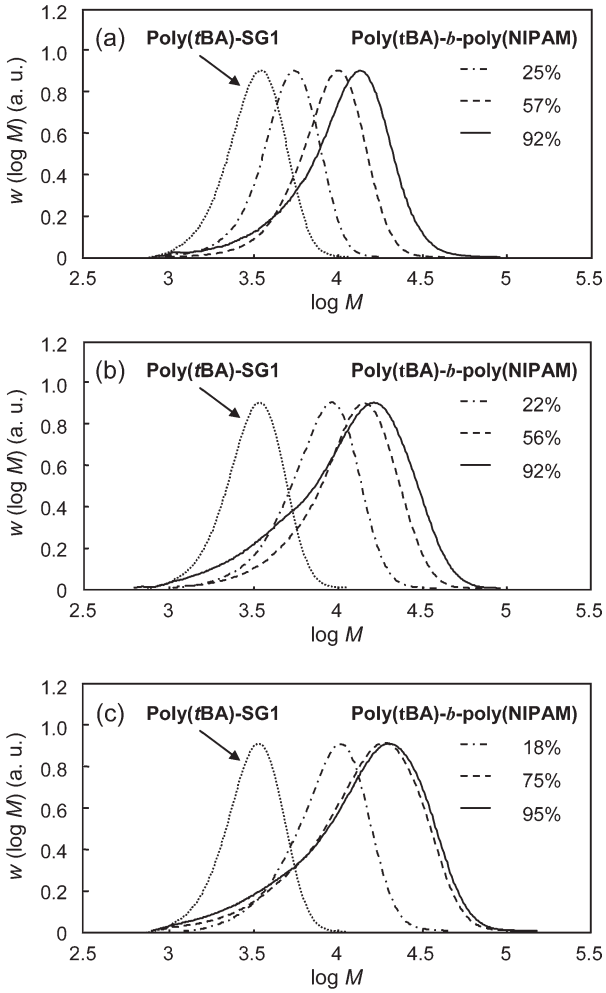

FIGURE 3 MWDs of poly(*t*BA)-*b*-poly(NIPAM) and original poly(*t*BA)-SG1 for $[M]_0/[MI]_0 = 100$ (a), 200 (b), 300 (c) with NIPAM conversions as indicated.

$$DP_n = \frac{\alpha[M]_0 + DP_{MI}[MI]_0}{[MI]_0 + \alpha[M]_0 C_{tr,M}} \quad (3)$$

In the case of chain transfer to solvent only, assuming also that [S] is constant, we can write:[40]

$$DP_n = \frac{\alpha[M]_0 + DP_{MI}[MI]_0}{[MI]_0 + C_{tr,S}[S]_0 \ln(1-\alpha)^{-1}} \quad (4)$$

Figure 5 shows M_n versus conversion computed from eq 3 for various values of $C_{tr,M}$ for $[M]_0/[MI]_0 = 200$. It is immediately obvious that regardless of the value of $C_{tr,M}$, the agreement with the experimental data is not satisfactory. A maximum in M_n versus conversion cannot be explained by chain transfer to monomer, regardless of the value of $C_{tr,M}$. Figure 4 shows experimental data of M_n versus conversion for three different $[M]_0/[MI]_0$ overlaid with predictions from eq 4 using $C_{tr,S} = 6.5 \times 10^{-4}$. The agreement between model and experiment is very good, and it is noted how eq 4 correctly predicts the maximum observed experimentally. Moreover, the datasets corresponding to all three MI concentrations can be successfully fitted with the same value of $C_{tr,S}$. The maximum M_n reached in the NMPs are all markedly lower than the maximum M_n as dictated by the expression $k_p[M]_0/k_{tr,S}[S]_0$ ($\approx$27,000 g mol^{-1} based on $C_{tr,S} = 6.5 \times 10^{-4}$, not considering M_n of the MI; see Limiting Molecular Weight section). The reason is that in NMP (and any CLRP), each chain transfer to solvent event generates a new living chain, thus increasing the number of chains over which the remaining monomer units are to be distributed (this is accounted for in eq 4).

It has very recently been reported[12] that nitroxide-mediated (SG1) radical polymerization of NIPAM in supercritical carbon dioxide (as an inverse suspension polymerization, that is, in the absence of solvent capable of undergoing chain transfer) proceeds to $M_n \approx 12{,}100$ g mol^{-1} with M_n versus conversion being a straight line close to $M_{n,th}$, thus providing strong evidence that chain transfer to monomer is not occurring to any significant extent in the present study either.

Chain-stopping events specific to NMP in general include (polymeric) alkoxyamine decomposition[41] and hydrogen

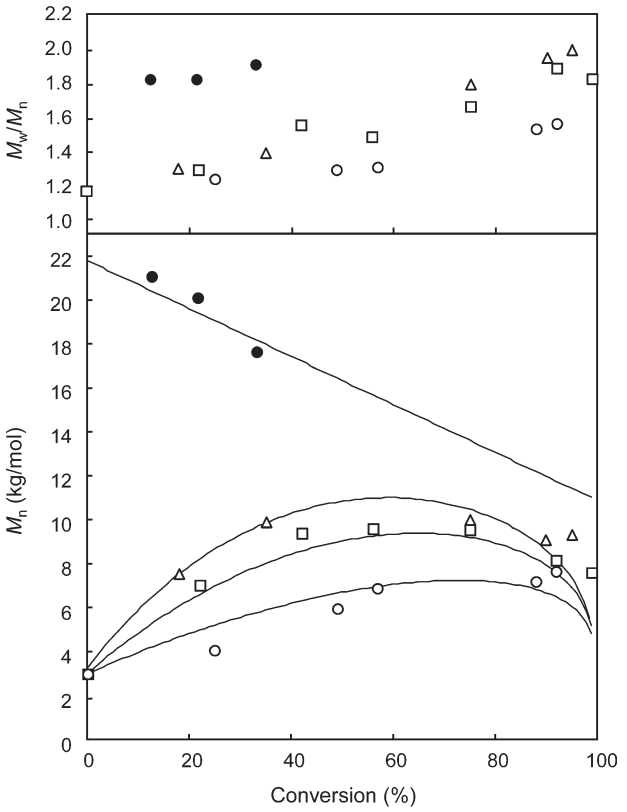

FIGURE 4 M_w/M_n (top) and M_n (bottom) versus conversion plots for NMP of NIPAM in DMF (2 M) at 120 °C with poly(*t*BA)-SG1 as macroinitiator with 25 mol % free SG1 relative to macroinitiator and $[M]_0/[MI]_0 = 100$ (○), 200 (□), and 300 (△), and conventional radical polymerization of NIPAM (2 M) with various concentrations of TBP as initiator (●) in DMF at 120 °C (each data point corresponding to a different $[TBP]_0$). The full lines are theoretical M_n using eqs 4 and 7 with $C_{tr,S} = 0.00065$ (NMP) and 0.0008 (conventional radical polymerization).

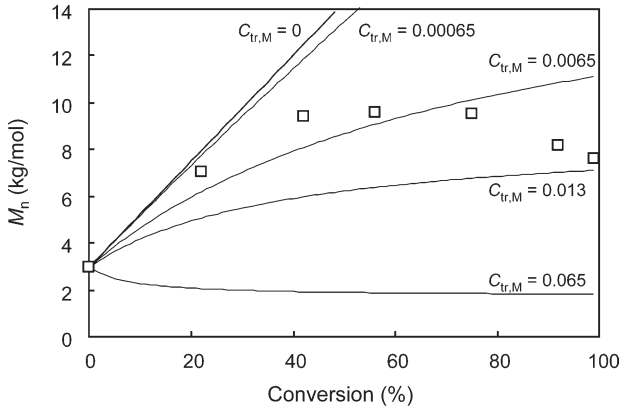

FIGURE 5 M_n versus conversion plots for NMP of NIPAM in DMF (2 M) at 120 °C with poly(*t*BA)-SG1 as macroinitiator with 25 mol % free SG1 relative to macroinitiator and $[M]_0/[MI]_0 = 200$. Solid lines are computed from eq 3 with various $C_{tr,M}$.

transfer from hydroxylamine (formed by hydrogen abstraction by nitroxide) to propagating radicals.[42] The rates of these reactions in the case of SG1 and NIPAM under the present conditions are not known. However, these reactions do not alter the number of chains, and, therefore, M_n is not expected to be affected. The fact that very similar chain transfer to solvent constants was obtained for conventional radical polymerization, and NMP, in this work, suggest that any influence of such side reactions is very minor at most.

In the case of conventional radical polymerization, the instantaneous DP_n is equal to $[M]/(\Sigma C_{tr,i}[X_i]) + DP_{n,0}$ (where $DP_{n,0}$ is DP_n in the absence of transfer) as given by the Mayo equation. The Mayo equation can be formulated as a function of [M], and the cumulative DP_n at a given conversion (i.e., the overall DP_n of the polymer formed between zero and a given conversion) is equal to:

$$DP_n = \frac{1}{[M] - [M]_0} \int_{[M]_0}^{[M]} \left(\frac{k_p[M]}{\sum_i k_{tr,i}[X_i] + (k_t + k_{td})[P^\bullet]} \right) d[M] \quad (5)$$

where k_t is the overall termination rate coefficient, k_{td} is the rate coefficient for termination by disproportionation, and $k_{tr,i}$ is the rate coefficient for chain transfer to species X_i. Under the assumption that all end-forming events are chain transfer to monomer (eq 6) or solvent (eq 7; with the additional assumption of constant [S]), DP_n can be expressed as functions of conversion as:

$$DP_n = \frac{1}{C_{tr,M}} \quad (6)$$

$$DP_n = \frac{[M]_0(2-\alpha)}{2[S]_0 C_{tr,S}} \quad (7)$$

Even if chain transfer to monomer or solvent is the predominant end-forming event, some fraction of propagating radicals will inevitably undergo bimolecular termination, which will cause deviation from DP_n as given by eqs 6 and 7. Note that eq 6 shows that the cumulative DP_n is the same as the instantaneous DP_n when chain transfer to monomer is the end-forming event. In the case of chain transfer to solvent being the end-forming event, however, the equation reveals that the cumulative DP_n decreases with conversion.

The conventional data at three different (low) initiator concentrations at 120 °C in DMF (from Fig. 1) were plotted as M_n versus conv. in Figure 4. Equation 7 was subsequently fitted to these data, resulting in good agreement with $C_{tr,S} = 8.0 \times 10^{-4}$. This value of $C_{tr,S}$ is very close to the value derived by fitting eq 4 to the NMP experiments ($C_{tr,S} = 6.5 \times 10^{-4}$). The somewhat higher value of $C_{tr,S}$ obtained in the case of conventional radical polymerization may be a result of bimolecular termination reactions between propagating radicals (which would cause propagating radicals to stop growing before reaching the chain transfer to solvent limit). Bimolecular termination would, of course, also occur to some minor extent in the NMP system, but the extent of such termination reactions in an NMP system without transfer reactions would obviously be much lower than in a conventional radical polymerization without chain transfer (in the latter case, all propagating radicals would undergo bimolecular termination). The data nicely illustrate how the same $C_{tr,S}$ (within experimental error, and allowing for the "error" due to termination in the conventional radical polymerization) can be used to (and also that $C_{tr,M}$ cannot) rationalize the polymerization behaviour of NIPAM in DMF with regard to chain transfer to solvent both in controlled/living (NMP) and conventional radical polymerization.

The four different scenarios, that is, chain transfer to monomer or solvent in conventional radical polymerization and NMP, are plotted in Figure 6. Conventional radical polymerization: In the case of chain transfer to monomer, theory predicts DP_n to remain constant with conversion, whereas in the case of chain transfer to solvent, DP_n decreases with conversion. CLRP: In the case of chain transfer to monomer, DP_n gradually deviates downward from the theoretical values (i.e., a straight line), whereas in the case of chain transfer to solvent, DP_n goes through a maximum.

Estimation of $C_{tr,S}$ via Mayo Plot

The value of $C_{tr,S}$ in the conventional radical polymerization of NIPAM in DMF at 120 °C was also estimated based on the classical Mayo treatment:

$$\frac{1}{DP_n} = \frac{1}{DP_{n,0}} + C_{tr,S}\frac{[S]}{[M]} \quad (8)$$

where $DP_{n,0}$ is DP_n when [S] = 0. The slope of the straight line obtained by plotting $1/DP_n$ versus [S]/[M] (Fig. 7) yields $C_{tr,S} = 9.2 \times 10^{-4}$, which is in relatively good agreement with $C_{tr,S} = 8.0 \times 10^{-4}$ (eq 7) and 6.5×10^{-4} (eq 4; Table 1).

Number of New Chains

Alternatively, the effects of chain transfer in NMP can be discussed based on the number of new chains generated as a function of conversion. Experimental values of the

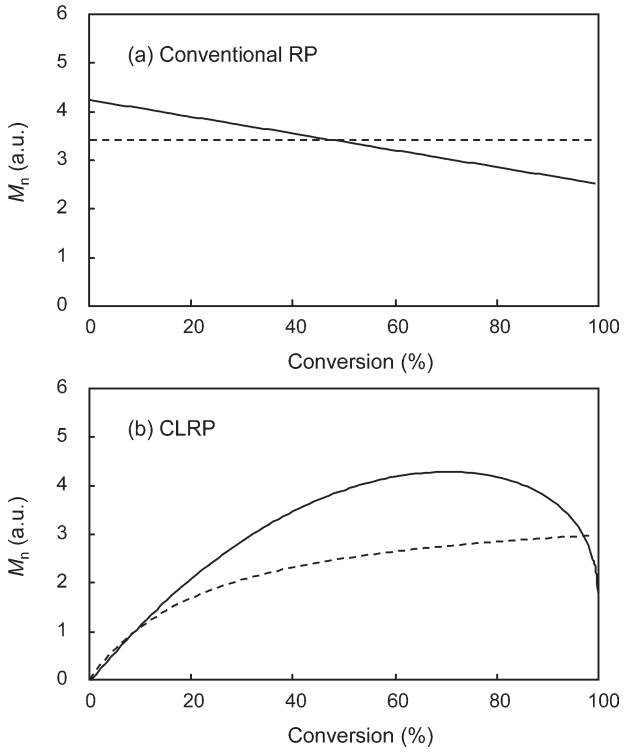

FIGURE 6 Typical traces of M_n against conversion in conventional radical polymerization (a) and controlled/living radical polymerization (b) with chain transfer to monomer (broken line) and chain transfer to solvent (solid line).

concentrations of new chains ($[chains]_{new}$) can be readily calculated from eq 9:

$$[chains]_{new} = [MI]_0((M_{n,th}/M_n) - 1) \quad (9)$$

Figure 8 shows the experimental $[chains]_{new}$ (from eq 9) as well as theoretical predictions based on chain transfer to monomer ($[chains]_{tr,M} = \alpha[M]_0 C_{tr,M}$) for $[M]_0/[MI]_0 = 200$, revealing that the theoretical prediction is in disagreement with the experimental data regardless of the value of $C_{tr,M}$. However, if we instead compute the concentration of new

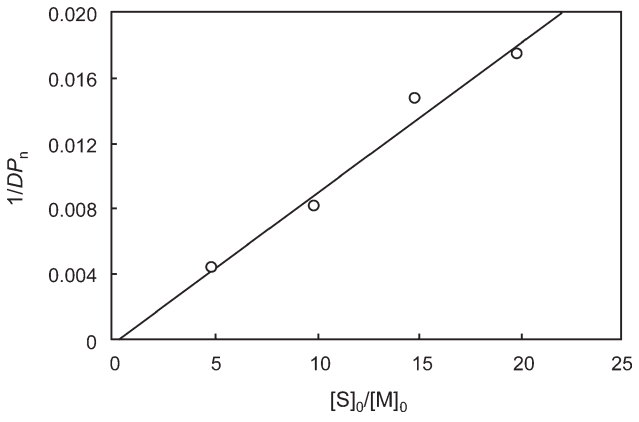

FIGURE 7 Mayo plot of NIPAM (2 M) in DMF initiated by TBP (0.41 mM) at 120 °C. The line is a best fit.

TABLE 1 Values of $C_{tr,S}$ for Radical Polymerization of NIPAM in DMF at 120 °C Estimated in This Work

$C_{tr,S}$ from Mayo plot (conv. rad. pol.)	$C_{tr,S}$ from eq 7 (conv. rad. pol.)	$C_{tr,S}$ from eq 4 (NMP)
9.2×10^{-4}	8.0×10^{-4}	6.5×10^{-4}

chains based on chain transfer to solvent ($[chains]_{tr,S} = C_{tr,S}[S]_0 \ln(1 - \alpha)^{-1}$; Fig. 9), the data for all three MI concentrations are in good agreement with theory for $C_{tr,S} = 6.5 \times 10^{-4}$ (the value obtained from fitting M_n vs. conversion). One single master curve is formed for all MI concentrations, because the number of new chains is a function of the total number of propagation steps and thus independent of $[MI]_0$ (as apparent from the term $C_{tr,S}[S]_0 \ln(1 - \alpha)^{-1}$ in eq 4).

Molecular Weight Distribution

A plot of M_w/M_n versus $[chains]_{tot}/[MI]_0$ (i.e., the total number of chains relative to the initial number of chains as given by the initial MI concentration; Fig. 10) for all three MI concentrations shows clearly how the generation of new chains is an important factor causing a gradual loss of control with increasing conversion. Interestingly, the data points for all three MI concentrations fall on the same master curve in this particular case. The effect of new chain generation on the MWD increases in magnitude with increasing $M_{n,th}$ (i.e., decreasing MI concentration, Fig. 4). The NMP data in Figure 4 reveal that M_n begins to deviate downward from $M_{n,th}$ with increasing conversion, consistent with chain transfer to solvent becoming increasingly significant. The newly generated radicals would have the same probability of propagation as longer living radical chains, and the low MW tail observed in the MWDs would, thus, mainly consist of living chains from chain transfer to solvent shifting to higher MW with conversion (Fig. 3). Consequently, even in the event of fairly significant chain transfer to solvent, the livingness may still

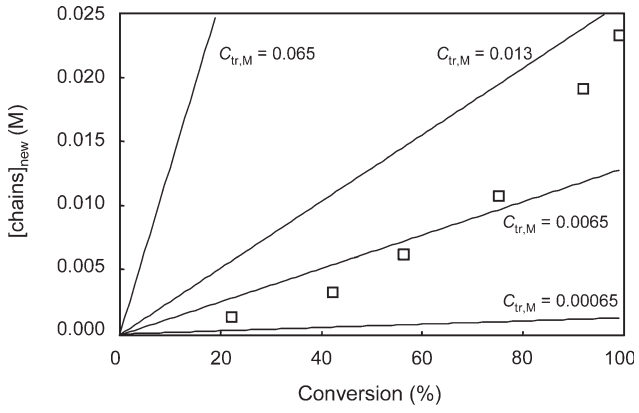

FIGURE 8 $[chains]_{new}$ versus conversion plots for NMP of NIPAM in DMF (2 M) at 120 °C using poly(*t*BA)-SG1 as macroinitiator with 25 mol % free SG1 relative to macroinitiator and $[M]_0/[MI]_0 = 200$. Solid lines correspond to $[chains]_{tr,M} = \alpha[M]_0 C_{tr,M}$ (see eq 3).

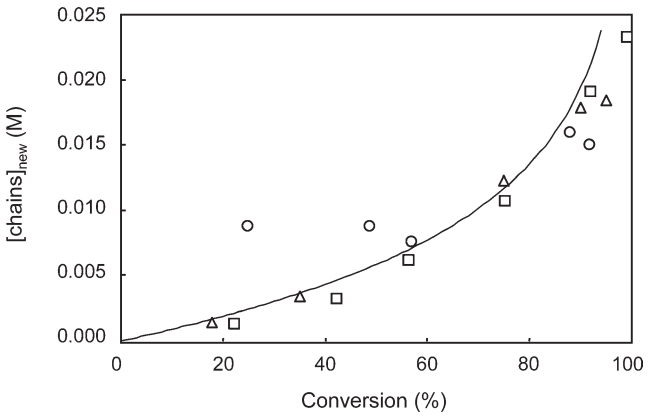

FIGURE 9 $[chains]_{new}$ versus conversion plots for NMP of NIPAM in DMF (2 M) at 120 °C using poly(*t*BA)-SG1 as macroinitiator with 25 mol % free SG1 relative to macroinitiator with $[M]_0/[MI]_0 = 100$ (○), 200 (□) and 300 (△). The line represents $[chains]_{tr,S} = C_{tr,S}[S]_0 \ln(1 - \alpha)^{-1}$ (see eq 4) for $C_{tr,S} = 6.5 \times 10^{-4}$.

be reasonable (especially considering the excess of free SG1 used in this work).

Effect of Poly(acrylate) Macroinitiator

Acrylate polymerization is complicated by the formation of mid-chain radicals (MCRs) that are formed by intra-(backbiting) or inter-molecular chain transfer reactions.[43–45] It has been reported recently that the extent of branch formation via MCRs is significantly lower in CLRP than conventional radical polymerization.[46] However, it is conceivable that MCRs may form during NMP due to the presence of the poly (acrylate) MI, and subsequent fragmentation of MCR would result in an increase in the number of chains and, thus, a decrease in M_n. However, if this occurred to any significant extent, the master curve of $[chains]_{new}$ versus conversion (Fig. 9) would not be observed, and furthermore, it would not be possible to fit all data (NMP for three different MI concentrations and conventional radical polymerization) with

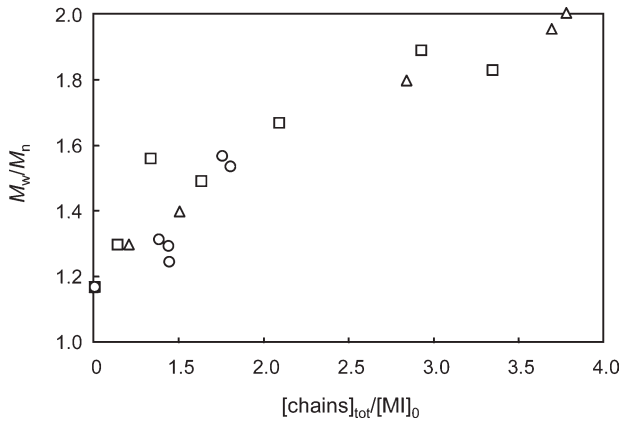

FIGURE 10 M_w/M_n versus $[chains]_{tot}/[MI]_0$ for NMP of NIPAM in DMF (2 M) at 120 °C using poly(*t*BA)-SG1 as macroinitiator with 25 mol % free SG1 relative to macroinitiator with $[M]_0/[MI]_0 = 100$ (○), 200 (□), and 300 (△).

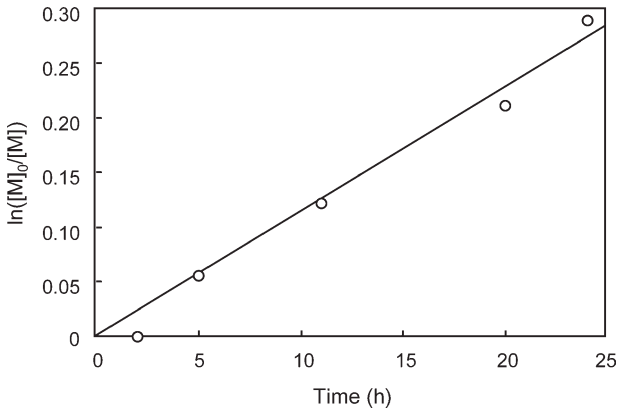

FIGURE 11 First-order plot of spontaneous polymerization (in the absence of initiator or nitroxide) of NIPAM (2 M) in DMF at 120 °C (the solid line is a best fit).

one single value of $C_{tr,s}$ (Figs. 4 and 9). It can, thus, be concluded that MCR formation followed by fragmentation is not a significant mechanism with regard to generation of new chains.

Spontaneous Initiation

Spontaneous (thermal) initiation (i.e., no initiator) has been previously reported in the polymerization of acrylates and acrylamides.[47–49] To estimate the extent of thermal generation of chains, polymerizations of NIPAM (2 M) in the absence of initiator and nitroxide were carried out in DMF at 120 °C. The rate of thermal initiation ($R_{i,th}$) can be estimated from the slope of a first-order plot (Fig. 11) according to eq 10:

$$\text{Slope} = k_p[P^\bullet] = k_p\left(\frac{R_{i,th}}{2k_t}\right)^{0.5} \quad (10)$$

Based on a slope of 3.19×10^{-6} and a literature value for $k_p/k_t^{0.5} = 0.24\ M^{0.5}s^{0.5}$ in DMF at 65 C,[50] one obtains $R_{i,th} = 1.8 \times 10^{-10}\ s^{-1}$. Assuming that $R_{i,th}$ is independent of conversion, the concentration of chains generated by spontaneous initiation is equal to $R_{i,th}$ multiplied by the polymerization time (longest time = 36 h), which gives 2.3×10^{-5} M. Considering that the MI concentration is 6.7×10^{-3} M or higher, it can be safely concluded that the contribution of spontaneous initiation to the overall number of chains in the system is insignificant (especially considering that the value of $k_p/k_t^{0.5}$ will be higher at 120 °C than at 65 °C).

Comparison with Literature

Table 1 lists the values of $C_{tr,S}$ estimated in this work based on eqs 4 (NMP) and 7 (conventional radical polymerization). To the best of our knowledge, $C_{tr,S}$ for NIPAM have to date not been reported for any solvent. Min et al.[51] studied the conventional radical polymerization of NIPAM initiated by γ-radiation in a wide range of solvents, reporting strong solvent effects on the molecular weights obtained, and speculated that this may be caused by differences in the extents of chain transfer to solvent. Of the solvents

investigated, the highest molecular weight was obtained for water and the lowest for THF (DMF not investigated). McCormick and coworkers[18] reported RAFT of NIPAM in DMF at 25 °C, obtaining close to linear M_n versus conversion plots with M_n as high as 44,500 g mol^{-1} with excellent control over the MWD. The absence of any apparent influence of chain transfer to DMF is most likely a result of the low polymerization temperature ($C_{tr,S}$ increases with temperature) as well as the higher ratio [monomer]/[solvent] in their work. Nitroxide-mediated stabilizer-free inverse suspension polymerization of NIPAM in supercritical CO_2 has recently been reported.[12] In this system, M_n did not deviate significantly from $M_{n,th}$ with increasing conversion, consistent with chain transfer to CO_2 being negligible (as well as chain transfer to monomer), and, thus, supporting the present results.

Conventional radical polymerization of St (60 °C) and *t*BA (115 °C) in DMF have been reported to proceed with $C_{tr,S} = 4 \times 10^{-4}$ [52] and 8.6×10^{-4},[31] respectively. The $C_{tr,S}$ values for these monomers are similar to $C_{tr,S}$ for NIPAM/DMF observed in this work. Downward deviations of M_n from $M_{n,th}$ with increasing conversion ($M_n < M_{n,th}$) have also been reported for other CLRPs in DMF, including the SG1-mediated polymerizations of *t*BA[31] and RAFT-mediated polymerizations of hydrophobic acrylamides,[53] consistent with chain transfer to solvent. Thus, chain transfer seems to be more significant to DMF than to other common polymerization solvents, possibly due to the greater stability of the DMF adduct radical. There are nevertheless scant reports of DMF generating radicals in small molecule reactions,[54] and DMF has continued to be widely used in the conventional radical polymerization and CLRP of NIPAM[6,8,10,11,18,22,26] and other monomers.[11,49,53,55–58] The wide literature use of NIPAM/DMF probably stems from its good solvent properties; our preliminary studies showed poly(NIPAM) to be poorly soluble (precipitates to form heterogeneous mixtures in NMPs) in benzene, anisole, and *m*-xylene under the polymerization conditions of the present article.

CONCLUSIONS

Chain transfer to solvent can be a significant factor in limiting the maximum attainable molecular weight in both conventional radical polymerization and NMP of NIPAM. Based on a theoretical treatment, it has been demonstrated that the same value of $C_{tr,S}$ (within experimental error) can be invoked to quantitatively rationalize experimental molecular weight data both in conventional radical polymerization and NMP in DMF at 120 °C under conditions where chain transfer to solvent is a significant end-forming event. The extent of chain transfer to solvent can have deleterious effects on both the control over the MWD (higher M_w/M_n) and the maximum attainable molecular weight in NMP (which is normally carried out at elevated temperatures). Chain transfer to solvent in NMP (or any CLRP technique) may lead to M_n going through a maximum with increasing conversion. This is distinctly different from the case of chain transfer to monomer, in which case M_n also deviates downward from $M_{n,th}$, but never goes through a maximum regardless of the extent of chain transfer to monomer.

This publication has emanated from research work conducted with financial support from Science Foundation Ireland (08/RFP/MTR1201).

REFERENCES AND NOTES

1 Heskins, M.; Guillet, J. E. J Macromol Sci Chem 1968, A2, 1441–1455.

2 Schild, H. G. Prog Polym Sci 1992, 17, 163–249.

3 Cho, E. C.; Lee, J.; Cho, K. Macromolecules 2003, 36, 9929–9934.

4 Kikuchi, A.; Okano, T. J Controlled Release 2005, 101, 69–84.

5 Wei, H.; Cheng, S. X.; Zhang, X. Z.; Zhuo, R. X. Prog Polym Sci 2009, 34, 893–910.

6 Bosman, A. W.; Vestberg, R.; Heumann, A.; Frechet, J. M. J.; Hawker, C. J. J Am Chem Soc 2003, 125, 715–728.

7 Savariar, E. N.; Thayumanavan, S. J Polym Sci Part A: Polym Chem 2004, 42, 6340–6345.

8 Kuroda, K.; Swager, T. M. Macromolecules 2004, 37, 716–724.

9 Schulte, T.; Siegenthaler, K. O.; Luftmann, H.; Letzel, M.; Studer, A. Macromolecules 2005, 38, 6833–6840.

10 Gibbons, O.; Carroll, W. M.; Aldabbagh, F.; Yamada, B. J Polym Sci Part A: Polym Chem 2006, 44, 6410–6418.

11 Binder, W. H.; Gloger, D.; Weinstabl, H.; Allmaier, G.; Pittenauer, E. Macromolecules 2007, 40, 3097–3107.

12 O'Connor, P.; Zetterlund, P. B.; Aldabbagh, F. J Polym Sci Part A: Polym Chem 2011, 49, 1719–1723.

13 Xia, Y.; Yin, X. C.; Burke, N. A. D.; Stover, H. D. H. Macromolecules 2005, 38, 5937–5943.

14 Rathfon, J. M.; Tew, G. N. Polymer 2008, 49, 1761–1769.

15 Ganachaud, F.; Monteiro, M. J.; Gilbert, R. G.; Dourges, M. A.; Thang, S. H.; Rizzardo, E. Macromolecules 2000, 33, 6738–6745.

16 Schilli, C.; Lanzendorfer, M. G.; Muller, A. H. E. Macromolecules 2002, 35, 6819–6827.

17 Ray, B.; Isobe, Y.; Morioka, K.; Habaue, S.; Okamoto, Y.; Kamigaito, M.; Sawamoto, M. Macromolecules 2003, 36, 543–545.

18 Convertine, A. J.; Ayres, N.; Scales, C. W.; Lowe, A. B.; McCormick, C. L. Biomacromolecules 2004, 5, 1177–1180.

19 Ray, B.; Isobe, Y.; Matsumoto, K.; Habaue, S.; Okamoto, Y.; Kamigaito, M.; Sawamoto, M. Macromolecules 2004, 37, 1702–1710.

20 Schilli, C. M.; Zhang, M. F.; Rizzardo, E.; Thang, S. H.; Chong, Y. K.; Edwards, K.; Karlsson, G.; Muller, A. H. E. Macromolecules 2004, 37, 7861–7866.

21 Liu, B.; Perrier, S. J Polym Sci Part A: Polym Chem 2005, 43, 3643–3654.

22 Carter, S.; Hunt, B.; Rimmer, S. Macromolecules 2005, 38, 4595–4603.

23 Smith, A. E.; Xu, X. W.; Kirkland-York, S. E.; Savin, D. A.; McCormick, C. L. Macromolecules 2010, 43, 1210–1217.

24 Millard, P. E.; Barner, L.; Reinhardt, J.; Buchmeiser, M. R.; Barner-Kowollik, C.; Muller, A. H. E. Polymer 2010, 51, 4319–4328.

25 Nuopponen, M.; Ojala, J.; Tenhu, H. Polymer 2004, 45, 3643–3650.

26 Yusa, S.; Yamago, S.; Sugahara, M.; Morikawa, S.; Yamamoto, T.; Morishima, Y. Macromolecules 2007, 40, 5907–5915.

27 Nguyen, N. H.; Rosen, B. M.; Percec, V. J Polym Sci Part A: Polym Chem 2010, 48, 1752–1763.

28 Zhou, S. Q.; Fan, S. Y.; Auyeung, S. C. F.; Wu, C. Polymer 1995, 36, 1341–1346.

29 Yu, T. L.; Lu, W. C.; Liu, W. H.; Lin, H. L.; Chiu, C. H. Polymer 2004, 45, 5579–5589.

30 Kukulj, D.; Davis, T. P.; Gilbert, R. G. Macromolecules 1998, 31, 994–999.

31 Lessard, B.; Tervo, C.; Maric, M. Macromol React Eng 2009, 3, 245–256.

32 Zetterlund, P. B.; Saka, Y.; McHale, R.; Nakamura, T.; Aldabbagh, F.; Okubo, M. Polymer 2006, 47, 7900–7908.

33 Cuervo-Rodriguez, R.; Bordege, V.; Fernandez-Monreal, M. C.; Fernandez-Garcia, M.; Madruga, E. L. J Polym Sci Part A: Polym Chem 2004, 42, 4168–4176.

34 O'Connor, P.; Zetterlund, P. B.; Aldabbagh, F. Macromolecules 2010, 43, 914–919.

35 Ishizone, T.; Ito, M. J Polym Sci Part A: Polym Chem 2002, 40, 4328–4332.

36 Ito, M.; Ishizone, T. J Polym Sci Part A: Polym Chem 2006, 44, 4832–4845.

37 Fukuda, T.; Terauchi, T.; Goto, A.; Ohno, K.; Tsujii, Y.; Miyamoto, T.; Kobatake, S.; Yamada, B. Macromolecules 1996, 29, 6393–6398.

38 Goto, A.; Fukuda, T. Prog Polym Sci 2004, 29, 329–385.

39 McHale, R.; Aldabbagh, F.; Zetterlund, P. B.; Minami, H.; Okubo, M. Macromolecules 2006, 39, 6853–6860.

40 Loiseau, J.; Doerr, N.; Suau, J. M.; Egraz, J. B.; Llauro, M. F.; Ladaviere, C. Macromolecules 2003, 36, 3066–3077.

41 Goto, A.; Kwak, Y.; Yoshikawa, C.; Tsujii, Y.; Sugiura, Y.; Fukuda, T. Macromolecules 2002, 35, 3520–3525.

42 Gridnev, A. A. Macromolecules 1997, 30, 7651–7654.

43 Sato, E.; Emoto, T.; Zetterlund, P. B.; Yamada, B. Macromol Chem Phys 2004, 205, 1829–1839.

44 Yamada, B.; Zetterlund, P. B.; Sato, E. Prog Polym Sci 2006, 31, 835–877.

45 Junkers, T.; Barner-Kowollik, C. J Polym Sci Part A: Polym Chem 2008, 46, 7585–7605.

46 Ahmad, N. M.; Charleux, B.; Farcet, C.; Ferguson, C. J.; Gaynor, S. G.; Hawkett, B. S.; Heatley, F.; Klumperman, B.; Konkolewicz, D.; Lovell, P. A.; Matyjaszewski, K.; Venkatesh, R. Macromol Rapid Commun 2009, 30, 2002–2021.

47 Ryan, J.; Aldabbagh, F.; Zetterlund, P. B.; Yamada, B. Macromol Rapid Commun 2004, 25, 930–934.

48 Moad, G.; Solomon, D. H. The Chemistry of Radical Polymerization; Elsevier: Oxford, 2006.

49 Gibbons, O.; Carroll, W. M.; Aldabbagh, F.; Zetterlund, P. B.; Yamada, B. Macromol Chem Phys 2008, 209, 2434–2444.

50 Costioli, M. D.; Berdat, D.; Freitag, R.; Andre, X.; Muller, A. H. E. Macromolecules 2005, 38, 3630–3637.

51 Min, Y.; Jun, L.; Hongfei, H. Radiat Phys Chem 1995, 46, 855–858.

52 Ueda, A.; Nagai, S. In Polymer Handbook; Brandrup, J.; Immergut, E. H.; Grulke, E. A., Eds.; Wiley: New York, 1999; p II/97.

53 de Lambert, B.; Charreyre, M. T.; Chaix, C.; Pichot, C. Polymer 2005, 46, 623–637.

54 Opstad, C. L.; Melo, T. B.; Sliwka, H. R.; Partali, V. Tetrahedron 2009, 65, 7616–7619.

55 Gotz, H.; Harth, E.; Schiller, S. M.; Frank, C. W.; Knoll, W.; Hawker, C. J. J Polym Sci Part A: Polym Chem 2002, 40, 3379–3391.

56 Xu, W. J.; Zhu, X. L.; Cheng, Z. P.; Chen, J. Y.; Lu, J. M. Macromol Res 2004, 12, 32–37.

57 Gonzalez, N.; Elvira, C.; Roman, J. S. Macromolecules 2005, 38, 9298–9303.

58 Eggenhuisen, T. M.; Becer, C. R.; Fijten, M. W. M.; Eckardt, R.; Hoogenboom, R.; Schubert, U. S. Macromolecules 2008, 41, 5132–5140.

Nitroxide-Mediated Stabilizer-Free Inverse Suspension Polymerization of *N*-Isopropylacrylamide in Supercritical Carbon Dioxide

PADRAIG O'CONNOR,[1] PER B. ZETTERLUND,[2] FAWAZ ALDABBAGH[1]

[1]School of Chemistry, National University of Ireland Galway, University Road, Galway, Ireland

[2]Centre for Advanced Macromolecular Design (CAMD), School of Chemical Engineering, The University of New South Wales, Sydney, New South Wales 2052, Australia

Received 7 December 2010; accepted 12 January 2011
DOI: 10.1002/pola.24580
Published online in Wiley Online Library (wileyonlinelibrary.com).

KEYWORDS: heterogeneous polymerization; living polymerization; particle nucleation; poly(*N*-isopropylacrylamide); radical polymerization

INTRODUCTION In recent years, benign supercritical carbon dioxide ($scCO_2$) has been widely used to perform heterogeneous (precipitation and dispersion)[1] controlled/living radical polymerization (CLRP) including nitroxide-mediated radical polymerization (NMP), atom transfer radical polymerization (ATRP), and reversible addition-fragmentation chain transfer (RAFT) polymerization.[2–5] These heterogeneous polymerizations rely upon the solubility of the monomer, initiator, and control agent in $scCO_2$, and the precipitation of polymer chains at a certain critical degree of polymerization (J_{crit}).[2,4] Beyond J_{crit}, the polymerization continues towards high conversion mainly in the monomer rich particle phase. A dispersion polymerization contains a stabilizer to prevent particle coagulation.

Poly(*N*-isopropylacrylamide, NIPAM) exhibits a phase transition at ~32 °C in water, which is known as the lower critical solution temperature (LCST). The proximity of the LCST to room and physiological temperature has resulted in extensive biotechnological and biomedical applications (including tissue engineering, biomolecule separation, and drug delivery).[6] NIPAM is a solid (mp = 60–63 °C), and is most commonly polymerized in solution of alcohols, dioxane, water, or DMF (*N*,*N*-dimethylformamide). The resultant polymer is usually isolated by precipitation from hydrophobic volatile organic compounds (VOC), including petroleum ether and diethyl ether, as non-solvent for poly(NIPAM). CLRP of NIPAM in solution using NMP,[7] ATRP,[8] RAFT,[9–11] TERP,[12] (organotellurium-mediated controlled radical polymerization), and SET-LRP (single-electron transfer living radical polymerization)[13] have been carried out, but CLRP of NIPAM in $scCO_2$ has to date not been reported. Low temperature (and microwave assisted) controlled/living aqueous homogeneous polymerizations of water soluble monomers, including acrylamides, have been reported using NMP.[14] It is noteworthy that aqueous CLRP of NIPAM relies on precipitation from VOC for polymer isolation,[11] and non-living aqueous precipitation and interfacial polymerizations use intensive dialysis (water exchange) and centrifugation, respectively, for purifying crosslinked poly(NIPAM) particles.[15] Recently, we have reported that the polymerization of NIPAM in VOC is prone to significant chain transfer to solvent (depending on the solvent) limiting the maximum attainable molecular weight.[16]

Literature precipitation and dispersion conventional (non-living) radical homo- and co-polymerizations of NIPAM (sparingly soluble) in $scCO_2$ use low monomer loadings to ensure that the monomer is initially soluble in the continuous phase.[17,18] In this communication, we show that CLRP of NIPAM can be carried out to high conversion using initial loadings of monomer, where the NIPAM is dispersed in $scCO_2$. NMP[19] is carried out in the absence of stabilizer (which is often expensive or requires prior synthesis) giving poly(NIPAM) as a dry powder, and circumventing the requirement for environmentally damaging VOC for polymerization and polymer isolation. It represents the first controlled/living dispersed phase polymerization or non-stabilized suspension polymerization[20] in $scCO_2$. The process is best described as an inverse suspension polymerization since it is contrary to a traditional suspension polymerizations, which employ oil-soluble monomers (acrylics or styrenics) suspended in an aqueous medium; in this case the water-soluble monomer (NIPAM) is suspended in a hydrophobic continuous phase ($scCO_2$).

RESULTS AND DISCUSSION

The nitroxide used is *N*-*tert*-butyl-*N*-[1-diethylphosphono-(2,2-dimethylpropyl)]nitroxide (SG1) and the initiator is 2,2′-azobisisobutyronitrile (AIBN), with $[SG1]_0/[AIBN]_0 = 2.5$ in all experiments. The sapphire windows allowed us to

Correspondence to: F. Aldabbagh (E-mail: fawaz.aldabbagh@nuigalway.ie) or P. B. Zetterlund (E-mail: p.zetterlund@unsw.edu.au)
Journal of Polymer Science: Part A: Polymer Chemistry, Vol. 000, 000–000 (2011)

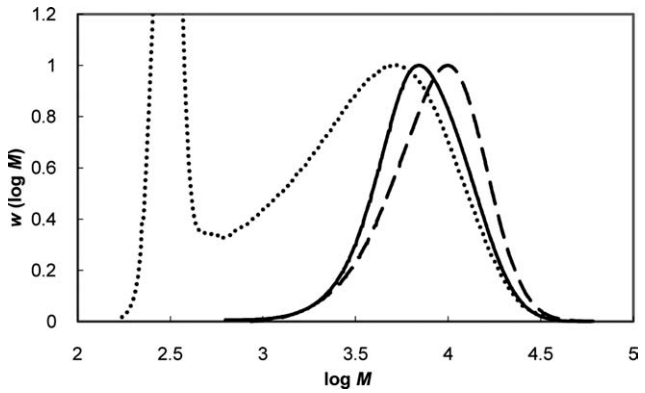

FIGURE 1 Influence of pressure on MWDs (normalized to peak height) for the NMP of 10% w/v NIPAM in $scCO_2$ at 120 °C for 24 h with $[SG1]_0/[AIBN]_0 = 2.5$. Dotted line = 10 MPa (not resolved from monomer), Conv. = 70%; Dashed line = 20 MPa, M_n = 7000 g/mol, M_w/M_n = 1.42, Conv. = 32% ($M_{n,th}$ = 4800 g/mol based on $f = 0.68$); Solid line = 30 MPa, M_n = 6000 g/mol, M_w/M_n = 1.39, Conv. = 37% ($M_{n,th}$ = 5500 g/mol based on $f = 0.68$).

visually observe initial monomer solubility in $scCO_2$, with >5% w/v NIPAM forming a whitish emulsion in $scCO_2$ at 120 °C and 10–30 MPa. It follows that for a 10% w/v NIPAM, approximately half the monomer will form large droplets suspended in $scCO_2$. Initially, NMP was carried out at three different pressures (Fig. 1). Very poor control was obtained at 10 MPa, as signified by the broad molecular weight distribution (MWD), however, at 20 and 30 MPa, lower polymerization rates and narrower MWDs were observed. The polymerization at 30 MPa offered marginally better control, and was more efficient in terms of apparent initiator efficiency compared to that at 20 MPa. The change in pressure influences the partitioning of reactants between the two phases, as well as the monomer solubility in $scCO_2$, and the AIBN initiator efficiency has been shown to be higher in $scCO_2$ than benzene.[21]

Control and polymerization rate did however not vary significantly with monomer loading (10–40% w/v) at 30 MPa (Fig. 2). This is consistent with (but does not prove) a suspension polymerization, whereby each monomer droplet essentially behaves as a "mini-bulk" system. In the case of 5% w/v NIPAM in $scCO_2$, the system initially appeared homogeneous and the polymerization proceeded as a precipitation polymerization with similar polymerization rate, but somewhat less control, than the inverse suspension polymerizations. The polymerization at 10% w/v NIPAM and 30 MPa proceeded with controlled/living character to high conversion (~70%) as indicated by MWDs remaining relatively narrow throughout (M_w/M_n = 1.35–1.50) and shifting to higher molecular weights with increasing conversion (Fig. 3). Significant coagulation was visible at 71% conversion (36 h), but the polymer and non-reacted monomer were nonetheless isolated as a dry crystalline white powder upon venting (depressurization) of CO_2.[22] At 82% conversion, there was a significant loss in control/livingness, as evidenced by a broad MWD (M_w/M_n = 2.1), although there is no obvious evidence of a limiting M_n (= 12,100 g/mol), which remains close to $M_{n,th}$ = 12,300 g/mol (using $f = 0.68$).

Despite the monomer being a solid under ambient conditions, it can be washed away from the poly(NIPAM) by purging the isolated polymer powder with $scCO_2$ two or three times at 50 °C (Figs. 4 and 5). The use of $scCO_2$ to purify poly(NIPAM) based materials prepared in (non-living) conventional radical precipitation polymerizations has been reported by others.[18] The cavities in the polymer shown in Figure 5 are attributed to expulsion of monomer by CO_2

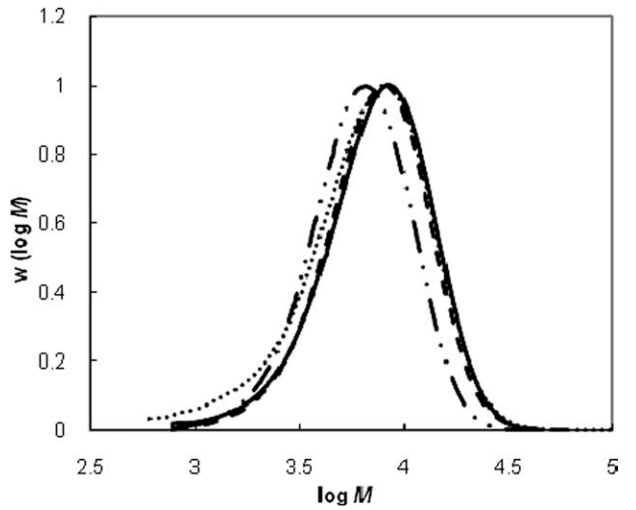

FIGURE 2 Influence of monomer loading on MWDs (normalized to peak height) for the NMP of NIPAM using 5% (dotted line; M_n = 5600 g/mol, M_w/M_n = 1.59, Conv. = 37%), 10% (solid line; M_n = 6000 g/mol, M_w/M_n = 1.39, Conv. = 37%), 20% (dashed line; M_n = 6900 g/mol, M_w/M_n = 1.34, Conv. = 39%), and 40% (dash-dot line; M_n = 5150 g/mol, M_w/M_n = 1.35, Conv. = 42%) w/v of NIPAM in $scCO_2$ for 24 h at 120 °C and 30 MPa using $[SG1]_0/[AIBN]_0 = 2.5$.

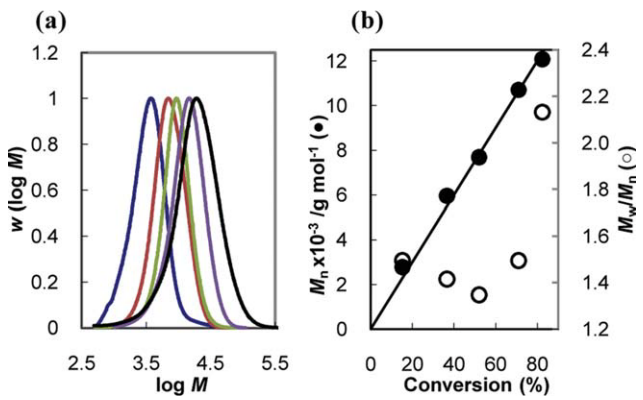

FIGURE 3 NMP of 10% w/v NIPAM in $scCO_2$ at 120 °C and 30 MPa (polymerization times are given within the brackets): (a) MWDs normalized to peak height corresponding to 15% (blue, 12 h), 37% (red, 24 h), 52% (green, 30 h), 71% (purple, 36 h), and 82% (black, 48 h) conversion and (b) M_n (●) and M_w/M_n (○) versus conversion. Line = M_{nth} based on initiator efficiency (f) = 0.68 obtained from the line of best fit ($M_{n,th}$ = 15,000 g/mol at 100% Conv.).

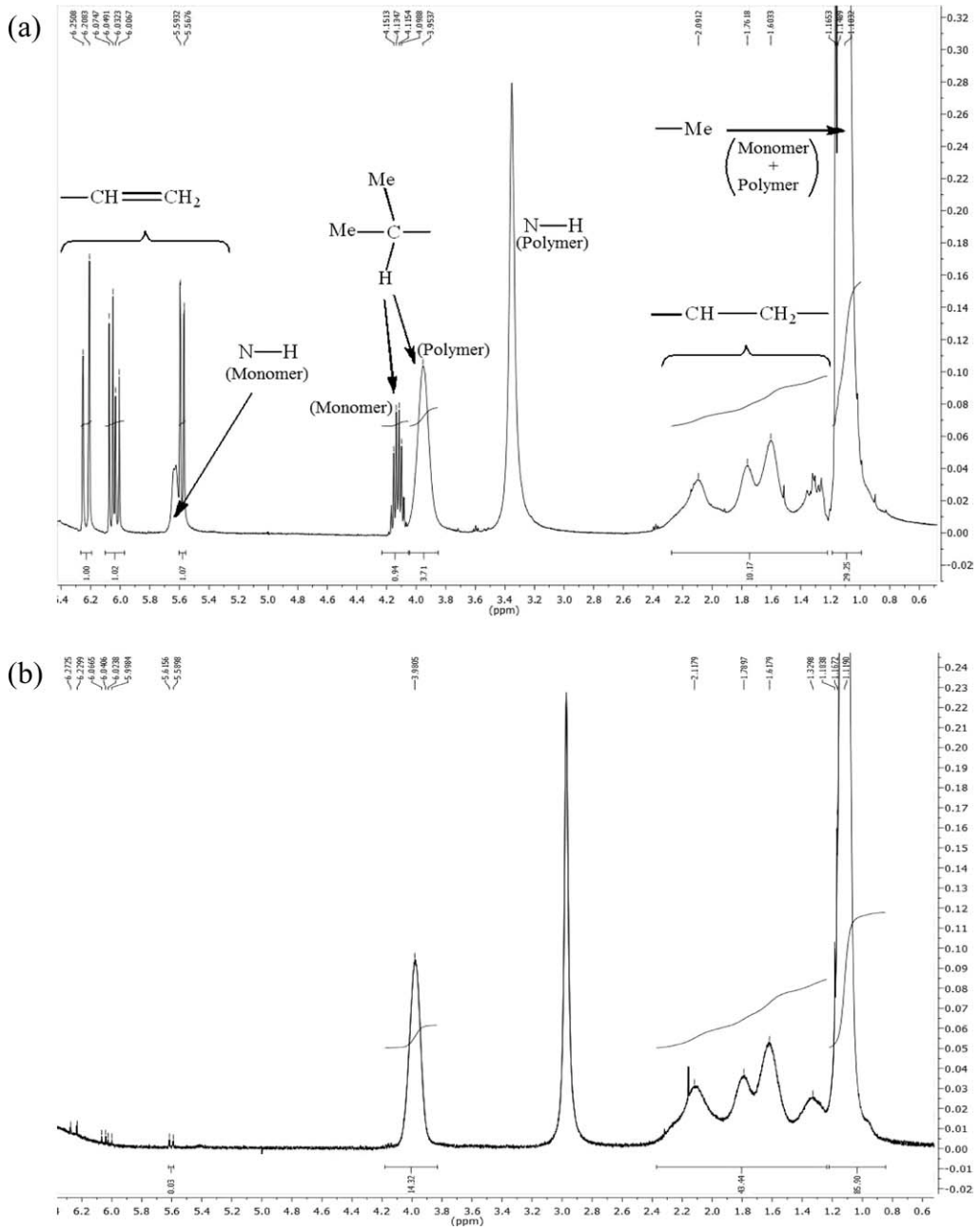

FIGURE 4 ^{1}H NMR spectra of dry polymer powder (71% Conv.) isolated from the NMP of 10% w/v NIPAM in $scCO_2$ at 120 °C and 30 MPa: (a) before (note that some monomer has been lost during venting) and (b) after purification by washing the sample [in Fig. 4(a)] with $scCO_2$ at 50 °C and 30 MPa.

upon venting. Thus, the technique circumvents the requirement for VOC, and avoids the loss of low molecular weight polymer, which often occurs with traditional precipitation methods using VOC. The absence of low molecular weight polymer in the CO_2 eluent was confirmed by venting the CO_2 into methanol followed by ^{1}H NMR analysis of the solid obtained upon evaporation of the methanol.

EXPERIMENTAL

Materials

N-Isopropylacrylamide (NIPAM, 97% Aldrich) was recrystallized from a mixture of 3:2 benzene/hexane before use. 2,2′-Azoisobutyronitrile (AIBN, DuPont Chemical Solution Enterprise) was recrystallized from methanol. *N-tert*-butyl-*N*-[1-diethylphosphono-(2,2-dimethylpropyl)]nitroxide SG1 (also known as DEPN) was synthesized according to the literature[23] with purity 96% determined using ^{1}H NMR spectroscopy from the reaction of SG1 radical with pentafluorophenylhydrazine (Aldrich, 97%). *N*,*N*-Dimethylformamide (DMF, Aldrich, HPLC grade), anhydrous lithium bromide (LiBr, BDH), methanol (Corcoran Chemicals, 99.9%), hexane (Fisher Scientific, reagent grade), benzene (BDH, reagent grade), and CO_2 (BOC, 99.8%) were all used as received.

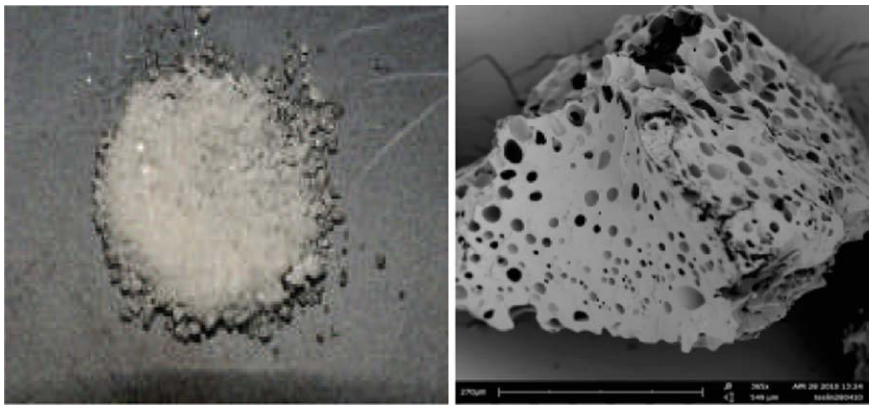

FIGURE 5 Photograph (left) and SEM image (right; scale bar is 270 μm) of purified poly(NIPAM) obtained at 71% conversion.

Equipment and Measurements

All polymerizations were carried out in a 100 mL stainless steel Thar reactor with 180° inline sapphire windows and overhead Magdrive maintaining stirring at ~1200 rpm. The pressure was produced and maintained by a Thar P-50 series high-pressure pump to within ±0.2 MPa. The temperature was regulated by a Thar CN6 controller to within ±1 °C. The maximum programable operating pressure and temperature of the reactor are 41.4 MPa and 125 °C, respectively. The reactor is connected to a Thar automated back pressure regulator (ABPR, a computer-controlled needle valve) for controlled venting. All GPC (gel permeation chromatography or size-exclusion chromatography) measurements were obtained on polymerization mixtures prior to purification by dissolving samples in DMF. M_n and polydispersity (M_w/M_n) were determined using a gel permeation chromatography (GPC) system consisting of a Viscotek DM 400 data manager, a Viscotek VE 3580 refractive-index detector, and two Viscotek Viscogel GMHHR-M columns. Measurements were carried out at 60 °C at a flow rate of 1.0 mL/min using HPLC grade DMF containing 0.01 M LiBr as the eluent. The columns were calibrated using six linear polystyrene standards (M_n = 376–2,570,000 g/mol). M_n measurements are not accurate. Control/livingness is assessed using MWD relative shifts, trends, and shapes. Similar GPC conditions for the analysis of control/livingness of NIPAM polymerizations have been used by others in the literature.[10,12,24] Conversions were measured by weighing the dry polymeric product after careful removal of any remaining monomer. The theoretical number-average molecular weights ($M_{n,th}$) were calculated according to:

$$M_{n,th} = \left(\frac{n_{NIPAM}}{2fn_{AIBN}}\right) \alpha MW_{NIPAM} \quad (1)$$

where n denotes the numbers of moles, f is the AIBN initiator efficiency, α is fractional monomer conversion, and MW_{NIPAM} is the molecular weight of NIPAM. ^{1}H NMR spectra were obtained using a JEOL 400 MHz spectrometer. All polymer samples were dissolved in $CDCl_3$ with Me_4Si used as the internal standard. Scanning Electron Microscopy (SEM) images were obtained using a FEI Phenom SEM with light optical magnification fixed at 20 times, electron optical magnification 120–20,000 times, and digital zoom of 12 times.

Polymerization Procedure

The reactor was loaded with NIPAM (10.0 g, 88.4 mmol, equivalent to 10% w/v), AIBN (80 mg, 0.49 mmol), and SG1 (0.36 g, 1.22 mmol). The reactor was sealed with the magnetically coupled stirring lid (Magdrive). The mixture was purged for 15 min by passing gaseous CO_2 through the mixture to remove air. Liquid CO_2 (~5 MPa) was added, and the temperature was raised to the reaction temperature of 120 °C, followed by the pressure to the reaction pressure by the addition of CO_2. The opaque reaction mixture was stirred at ~1200 rpm throughout. At the desired time, heating was stopped, and rapid external cooling using dry ice was carried out (this caused the temperature of the reactor to drop to ~80 °C in 10 min). The CO_2 was vented slowly from the reactor (when at approximately room temperature after 30 min of cooling) through methanol to prevent the loss of polymer and opened using the ABPR. Upon opening the reactor, at low conversion, the polymerization mixture appeared as a gel (which hardens with time), which was dissolved in methanol and the polymer precipitated from excess hexane. At 71% and higher conversion, a white crystalline powder containing polymer and non-reacted monomer was obtained. This was purified by two or three washings using fresh $scCO_2$ in the reactor at 50 °C and 30 MPa. The vented CO_2 was bubbled through methanol, which was evaporated to dryness under vacuum, and the resultant solid shown to be NIPAM monomer free of polymer by ^{1}H NMR spectroscopy.

CONCLUSIONS

Nitroxide-mediated stabilizer-free inverse suspension polymerization of NIPAM has been performed successfully in $scCO_2$—this is the first report of an inverse dispersed phase CLRP in $scCO_2$. This new heterogeneous polymerization technique using benign $scCO_2$ offers significant advantages from a technical, commercial, as well as an environmental perspective. We are currently pursuing a stabilized controlled/living polymerization of NIPAM in $scCO_2$, which is anticipated to yield smaller spherical particles.

This publication has emanated from research work conducted with financial support from Science Foundation Ireland (08/RFP/MTR1201). The authors thank the National Centre of Laser Applications (NCLA), NUI Galway for SEM, obtained

under the framework of the Inspire program, funded by Cycle 4, National Development Plan 2007–2013.

REFERENCES AND NOTES

1 (a) Kendall, J. L.; Canelas, D. A.; Young, J. L.; DeSimone, J. M. Chem Rev 1999, 99, 543–563; (b) Cooper, A. I. J Mater Chem 2000, 10, 207–234; (c) Firetto, V.; Scialdone, O.; Silvestri, G.; Spinella, A.; Galia, A. J Polym Sci Part A: Polym Chem 2010, 48, 109–121.

2 For a recent review on heterogeneous CLRP in $scCO_2$, see: Zetterlund, P. B.; Aldabbagh, F.; Okubo, M. J Polym Sci Part A: Polym Chem 2009, 47, 3711–3728.

3 For a recent review on dispersion CLRP in $scCO_2$, see: Thurecht, K. J.; Howdle, S. M. Aust J Chem 2009, 62, 786–789.

4 O'Connor, P.; Zetterlund, P. B.; Aldabbagh, F. Macromolecules 2010, 43, 914–919.

5 Grignard, B.; Phan, T.; Bertin, D.; Gigmes, D.; Jerome, C.; Detrembleur, C. Polym Chem 2010, 1, 837–840.

6 (a) Schild, H. G. Prog Polym Sci 1992, 17, 163–249; (b) Kikuchi, A.; Okano, T. J Control Release 2005, 101, 69–84; (c) Wei, H.; Cheng, S.-X.; Zhang, X.-Z.; Zhou, R.-X. Prog Polym Sci 2009, 34, 893–910.

7 For examples of NMP of NIPAM, see: (a) Bosman, A. W.; Vestberg, R.; Heumann, A.; Frechet, J. M. J.; Hawker, C. J. J Am Chem 2003, 125, 715–728; (b) Schulte, T.; Siegenthaler, K. O.; Luftmann, H.; Letzel, M.; Studer, A. Macromolecules 2005, 38, 6833–6840; (c) Binder, W. H.; Gloger, D.; Weinstabl, H.; Allmaier, G.; Pittenauer, E. Macromolecules 2007, 40, 3097–3107.

8 Xia, Y.; Yin, X.; Burke, N. A. D.; Stöver, H. D. H. Macromolecules 2005, 38, 5937–5943.

9 For examples of RAFT of NIPAM in VOC, see: (a) Ganachaud, F.; Monteiro, M. J.; Gilbert, R. G.; Dourges, M.-A.; Thang, S. H.; Rizzardo, E. Macromolecules 2000, 33, 6738–6745; (b) Schilli, C.; Lanzendörfer, M. G.; Müller, A. H. E. Macromolecules 2002, 35, 6819–6827; (c) Convertine, A. J.; Ayres, N.; Scales, C. W.; Lowe, A. B.; McCormick, C. L. Biomacromolecules 2004, 5, 1177–1180.

10 (a) Biswajit, R.; Isobe, Y.; Morioka, K.; Habaue, S.; Okamoto, Y.; Kamigaito, M.; Sawamoto, M. Macromolecules 2003, 36, 543–545; (b) Biswajit, R.; Isobe, Y.; Matsumoto, K.; Habaue, S.; Okamoto, Y.; Kamigaito, M.; Sawamoto, M. Macromolecules 2004, 37, 1702–1710.

11 For examples of RAFT of NIPAM in water, see: (a) Millard, P.-E.; Barner, L.; Stenzel, M. H.; Davis, T. P.; Barner-Kowollik, C.; Müller, A. H. E. Macromol Rapid Commun 2006, 27, 821–828; (b) Boyer, C.; Bulmus, V.; Liu, J.; Davis, T. P.; Stenzel, M. H.; Barner-Kowollik, C. J Am Chem Soc 2007, 129, 7145–7154; (c) Bai, W.; Zhang, L.; Bai, R.; Zhang, G. Macromol Rapid Commun 2008, 29, 562–566; (d) Millard, P.-E.; Barner, L.; Reinhardt, J.; Buchmeiser, M. R.; Barner-Kowollik, C.; Müller, A. H. E. Polymer 2010, 51, 4319–4328; RAFT of 2-aminoethylmethacrylate in water, see: (e) Alidedeoglu, A. H.; York, A. W.; McCormick, C. L.; Morgan, S. E. J Polym Sci Part A: Polym Chem 2009, 47, 5405–5415.

12 Yusa, S.-I; Yamago, S.; Sugahara, M.; Morikawa, S.; Yamamoto, T.; Morishima, Y. Macromolecules 2007, 40, 5907–5915.

13 Nguyen, N. H.; Rosen, B. M.; Percec, V. J Polym Sci Part A: Polym Chem 2010, 48, 1752–1763.

14 (a) Nicolaÿ, R.; Marx, L.; Hémery, P.; Matyjaszewski, K. Macromolecules 2007, 40, 6067–6075; (b) Phan, T. N. T.; Bertin, D. Macromolecules 2008, 41, 1886–1895; (c) Rigolini, J.; Grassl, B.; Billon, L.; Reynaud, S.; Donard, O. F. X. J Polym Sci Part A: Polym Chem 2009, 47, 6919–6931; (d) Rigolini, J.; Grassl, B.; Reynaud, S.; Billon, L. J Polym Sci Part A: Polym Chem 2010, 48, 5775–5782.

15 (a) Karg, M.; Lu, Y.; Carbó-Argibay, E.; Pastoriza-Santos, I.; Pérez-Juste, J.; Liz-Marzán, L. M.; Hellweg, T. Langmuir 2009, 25, 3163–3167; (b) Sánchez-Iglesias, A.; Grzelczak, M.; Rodríguez-González, B.; Guardi-Girós, P.; Pastoriza-Santos, I.; Pérez-Juste, J.; Prato, M.; Liz-Marzán, L. M. ACS Nano 2009, 3, 3184–3190.

16 Sugihara, Y.; O'Connor, P.; Zetterlund, P. B.; Aldabbagh, F. J Polym Sci Part A: Polym Chem, in press.

17 (a) Temtem, M.; Casimiro, T.; Mano, J. F.; Aguiar-Ricardo, A. Green Chem 2007, 9, 75–79; (b) Hu, Y.; Cao, L.; Xiao, F.; Wang, J. Polym Adv Technol 2010, 21, 386–391.

18 (a) Cao, L.; Chen, L.; Lai, W. J Polym Sci Part A: Polym Chem 2007, 45, 955–962; (b) Wang, C.; Wang, J.; Gao, W.; Jiao, J.; Feng, H.; Liu, X.; Chen, L. J Colloid Interface Sci 2010, 343, 141–148.

19 For recent NMP, see: (a) Pu, D. W.; Lucien, F. P.; Zetterlund, P. B. J Polym Sci Part A: Polym Chem 2010, 48, 5636–5641; (b) Edeleva, M. V.; Kirilyuk, I. A.; Zubenko, D. P.; Zhurko, I. F.; Marque, S. R. A.; Gigmes, D.; Guillaneuf, Y.; Bagryanskaya, E. G. J Polym Sci Part A: Polym Chem 2009, 47, 6579–6595.

20 Cooper, A. I.; Hems, W. P.; Holmes, A. B. Macromol Rapid Commun 1998, 19, 353–357.

21 Guan, Z.; Combes, J. R.; Menceloglu, Y. Z.; DeSimone, J. M. Macromolecules 1993, 26, 2663–2669.

22 SEM images of nonpurified polymer did not show well-defined particles, and it is not possible to isolate the polymer from monomer retaining the morphology. Coagulation led to particulate matter of too large size to enable particle size and particle size distribution data to be obtained.

23 Cuervo-Rodriguez, R.; Bordegé, V.; Fernández-Monreal, M. C.; Fernández-García, M.; Madruga, E. L. J Polym Sci Part A: Polym Chem 2004, 42, 4168–4176.

24 (a) Ishizone, T.; Ito, M. J Polym Sci Part A: Polym Chem 2002, 40, 4328–4332; (b) Ito, M.; Ishizone, T. J. Polym Sci Part A: Polym Chem 2006, 44, 4832–4845.

European Polymer Journal xxx (2012) xxx–xxx

Contents lists available at SciVerse ScienceDirect

European Polymer Journal

journal homepage: www.elsevier.com/locate/europolj

Facile synthesis of thermoresponsive block copolymers of *N*-isopropylacrylamide using heterogeneous controlled/living nitroxide-mediated polymerizations in supercritical carbon dioxide

Padraig O'Connor, Rongbing Yang, William M. Carroll, Yury Rochev, Fawaz Aldabbagh *

School of Chemistry, National University of Ireland Galway, University Road, Galway, Ireland

ARTICLE INFO

Article history:
Received 9 December 2011
Received in revised form 16 April 2012
Accepted 21 April 2012
Available online xxxx

Keywords:
Macroinitiator
Radical
Polymer
Precipitation polymerisation
Reversible-deactivation
Suspension polymerisation

ABSTRACT

A new protocol for preparation of thermoresponsive poly(*N*-isopropylacrylamide, NIPAM) containing block copolymers is described. It involves two successive heterogeneous controlled/living nitroxide-mediated polymerizations (NMPs) in supercritical carbon dioxide ($scCO_2$) using *N*-*tert*-butyl-*N*-[1-diethylphosphono-(2,2-dimethylpropyl)]nitroxide (SG1), as the nitroxide. Precipitation NMPs give narrow dispersity macroinitiators (MIs), and a first report of the controlled/living polymerization of *N*,*N*-dimethylacrylamide (DMA) in $scCO_2$ is described. The MI is then used in an inverse suspension NMP of NIPAM in $scCO_2$ resulting in the efficient preparation of block copolymers containing DMA, *tert*-butyl acrylate and styrene. Aqueous cloud point temperature analysis for poly(DMA)-*b*-poly(NIPAM) and poly(acrylic acid)-*b*-poly(NIPAM) shows a significant dependence on poly(NIPAM) chain length for a given AB block copolymer.

1. Introduction

The first preparation of well-defined block copolymers using controlled/living chain growth polymerizations that minimize termination and transfer reactions is attributed to Szwarc et al. by means of living anionic polymerizations and date back to the 1950s [1,2]. The recognised disadvantages of anionic and cationic polymerizations are the low temperatures, scrupulous drying and purification of both monomers and solvents required [3], the non-compatibility of monomer classes with the propagating chain [4], and the requirement for protecting groups (e.g. in the anionic polymerization of *N*-isopropylacrylamide, NIPAM) [5,6]. Since the early 1990s the more versatile controlled/living radical polymerization (CLRP) techniques have largely superseded living ionic polymerizations for forming block copolymers and other well-defined polymers with narrow molecular weight distributions (MWDs) and various topologies. CLRPs are based on dissociation-combination, atom transfer and degenerative chain transfer mechanisms/techniques. Well-known CLRPs using the first two techniques are nitroxide-mediated polymerization (NMP) [7,8] and atom transfer radical polymerization (ATRP) [9,10], respectively. More recently, atom transfer techniques that reduce the amount of metal salt catalyst used have been popularized [11,12]. The most common degenerative transfer methodologies are reversible addition-fragmentation chain transfer (RAFT) [13,14], and macromolecular design by interchange of xanthate (MADIX) [15]. Organotellurium-mediated radical polymerization (TERP) is thought to achieve living character using more than one of these mechanisms [16]. In all cases, controlled/living character is achieved by rapid reversible deactivation of propagating radicals ($P^{\bullet}$), which is required to minimise the contribution of irreversible bimolecular terminations (and chain transfer), in contrast to a conventional "non-living" radical polymerization where irreversible terminations are the major chain-end forming events [17].

* Corresponding author. Tel.: +353 91 493120; fax: +353 91 495576.
E-mail address: Fawaz.Aldabbagh@nuigalway.ie (F. Aldabbagh).

0014-3057/$ - see front matter © 2012 Elsevier Ltd. All rights reserved.
http://dx.doi.org/10.1016/j.eurpolymj.2012.04.011

Poly(NIPAM) is a thermoresponsive polymer exhibiting a lower critical solution temperature (LCST) in water of ~32 °C leading to biomedical and drug delivery applications [18–20]. The manipulation of the polymer's LCST by incorporating additional monomers has attracted much interest with block copolymers prepared by a variety of CLRPs, including solution NMPs of NIPAM [21–24]. Block copolymers of NIPAM and acrylic acid (AA) have attracted much interest, because they form thermo- and pH-responsive micelles, useful in drug-delivery [25–29]. The combination of NIPAM with the hydrophilic monomer *N*,*N*-dimethylacrylamide (DMA) gives copolymers with elevated LCST [30–36], which may be closer to physiological temperature of ~37 °C.

Supercritical carbon dioxide ($scCO_2$) is a benign reaction medium, which can be used to circumvent the requirement for toxic and hazardous volatile organic compound (VOC). $ScCO_2$ is a continuous phase of CO_2 above its critical point exhibiting liquid-like densities and gas-like diffusivity. As a polymerization medium $scCO_2$ can generally dissolve most organic molecules (including monomers), but does not dissolve the resulting polymers [37,38]. This makes $scCO_2$ a useful medium for industrially important heterogeneous polymerizations that allow the synthesis of sub-micron sized polymer particles [39,40]. Controlled/living precipitation NMPs [41–44] and dispersion (with added stabilizer) NMPs [45–49] in $scCO_2$ have been reported, as well as dispersion polymerizations using ATRP [50–54] and RAFT [55–57] in $scCO_2$. The dispersion CLRP allows simultaneous control over particle size distribution and MWD of polymers [38,58].

Using the NMP of styrene (St) and *tert*-butyl acrylate (*t*-BA) in $scCO_2$, polymer chains have been shown to be soluble up to a certain critical degree of polymerization (J_{crit}) prior to precipitation, after which the polymerization continues in the monomer rich particle phase [44]. J_{crit} or the particle nucleation step can be predicted based on the targeted molecular weight and initial monomer loading, and J_{crit} or polymer solubility can be increased approximately linearly with pressure [44]. Control in terms of MWDs being narrower than in an equivalent nitroxide-mediated solution polymerization can be obtained under conditions where J_{crit} is high, and is attributed to an enhanced deactivation rate due to predicted increased nitroxide mobility in $scCO_2$ [42]. However it is not possible to carry out precipitation or dispersion polymerizations of NIPAM in $scCO_2$ at higher loadings than approximately 5% w/v because of the poor solubility of the monomer. Nevertheless in a recent communication [59], the inverse suspension NMP of NIPAM at loadings 10–40% w/v in $scCO_2$ using the 2,2′-azoisobutyronitrile (AIBN)/*N*-*tert*-butyl-*N*-[1-diethylphosphono-(2,2-dimethylpropyl)]nitroxide (SG1) [60] system, was reported with good control/living character established up to high conversion. An inverse suspension refers to a water soluble monomer (e.g. NIPAM) suspended in a hydrophobic phase (e.g. $scCO_2$). Amongst the benefits of using $scCO_2$ include elimination of chain transfer to solvent, which has been shown to be significant in the polymerizations of NIPAM in *N*,*N*-dimethylformamide (DMF). Chain transfer to solvent gives a maximum attainable MW for a given set of conditions in both conventional radical polymerization and CLRP [24]. In CLRPs chain transfer to organic solvent or monomer impedes control by leading to low MW tailing in MWDs at high conversions because of the accumulation of shorter chains [41,61,62]. This is particularly significant, for NMP where relatively high temperatures are required for the dissociation-combination equilibrium.

In the present article we report the facile preparation of various well-defined thermoresponsive block copolymers through controlled/living radical inverse suspension NMP of NIPAM in $scCO_2$. The polymeric alkoxyamines or macroinitiators (MI) are prepared by precipitation NMP in $scCO_2$ and a first report of the controlled/living polymerization of DMA in $scCO_2$ is described. There are in fact few heterogeneous controlled/living polymerizations of DMA, with only inverse microemulsion RAFT polymerizations reported, [63,64]. Further the thermal responsive properties of the block copolymers prepared using heterogeneous polymerizations in $scCO_2$; poly(DMA)-*b*-poly(NIPAM), poly(*t*-BA)-*b*-poly(NIPAM), poly(AA)-*b*-poly(NIPAM), and poly(St)-*b*-poly(NIPAM) are examined.

2. Experimental

2.1. Materials

N-Isopropylacrylamide (NIPAM, 98% TCI) was recrystallized from a mixture of 3:2 benzene/hexane before use. Styrene (St, Aldrich, >99%), *tert*-butyl acrylate (*t*-BA, Aldrich, 98%) and *N*,*N*-dimethylacrylamide (DMA, TCI, >99%) were distiled under reduced pressure before use. 2,2'-Azoisobutyronitrile (AIBN, DuPont Chemical Solution Enterprise) was recrystallized twice from methanol. *N*-*tert*-butyl-*N*-[1-diethylphosphono-(2,2-dimethylpropyl)]nitroxide, SG1 (also known as DEPN) was synthesized according to the literature [65], with purity 96% determined using ^{1}H NMR spectroscopy from the reaction of the SG1 radical with pentafluorophenylhydrazine (Aldrich 97%). Macroinitiators (MI) of poly(*t*-BA)-SG1(M_n = 8000 g mol^{-1}, M_w/M_n = 1.17) and poly(St)-SG1 (M_n = 6450 g mol^{-1}, M_w/M_n = 1.13) were prepared by precipitation NMP in $scCO_2$ as outlined in our published procedure [44]. Table 1 details the conditions for the synthesis of MIs. Sodium hydroxide (Aldrich ⩾97%), *N*,*N*-dimethlyformamide (DMF, Fisher, GPC grade), tetrahydrofuran (THF, Aldrich, 99.9%), dichloromethane (DCM, Aldrich 99%), anhydrous methanol (MeOH, Corcoran Chemicals 99.9%), acetone (Corcoran Chemicals 99.5%), hexane (Fisher Scientific, reagent grade), benzene (BDH, reagent grade), diethyl ether (Aldrich, reagent grade), trifluoroacetic acid (TFA, Aldrich, 99%), (trimethylsilyl)diazomethane solution in 2.0 M hexanes (Aldrich), lithium bromide (BDH, >97%), and CO_2 (BOC, 99.8%) were all used as received.

2.2. Equipment and measurements

All polymerizations in supercritical carbon dioxide ($scCO_2$) were conducted in a 100 mL stainless steel Thar reactor with 180° inline sapphire windows and overhead Magdrive stirrer with maximum programmable operating

Please cite this article in press as: O'Connor P et al. Facile synthesis of thermoresponsive block copolymers of *N*-isopropylacrylamide using heterogeneous controlled/living nitroxide-mediated polymerizations in supercritical carbon dioxide. Eur Polym J (2012), http://dx.doi.org/10.1016/j.eurpolymj.2012.04.011

Table 1
Experimental conditions for the synthesis of polymers shown in Table 2.[a]

Polymer[b]	$[Monomer]_0$ (% w/v)	Reagents	Polymerization Times (h)
Poly(DMA)-SG1 (MI)	20	$[SG1]_0/[AIBN]_0 = 3.3$	3.3
Poly(DMA)$_n$-*b*-poly(NIPAM)$_m$	10	$[MI]_0 = 0.14$ mmol, $[SG1]_0/[MI]_0 = 0.5$	12, 20, 28
Poly(*t*-BA)-SG1 (MI)	50	$[SG1]_0/[AIBN]_0 = 2.5$	8
Poly(*t*-BA)$_n$-*b*-poly(NIPAM)$_m$	10	$[MI]_0 = 0.14$ mmol, $[SG1]_0/[MI]_0 = 0.5$	20, 28, 31
Poly(St)-SG1 (MI)	60	$[SG1]_0/[AIBN]_0 = 2.0$	2.8
Poly(St)$_n$-*b*-poly(NIPAM)$_m$	20	$[MI]_0 = 0.28$ mmol, $[SG1]_0/[MI]_0 = 0.75$	36

[a] All polymerizations carried out in $scCO_2$ at 120 °C and 30 MPa using initial monomer loading $[Monomer]_0$.
[b] See Figs. 2–5 and Table 2 for GPC data before and after purification of polymers respectively.

pressure and temperature of 41.4 MPa and 125 °C, respectively. The pressure was produced and maintained by a Thar P-50 series high-pressure pump to within ±0.2 MPa. The temperature was regulated by a Thar CN6 controller to within ±1 °C. The reactor is connected to a Thar automated back pressure regulator (ABPR, a computer-controlled needle valve) for controlled venting.

M_n and polydispersity (M_w/M_n) were determined using a gel permeation chromatography (GPC) system consisting of a Viscotek DM 400 data manager, a Viscotek VE 3580 refractive-index detector, and two Viscotek Viscogel GMHHR-M columns. Measurements were carried out at 60 °C at a flow rate of 1.0 mL min^{-1} using GPC grade DMF containing 0.01 M LiBr as the eluent [5,6,23,24,59,61]. The columns were calibrated using six linear poly(St) standards (M_n = 376–2570,000). The M_n(GPC) values are given as grams per mole throughout, and are not absolute, but relative to linear poly(St) standards. Theoretical (M_n) or $M_{n,th}$ are not quoted due to the use of relative M_n(GPC) values and uncertainties in initiator efficiencies. Control/livingness is assessed using MWD relative shifts, trends and shapes. All GPC data corresponds to polymer before purification, unless otherwise stated.

^{1}H NMR spectra were obtained using a JEOL 400 MHz spectrometer. Samples containing poly(acrylic acid, AA) were recorded in $(CD_3)_2SO$, and all other samples were analysed in $CDCl_3$ with Me_4Si used as the internal standard. M_n(NMR) of purified block copolymers is calculated according to eq. (1: where $DP_{n(MI)}$ is the average degree of polymerization of each MI obtained from $M_n(GPC) = M_{n(MI)}$ divided by the MW of the constituent monomer; x is the ratio of poly(NIPAM) relative to MI incorporated in the block copolymer obtained from integration of poly(NIPAM) N–C–H ($\delta_H \sim 3.8$–4.1 ppm, 1H) resonance, and resonances at $\delta_H \sim 1.0$–2.4 ppm due to each individual incorporated MI plus poly(NIPAM) (see Figs. S5–S7 in Supplementary data). E.g. In the case of poly(-DMA)-*b*-poly(NIPAM), δ_H 0.90–2.0 ppm represents 3H (CH–CH_2) of poly(DMA) plus 9H (CH–CH_2 and 2 × Me) of poly(NIPAM) (Fig. S5). $MW_{[NIPAM]}$ is the molecular weight of NIPAM monomer.

$$M_n(NMR) = \{DP_{n(MI)} \times x\} \times MW_{[NIPAM]} + M_{n(MI)} \quad (1)$$

2.3. Precipitation NMP of DMA in $scCO_2$

DMA (20.0 g, 0.20 mol), AIBN (66 mg, 0.40 mmol) and SG1 (0.393 g, 1.33 mmol) were loaded into the $scCO_2$ reactor. The reactor was sealed with the magnetically coupled stirring lid (Magdrive). The mixture was purged for 15 min by passing gaseous CO_2 through the mixture to remove oxygen. Liquid CO_2 (~5 MPa) was added and the temperature was raised to the reaction temperature of 120 °C followed by the pressure to the reaction pressure (in this case 30 MPa) by the addition of CO_2. The reaction mixture was stirred at ~1200 rpm throughout and monitored through the inline sapphire windows. At the start the viewing window indicated a transparent solution, which became opaque at J_{crit} or the particle nucleation stage [44]. Heating was stopped and rapid external cooling using a cooling fan applied (this caused the temperature of the reactor to drop to ~80 °C in 10 min). When at approximately room temperature the CO_2 was vented slowly from the reactor through DCM to prevent the loss of polymer and opened using the ABPR. The reaction mixture was pipetted directly from the reactor. The polymer was precipitated into excess hexane, filtered and dried prior to conversion measurement by gravimetry. Polymerizations were then carried out to higher conversions beyond J_{crit}.

2.4. Test for livingness: chain extension of MI with bulk St

MI (0.025 mmol, based on the M_n of the purified polymer), St (2.0 g, 19.2 mmol), and SG1 (5.2 mg, 17.7 μmol) were charged in glass ampoules and subjected to several freeze/thaw degas cycles. After sealing under vacuum, the ampoules were heated at 110 °C in an aluminium heating block for 15 h. The polymerizations were quenched by immersing the ampoule into an ice-water bath. Each polymer was precipitated into an excess of methanol, filtered and dried prior to conversion measurement by gravimetry. Conversion was obtained from the increase in weight of polymeric material.

2.5. MI-initiated inverse suspension NMP of NIPAM in $scCO_2$

NIPAM (10.0 g, 88.4 mmol), MI (0.14 mmol, based on the M_n of the purified polymer; e.g. poly(*t*-BA)-SG1 = 1.12 g) and SG1 (20.6 mg, 0.07 mmol) were loaded into the reactor. Poly(St)-SG1 initiated polymerization was carried out at 20% w/v NIPAM loading (20.0 g, 0.177 mol) using poly(St)-SG1 (1.81 g, 0.28 mmol) and SG1 (61.8 mg, 0.21 mmol). The polymerizations were carried out as above (Section 2.3) at 120 °C and 30 MPa and stopped at various times. Poly(*t*-BA)-*b*-poly(NIPAM) and poly(St)-*b*-poly(NIPAM) were dissolved in MeOH and

Please cite this article in press as: O'Connor P et al. Facile synthesis of thermoresponsive block copolymers of *N*-isopropylacrylamide using heterogeneous controlled/living nitroxide-mediated polymerizations in supercritical carbon dioxide. Eur Polym J (2012), http://dx.doi.org/10.1016/j.eurpolymj.2012.04.011

acetone respectively and precipitated into excess petroleum ether and poly(DMA)-*b*-poly(NIPAM) was dissolved in DCM and precipitated into excess hexane. All copolymer samples were filtered and dried prior to conversion measurement by gravimetry. Table 1 details the conditions for the synthesis of block copolymers.

2.6. Hydrolysis of poly(t-BA)-b-poly(NIPAM)

Poly(*t*-BA)-*b*-poly(NIPAM) (1.5 g) was dissolved in DCM (15 mL) and a tenfold molar excess of TFA was added and the mixture stirred at room temperature for 24 h. The reaction was evaporated to dryness and the solid dissolved in methanol. The polymer was precipitated into excess diethyl ether, filtered and dried under vacuum. ^{1}H NMR spectra verified the hydrolysis of the *tert*-butyl groups (~1.4 ppm) had occurred quantitatively (see Fig. S6).

2.7. Aqueous cloud point measurements of block copolymers

These were carried out using a Cary 100 UV–vis spectrophotometer at 500 nm, with temperature ramping at 0.1 °C/min. Polymers solutions (0.1% w/v) were prepared in Millipore water. NaOH solutions were used to adjust the pH of samples containing poly(AA) blocks. Samples were allowed to equilibrate for several hours before analysis. Commercial poly(NIPAM) with M_n = 56,000 and M_w/M_n = 2.70 using the above GPC conditions, was used as reference.

3. Results and discussion

3.1. Precipitation NMP of N,N-dimethylacrylamide (DMA) in scCO$_2$

DMA has a large propagation rate constant (k_p), and NMP with good control/living character is reported with bulk monomer in the presence of an excess of the nitroxide, SG1 [66,67]. For precipitation and dispersion NMP of St in scCO$_2$, a larger amount of free nitroxide is necessary compared to the solution or bulk polymerization of St because of the partitioning of some of the mediating nitroxide away from the locus of polymerization (i.e. the monomer rich particle) upon precipitation of the propagating radical from the continuous phase [41,43,47]. Polymerizations of 20% w/v DMA (i.e. 20 g DMA in 100 mL reactor) in scCO$_2$ with initial ratios of $[SG1]_0/[AIBN]_0$ = 2.5, 3.0 and 3.3 were carried out at 120 °C and 30 MPa, in order to give an optimal ratio required to achieve control/living character, as well as reasonable polymerization rates (Fig. 1). The highest ratio of $[SG1]_0/[AIBN]_0$ was found to give the narrowest MWD with negligible effect on rate and was used in subsequent polymerizations. The solubility of DMA in scCO$_2$ using these polymerization conditions was deciphered by observation of the reaction through the inline sapphire windows. The monomer was found to be soluble beyond 40% w/v loading and thus amenable to a precipitation polymerization. At 20% w/v monomer loading, precipitation occurred after 37 min at the above conditions with J_{crit} occurring at 6% conversion (M_n = 1600 g/mol and M_w/M_n = 1.22). Poly(DMA) has comparable solubility to poly(*t*-BA) in scCO$_2$, which has been shown to be more soluble than poly(St) under similar conditions [44]. A series of polymerizations were then performed to high conversion and despite the large excess of nitroxide used, the NMP remained relatively fast reaching 66% conversion in about 12 h (Fig. 2). Controlled/living character is demonstrated by uniform MWDs remaining relatively narrow throughout (1.22–1.37) and M_n increasing linearly with conversion. It is interesting that the polydispersity index also increases approximately linearly with conversion (over this narrow range) with the initial rise in M_w/M_n presumably because of the partitioning of the nitroxide between the continuous and particle phase causing a small depreciation in control (see earlier discussion). Livingness was assessed by chain extension of the isolated poly(DMA)-SG1 at 24% conversion with bulk styrene (Fig. 3). After conversion of the chain extended GPC trace, to its number distribution curve (P(*M*) *vs. M*, Fig. 3b), [47,62,68] and integration of the distinctive low molecular weight peak (non-extended chains, M_n < ~5700 g/mol) relative to the overall distribution, it is calculated that 82% of poly(DMA) chains contain the SG1 end-group.

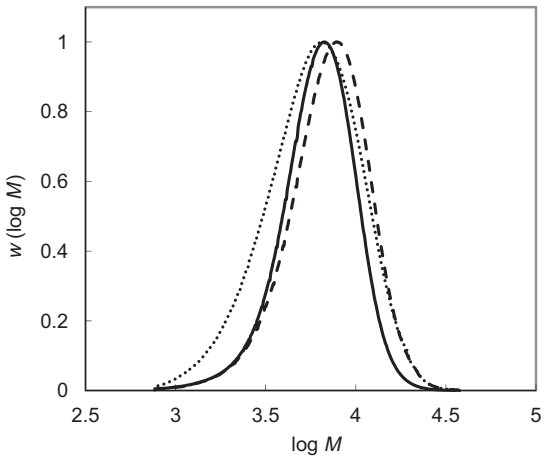

Fig. 1. Influence of initial nitroxide concentration on MWDs (normalised to peak height) for the precipitation NMPs of 20% w/v initial loading of DMA in scCO$_2$ at 120 °C and 30 MPa. $[SG1]_0/[AIBN]_0$ = 2.5 (dotted line), 3.0 (dashed line) and 3.3 (continuous line), where M_n = 4750 g/mol, M_w/M_n = 1.45, 16% conversion; M_n = 6100 g/mol, M_w/M_n = 1.32, 28% conversion; and M_n = 5450 g/mol, M_w/M_n = 1.26, 24% conversion; respectively.

3.2. MI-initiated inverse suspension polymerizations of N-isopropylacrylamide (NIPAM) in scCO$_2$

The block copolymers were prepared by inverse suspension NMP of NIPAM in scCO$_2$ at 120 °C and 30 MPa [59]. The latter optimised conditions (particularly pressure) are thought to reduce the influences of NIPAM solubility in scCO$_2$, as well as reagent partitioning between the two phases. The poly(DMA)-SG1 sample at 24% conversion in Fig. 2 was used as MI, and the poly(*t*-BA)-SG1 MI synthesis is previously reported [44]. Since the MIs were obtained using precipitation NMPs in scCO$_2$, it follows that the polymeric initiators would be expected to have a lower

Please cite this article in press as: O'Connor P et al. Facile synthesis of thermoresponsive block copolymers of *N*-isopropylacrylamide using heterogeneous controlled/living nitroxide-mediated polymerizations in supercritical carbon dioxide. Eur Polym J (2012), http://dx.doi.org/10.1016/j.eurpolymj.2012.04.011

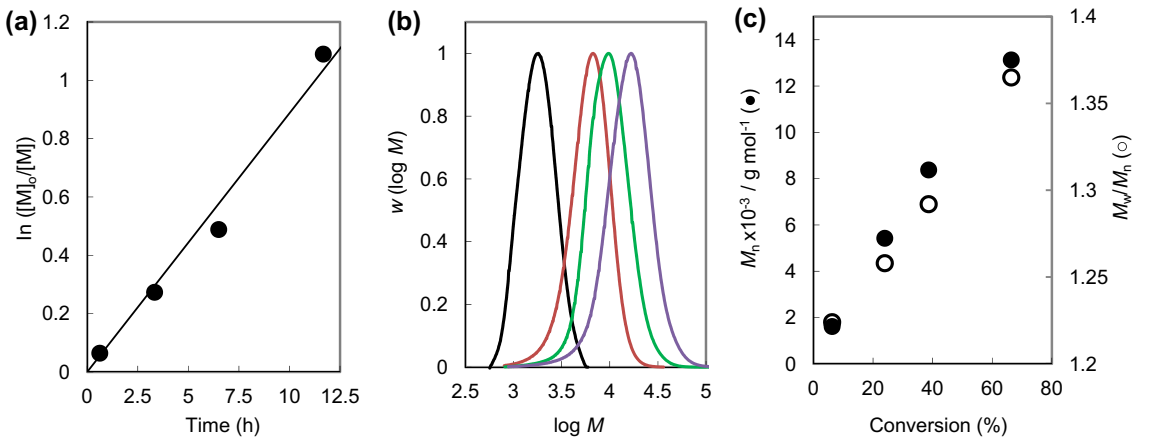

Fig. 2. Precipitation NMPs of 20% w/v initial loading of DMA in $scCO_2$ at 120 °C and 30 MPa, where $[SG1]_0/[AIBN]_0 = 3.3$. (a) First order rate plot (b) MWDs (normalized to peak height) and (c) GPC M_n (●) and M_w/M_n (○) versus conversion plots. J_{crit} is at 6% conversion.

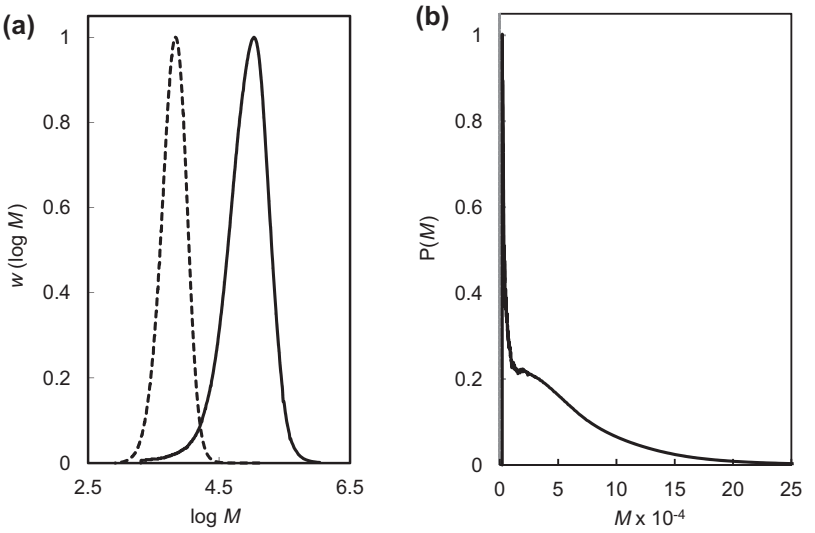

Fig. 3. Chain extension of poly(DMA)-SG1 with bulk St at 110 °C for 15 h: (a) GPC traces of purified MI (dashed line) from precipitation NMP of DMA in $scCO_2$ at 24% conversion (see Fig. 2), M_n = 5700 g/mol, M_w/M_n = 1.23 and chain extension in bulk St in the presence of 70% free SG1 (solid line) M_n = 60,250 g/mol, M_w/M_n = 1.78 and (b) *P(M) vs M* (number distribution curve) of the chain extended polymer. All peaks normalized to peak height.

solubility in the continuous phase, and would be located mostly in the monomer-rich suspended droplets at the start of the polymerization. NMP of 10% w/v NIPAM was initiated by the MIs in the presence of a 50 mol% excess of free SG1 (Fig. 4). There is an induction period in the polymerizations using two different concentrations of poly(*t*-BA)-SG1, which is absent when using poly(DMA)-SG1, as MI (Fig. 4a). This however is not be due to the dispersed nature of the polymerization mixture, but is a feature of the kinetics of this particular NMP, given that a similar ~12 h delay in polymerization was observed in the solution NMP of NIPAM in DMF using a similar poly(*t*-BA)-SG1 MI (with 25% excess free SG1) [24]. This may be attributed to the dissociation rate constant (k_d) of the MI, which is likely to be about two times greater for poly(DMA)-SG1 compared to poly(*t*-BA)-SG1, based on literature k_d data available for analogous small molecule alkoxyamines of SG1 at 120 °C [69]. It is thus expected that in the polymerizations initiated by poly(*t*-BA)-SG1, there is a greater tendency for the initiation equilibrium to lie towards the dormant state (i.e. non-dissociated MI). Halving the ratio of $[NIPAM]_0/[poly(t\text{-}BA)\text{-}SG1]_0$ by doubling the number of initiated chains, with the $[MI]_0/[free\ SG1]_0$ ratio maintained, gives no increase in the rate of polymerization (Fig. 4a). This indicates that stationary state kinetics apply, whereby the $[P^{\bullet}]$ is not affected by $[MI]_0$ [17]. The rate of spontaneous thermal initiation is negligible in this system [24], and rate which is proportional to $[P^{\bullet}]$ (evidenced by the linear first order plot) will be dictated by the high excess of free nitroxide available for a given $[MI]_0/[SG1]_0$ [41,43,47]. It is also evident from the identical rates of polymerization for the two different $[poly(t\text{-}BA)\text{-}SG1]_0$

Please cite this article in press as: O'Connor P et al. Facile synthesis of thermoresponsive block copolymers of *N*-isopropylacrylamide using heterogeneous controlled/living nitroxide-mediated polymerizations in supercritical carbon dioxide. Eur Polym J (2012), http://dx.doi.org/10.1016/j.eurpolymj.2012.04.011

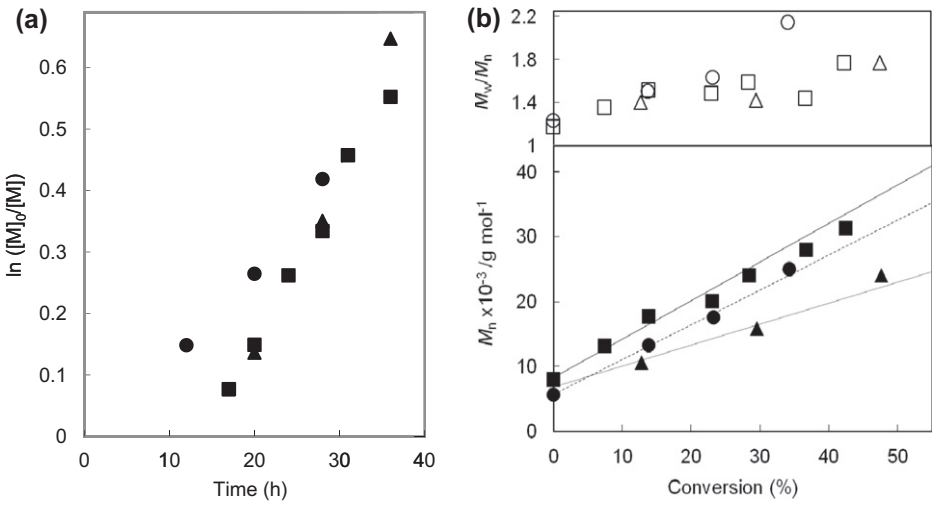

Fig. 4. Inverse suspension NMPs of 10% w/v initial loading of NIPAM in $scCO_2$ at 120 °C and 30 MPa initiated by poly(*t*-BA)-SG1 = 0.14 mmol (■, □), poly(*t*-BA)-SG1 = 0.28 mmol (▲,△) and poly(DMA)-SG1 = 0.14 mmol (●,○) in the presence of 50 mol% free SG1. (a) First order rate plot and (b) GPC M_n (closed symbols with trend lines) and M_w/M_n (open symbols) versus conversion plots.

initiated polymerizations that the level of partitioning of SG1 between phases is proportionate. Fig. 4b shows the increase in the poly(*t*-BA)-SG1 concentration by a factor of two resulted in a decrease in M_n by close to a factor of two, as expected for a controlled/living system. This increase in $[MI]_0$ has however no effect on the rate of monomer consumption because of an increase in the average number of activation-deactivation cycles for the higher $[MI]_0$ is accompanied by a proportional decrease in the number of monomer units incorporated into each living polymer chain per cycle, in accordance with ideal CLRP kinetics [17]. The monomodal MWDs demonstrated that the polymerizations took place mainly in the suspended particles and that polymerization in the $scCO_2$ phase is less significant (see Supplementary Figs. S1–S3). Therefore the polymerizations initiated by poly(DMA)-SG1 and poly(*t*-

Table 2
Characterization of macroinitiators (MI) and poly(NIPAM) containing block copolymers used in aqueous cloud point analysis.

Polymers[a]	M_n(GPC) (M_w/M_n)[b]	M_n (NMR)[c]
Poly(DMA)-SG1 (MI)	5700 (1.23)	–
Poly(DMA)$_{(58)}$-*b*-poly(NIPAM)$_{(82)}$	13400 (1.48)	15000
Poly(DMA)$_{(58)}$-*b*-poly(NIPAM)$_{(117)}$	21400 (1.55)	18950
Poly(DMA)$_{(58)}$-*b*-poly(NIPAM)$_{(217)}$	29250 (2.07)	30250
Poly(*t*-BA)-SG1 (MI)	8000 (1.17)	–
Poly(*t*-BA)$_{(62)}$-*b*-poly(NIPAM)$_{(81)}$	20600 (1.42)	17200
Poly(*t*-BA)$_{(62)}$-*b*-poly(NIPAM)$_{(192)}$	30750 (1.33)	29700
Poly(*t*-BA)$_{(62)}$-*b*-poly(NIPAM)$_{(254)}$	34550 (1.31)	36750
Poly(St)-SG1 (MI)	6450 (1.13)	–
Poly(St)$_{(62)}$-*b*-poly(NIPAM)$_{(266)}$	34200 (1.51)	36500

[a] DP_n of block copolymers is calculated from M_n(GPC) for the first block relative to overall M_n(NMR) of the block copolymer.
[b] After purification.
[c] Calculated from ^{1}H NMR according to Eq. (1).

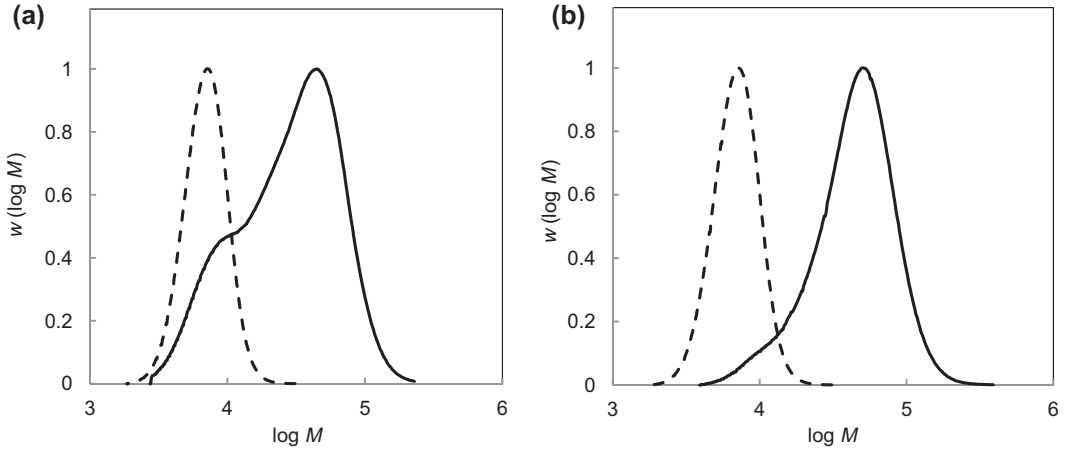

Fig. 5. Inverse suspension NMPs of NIPAM in $scCO_2$ at 120 °C and 30 MPa initiated by (a) 0.14 mmol and (b) 0.28 mmol poly(St)-SG1 (dashed lines, M_n = 6450, M_w/M_n = 1.13). MWDs for (a) 10% w/v initial monomer loading with 50 mol% free SG1 (solid line, M_n = 18450, M_w/M_n = 2.00, 14% conv.) and (b) 20% w/v initial monomer loading with 75 mol% free SG1 (solid line, M_n = 30700, M_w/M_n = 1.63, 51% conv.). All peaks normalized to peak height.

Please cite this article in press as: O'Connor P et al. Facile synthesis of thermoresponsive block copolymers of *N*-isopropylacrylamide using heterogeneous controlled/living nitroxide-mediated polymerizations in supercritical carbon dioxide. Eur Polym J (2012), http://dx.doi.org/10.1016/j.eurpolymj.2012.04.011

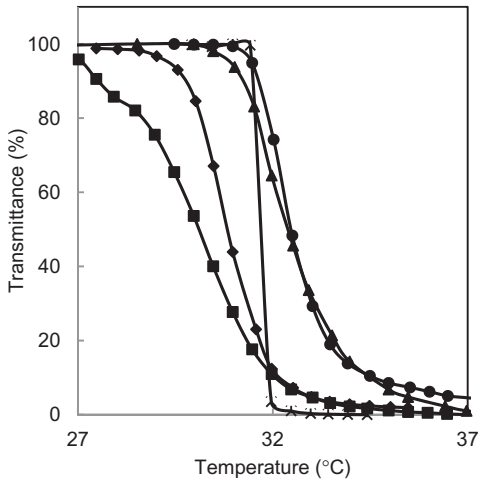

Fig. 6. Light transmittance as a function of temperature of 0.1% w/v aqueous solutions at pH 7 of commercial poly(NIPAM) (☼), poly(-DMA)$_{(58)}$-*b*-poly(NIPAM)$_{(217)}$ (●), poly(*t*-BA)$_{(62)}$-*b*-poly(NIPAM)$_{(192)}$ (■), poly(AA)$_{(62)}$-*b*-poly(NIPAM)$_{(192)}$ (▲), and poly(St)$_{(62)}$-*b*-poly(NIPAM)$_{(266)}$ (♦).

BA)-SG1 (at two different [MI]$_0$) proceeded with good controlled/living character, since M_n increases linearly with conversion starting from each $M_{n(MI)}$. Polydispersities remain reasonably low, although some broadening occurs up to intermediate conversion especially for the poly(-DMA)-SG1 initiated system.

The initial inverse suspension polymerization of NIPAM in $scCO_2$ initiated by poly(St)-SG1 was carried out using the same conditions that proved successful using the polyamide and polyacrylate MIs (shown above). However poor control/livingness was obtained, as indicated by a prominent low MW shoulder corresponding to non-extended MI (Fig. 5a). Simultaneous doubling of the monomer loading, concentration of MI, and an increase in the excess free SG1 (Fig. 5b) gave a clear shift in the MWD of MI (at M_n = 6450 and M_w/M_n = 1.13) to higher MW block copolymer (at M_n = 30,700 and M_w/M_n = 1.63). The minor low MW tail in Fig. 5b is attributed to mainly dead poly(St) chains that did not initiate the polymerization of NIPAM, based on a 70% calculation of livingness of the MI (Fig. S4).

Prior to aqueous cloud point analysis of block copolymers, any traces of unreacted MI, and NIPAM were removed by selective precipitation procedures using an anti-solvent for the block copolymers, which dissolved monomer and any non-extended MI (see Section 2). M_n(GPC) of purified block copolymers are in reasonable agreement with M_n(NMR) in Table 2, indicating good accuracy in the estimation of the average degrees of polymerization of block copolymers (^{1}H NMR spectra of block copolymers are given in Supplementary data, see Figs. S5–S7).

3.3. Hydrolysis of Poly(t-BA)-b-Poly(NIPAM)

The required pH-sensitive thermal response polymer, poly(AA)-*b*-poly(NIPAM) was obtained through hydrolysis of the *tert*-butyl groups of poly(*t*-BA)-*b*-poly(NIPAM) with an excess of TFA (Fig. S6). The poly(AA) copolymer was then methylated using $Me_3SiCH = N_2$, and its MWD shown to be similar to that of the poly(*t*-BA) precursor before hydrolysis, indicating both negligible loss of polymer chains, and decomposition of the poly(NIPAM) part during the hydrolysis process (Fig. S8). The average degrees of polymerization for each poly(AA)-*b*-poly(NIPAM) are assumed to be the same as the *t*-BA precursor prior to hydrolysis (Table 2).

3.4. Aqueous cloud point analysis of block copolymers

This involved the preparation of purified and dried block copolymer samples (0.1% w/v) in de-ionised water. Upon heating at pH 7, the solutions became turbid above

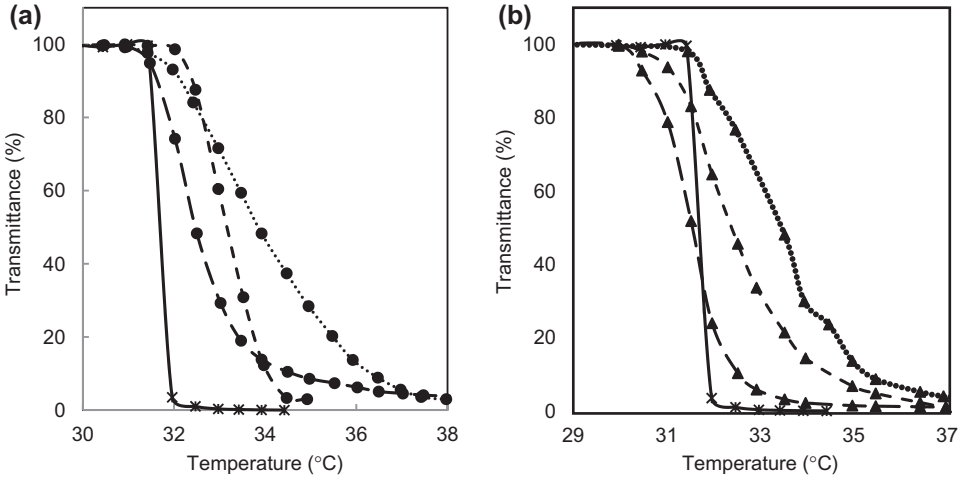

Fig. 7. Light transmittance as a function of temperature of 0.1% w/v aqueous solution at pH 7 of (a) commercial poly(NIPAM) (continuous line), poly(DMA)$_{(58)}$-*b*-poly(NIPAM)$_{(82)}$ (dotted line), poly(DMA)$_{(58)}$-*b*-poly(NIPAM)$_{(117)}$ (dashed line) and poly(DMA)$_{(58)}$-*b*-poly(NIPAM)$_{(217)}$ (long dashed line) and (b) commercial poly(NIPAM) (continuous line), poly(AA)$_{(62)}$-*b*-poly(NIPAM)$_{(81)}$ (dotted line), poly(AA)$_{(62)}$-*b*-poly(NIPAM)$_{(192)}$ (dashed line) and poly(AA)$_{(62)}$-*b*-poly(NIPAM)$_{(254)}$ (long dashed line).

Please cite this article in press as: O'Connor P et al. Facile synthesis of thermoresponsive block copolymers of *N*-isopropylacrylamide using heterogeneous controlled/living nitroxide-mediated polymerizations in supercritical carbon dioxide. Eur Polym J (2012), http://dx.doi.org/10.1016/j.eurpolymj.2012.04.011

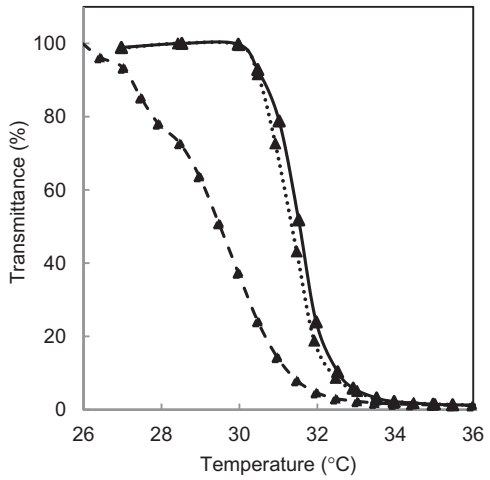

Fig. 8. Light transmittance as a function of temperature of 0.1% w/v aqueous solution of poly(AA)$_{(62)}$-*b*-poly(NIPAM)$_{(254)}$, at pH = 4 (dashed line), pH = 7 (dotted line) and pH = 10 (continuous line).

the LCST, which corresponds to 50% transmittance on the heating curves in Figs. 6–8, with commercially available high MW polydisperse poly(NIPAM) (LCST = 31.7 °C) used as a reference. Our study assumes negligible end-group influences and similar relative GPC error for all samples (see Section 2). The MI incorporated part of the AB poly(NIPAM) block copolymer is of similar length in each case, and this study shows the effect of changing the chemical composition of the MI block on the observed LCST of poly(NIPAM). Fig. 6 shows the block copolymer solutions containing a hydrophobic poly(St) and poly(*t*-BA) parts become turbid at lower temperatures than those block copolymers incorporating hydrophilic poly(AA) and poly(-DMA) parts. The formation of aggregates or micelles for the poly(St) and poly(*t*-BA) containing block copolymers prior to the LCST is possible [27,28], and could influence cloud point measurements shown in Fig. 6. The controlled/living polymerization technique allowed us to analyse the effect of extending the poly(NIPAM) block length, while maintaining identical MI incorporated block sizes. Fig. 7a and b, respectively show this for the poly(DMA) and poly(AA) containing block copolymers. As a greater number of NIPAM monomeric units are incorporated in each case, the copolymers reach the cloud point at temperatures closer to that of commercial poly(NIPAM). The differences in polydispersity have less effect on cloud points, as indicated upon examination of Table 2. Strong decreases in the phase transition temperature with increasing MW of poly(NIPAM) have been reported by Stöver and co-workers for narrow dispersity homopolymers prepared using room temperature ATRP [70]. Poly(AA)-*b*-poly(NIPAM) is a well-studied dual responsive copolymer [25,27–29], and it is now observed that the cloud point is lowered significantly at pH4 close to the pK_a (≈4.5–5.0) of the poly(AA) part, where it is the most hydrophobic (Fig. 8). This is in agreement with the findings of Kulkarni et al. [26] with the dependence of cloud point measurements on pH being small once the p*K*a is exceeded.

4. Conclusion

DMA is found to be appreciably soluble in $scCO_2$, and amenable to a precipitation polymerization. Precipitation NMP of 20% w/v DMA was carried out in $scCO_2$ at 120 °C and 30 MPa with good control/living character demonstrated. Under these conditions the polymer becomes insoluble at the critical degree of polymerization (J_{crit}) at 6% conversion, M_n = 1600 g/mol and M_w/M_n = 1.22. This indicates a similar solubility to polyacrylates in $scCO_2$ [44]. Poly(DMA) at 24% conversion was used as MI, which was estimated to contain ≈82% living chains based on chain extension with bulk styrene. Inverse suspension NMP of 10% w/v NIPAM in $scCO_2$ using various MIs (prepared by precipitation NMPs) was then carried out with controlled/living stationary state kinetics observed, when using poly(*t*-BA)-SG1 (at two different $[MI]_0$). Different conditions were required to establish control for poly(St)-SG1 initiated inverse suspension polymerization of NIPAM in $scCO_2$, in comparison to poly(DMA)-SG1 and poly(*t*-BA)-SG1 initiated polymerizations. The MIs incorporated are shown to greatly influence the aqueous cloud point temperature, and cloud points approach commercial polydisperse high MW poly(NIPAM) as a greater number of NIPAM units are incorporated. Future work will focus on stabilizing heterogeneous NMPs of hydrophilic NIPAM and DMA monomers, which is not possible in aqueous or organic solution environments.

Acknowledgment

This publication has emanated from research work conducted with financial support from Science Foundation Ireland (08/RFP/MTR1201).

Appendix A. Supplementary data

Supplementary data associated with this article can be found, in the online version, at http://dx.doi.org/10.1016/j.eurpolymj.2012.04.011.

References

[1] Szwarc M. "Living" polymers. Nature 1956;178:1168–9.
[2] Szwarc M, Levy M, Milkovich R. Polymerization initiated by electron transfer to monomer. A new method of formation of block polymers. J Am Chem Soc 1956;78:2656–7.
[3] Uhrig D, Mays JW. Experimental techniques in high-vacuum anionic polymerization. J Polym Sci Part A Polym Chem 2005;43:6179–222.
[4] Aldabbagh F, Gibbons O. Polystyrenes. Sci Synthesis 2010;45b:723–44.
[5] Ito M, Ishizone T. Synthesis of well-defined block copolymers containing poly(*N*-isopropylacrylamide) segment by anionic block copolymerization of N-methoxymethyl-*N*-isopropylacrylamide. Des Monomers Polym 2004;7:11–24.
[6] Ito M, Ishizone T. Living anionic polymerization of *N*-methoxymethyl-N-isopropylacrylamide: synthesis of well-defined poly(*N*-isopropylacrylamide) having various stereoregularity. J Polym Sci Part A Polym Chem 2006;44:4832–45.
[7] Georges MK, Veregin RPN, Kazmaier PM, Hamer GK. Narrow molecular weight resins by a free radical polymerization process. Macromolecules 1993;26:2987–8.
[8] Grubbs RB. Nitroxide-mediated radical polymerization: limitations and versatility. Polym Rev 2011;51:104–37.
[9] Wang J-S, Matyjaszewski K. Controlled/"living" radical polymerization. Atom transfer radical polymerization in the

presence of transition-metal complexes. J Am Chem Soc 1995;117:5614–5.
[10] Kato M, Kamigaito M, Sawamoto M, Higashimura T. Polymerization of methyl methacrylate with carbon tetrachloride/dichlorotris(triphenylphosphine)ruthenium (II)/methylaluminum bis(2,6-di-tert-butylphenoxide) initiating system: possibility of living radical polymerization. Macromolecules 1995;28:1721–3.
[11] Pintauer T, Matyjaszewski K. Atom transfer radical addition and polymerization reactions catalyzed by ppm amounts of copper complexes. Chem Soc Rev 2008;37:1087–97.
[12] Rosen BM, Percec V. Single-electron transfer and single-electron transfer degenerative chain transfer living radical polymerization. Chem Rev 2009;109:5069–119.
[13] Chiefari J, Chong YK, Ercole F, Krstina J, Jeffery J, Le TPT, et al. Living free-radical polymerization by reversible addition-fragmentation chain transfer: the RAFT process. Macromolecules 1998;31:5559–62.
[14] Destarac M. On the critical role of RAFT agent design in reversible addition-fragmentation chain Transfer (RAFT) polymerization. Polym Rev 2011;51:163–87.
[15] Perrier S, Takolpuckdee P. Macromolecular design via reversible addition–fragmentation chain transfer (RAFT)/xanthates (MADIX) polymerization. J Polym Sci Part A Polym Chem 2005;43:5347–93.
[16] Yamago S. Development of organotellurium-mediated and organostibine-mediated living radical polymerization reactions. J Polym Sci Part A Polym Chem 2006;44:1–12.
[17] Goto A, Fukuda T. Kinetics of living radical polymerization. Prog Polym Sci 2004;29:329–85.
[18] Schild HG. Poly(N-isopropylacrylamide): experiment, theory and application. Prog Polym Sci 1992;17:163–249.
[19] Kikuchi A, Okano T. Nanostructured designs of biomedical materials: applications of cell sheet engineering to functional regenerative tissues and organs. J Control Release 2005;101:69–84.
[20] Wei H, Cheng S-X, Zhang X-Z, Zhuo R-X. Thermo-sensitive polymeric micelles based on poly(*N*-isopropylacrylamide) as drug carriers. Prog Polym Sci 2009;34:893–910.
[21] Harth E, Bosman A, Benoit D, Helms B, Fréchet JMJ, Hawker CJ. A practical approach to the living polymerization of functionalized monomers: application to block copolymers and 3-dimensional macromolecular architectures. Macromol Symp 2001;174:85–92.
[22] Kuroda K, Swager TM. Fluorescent semiconducting polymer conjugates of poly(*N*-isopropylacrylamide) for thermal precipitation assays. Macromolecules 2004;37:716–24.
[23] Gibbons O, Carroll WM, Aldabbagh F, Yamada B. Nitroxide-mediated controlled statistical copolymerizations of *N*-isopropylacrylamide with *N*-tert-butylacrylamide. J Polym Sci Part A Polym Chem 2006;44:6410–8.
[24] Sugihara Y, O'Connor P, Zetterlund PB, Aldabbagh F. Chain transfer to solvent in the radical polymerization of *N*-isopropylacrylamide. J Polym Sci Part A Polym Chem 2011;49:1856–64.
[25] Schilli CM, Zhang M, Rizzardo E, Thang SH, Chong YK, Edwards K, et al. A new double-responsive block copolymer synthesized via RAFT polymerization: poly(*N*-isopropylacrylamide)-block-poly(acrylic acid). Macromolecules 2004;37:7861–6.
[26] Kulkarni S, Schilli C, Grin B, Müller AHE, Hoffman AS, Stayton PS. Controlling the aggregation of conjugates of streptavidin with smart block copolymers prepared via the RAFT copolymerization technique. Biomacromolecules 2006;7:2736–41.
[27] Li G, Shi L, An Y, Zhang W, Ma R. Double-responsive core–shell–corona micelles from self-assembly of diblock copolymer of poly(t-butyl acrylate-co-acrylic acid)-b-poly(*N*-isopropylacrylamide). Polymer 2006;47:4581–7.
[28] Li G, Shi L, Ma R, An Y, Huang N. Formation of complex micelles with double-responsive channels from self-assembly of two diblock copolymers. Angew Chem Int Ed 2006;45:4959–62.
[29] Li G, Song S, Guo L, Ma S. Self-assembly of thermo- and pH-responsive poly(acrylic acid)-b-poly(*N*-isopropylacrylamide) micelles for drug delivery. J Polym Sci Part A Polym Chem 2008;46:5028–35.
[30] Masci G, Giacomelli L, Crescenzi V. Atom transfer radical polymerization of N-Isopropylacrylamide. Macromol Rapid Commun 2004;25:559–64.
[31] Convertine AJ, Lokitz BS, Vasileva Y, Myrick LJ, Scales CW, Lowe AB, et al. Direct synthesis of thermally responsive DMA/NIPAM diblock and DMA/NIPAM/DMA triblock copolymers via aqueous, room temperature RAFT polymerization. Macromolecules 2006;39:1724–30.
[32] Li Y, Lokitz BS, McCormick CL. RAFT Synthesis of a thermally responsive ABC triblock copolymer incorporating *N*-acryloxysuccinimide for facile in situ formation of shell cross-linked micelles in aqueous media. Macromolecules 2006;39:81–9.
[33] An Z, Shi Q, Tang W, Tsung C-K, Hawker CJ, Stucky GD. Facile RAFT precipitation polymerization for the microwave-assisted synthesis of well-defined, double hydrophilic block copolymers and nanostructured hydrogels. J Am Chem Soc 2007;129:14493–9.
[34] Xie D, Ye X, Ding Y, Zhang G, Zhao N, Wu K, et al. Multistep thermosensitivity of poly(*N*-isopropylacrylamide)-block-poly(*N*-isopropylacrylamide)-block-poly(*N*,*N*-ethylmethylacrylamide) triblock terpolymers in aqueous solutions as studied by static and dynamic light scattering. Macromolecules 2009;42:2715–20.
[35] Sun X-L, He W-D, Li J, Li L-Y, Zhang B-Y, Pan T-T. RAFT cryopolymerizations of *N*,*N*-dimethylacrylamide and *N*-isopropylacrylamide in moderately frozen aqueous solution. J Polym Sci Part A Polym Chem 2009;47:6863–72.
[36] Li K, Cao Y. Thermo-responsive behavior of block and random copolymers of *N*-Isopropylamide/*N*,*N*-dimethylacrylamide synthesized via reversible addition—fragmentation chain transfer polymerization. Soft Matter 2010;8:226–38.
[37] Kendall JL, Canelas DA, Young JL, DeSimone JM. Polymerizations in supercritical carbon dioxide. Chem Rev 1999;99:543–64.
[38] Zetterlund PB, Aldabbagh F, Okubo M. Controlled/living heterogeneous radical polymerization in supercritical carbon dioxide. J Polym Sci Part A Polym Chem 2009;47:3711–28.
[39] Zetterlund PB, Kagawa Y, Okubo M. Controlled/living radical polymerization in dispersed systems. Chem Rev 2008;108:3747–94.
[40] Cunningham MF. Controlled/living radical polymerization in aqueous dispersed systems. Prog Polym Sci 2008;33:365–98.
[41] McHale R, Aldabbagh F, Zetterlund PB, Okubo M. Nitroxide-mediated radical precipitation polymerization of styrene in supercritical carbon dioxide. Macromol Chem Phys 2007;208:1813–22.
[42] Aldabbagh F, Zetterlund PB, Okubo M. Improved control in nitroxide-mediated radical polymerization using supercritical carbon dioxide. Macromolecules 2008;41:2732–4.
[43] Aldabbagh F, Zetterlund PB, Okubo M. Nitroxide-mediated precipitation polymerization of styrene in supercritical carbon dioxide: effects of monomer loading and nitroxide partitioning on control. Eur Polym J 2008;44:4037–46.
[44] O'Connor P, Zetterlund PB, Aldabbagh F. Effect of monomer loading and pressure on particle formation in nitroxide-mediated precipitation polymerization in supercritical carbon dioxide. Macromolecules 2009;43:914–9.
[45] Ryan J, Aldabbagh F, Zetterlund PB, Okubo M. First nitroxide-mediated free radical dispersion polymerizations of styrene in supercritical carbon dioxide. Polymer 2005;46:9769–77.
[46] McHale R, Aldabbagh F, Zetterlund PB, Okubo M. Nitroxide-mediated radical dispersion polymerization of styrene in supercritical carbon dioxide using poly(dimethylsiloxane-b-styrene) alkoxyamine as initiator and stabilizer. Macromol Rapid Commun 2006;27:1465–71.
[47] McHale R, Aldabbagh F, Zetterlund PB, Minami H, Okubo M. Nitroxide-mediated radical dispersion polymerization of styrene in supercritical carbon dioxide using a poly(dimethylsiloxane-b-methyl methacrylate) stabilizer. Macromolecules 2006;39:6853–60.
[48] Ramírez-Wong DG, Posada-Vélez CA, Saldívar-Guerra E, Luna-Bárcenas JG, Ott C, Schubert US. Silicon-based and fluorinated polymeric surfactants for nitroxide mediated dispersion polymerization in supercritical carbon dioxide. Macromol Symp 2009;283–284:120–9.
[49] Grignard B, Phan T, Bertin D, Gigmes D, Jérôme C, Detrembleur C. Dispersion nitroxide mediated polymerization of methyl methacrylate in supercritical carbon dioxide using in situ formed stabilizers. Polym Chem 2010;1:837–40.
[50] Xia J, Johnson T, Gaynor SG, Matyjaszewski K, DeSimone J. Atom transfer radical polymerization in supercritical carbon dioxide. Macromolecules 1999;32:4802–5.
[51] Minami H, Kagawa Y, Kuwahara S, Shigematsu J, Fujii S, Okubo M. Dispersion atom transfer radical polymerization of methyl methacrylate with bromo-terminated poly(dimethylsiloxane) in supercritical carbon dioxide. Des Monomers Polym 2004;7:553–62.
[52] Grignard B, Jérôme C, Calberg Cd, Jérôme R, Wang W, Howdle SM, Detrembleur C. Dispersion atom transfer radical polymerization of vinyl monomers in supercritical carbon dioxide. Macromolecules 2008;41:8575–83.
[53] Grignard B, Jérôme C, Calberg C, Jérôme R, Detrembleur C. Atom transfer radical polymerization of MMA with a macromolecular ligand in a fluorinated solvent and in supercritical carbon dioxide. Eur Polym J 2008;44:861–71.
[54] Grignard B, Jérôme C, Calberg C, Jérôme R, Wang W, Howdle SM, Detrembleur C. Copper bromide complexed by fluorinated

Please cite this article in press as: O'Connor P et al. Facile synthesis of thermoresponsive block copolymers of *N*-isopropylacrylamide using heterogeneous controlled/living nitroxide-mediated polymerizations in supercritical carbon dioxide. Eur Polym J (2012), http://dx.doi.org/10.1016/j.eurpolymj.2012.04.011

macroligands: towards microspheres by ATRP of vinyl monomers in scCO2. Chem Commun 2008: 314–316.
[55] Thurecht KJ, Gregory AM, Wang W, Howdle SM. "Living" polymer beads in supercritical CO_2. Macromolecules 2007;40:2965–7.
[56] Zong M, Thurecht KJ, Howdle SM. Dispersion polymerisation in supercritical CO_2 using macro-RAFT agents. Chem Commun 2008;45:5942–4.
[57] Gregory AM, Thurecht KJ, Howdle SM. Controlled dispersion polymerization of methyl methacrylate in supercritical carbon dioxide via RAFT. Macromolecules 2008;41:1215–22.
[58] Thurecht KJ, Howdle SM. Controlled dispersion polymerization in supercritical carbon dioxide. Aust J Chem 2009;62:786–9.
[59] O'Connor P, Zetterlund PB, Aldabbagh F. Nitroxide-mediated stabilizer-free inverse suspension polymerization of N-isopropylacrylamide in supercritical carbon dioxide. J Polym Sci Part A Polym Chem 2011;49:1719–23.
[60] Benoit D, Grimaldi S, Finet JP, Tordo P, Fontanille M, Gnanou Y. Controlled free-radical polymerization in the presence of a novel asymmetric nitroxyl radical. Polym Prepr (Am Chem Soc, Div Polym Chem) 1997; 38: 729–730.
[61] Gibbons O, Carroll WM, Aldabbagh F, Zetterlund PB, Yamada B. Nitroxide-mediated radical polymerization of N-tert-butylacrylamide. Macromol Chem Phys 2008;209:2434–44.
[62] Zetterlund PB, Saka Y, McHale R, Nakamura T, Aldabbagh F, Okubo M. Nitroxide-mediated radical polymerization of styrene: experimental evidence of chain transfer to monomer. Polymer 2006;47:7900–8.
[63] Sogabe A, McCormick CL. Reversible addition–fragmentation chain transfer (RAFT) polymerization in an inverse microemulsion system: homopolymerization, chain extension, and block copolymerization. Macromolecules 2009;42:5043–52.
[64] Sogabe A, Flores JD, McCormick CL. Reversible addition–fragmentation chain transfer (RAFT) polymerization in an inverse microemulsion: partitioning of chain transfer agent (CTA) and its effects on polymer molecular weight. Macromolecules 2010;43:6599–607.
[65] Cuervo-Rodriguez R, Bordegé V, Fernández-Monreal MC, Fernández-García M, Madruga EL. Nitroxide-mediated free-radical copolymerization of styrene with butyl acrylate. J Polym Sci Part A Polym Chem 2004;42:4168–76.
[66] Schierholz K, Givehchi M, Fabre P, Nallet F, Papon E, Guerret O, et al. Acrylamide-based amphiphilic block copolymers via nitroxide-mediated radical polymerization. Macromolecules 2003;36:5995–9.
[67] Diaz T, Fischer A, Jonquières A, Brembilla A, Lochon P. Controlled polymerization of functional monomers and synthesis of block copolymers using a β-phosphonylated nitroxide. Macromolecules 2003;36:2235–41.
[68] Gilbert RG. Molecular weight distributions in free-radical polymerizations: their cause and cure. Trends Polym Sci 1995;3: 222–6.
[69] Bertin D, Dufils P-E, Durand I, Gigmes D, Giovanetti B, Guillaneuf Y, et al. Effect of the penultimate unit on the C–ON bond homolysis in SG1-based alkoxyamines. Macromol Chem Phys 2008;209:220–4.
[70] Xia Y, Yin X, Burke NAD, Stöver HDH. Thermal response of narrow-disperse poly(N-isopropylacrylamide) prepared by atom transfer radical polymerization. Macromolecules 2005;38:5937–43.

Please cite this article in press as: O'Connor P et al. Facile synthesis of thermoresponsive block copolymers of *N*-isopropylacrylamide using heterogeneous controlled/living nitroxide-mediated polymerizations in supercritical carbon dioxide. Eur Polym J (2012), http://dx.doi.org/10.1016/j.eurpolymj.2012.04.011